OCS Study
MMS 93-0025

Preliminary Assessment of Gulf of Mexico OCS Contributions to Ozone Formation in Onshore Areas Using the Regional Oxidant Model

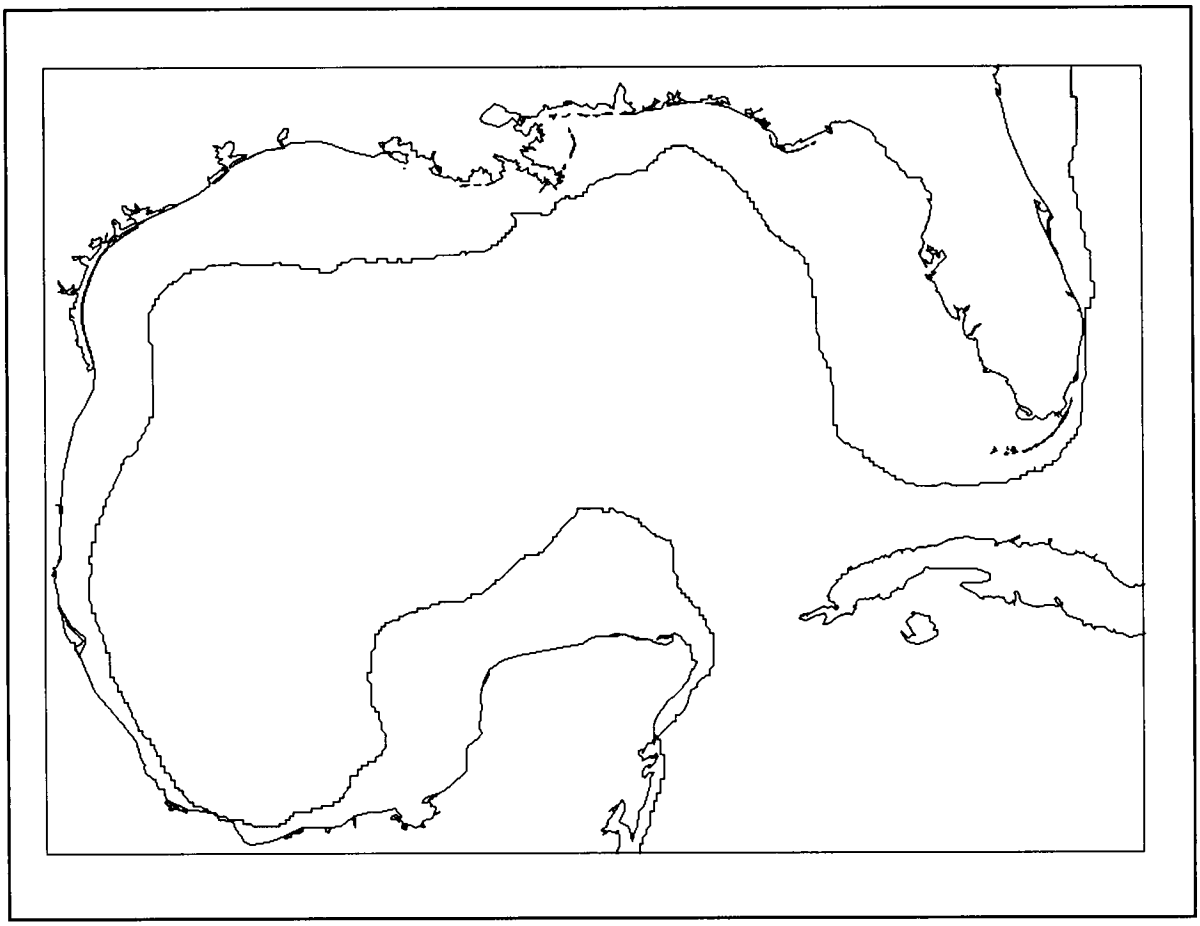

Gulf of Mexico

MMS
U.S. Department of the Interior
Minerals Management Service
Gulf of Mexico OCS Region

OCS Study
MMS 93-0025

Preliminary Assessment of Gulf of Mexico OCS Contributions to Ozone Formation in Onshore Areas Using the Regional Oxidant Model

Prepared by

U.S. Environmental Protection Agency
Office of Air Quality Planning and Standards
Technical Support Division
Research Triangle Park, North Carolina 27711

Prepared under Interagency Agreement 16198

Published by

U.S. Department of the Interior
Minerals Management Service
Gulf of Mexico OCS Region

New Orleans
November 1993

DISCLAIMER

This report was prepared under an Interagency Agreement between the Minerals Management Service (MMS) and the U.S. Environmental Protection Agency. This report has been technically reviewed by the MMS and approved for publication. Approval does not signify that the contents necessarily reflect the views and policies of the Service, nor does the mention of trade names or commercial products constitute endorsement or recommendation for use. It is, however, exempt from review and compliance with MMS editorial standards.

REPORT AVAILABILITY

Extra copies of the report may be obtained from the Public Information Unit (Mail Stop 5034) at the following address:

U.S. Department of the Interior
Minerals Management Service
Gulf of Mexico OCS Region
Public Information Unit (MS 5034)
1201 Elmwood Park Boulevard
New Orleans, Louisiana 70123-2394
Telephone: (504) 736-2519

CITATION

Suggested citation:

U.S. Environmental Protection Agency. 1993. Preliminary assessment of Gulf of Mexico OCS contributions to ozone formation in onshore areas using the regional oxidant model. Prepared by the U.S. Environmental Protection Agency, Office of Air Quality Planning and Standards, Technical Support Division, Research Triangle Park, N.C. OCS Study MMS 93-0025. 214 pp.

ABSTRACT

A preliminary assessment of ozone contributions from outer continental shelf (OCS) to onshore areas using the U.S. Environmental Protection Agency's Regional Oxidant Model (ROM) in the Gulf of Mexico examined five nonattainment areas: Baton Rouge, Baton Rouge-New Orleans (Louisiana), Lake Charles-Beaumont, Houston-Galveston, and Corpus Christi. The study represents the first assessment of OCS contributions to ozone in the Gulf of Mexico. Two ozone episodes (July 20-August 6, 1988, and July 24-August 1, 1990), which had onshore winds for transporting OCS-derived ozone to onshore areas, were selected for analysis. The model's onshore emissions input consisted of the 1985 National Acid Precipitation and Assessment inventory, the Biogenic Emissions Inventory System, and mobile sources from the 1986 vehicle traveled data adjusted to 1988. Offshore emissions inputs were supplied by Texas' 1985 inventory, Louisiana's 1990 inventory, and the Minerals Management Service's 1985 platform inventory. The OCS platforms emit about 115,592 tons/year of NO_x and about 43,872 tons/year of THC. The OCS contributions to ozone are greatest over water, 29 parts per billion (ppb), while contributions to onshore average 5-8 ppb during these episodes. Daily ozone contributions under appropriate meteorological conditions can be as high as 12-16 ppb. The model's performance evaluation reveals an average normalized gross error of 31%, while the paired accuracy of peaks averaged 22.8%. The results of this assessment suggest that a similar study using an improved emissions database and a photochemical model with finer spatial resolution to gain a better understanding of OCS contributions is desirable.

TABLE OF CONTENTS

	Page
LIST OF FIGURES	ix
LIST OF TABLES	xi
1. INTRODUCTION	1
2. EXPERIMENTAL DESIGN	1
3. MODELING SYSTEM	3
4. EMISSIONS PROCESSING AND ANALYSIS	7
5. BASE CASE SIMULATION	11
6. AMBIENT OZONE IMPACT ANALYSIS	18
7. CONCLUSIONS	27
8. REFERENCES	31
9. APPENDICES	
APPENDIX A. GRAPHICS DEPICTING MODEL PERFORMANCE	A-3
APPENDIX B. PERFORMANCE MEASURE FORMULATIONS	B-3
APPENDIX C. ALGORITHMS FOR CELL-AGGREGATION	C-3
APPENDIX D. EPISODIC AND DAILY VALUE PLOTS OF PREDICTED OZONE DIFFERENCES BETWEEN THE SCENARIOS AND BASE CASE	D-3

LIST OF FIGURES

		Page
Figure 2-1	ROM modeling domain and 5 MMS selected subregions	2
Figure 3-1	ROM vertical structure and pollutants dispersion (a) daytime; (b) nighttime	5
Figure 5-1	Scatter plot of hourly O3 (paired in space and time) for MMS, Baton Rouge-New Orleans, Episode #1	13
Figure 5-2	Quantile-quantile plot of ozone concentrations for MMS, Baton Rouge-New Orleans, Episode #1	14
Figure 5-3	Maximum hourly O3 concentrations for MMS, Baton Rouge-New Orleans, Episode #1	15
Figure 6-1	Difference: Base without OCS - Base. Maximum Ozone, Layer 1 -- July 25-31, 1988	19
Figure 6-2	Difference: Base without OCS - Base. Maximum Ozone, Layer 1 -- August 1-6, 1988	20
Figure 6-3	Difference: Base with double OCS - Base. Maximum Ozone, Layer 1 -- July 25-31, 1988	21
Figure 6-4	Difference: Base with double OCS - Base. Maximum Ozone, Layer 1 -- August 1-6, 1988	22
Figure 6-5	Difference: Base without OCS - Base. Maximum Ozone, Layer 1 -- July 26-31, 1990	24
Figure 6-6	Difference: Base with double OCS - Base. Maximum Ozone, Layer 1 -- July 26-31, 1990	25
Figure 6-7	Difference: MMS Base without OCS - MMS Base. Daily Maximum Ozone, Layer 1 -- July 29, 1990	26
Figure 6-8	Box plot of OCS impact on MMS subregions, Episode #1: July 25 - August 6, 1988 (8 a.m. - 7 p.m.)	28
Figure 6-9	Box plot of OCS impact on MMS subregions, Episode #1: July 26 - July 31, 1990 (8 a.m. - 7 p.m.)	29

LIST OF TABLES

		Page
Table 4-1	Emissions data summaries for the offshore point source data (tons/year)	10
Table 5-1	Monitor locations and number of observations used by subregion (daylight hours)	12
Table 5-2	Numerical measurements of model performance based on MMS episode #1/July 25 - August 6, 1990	16
Table 5-3	Numerical measurements of model performance based on MMS episode #2/July 26 - July 31, 1990	17

1. INTRODUCTION

This project was initiated under the interagency agreement between the Department of Interior (DOI Reference: 16198) and the United States Environmental Agency (EPA Reference: RW14935350-01-0). According to this agreement, the U.S. EPA has conducted a preliminary study of the potential impact of Gulf of Mexico outer continental shelf (OCS) source emissions on onshore ozone concentrations using the regional oxidant model (ROM)[1,2]. The main objective of this proposed ROM study is to assess at an "order of magnitude" level the contributions of Gulf of Mexico OCS activities to ozone concentrations in onshore areas. The ROM results will be evaluated by the Minerals Management Service (MMS) for possible use in the air quality impact analysis in the Environmental Impact Statement.

2. EXPERIMENTAL DESIGN

2.1. *Modeling Domain.*

In this application, the geographic area of interest is the Gulf of Mexico offshore OCS areas and onshore areas of neighboring states. The ROM domain and 5 MMS selected subregions are shown in Figure 2-1. The domain is defined by a curvilinear coordinate system from 26° N to 37.67° N and from 99° W to 81° W, with a horizontal grid resolution of (1/4)° longitude by (1/6)° latitude, a total of 5040 (72 columns x 70 rows) model grid cells. Only the data in the 5 subregions are used to calculate all the statistics.

2.2. *Episode Selection.*

An episodic day for ozone is defined as a day in which at least two urban areas in the ROM modeling domain recorded exceedances of the concentration specified in the National Ambient Air Quality Standard (NAAQS) for ozone (0.12 ppm). An ozone episode may consist of any number of consecutive ozone episodic days. To minimize the influences not relevant to the episode to be simulated, the ROM is initialized with a clean background. Thus, a ROM episode usually starts a few days before an episode begins.

The episode selection criteria for this study, however, are somewhat different from those which are typically used. These differences are due to the unique purpose of this study as stated in section 1 of this report to evaluate the possible impact of Gulf of Mexico OCS emissions on onshore ozone formation. The MMS has requested two high ozone episodes to be selected during the period of 1987-1990. The selection process started with ranking all ozone episodes during the 1987-1990 period according to their severity, spatial coverage and persistence. Then the episodes with well-defined onshore trajectories from the Gulf of Mexico are pooled together. Among these episodes, two are selected for ROM modeling.

1. July 20 - August 6, 1988

2. July 24 - August 1, 1990

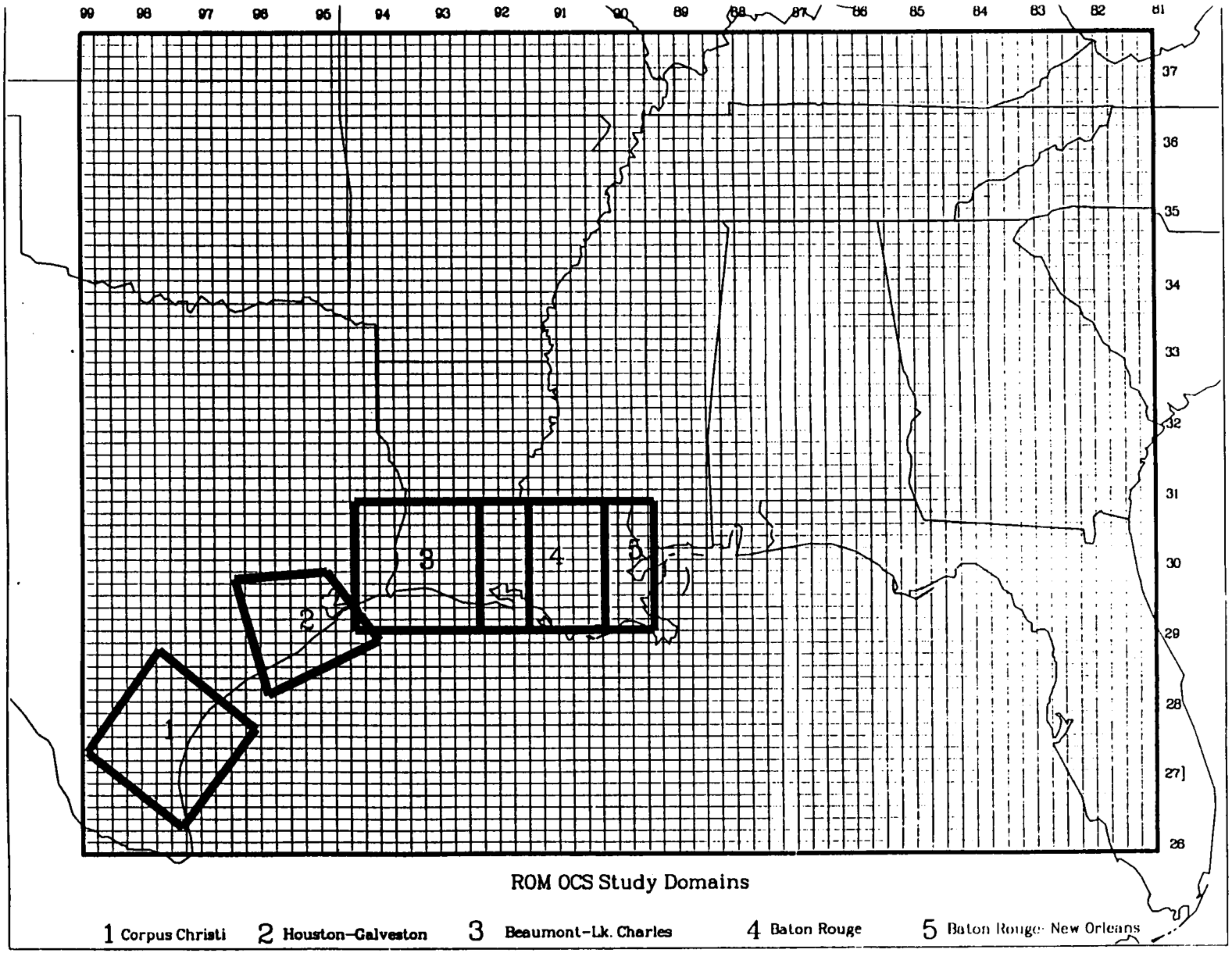

Figure 2-1. ROM modeling domain and 5 MMS selected subregions.

The 1988 episode is a historic episode of moderate intensity. The 1990 episode is a more recent one with much stronger intensity. Both episodes occur under the influence of stagnant high pressure systems and have predominantly light onshore flows.

2.3. *Modeling Strategies.*

The model is first run for the existing onshore and offshore emissions (both anthropogenic and biogenic) to establish the base case scenario. Then, two modeling strategies are developed to test the sensitivity of coastal ozone concentrations to changes in the Gulf of Mexico OCS emissions. The first strategy is to examine the differences between ozone concentrations predicted by the base case emissions and those predicted when the OCS sources are totally eliminated. The second strategy is to compare the base case model prediction of ozone with a scenario in which the existing OCS source emissions are doubled.

3. MODELING SYSTEM

3.1. *Model Characteristics*

The current version of Regional Oxidant Model (ROM 2.2) is a three-dimensional Eulerian model designed to simulate most of the important chemical and physical processes that are responsible for the photochemical production of ozone over a domain of 1000 km or more and for episodes ranging from a few days to well above two weeks. These processes include (1) horizontal transport, (2) atmospheric chemistry, (3) the effects of cumulus clouds on vertical mass transport and photochemical reaction rates, (4) mesoscale vertical motions induced by terrain and large scale flow, 5) terrain effects on advection, diffusion and deposition, (6) emissions of natural and anthropogenic ozone precursors, and (7) dry deposion. The ROM is essentially a planetary boundary layer model with a horizontal grid resolution of (1/4)° longitude by (1/6)° latitude, or about 18.5 km x 18.5 km. In the vertical, the planetary boundary layer and the capping inversion or cloud layer are simulated by the ROM using three dynamic layers, which are free to expand and contract locally in response to changes in the physical processes occurring therein. During an entire simulation period, horizontal advection and diffusion and gas-phase chemistry are modeled prognostically in the three vertical layers. Pollutant concentrations are calculated every 30 minutes, but the ROM predictions are aggregated hourly. Pollutant concentrations predicted at layer 1 are used as surrogates for surface concentrations.

3.2 *Physical Processes Treated in Layers 1, 2 and 3*

During the daytime, layers 1 and 2 model the mixed layer while layer 3 models the cloud layer or the synoptic-scale subsidence inversion, the base of which is typically 1-2 km above the ground. Near coastal areas there often exists a thermal internal boundary layer that is modeled in layer 1. Two other processes are also treated in layer 1: namely, some localized strong low level wind shear and deposition on terrain features that protrude above the surface layer. During the nighttime, as a nocturnal inversion forms near the surface, layer 1 decouples with the upper 2 layers to become the only stable boundary layer and layer 2 represents the residual layer which effectively contains the remains of the daytime mixed layer. Ozone and the remnants of other

photochemical reaction products may remain in layers 2 and 3 during the night and can be transported long distances downwind by a nocturnal jet. Figures 3-1 (a) and (b) show the vertical layer structure of the model for a typical daytime and nighttime, respectively.

Horizontal transport within the ROM system is governed by hourly wind fields interpolated from periodic wind observations made from upper air soundings and surface measurements. Horizontal turbulent fluxes are approximated using gradient transport theory. The horizontal eddy diffusivity coefficient is parameterized by empirical relationships of convective velocity scale and layer height during unstable conditions and is considered to be zero during stable conditions.

The flux of mass into and out of each model layer is determined for both the bottom and top surfaces of the layer. Several physical processes cause air to pass through these surfaces. Vertical advection (caused by surface convergence or divergence), turbulent eddies, changes in layer height, deposition fluxes (for the lower layers), horizontal winds (depending upon the slope of the layer interface), terrain forcing, and cumulus cloud updrafts can cause air to move across one of these surfaces. In local areas where strong winds exist and the surface heat flux is weak there can exist substantial wind shear in the lowest few hundred meters above ground. This phenomenon is treated separately in layer 1. At night, emissions from tall stacks and warm cities are injected directly into layer 2 aloft. Otherwise, surface emissions are specified as a mass flux into layer 1. Within the ROM system, a submodel simulates the cloud flux process and its impact on the material fluxes among all the model's layers[3]. The magnitude of the mass flux proceeding directly from the surface layer to the cloud layer is modeled as being proportional to the observed amount of cumulus cloud coverage and inversely proportional to the observed depth of the clouds. The model solves a complex set of equations governing each of these processes to obtain mass fluxes from one layer to the next for each pollutant species.

3.3 *Model Chemistry*

The chemical kinetic mechanism embedded in ROM is the Carbon Bond Mechanism IV (CB-IV)[4]. This mechanism simulates the significant reaction pathways responsible for gas-phase production and destruction of photochemical smog constituents on regional scales. The mechanism consists of 83 reactions including 33 individual species. The ROM's chemical solution scheme makes no a priori assumptions concerning local steady states. Therefore all species are advected, diffused, and chemically reacted within the model domain. Chemical time steps vary depending on chemical reaction rates but typically range from 10 to 60 *s*. Liquid-phase chemistry is not modeled in the current implementation of the chemical kinetics, and thus part of the effects from the cloud flux processes are not accounted for in the simulations. A solar radiation algorithm[5] is used to compute photolytic rate constants and implicitly considers the effect of haze on the solar intensity. A cloud cover correction factor for photolysis rates[6] is applied using observed cloud cover data.

The CB-IV contains a standard set of reactions for atmospheric inorganic chemical species, including O_3, NO, NO_2, CO and other intermediate and radical species. Organic chemistry is partitioned along reactivity lines based on the carbon structures of the molecules. Ten categories of organics are represented to account for the chemistry of hundreds of organic

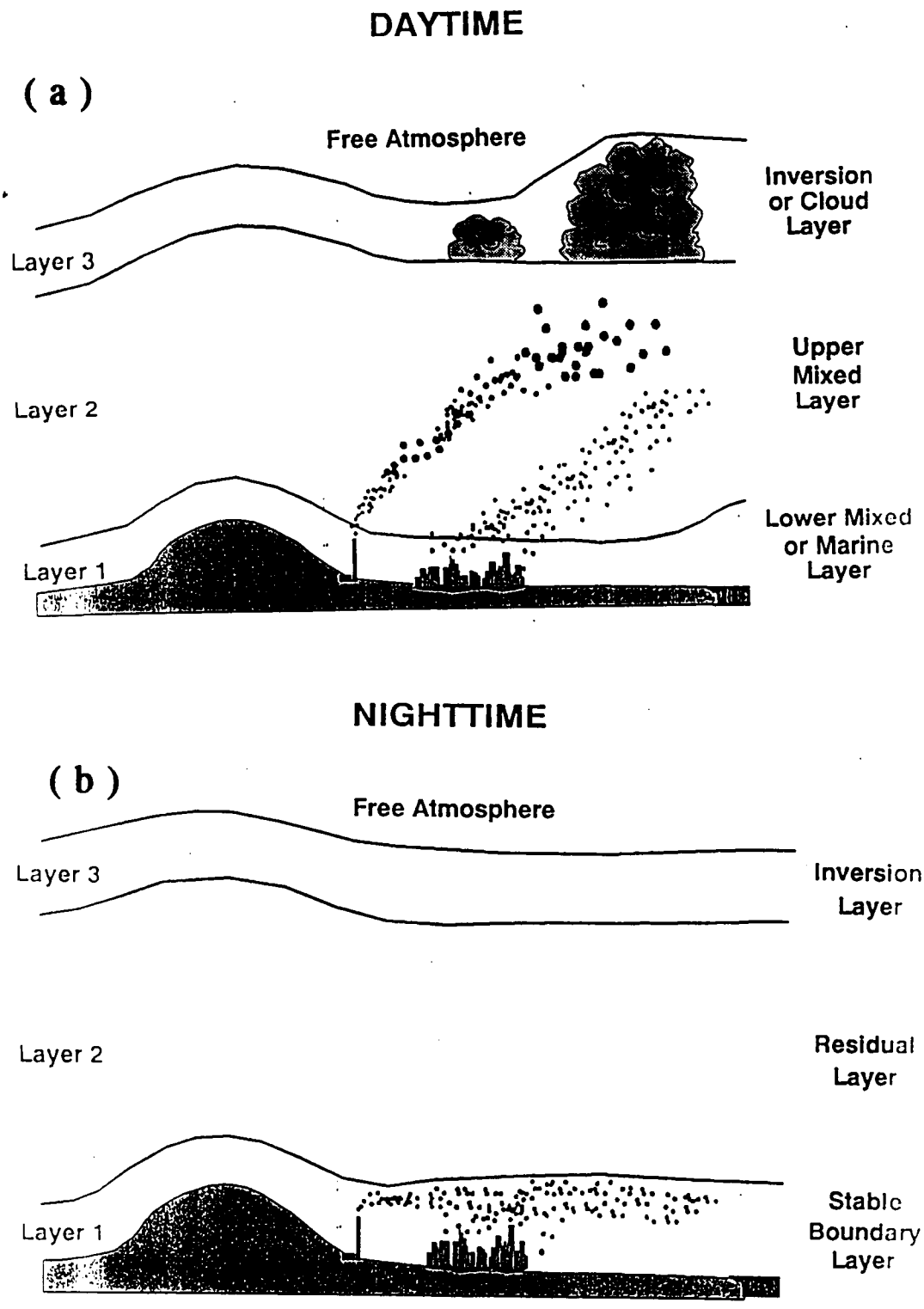

Figure 3-1. ROM vertical structure and pollutants dispersion. (a) daytime; (b) nighttime.

molecules existing in the ambient atmosphere:

* ETH, an explicit representation of ethene;

* FORM, an explicit representation of formaldehyde;

* OLE, a double-bonded lumped structure including two carbons (e.g., olefin);

* PAR, a single-bond, single carbon structure (e.g., paraffins);

* ALD2, the oxygenated two-carbon structure of the higher aldehydes;

* TOL, the aromatic structure of molecules with only one functional group (e.g., toluene);

* XYL, the structure of molecules with multifunctional aromatic rings (e.g., xylene);

* ISOP, the five-carbon isoprene molecule;

* NONR, a single-carbon organic structure not significantly participating in the reaction sequence; and

* MTHL, methanol, for use with control strategies that include methanol-powered vehicles.

3.4 *Input Data Requirements*

3.4.1. *Initial and boundary conditions.* Prior to setting either initial or boundary conditions for pollutant concentrations, a set of concentrations are derived to represent the background atmosphere. These background concentrations are obtained by taking mean tropospheric concentrations of gases (100 ppb of CO, 2 ppb of NO_x, and 14 ppbC of NMHC)[7], and equilibrating these using the CBM-IV for a 24-hour period, using constant daytime "clear-sky" photolysis rates for the first 12 hours and then using constant nighttime rates for the last 12 hours. This procedure is performed for each model layer. Concentrations representing the daytime background atmosphere are taken toward the end of the first 12 hours, and those representing nighttime are taken toward the end of the final 12-hour period. Chemically equilibrated states are formed between all the species, with O_3 reaching a level of $\sim$ 30 ppb in all three layers for both daytime and nighttime.

The model is initialized with the daytime background concentrations, computed as described above, for each model grid cell. The meteorological episode was chosen such that the initial conditions resembled the actual state of the atmosphere. The simulations presented here begin on a day with relatively clean air. Nevertheless, it is impossible to match the initial conditions exactly with the actual atmosphere; therefore the first 24-36 hours were considered an initialization period. The effects of the initial conditions are considered to be removed after the first day or so. The same initial conditions are used in all three emission scenarios.

Temporally varying boundary conditions are specified for all four sides of the modeling domain. Ozone observations in the vicinity of the model's boundaries are aggregated into day and night values for each simulation day. The background values, described above, for other chemical species are equilibrated with the specified boundary O_3 value, to arrive at a boundary condition set. Relatively clean tropospheric air is assumed to exist above layer 3 at all times, and therefore background values equilibrated with an O_3 level of 40 ppb are used for the top boundary condition. The same boundary conditions were used in each of the three emission scenarios analyzed here.

3.4.2. *Meteorological data.* Several sets of meteorological data are required by the model, including surface and upper air observations, as well as data from buoys. Many levels of data preprocessing occur in preparing these data for the model, along with quality control procedures at each level to filter out erroneous data. Surface and buoy data are merged and subjected to objective analysis to obtain gridded values for various meteorological parameters. Hourly upper air profiles are produced by interpolating upper air data between observation times and by adjusting the interpolated profiles to account for hourly surface conditions. Objective analysis is then used to grid horizontally other derived meteorological parameters based on these hourly profiles. In addition to the standard meteorological parameters required by the model turbulence parameters are computed using the observed meteorological data and provided to the model.

2.4.3. *Emission inventories.* Two sets of emissions data were developed for this study. Anthropogenic estimates, consisting of gridded hourly rates of NMHC and NO_x, were derived from the 1985 National Acid Precipitation Assessment Program (NAPAP) inventory[8]. Emissions for major point, area and mobile sources were included in this set. They varied daily (Saturday, Sunday, or weekday) and hourly. Biogenic emission estimates were obtained from the Biogenic Emissions Inventory System (BEIS)[9].

4. EMISSIONS PROCESSING AND ANALYSIS

4.1. *Base Case Emissions.*

4.1.1. *Onshore Emissions.*

The anthropogenic emissions data used in the Regional Oxidant Model (ROM) Minerals Management Service (MMS) study are divided into four primary components: point source data, stationary area source data, mobile source data and offshore point source data. Each component is processed independently, however, the area, mobile, offshore point and minor onshore point source data are later combined into a single gridded, speciated data file. Thus, it is assumed that plume rise associated with OCS emissions is insufficient to lead to an effective plume height higher than the models level 1 cells. The major point sources over land are treated separately to allow for proper layering of the emissions based on plume rise.

The onshore point source and stationary area source data were generated using the 1985 National Acid Precipitation and Assessment (NAPAP) annual NOx, THC and CO emissions estimates. The mobile source data were based on 1986 vehicle miles travelled (VMT) data

projected to 1988 and 1988 mobile emission factors generated using the MOBILE4.1 model. The projections were calculated using motor vehicle gasoline consumption data for each State and average roadway fuel economy data. The fuel consumption data were multiplied by the roadway miles per gallon (MPG) to estimate State-level VMT. The growth rates were then calculated using the following formula:

$$GROWTHRATE = \left[\left(\frac{1988\,VMT}{1986\,VMT} \right)^{1/2} - 1 \right] * 100$$

4.1.2. *Offshore Emissions.*

The offshore point source data were processed in three independent groups: Texas, Louisiana and Minerals Management Service. The Texas State offshore data were received from the EPA Region VI office in Dallas, Texas and contained 1985 annual emission estimates of NOx, VOC and CO, location coordinates, stack parameter information, and point source identification codes for 18 sources. We were directed by Region VI to assume operating schedules of 24 hours/day for 365 days/year.

The MMS data were received from Mr. Y.P. Desai at MMS and contained 1985 annual emission estimates of NOx, THC, CO, SOx and TSP, location coordinates, and point source identification codes for 1087 sources. We were directed by Mr. Desai to assume operating schedules of 24 hours/day for 365 days/year.

The Louisiana State offshore point source data were received from the State of Louisiana, Department of Environmental Quality through EPA Region VI and contained 1990 annual emission estimates of NOx, VOC, CO and SOx, location coordinates, stack parameter information and point source identification codes for 3,356 point sources. Unlike the Texas and MMS data, these data contained many of the same sources already included in the 1985 NAPAP point source inventory. Of the 3,356 point sources, 842 sources were removed as NAPAP duplicates. Of the remaining 2,514 sources, 63 were considered major (>100 tons/year NOx, VOC), 1,224 had zero NOx, VOC and CO emissions and 1,227 were considered minor (<=100 tons/year NOx, VOC).

Initially, there was concern that the non-NAPAP minor sources might have been included in the 1985 NAPAP area source inventory. To investigate this issue, the 1,227 minor non-NAPAP point sources were analyzed by source category. The results were discussed with Mr. David Mobley, Chief of the Office of Air Quality Planning and Standards. Emissions Inventory Branch and it was determined that these sources would not have been included in the NAPAP area source inventory. Therefore, the 63 major point sources and the 1,227 minor point sources were processed as offshore sources for the State of Louisiana. It should be noted that the 63 major sources accounted for approximately 50% of the total 1,290 non-NAPAP sources.

All of the anthropogenic emissions data were processed through the Flexible Regional Emissions Data System (FREDS)[10], where they were gridded, temporally allocated and speciated consistently for use as hourly emissions in the ROM grid system of 1/4° longitude by 1/6°

latitude grid cells. The speciation involved distributing the NOx into NO and NO_2 and allocating the THC or VOC emissions into the appropriate Carbon Bond IV classes.

4.1.3. *Biogenic Emissions.*

The biogenic emissions for this study were derived using the Biogenic Emissions Inventory System (BEIS). The resulting gridded, speciated, hourly emission estimates were then merged with the area sources estimates prior to insertion into the ROM.

4.1.4. *Base Case Emissions Summaries.*

Base case emission estimates are summarized in Table 4-1 of the following page.

4.2. *Developing Scenario Emissions.*

The modeling strategies involved the development of model emission inputs for two other scenarios associated with the MMS offshore data. The first strategy involved eliminating the MMS offshore point sources from the current base case emissions and the second involved doubling the existing MMS offshore sources. Since the offshore data were processed independently, this analysis was easily accomplished by omitting the MMS data from the base case data set for one strategy and by applying an across the board factor of 2 to the existing MMS data for the second strategy.

4.3. *Quality Assurance/control.*

Color tile gridded emissions density plots of the total anthropogenic emissions for the modeling domain and offshore point source emissions for the MMS, Texas and Louisiana State data were generated to assist in quality assurance. These plots are in units of tons/day for CO, NOx and VOC and are included as attachments to this report. In addition, the hourly totals output from the FREDS system for input into the ROM were summed to derive daily totals and then multiplied by 365 to get annual estimates and compared with the original annual data. These totals were presented in Table 4-1.

TABLE 4-1

EMISSIONS DATA SUMMARIES FOR THE OFFSHORE POINT SOURCE DATA
(tons/year)

Totals from-FREDS:

	NOx	THC	CO	VOC
LOUISIANA	22,619.00	14,751.17	4,460.00	7,228.22
TEXAS	1,473.10	73.19	253.70	17.06
MMS	115,591.70	43,871.86	15,304.20	10,226.53
TOTAL	139,683.80	58,696.22	20,017.90	17,471.81

Totals RAW Data:

	NOx	THC	CO	VOC
LOUISIANA	22,619.00	14,238.00	4,460.00	---
(- outliers)	22,404.00	14,233.00	4,446.00	---
TEXAS	1,473.10	72.60	253.70	---
MMS	115,591.70	43,516.50	15,304.20	---
TOTAL	139,683.80	57,827.10	20,017.90	---

1) Outliers in Louisiana represent data points that were located in Florida and in Baton Rouge, La. and thus should not have been included in the offshore inventory for Louisiana.

2) THC values differ for FREDS totals and the RAW data totals because of the aldehyde augmentation applied in the HCPREP module of FREDS.

3) The large differences between THC and VOC occur because VOC does not include methane which, for source category 20200202 (which most of the offshore sources are), accounts for 76% of the total hydrocarbon emissions.

5. BASE CASE SIMULATION

5.1. *Base Case Model Performance*

The model was first evaluated for its ability to predict the base case ozone concentrations in the 5 subregions which MMS selected (see Figure 2-1). The EPA Regional Evaluation Support System (RESS) was applied to compare the model predicted ozone concentrations with the observations. The hourly ozone monitoring data of all monitors within the 5 subregions were retrieved from the EPA's Aerometric Information Retrieval System (AIRS). The description of these monitoring data is summarized in Table 5-1. For reasons to be discussed later in this section, only daytime model predictions were used in numerical comparison with monitoring data. Various statistics were calculated based on these comparisons. In paired comparison, monitoring data are compared with a weighted average of model predictions of the nearest four grid cells (see Appendix C). Figures 5-1 to 5-3 are examples of these plots. Despite some geographical differences, the inference drawn from these examples is generally supported by the statistics at other subregions in both episodes. A complete set of graphics of model evaluation statistics is available in Appendix A.

The model evaluation statistics suggest that the model has a tendency to over-predict ozone at low observed concentrations (< about 70 ppb) and under-predict at high concentrations (> about 110 ppb) (e.g., see Figures 5-1 and 5-2). Because of the model's poor resolution in the vertical, it is unable to simulate the scavenging effect within the nocturnal inversion close to the ground after sunset. As a result, the model almost always over-predicted the nighttime ozone concentrations and often delayed the model predicted ozone peak hour by 2-6 hours in comparison with observed peaks (e.g., see Figure 5-3). Fortunately, this weakness has little impact after inversion breakup in the morning. That is why only daytime predictions are entered in the numerical evaluation of the model. These findings are consistent with what have been found in the evaluation of an earlier version of ROM[11].

Based on the two simulated episodes, the model, on the average, under-predicted daily maximum ozone concentrations by 21%. The average normalized gross error for these two episodes is 31%. These statistics are calculated from three non-overlaping subregions, Baton Rouge-New Orleans region, Lake Charles-Beaumont region and Houston-Galveston region. Subregion Corpus Christi is omitted, because it has only two monitors. Numerical measurements of model performance are summarized in Tables 5-2 and 5-3. All numbers, except the mean bias, are dimensionless. The mean bias is measured in parts per billion (ppb). The meaning and manner of calculation are described more fully in Appendix B.

One caution has to be made here for the readers in inferring the model performance. Due to the screening nature of this study and nature of available emissions data, the emission inputs to the model are **not** day-specific, only the meteorology inputs are day-specific. Further, the model predictions in this study assume that the 1988 and 1990 OCS emissions are similar to the 1985 OCS emission inventory. Furthermore, the uncertainty in the emissions inventory could be very large. Given these concerns, the model performance presented here is considered to be adequate.

Table 5-1. Monitor Locations and Number of Observations Used by Subregion (Daylight Hours)

Region	Monitor Id.	City	Lat.	Lon.	# of Observations Eps #1	Eps #2
BR-NO	220330003442011	BATON ROUGE	30.419	91.183	146	70
BR-NO	220330004442012	BATON ROUGE	30.461	91.188	147	--
BR-NO	220330006442011	BATON ROUGE	30.464	91.188	---	70
BR-NO	220331001442012	NOT IN A CITY	30.587	91.207	149	71
BR-NO	220470002442011	NOT IN A CITY	30.200	91.100	150	69
BR-NO	220511001442012	KENNER	30.043	90.275	148	68
BR-NO	220570002442011	THIBODAUX	29.792	90.804	---	71
BR-NO	220710012442012	NEW ORLEANS	29.994	90.103	148	71
BR-NO	220770001442011	NEW ROADS	30.685	91.367	---	70
BR-NO	220870002442011	NOT IN A CITY	29.982	89.999	151	66
BR-NO	220930002442011	NOT IN A CITY	29.994	90.820	---	65
BR-NO	220950002442011	NOT IN A CITY	30.058	90.608	151	68
BR-NO	221010003442011	MORGAN CITY	29.715	91.210	---	48
BR-NO	221210001442011	PORT ALLEN	30.502	91.210	144	72
BR-NO	221210001442012	PORT ALLEN	30.502	91.210	144	--
BR-NO	220512001442011	MARRERO	29.883	90.083	150	--
BR1	220330003442011	BATON ROUGE	30.419	91.183	146	70
BR1	220330004442012	BATON ROUGE	30.461	91.188	147	--
BR1	220330006442011	BATON ROUGE	30.464	91.188	---	70
BR1	220331001442012	NOT IN A CITY	30.587	91.207	149	71
BR1	220470002442011	NOT IN A CITY	30.200	91.100	150	69
BR1	220511001442012	KENNER	30.043	90.275	148	68
BR1	220550003442011	LAFAYETTE	30.233	92.017	136	20
BR1	220570002442011	THIBODAUX	29.792	90.804	---	71
BR1	220710012442012	NEW ORLEANS	29.994	90.103	148	71
BR1	220770001442011	NEW ROADS	30.685	91.367	---	70
BR1	220930002442011	NOT IN A CITY	29.994	90.820	---	65
BR1	220950002442011	NOT IN A CITY	30.058	90.608	151	68
BR1	221010003442011	MORGAN CITY	29.715	91.210	---	48
BR1	221210001442011	PORT ALLEN	30.502	91.210	144	72
BR1	221210001442012	PORT ALLEN	30.502	91.210	144	--
BR1	220512001442011	MARRERO	29.883	90.083	150	--
LC-B	220110002442011	NOT IN A CITY	30.492	93.144	---	69
LC-B	220190002442011	NOT IN A CITY	30.143	93.372	149	70
LC-B	220191003442011	WESTLAKE	30.326	93.323	148	69
LC-B	481990002442011	KOUNTZE	30.381	94.316	---	64
LC-B	482450009442012	BEAUMONT	30.039	94.075	146	63
LC-B	482450011442011	PORT ARTHUR	29.894	93.988	151	29
LC-B	483611001442012	WEST ORANGE	30.058	93.764	---	69
LC-B	484570101442011	NOT IN A CITY	30.544	94.346	---	24
H-G	480391003442012	CLUTE	29.008	95.392	156	69
H-G	481570004442011	ROSENBERG	29.565	95.799	---	72
H-G	482010024442012	NOT IN A CITY	29.875	95.326	156	12
H-G	482010026442012	NOT IN A CITY	29.802	95.125	42	12
H-G	482010046442011	HOUSTON	29.827	95.284	139	13
H-G	482010047442012	HOUSTON	29.835	95.496	147	62
H-G	482010051442012	HOUSTON	29.624	95.474	145	71
H-G	482010059442011	HOUSTON	29.706	95.281	149	72
H-G	482010062442011	HOUSTON	29.631	95.267	151	67
H-G	482011003442012	DEER PARK	29.679	95.131	154	72
H-G	482011034442012	HOUSTON	29.771	95.222	147	72
H-G	482011035442013	HOUSTON	29.733	95.257	136	69
H-G	482011037442012	HOUSTON	29.752	95.361	140	71
CC	483550025442012	CORPUS CHRISTI	27.764	97.433	155	72
CC	483550026442011	CORPUS CHRISTI	27.835	97.557	152	70

Figure 5-1. SCATTER PLOT OF HOURLY O3 (PAIRED IN SPACE & TIME)
FOR MMS BATON ROUGE–NEW ORLEANS, EPISODE #1
JULY 25 – AUGUST 6, 1988 (8 a.m. – 7 p.m.)

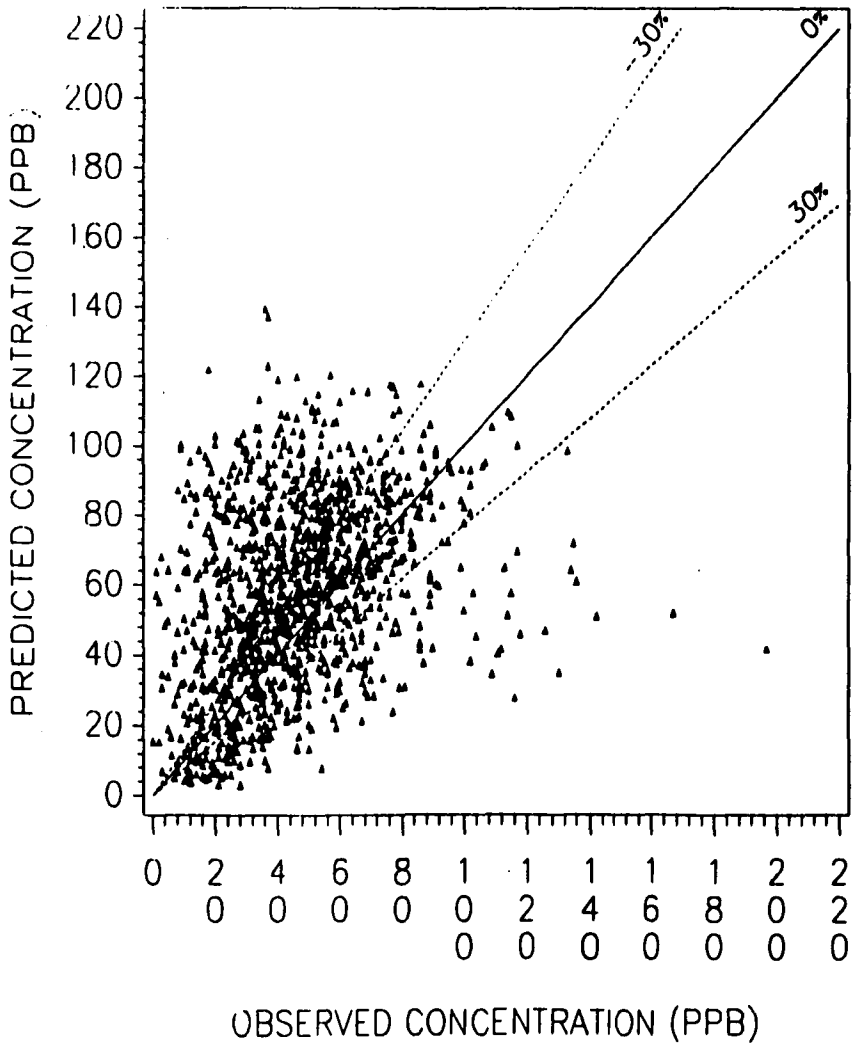

McIDAS
WT4CELL

Figure 5-2. QUANTILE – QUANTILE PLOT OF OZONE CONCENTRATIONS
FOR MMS BATON ROUGE–NEW ORLEANS
JULY 25 – AUGUST 6, 1988 (8 a.m. – 7 p.m.)

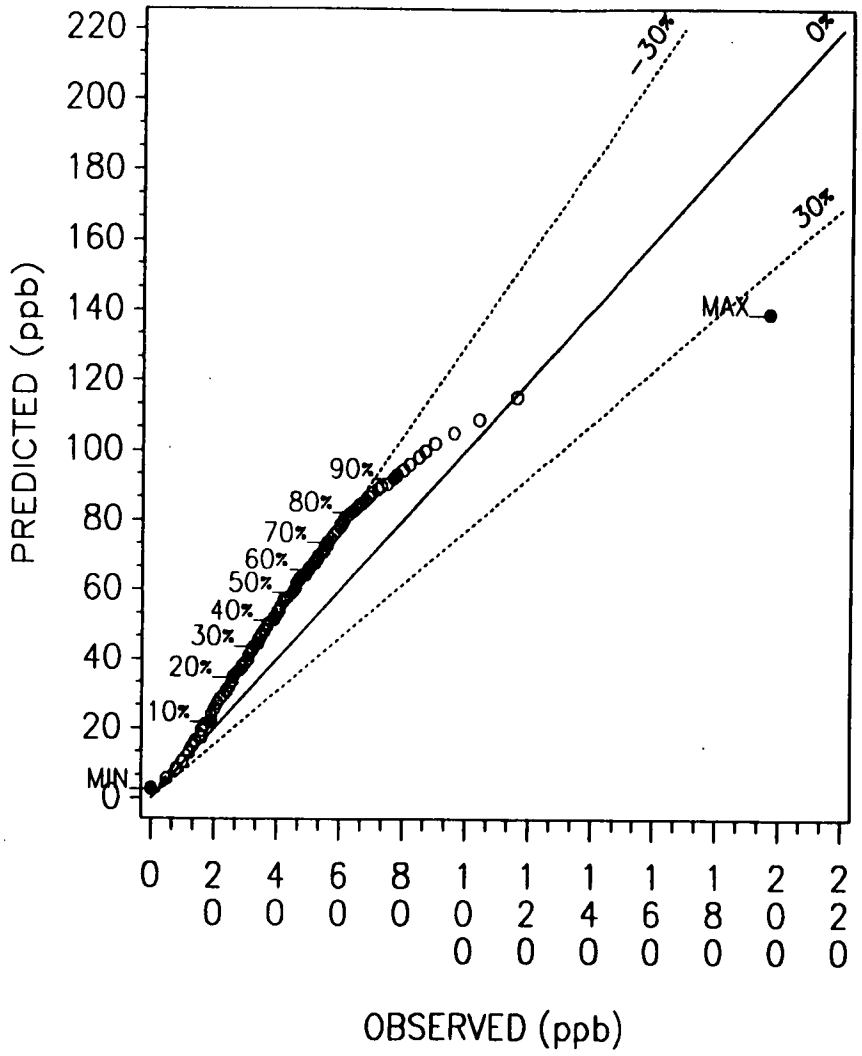

McIDAS
WT4CELL

Figure 5-3. MAXIMUM HOURLY O3 CONCENTRATIONS
FOR MMS BATON ROUGE–NEW ORLEANS, EPISODE #1
JULY 25 – AUGUST 6, 1988

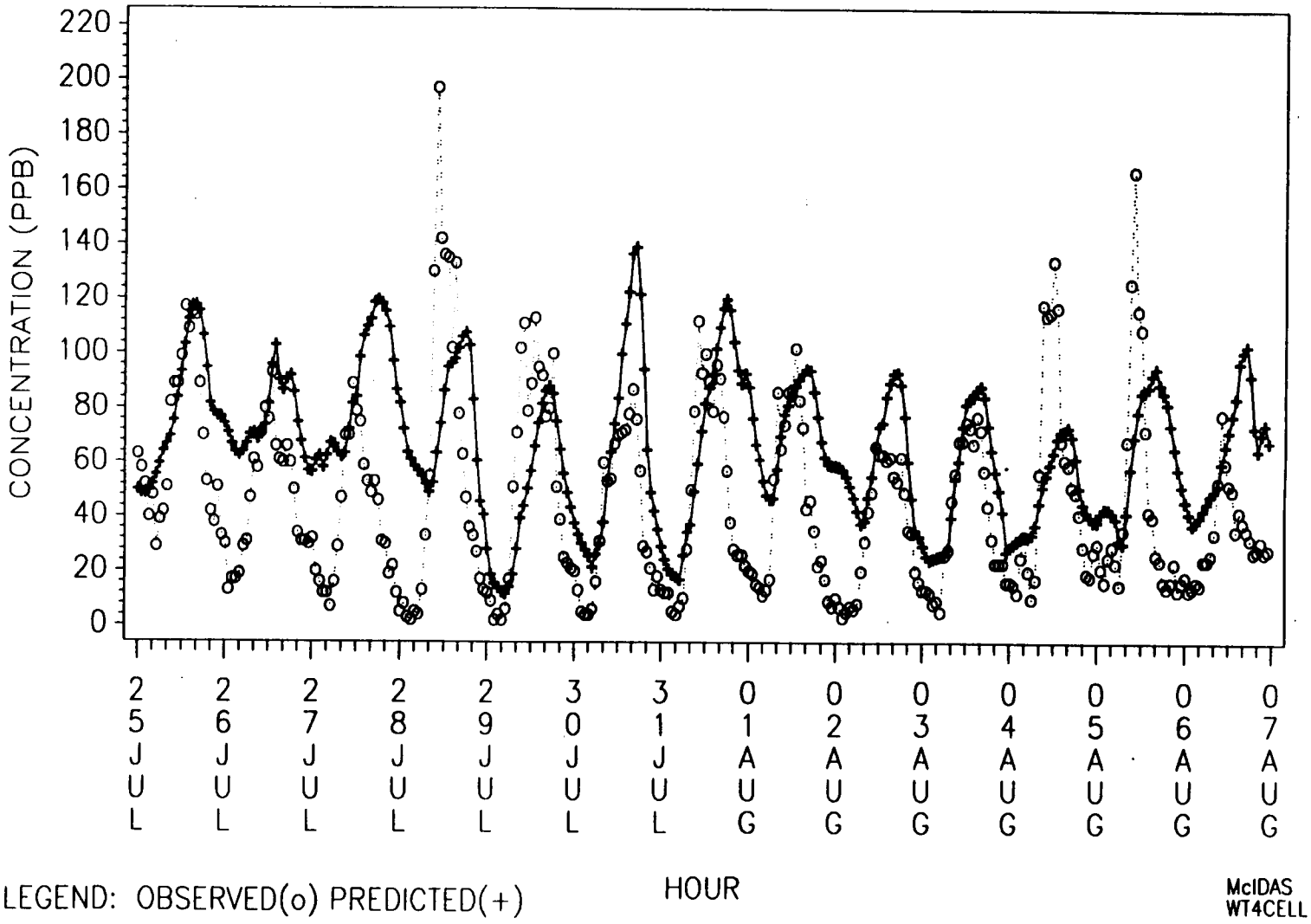

Table 5-2

Numerical Measurements of Model Performance#
Based on MMS Episode #1
July 25 - August 6, 1990

Subregion	Paired Accuracy of Peaks@ (%)	Unpaired Accuracy of Peaks@ (%)	Mean Bias@ (ppb)	Mean Normalized Bias@ (fraction)	Normalized Gross Error@ (fraction)	Fractional Bias@ (fraction)
Baton Rouge-New Orleans	17.80	5.01	-6.41*	-0.19*	0.34	0.04
Baton Rouge I	17.80	4.08	-7.11*	-0.20*	0.34	0.02
Lake Charles-Beaumont	9.60	-15.81*	-1.00*	-0.09*	0.28	0.16
Houston-Galveston	32.60	28.70	6.40	-0.22*	0.53	0.15
Corpus Christi	-100.38*	-100.71*	-25.32*	-1.69*	1.69	-0.58

The total number of observations (monitoring data) used in calculating these statistics are listed in Table 5-1.

@ The formulae are explained in Appendix B.

* Negative value means overprediction.

Table 5-3

Numerical Measurements of Model Performance#
Based on MMS Episode #2
July 26 - July 31, 1990

Subregion	Paired Accuracy of peaks@ (%)	Unpaired Accuracy of peaks@ (%)	Mean Bias@ (ppb)	Mean Normalized Bias@ (fraction)	Normalized Gross Error@ (fraction)	Fractional Bias@ (fraction)
Baton Rouge-New Orleans	37.18	13.40	5.28	0.00	0.23	-0.02*
Baton Rouge I	37.18	13.14	4.65	0.00	0.23	-0.02*
Lake Charles-Beaumont	17.54	-0.52*	8.08	0.07	0.27	0.03
Houston-Galveston	11.75	7.93	2.92	-0.01*	0.21	0.02
Corpus Christi	-1.05*	-1.05*	2.11	-0.03*	0.19	0.08

The total number of observations (monitoring data) used in calculating these statistics are listed in Table 5-1.

@ The formulae are explained in Appendix B.

* Negative value means overprediction.

6. AMBIENT OZONE IMPACT ANALYSIS

Ambient ozone impact is evaluated according to the difference of model-predicted maximum (episodic) ozone concentrations between the emission-varying scenarios and base case for each grid cell during each episode. Because the two ozone episodes reflect different meteorological conditions, the impacts are evaluated independently. Also, due to the purpose of the study, the impacts over land and over water are also discussed separately for the current OCS emissions and for the case when current OCS emissions are doubled.

6.1. *Episode # 1 - Episodic Ozone Differences*

Episode #1 (July 25 - August 6, 1988) has two distinct periods of onshore winds. From July 25 to July 31, the prevalent wind direction is from the southwest while from August 1 to August 6, the winds were generally from the southeast. Because of the difference in onshore winds, the impact areas over land could be different. Thus, separate figures are prepared for the following discussion.

6.1.1. *Without OCS Emissions*

Figures 6-1 and 6-2 are difference maps of episodic ozone concentrations between the base case and the scenario when all the OCS emissions are eliminated. Figure 6-1 shows the impact areas during the first period of the episode when the onshore winds are from the southwest. Figure 6-2 shows the impact areas during the second period of the episode when the onshore winds are from the southeast. The color code is shown on the bottom of the plot. It is obvious that the major impact of OCS emissions is over the water. The maximum episodic ozone concentrations could decrease by 25 ppb over water and 8 ppb over land if the currently estimated OCS emissions were eliminated. Although the impact is perceptible further inland, the major impact over land areas is along a very narrow strip of the Gulf Coast. There were also a few grid squares over New Orleans and Houston where ROM predicted an increase of ozone by a couple of ppb.

6.1.2. *Double OCS Emissions*

Figures 6-3 and 6-4 are similar to Figures 6-1 and 6-2, but they are the model predicted difference in ambient ozone concentrations if the currently estimated OCS emissions were doubled. The predicted increases in ambient episodic maximum ozone concentrations due to doubling the OCS emissions is 11 ppb over water and 6 ppb over land. The nonlinear response between without and double OCS emissions could be due to the fact that most of the OCS emissions are NO_x sources and the amount of available VOC over water is limited. When only NO_x emissions are doubled in an environment of limited VOC, some of the NO_x will not be able to be oxidized by organic radicals to create more ozone. Instead, they will be oxidized by available ozone and result in a titration effect on ambient ozone. The titration on episodic maximum ozone as much as 11-13 ppb was actually predicted at a few grid squares over Gulf waters just south of New Orleans for this episode. Thus, doubling NO_x emissions in an environment of limited VOC generally does not proportionally create more ozone.

Figure 6-1. Difference: Base without OCS – Base
Maximum Ozone, Layer 1 – – July 25–31, 1988

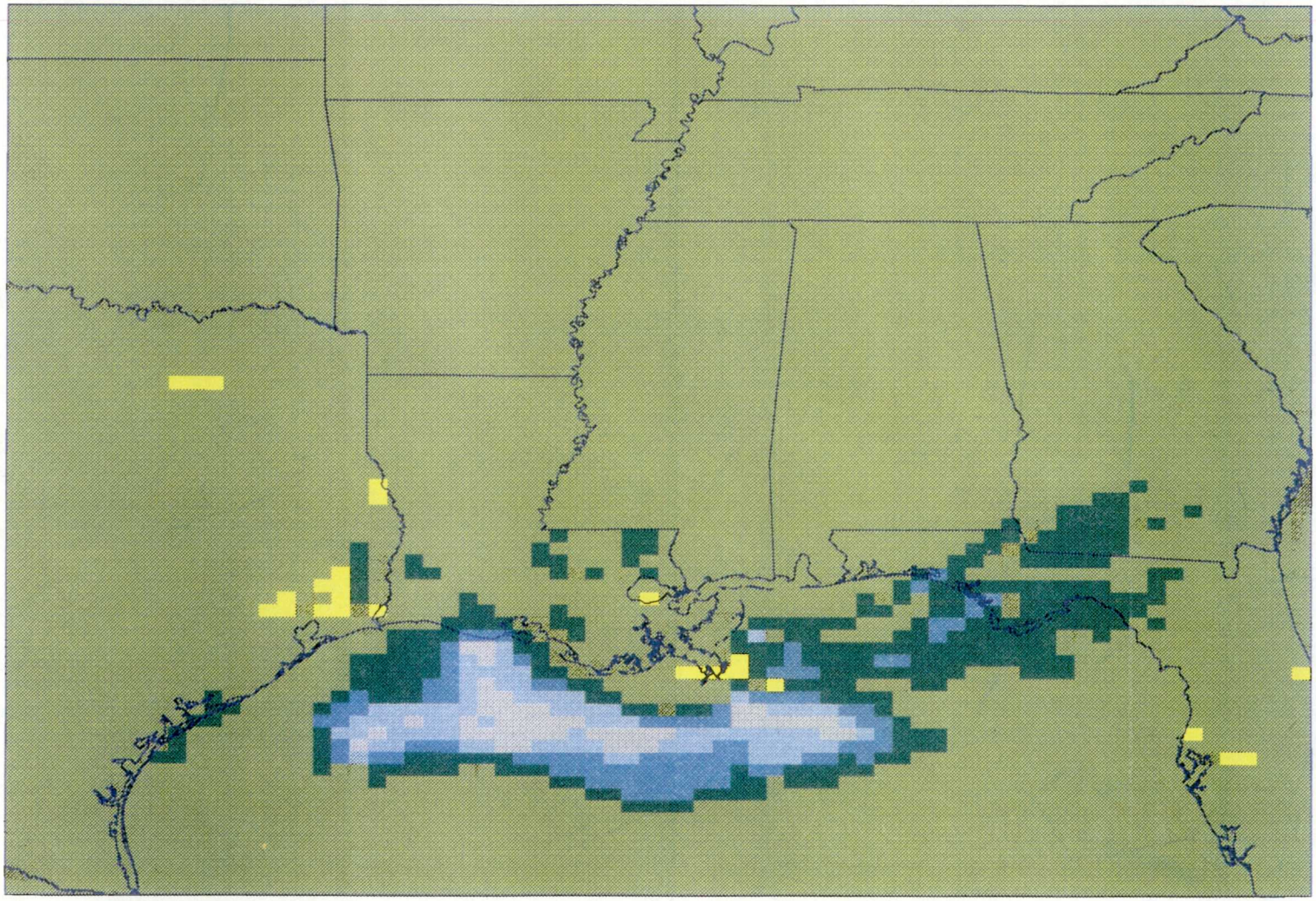

Figure 6-2. Difference: Base without OCS – Base
Maximum Ozone, Layer 1 – – August 1–6, 1988

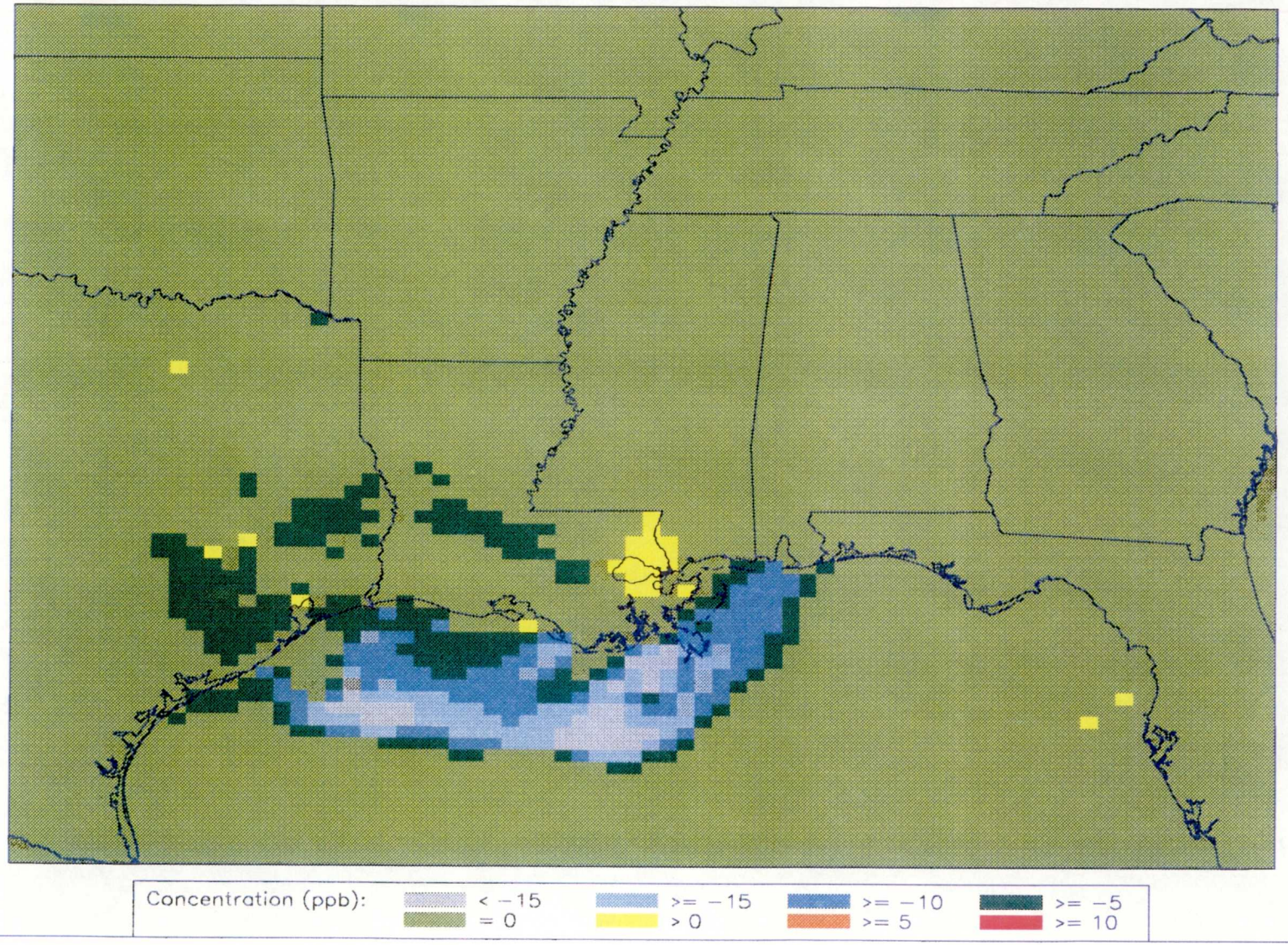

Figure 6-3. Difference: Base with Double OCS – Base
Maximum Ozone, Layer 1 – – July 25–31, 1988

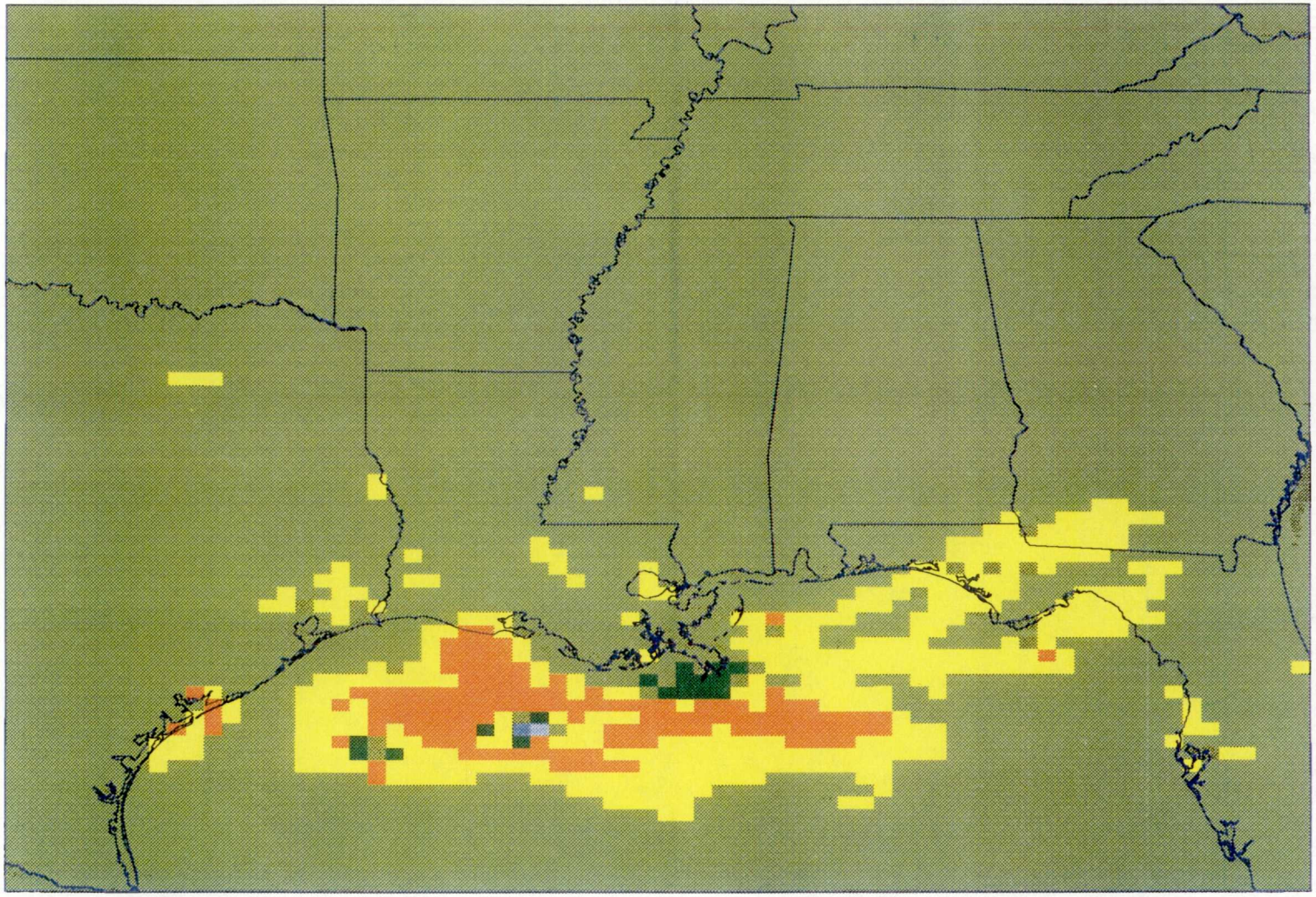

Figure 6-4. Difference: Base with Double OCS – Base
Maximum Ozone, Layer 1 – – August 1–6, 1988

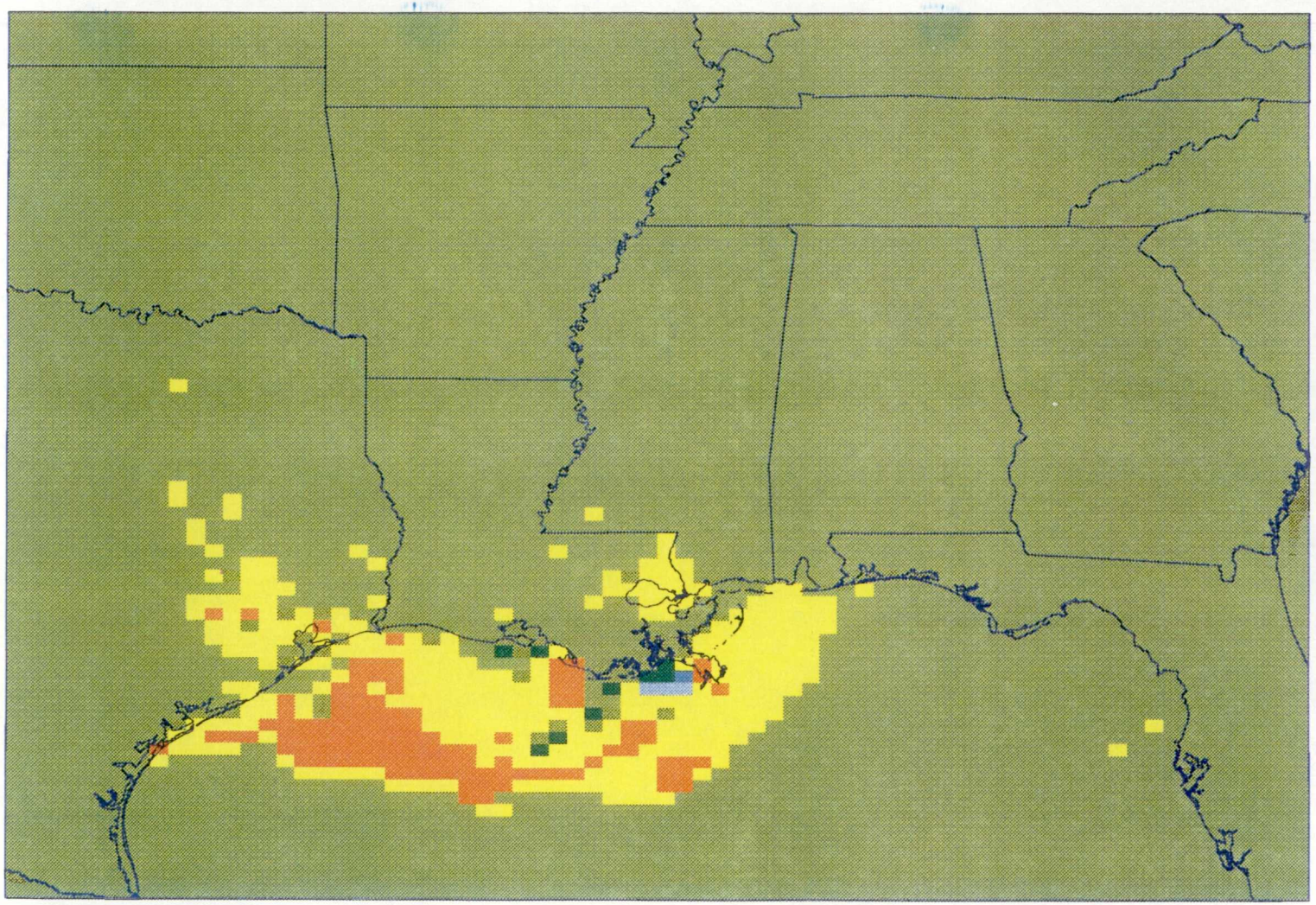

6.2. *Episode # 2 - Episodic Ozone Differences*

Different from episode #1, this episode (July 26-31, 1990) has only one prevalent onshore flow. The general wind direction was from east to southeast.

6.2.1. *Without OCS Emissions*

Figure 6-5, like Figures 6-1 and 6-2, is a difference map of episodic ozone concentrations between the base case and the scenario when all the OCS emissions were eliminated. The maximum impact is still over the water. The episodic ambient ozone concentrations could be reduced by as much as 29 ppb over water and 5 ppb over land if all the OCS emissions could be eliminated. Some titration effect of current OCS emissions on ozone by as much as 11 ppb were also predicted in a few grid squares over Gulf waters south of New Orleans. Despite the fact that episode #2 observed much higher ozone over land than was true for episode #1, the impact of OCS emissions over land was still small. The reason for such a small impact can be attributed to the more stagnant meteorological conditions of this episode. Under fairly stagnant conditions, most of the high ozone concentrations observed over land are likely due to local sources. In this episode, the weak transport of pollutants by the onshore winds resulted in the OCS emissions playing a relatively minor role in contributing to predicted episode maximum concentrations in grid squares over land.

6.2.2. *Double OCS Emissions*

Figure 6-6, like Figures 6-3 and 6-4, depicts the difference of episodic ozone concentrations between the base case and the scenario when OCS emissions are doubled. Over land, a response similar to the one shown for the 1st episode was predicted. ROM predicted an episodic maximum ozone increase by as much as 6 ppb over land, but only 16 ppb over water, in contrast to the 29 ppb difference over water between the base case and scenario without OCS emissions. As expected, some titration of ozone by doubling OCS emissions were predicted but only at a few grids over the Gulf waters.

6.3. *Daily vs Episodic*

Comparison of episodic ozone maxima among scenarios allow the reader to see the differences among episodic ozone peaks at each grid. However, the day-to-day impact is also important because the increase of ozone due to existing or doubling OCS emissions on a relatively high ozone day could be the difference of exceeding or not exceeding the NAAQS for ozone at some grids. Thus, it is of interest to investigate the difference of daily maximum ozone concentrations between the base case and emission-varying scenarios. It is found that on some days, the ozone differences at certain grids were much larger than the difference of episodic maxima even though the average impact remains the same. This is because the episodic maximua for different scenarios at a given grid could be on different days. Figure 6-7 is an example for July 29, 1988. On this day, the predicted difference in daily maximum ozone at Pecan Island, LA, between the base case and the scenario without OCS emissions was 16 ppb comparing to a difference in episodic maxima of 8 ppb at this location. New Orleans also had a predicted 12 ppb difference in daily maximum ozone

Figure 6-5. Difference: MMS Base Without OCS – MMS Base
Maximum Ozone, Layer 1 – – July 26 – July 31, 1990

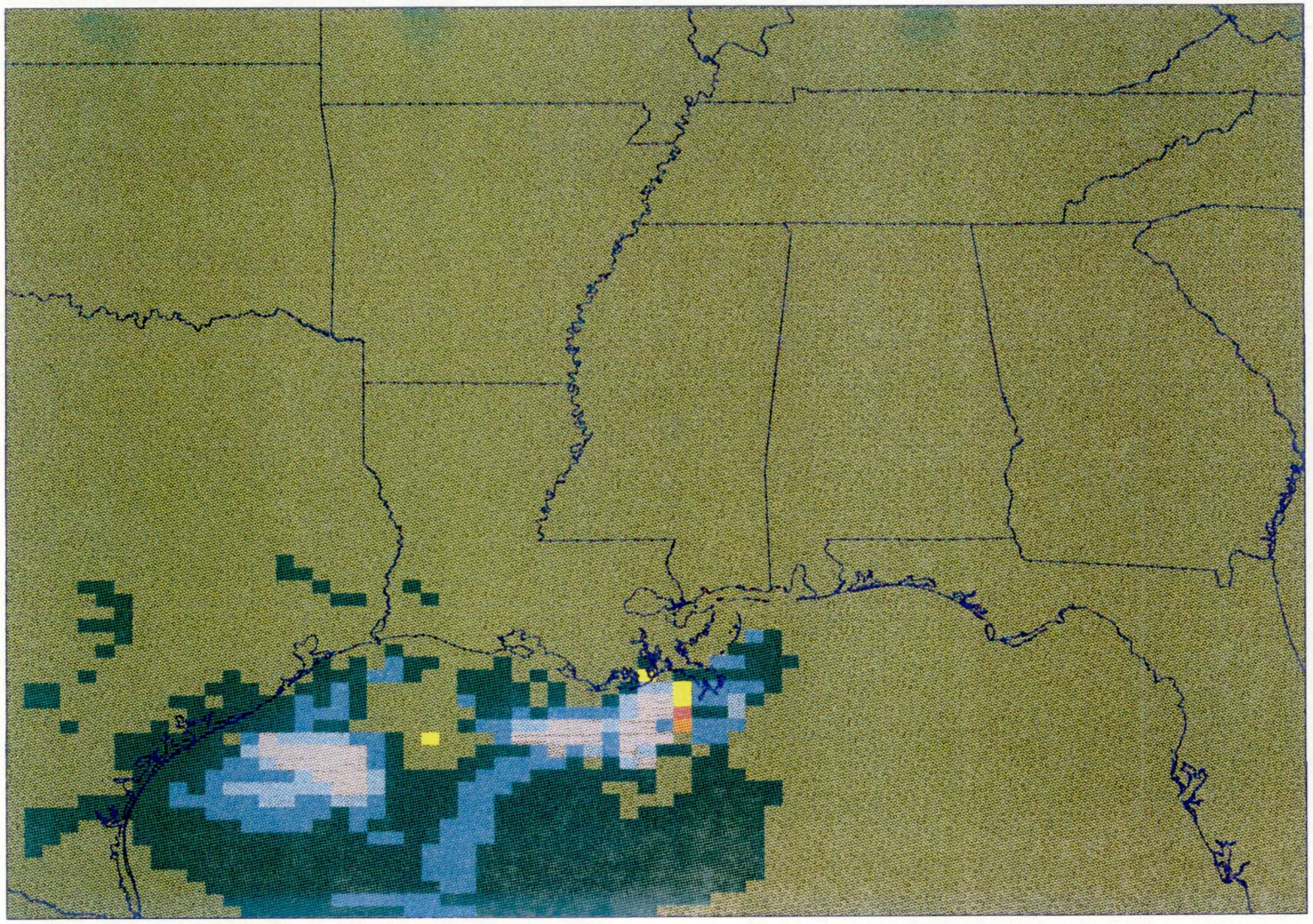

Figure 6-6. Difference: MMS Base With Double OCS – MMS Base
Maximum Ozone, Layer 1 – – July 26 – July 31, 1990

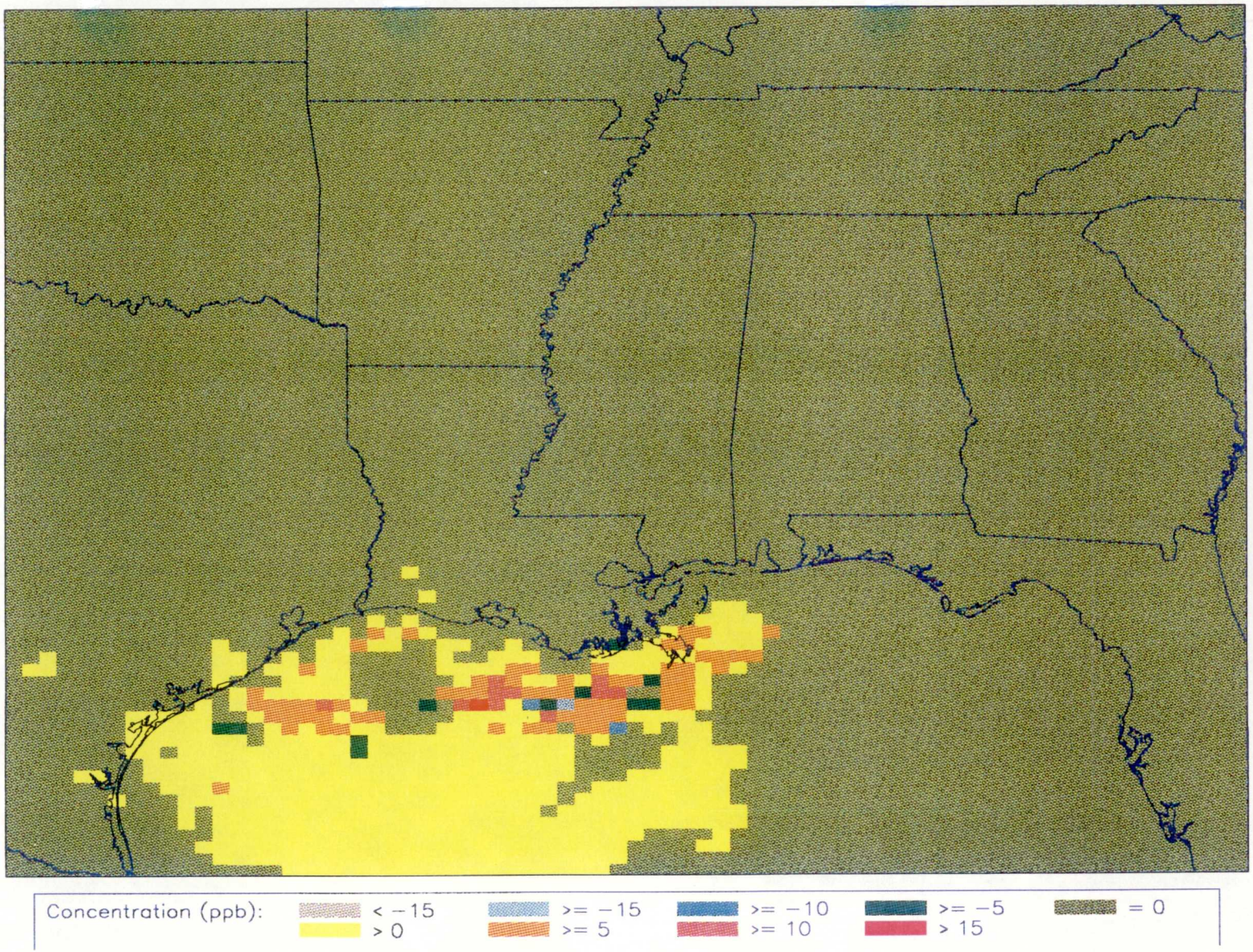

Figure 6-7. Difference: MMS Base Without OCS - MMS Base
Daily Maximum Ozone, Layer 1 – JULY 29, 1988

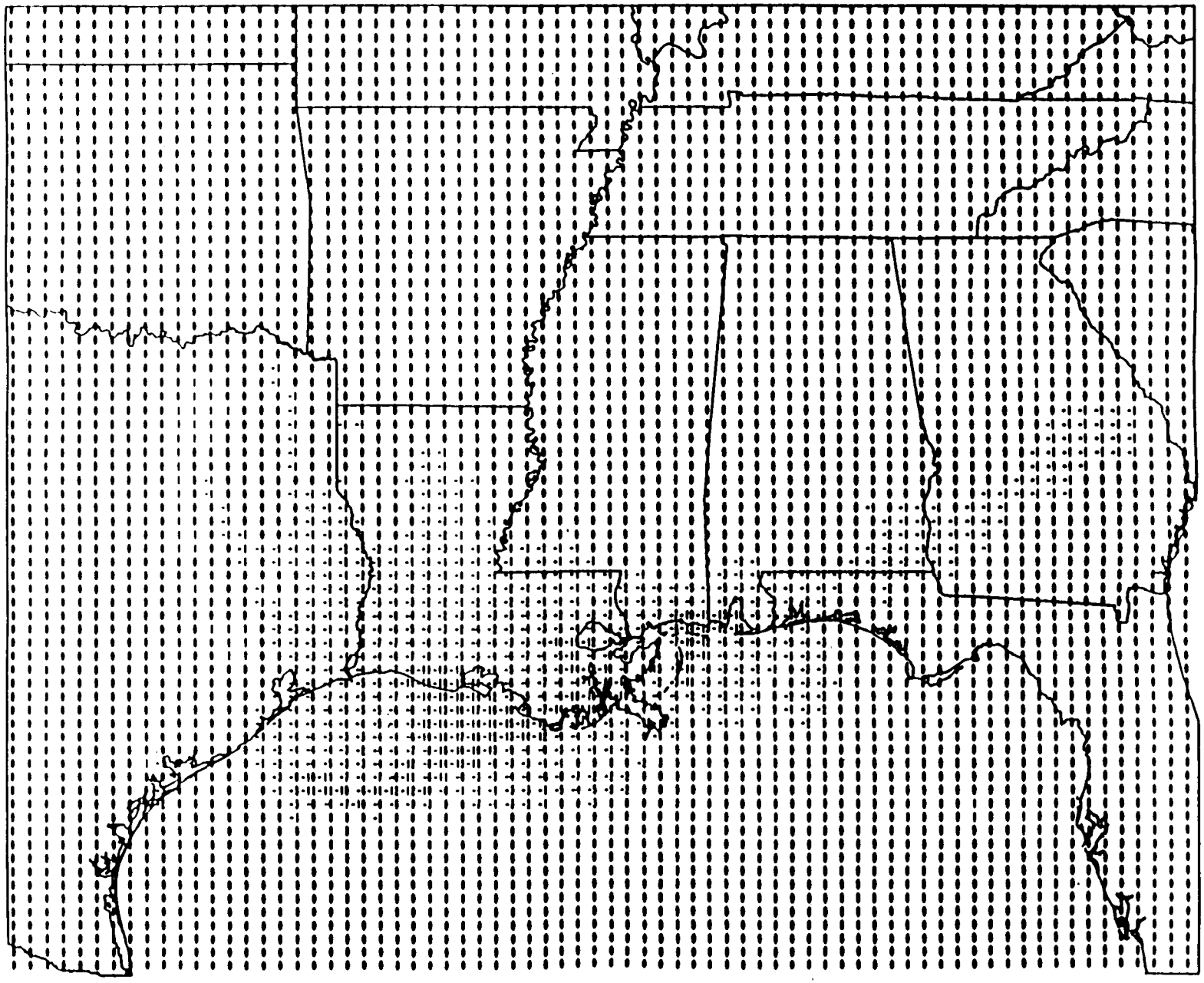

concentration on the same day. The findings suggest that for any given day of an ozone episode when the meteorological conditions are most favorable, the impact of OCS emissions on coastal ambient ozone concentrations could be about 10 to 20 ppb. This could raise ambient ozone at some coastal grids above the ozone NAAQS if their local prduction of ozone is already close to the NAAQS. A complete set of ROM predicted episodic and daily maximum ozone differences between base case and the two emission scenarios is plotted as value plots and is available in Appendix D.

Thus, it is important to acknowledge that even though the difference in episodic maxima over land between the base case and the test scenarios are generally less than 10 ppb, on some specific days, when meteorological conditions are most favorable, the difference could be much larger at some locations along the Gulf coast. Though the study considered only the very extreme scenarios (i.e., eliminate all OCS emissions and double the current OCS emissions), the ROM results suggest that the magnitude of total impact of OCS emissions on ambient ozone at some locations along the coast on some episodic days may not be trivial.

6.4. *Summary Statistics and Cautions on Interpretation the Results*

Figures 6-8 and 6-9 are box plots showing the distribution of difference in episodic maxima between scenarios and base case in each of the 5 subregions for episodes 1 and 2 respectively. The whiskers represent the 10th and the 90th percentile of the ozone concentration differences. The top and bottom of the boxes represent the 75th and 25th percentile and the horizontal line in the box represents the 50th percentile. The maximum, minimum and mean are drawn by symbols, * or .. From these two figures, it is obvious that in over 90% of the grid squares in the 5 subregions the impact is less than 10 ppb. The largest differences shown here are actually predicted over Gulf waters.

Caution is necessary in interpreting these results. Like all numerical modeling studies the accuracy of the modeling results is subject to the accuracy of the model, the input and the representativeness of the episodes. The largest uncertainty in this study lies in the emissions inventory. The model itself is known to have a tendency to under-estimate high ozone concentrations and over-estimate low ozone concentrations. This could result in under-estimation of the ozone difference between the base and emission-varying scenarios. Another built-in drawback of the model is its coarse spatial resolution, 18.5 km x 18.5 km x 3 vertical layers. This coarse resolution cannot adequately resolve the subgrid scale phenomena such as seabreeze convergence zone near coastlines, where highest ozone concentrations are often monitored. Further, only two episodes have been simulated. Results may vary under other meteorological conditions.

7. CONCLUSIONS

Based on the current 1985 MMS emissions inventory, the ROM results suggest that the major impact of OCS emissions on ambient ozone concentrations are over the Gulf waters. The impact of current OCS emissions on predicted episodic maximum ozone

Figure 6-8. BOX PLOT OF OCS IMPACT ON MMS SUBREGIONS
EPISODE #1: JULY 25 – AUGUST 6, 1988 (8 a.m. – 7 p.m.)

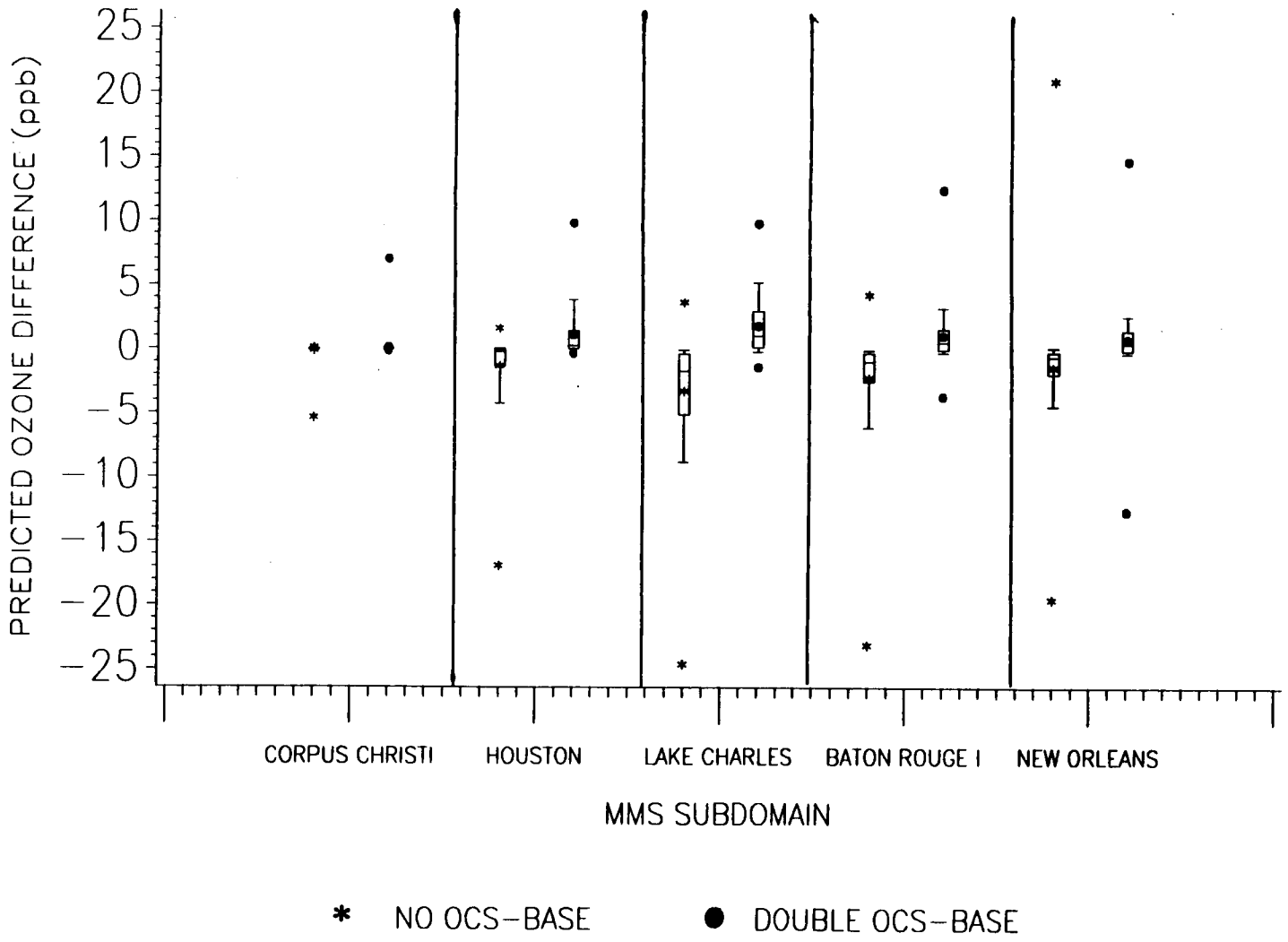

Figure 6-9. BOX PLOT OF OCS IMPACT ON MMS SUBREGIONS
EPISODE #2: JULY 26 – JULY 31, 1990 (8 a.m. – 7 p.m.)

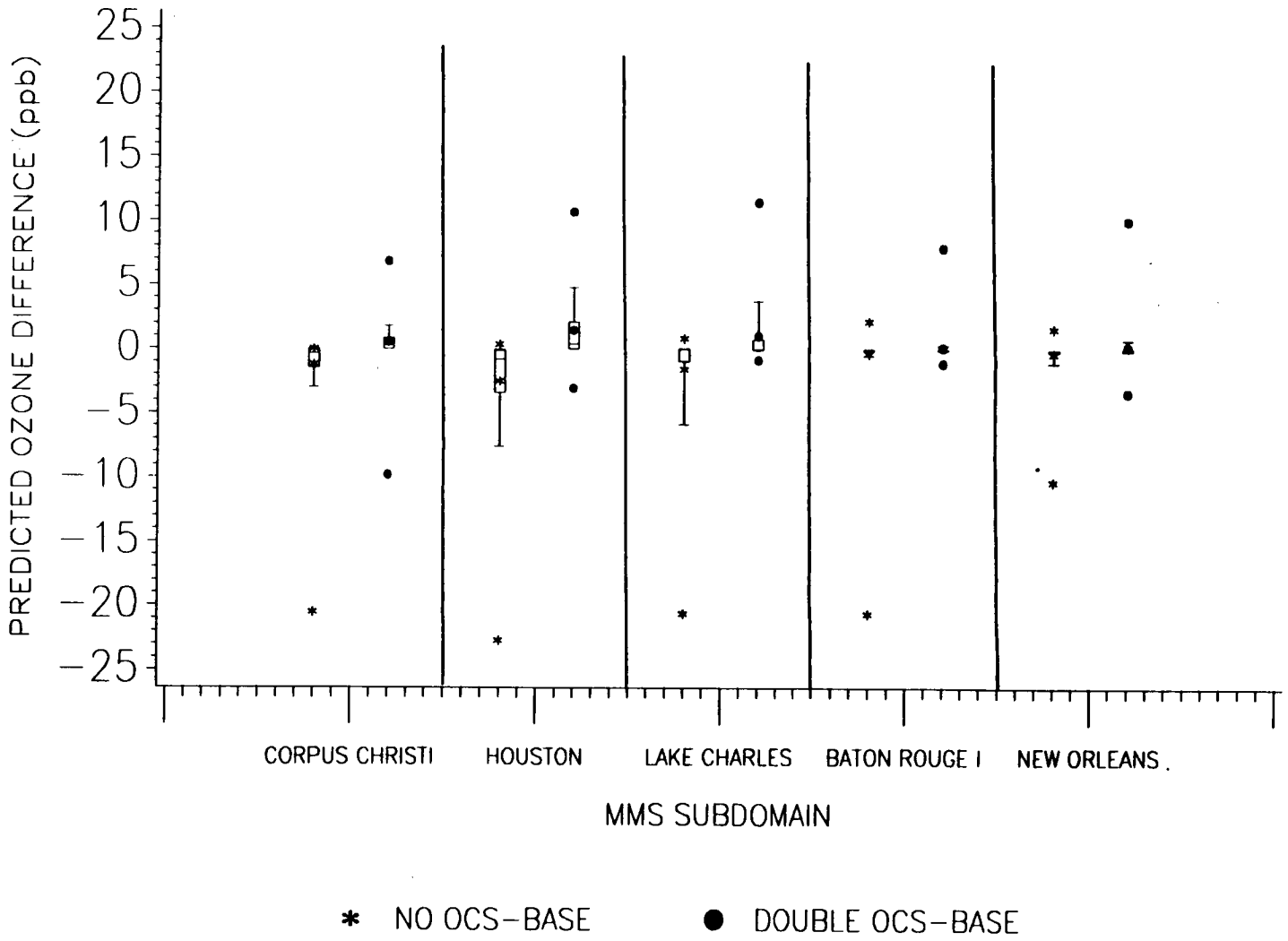

concentrations over land ranges from 5-8 ppb while the impact over the water ranges from 25 to 29 ppb. However, if the current OCS emissions were doubled, the predicted episodic maximum ozone concentration could increase by as much as 6 ppb over land and about 11 to 16 ppb over water. The summary statistics indicate that in over 90% of the grid squares in the 5 subregions the impact is less than 10 ppb. However, on some specific day(s) when the meteorological conditions are most favorable, the impact over land could be larger. Daily maximum ozone differences as large as 10-20 ppb were predicted between the base case and the two emission scenarios.

Although the impact on maximum episodic ozone concentrations predicted over land due to OCS emissions is small (5-10 ppb) in this screening analysis, the impact on some specific day(s) is considerably larger (10-20 ppb). This could result in ambient ozone concentrations at some coastal grid(s) exceeding the NAAQS for ozone if the local production of ozone is already close to the ozone standard. For a more detailed understanding of the magnitude of OCS emissions impact on coastal ambient ozone, it is suggested that an improved emissions data base be used in concert with a finer resolution photochemical model.

8. REFERENCES

1. Lamb, R.G., A Regional Scale (1000 km) Model of Photochemical Air Pollution: Part 1. Theoretical Formulation, EPA-600/3-83-035, 227 pp., U.S. Environmental Protection Agency, Research Triangle Park, NC, 1983.

2. Young, J., M. Aissa, T. Boehm, C. Coats, J. Eichinger, D. Grimes, S. Hallyburton, D. Olerud, S. Roselle, A. Van Meter, R. Wayland, and T. Pierce, Development of the Regional Oxidant Model Version 2.1, EPA-600/3-89-044, 55 pp., U.S. Environmental Protection Agency, Research Triangle Park, NC, 1989.

3. Vukovich, F.M. and J.K.S. Ching, "A Semi-Empirical Approach to Estimate Vertical Transport by Nonpreciputating Convective Clouds on a Regional Scale," Atmos. Environ., Part A, 24, pp 2153-2168, 1990.

4. Gery,, M., G. Whitten, J. Killus, and M. Dodge, "A Photochemical Kinetics Mechanism for Urban and Regional Scale Computer Modeling," J. Geophys. Res., 94, pp 12,925-12,956, 1989.

5. Demerjian, K.L., K.L. Schere and J.T. Peterson, "Theoretical Estimates of Actinic (Spherically Integrated) Flux and Photolytic Rate Constants of Atmospheric Species in the Lower Troposphere," Adv. Environ. Sci. and Technol., 10, pp 369-459, 1980.

6. Jones, F.L., R.W. Miksad and A.R. Laird, "A Simple Method for Estimating the Influence of Cloud Cover on the NO_2 Photolysis Rate Constant," JAPCA, 31, pp 42-45, 1981.

7. Killus, J.P. and G.Z. Whitten, Technical Discussion Relating to the Use of Carbon Bond Mechanism in OZIP/EKMA, EPA-450/4-84-009, 92 pp., U.S. Environmental Protection Agency, Research Triangle Park, NC, 1984.

8. Saeger, M., J. Langstaff, R. Walters, L. Modica, D. Zimmerman, D. Fratt, D. Bulleba, R. Ryan, J. Demmy, W. Tax, D. Sprague, D. Mudgett and A. Werner, The NAPAP Emissions Inventory (Version 2): Development of the Annual Data and Modeler's Tapes, EPA-600/7-89-012a, U.S. Environmental Protection Agency, Research Triangle Park, NC, 692 pp., 1989.

9. Pierce, T.E., B.K. Lamb, and A.R. van Meter, "Development of a Biogenic Emissions Inventory System for Regional Scale Air Pollution Models," in Proceedings of the 83rd Air and Waste Management Association Annual Meeting, Pittsburgh, PA, 16 pp., 1990a.

10. Modica, L.G., D.R. Dulleba, R.A. Walters, and J.E. Langstaff, Flexible Regional Emissions Data System (FREDS) Documentation for the 1985 NAPAP Emission Inventory, EPA-600/9-89-047, 411 pp., U.S. Environmental Protection Agency, Research Triangle Park, NC, 1989.

11. Pierce, T.E., K.L. Schere, D.C. Doll, and W.E. Heilman, Evaluation of the Regional Oxidant Model (Version 2.1) Using Ambient and Diagnostic Simulations, EPA/600/3-90-046, U.S. Environmental Protection Agency, Research Triangle Park, NC, 105 pp., 1990b.

9. APPENDICES

APPENDIX A

GRAPHICS DEPICTING MODEL PERFORMANCE

APPENDIX A

GRAPHICS DEPICTING MODEL PERFORMANCE

Graphical means of displaying model performance are shown in this appendix. Nine types of plots are used. They are:

1. Scatter Plots of Hourly Ozone (Paired in Space & Time),
2. Quantile-Quantile Plots of Ozone Concentrations,
3. Time Series Plots of Maximum Hourly Ozone Concentrations,
4. Daily Box-Plots of Observed and Predicted Hourly Ozone,
5. Box-Plots of Bias (Obs.-Pred.),
6. Box-Plots of Normalized Bias,
7. Box-Plots of Normalized Gross Error,
8. Plots of Daily Paired Accuracy by Subregion,
9. Plots of Daily Unpaired Accuracy by Subregion.

A brief description of the 9 types of plots is given in the following Sections. All except the time series plots are for daytime (8 a.m. - 7 p.m.) only. Time series are plotted 24 hours a day. For types 1, 5, 6 and 7, the prediction and the observation are paired both in time and space. For type 3, the data is paired only in time, while for type 8, the data is paired only in space. For temporal pairing, the predicted and the observed ozone concentrations are paired hour by hour. The methodology for selecting appropriate predictions to spatially pair with a monitored observation is described in Appendix C.

1. Scatter Plots of Hourly Ozone (Paired in Spaced & Time)

These are scatter plots of predicted vs. observed hourly ozone concentrations. The predicted and observed values are paired in space and time. The temporal pairing is paired hour by hour. The diagonal (0%) line indicates perfect match between prediction and observation; above this line (negative) means overprediction; below this line (positive) means underprediction.

2. Quantile-Quantile Plots of Ozone Concentrations

These are plots of the distribution of predicted vs. observed ozone concentrations

expressed in percentiles of the distribution. They are not paired in space nor in time. The diagonal (0%) line indicates perfect match between prediction and observation; above this line (negative) means overprediction; below this line (positive) means underprediction.

3. Time Series Plots of Maximum Hourly Ozone Concentrations

These are time series plots of temporally paired hourly maximum ozone concentrations, predicted vs observed in the subregion.

4. Daily Box-Plots of Observed and Predicted Hourly Ozone

These graphs plot, side by side, the daily distribution of predicted and observed hourly ozone concentrations in the subregion. The whiskers represent the 10th and the 90th percentile of the ozone concentration differences. The top and bottom of the boxes represent the 75th and 25th percentile and the horizontal line in the box represents the 50th percentile. The maximum, minimum and mean are drawn by symbols, ° or *.

5. Box-Plots of Bias (Obs.-Pred.)

These are plots of the distribution of ozone concentration differences of the observed minus the predicted. The predicted and the observed are paired both temporally and spatially. The symbols are defined the same way as those explained in Section 4 of Appendix A. The mean bias in each subregion is given in Table 5-2 and 5-3 in the text; and the numerical formula is described in Appendix B. For each subregion, two plots are generated: 1) Bias is plotted against day. 2) Bias is plotted against observed ozone concentrations.

6. Box-Plots of Normalized Bias

The normalized bias is a non-dimensional quantity which measures the extent of model prediction bias relative to the observed ozone concentration. The predicted and observed ozone concentrations are paired in time and space. The mean normalized bias for each subregion is given in Table 5-2 and 5-3 in the text; and the numerical formula is described in Appendix B. The distribution of the normalized bias for each subregion is plotted in two ways: 1) Normalized bias is plotted against day. 2) Normalized bias is plotted against observed ozone concentrations. The symbols are defined the same way as those explained in Section 4 of Appendix A.

7. Box-Plots of Normalized Gross Error

The gross error is the absolute value of the difference between the spatially paired observed and predicted ozone concentrations. When the gross error is normalized by the observed ozone concentration, it is called the normalized gross error. It is a non-dimensional quantity. The averaged normalized gross error for each subregion is given in Table 5-2 and 5-3 in the text; and the numerical formula is described in Appendix B. The distribution of the

normalized gross error for each subregion is plotted in two ways: 1) Normalized gross error is plotted against day. 2) Normalized gross error is plotted against observed ozone concentrations. The symbols are defined the same way as those explained in Section 4 of Appendix A.

8. Plots of Daily Paired Accuracy by Subregion

The daily paired accuracy is calculated as a percentage of the difference (the observed minus the predicted daily maximum ozone concentrations) divided by observed daily maximum ozone concentration. The prediction and the observation are spatially paired but temporally windowed (+/- 3 hours of the observed daily maximum). The line plots reflect the ability of the model to predict daily maximum ozone concentrations. The averaged daily paired accuracy for each subregion is given in Table 5-2 and 5-3 in the text; and the numerical formula is described in Appendix B.

9. Plots of Daily Unpaired Accuracy by Subregion

The calculation is the same as daily paired accuracy except that the prediction and observation are not necessarily paired. It is also a percentage quantity. The line plots reflect the ability of the model to predict daily maximum ozone concentrations. The averaged daily paired accuracy for each subregion is given in Table 5-2 and 5-3 in the text; and the numerical formula is described in Appendix B.

1 (a). Scatter Plots of Hourly Ozone (Paired in Spaced & Time)

For Episode #1, July 25 - August 6, 1988

SCATTER PLOT OF HOURLY O3 (PAIRED IN SPACE & TIME)

FOR MMS BATON ROUGE–NEW ORLEANS, EPISODE #1

JULY 25 – AUGUST 6, 1988 (8 a.m. – 7 p.m.)

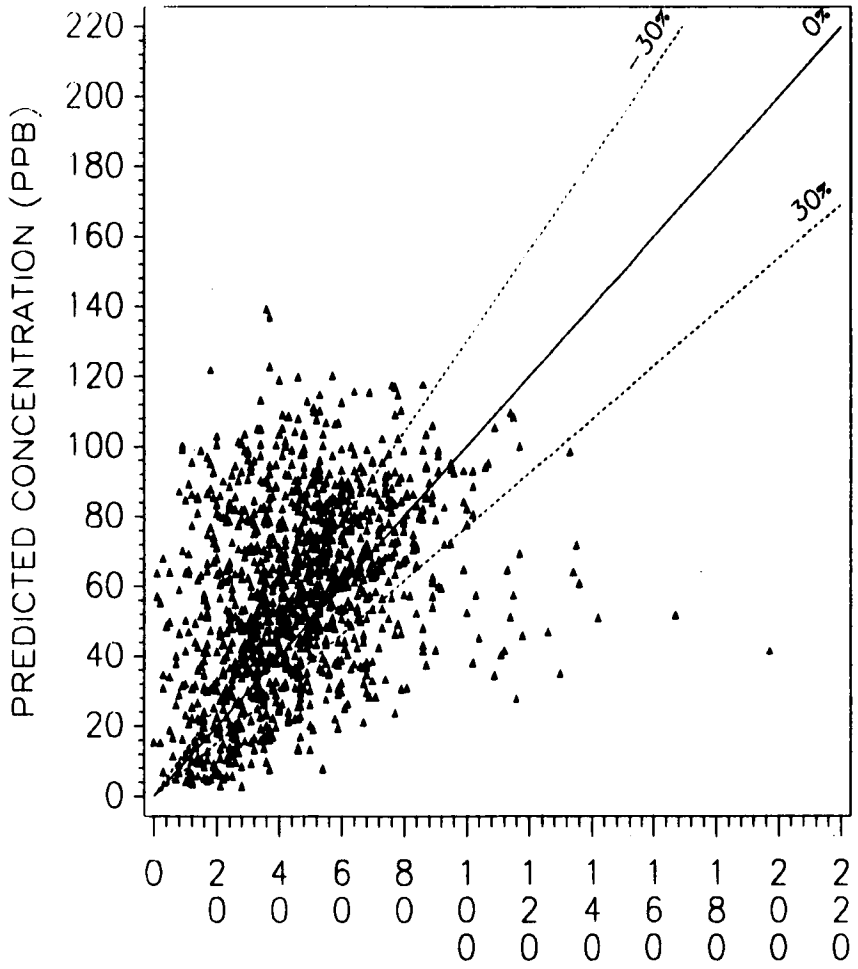

McIDAS
WT4CELL

SCATTER PLOT OF HOURLY O3 (PAIRED IN SPACE & TIME)

FOR MMS BATON ROUGE I, EPISODE #1

JULY 25 – AUGUST 6, 1988 (8 a.m. – 7 p.m.)

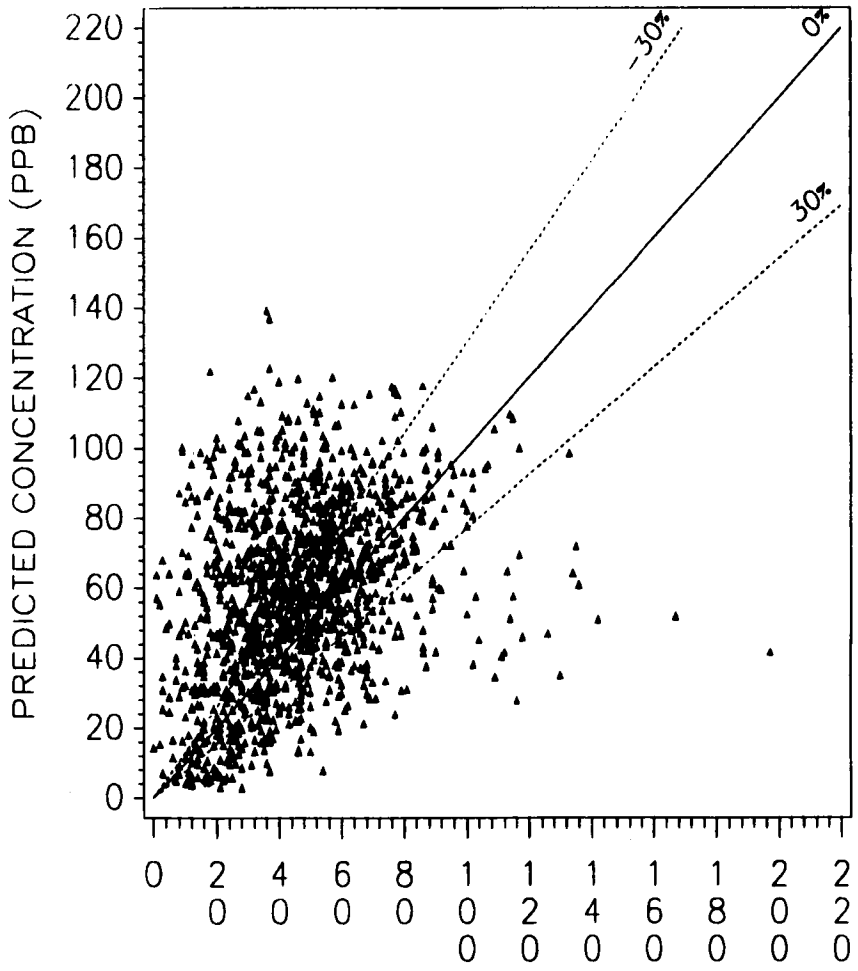

McIDAS
WT4CELL

SCATTER PLOT OF HOURLY O3 (PAIRED IN SPACE & TIME)

FOR MMS LAKE CHARLES–BEAUMONT, EPISODE #1

JULY 25 – AUGUST 6, 1988 (8 a.m. – 7 p.m.)

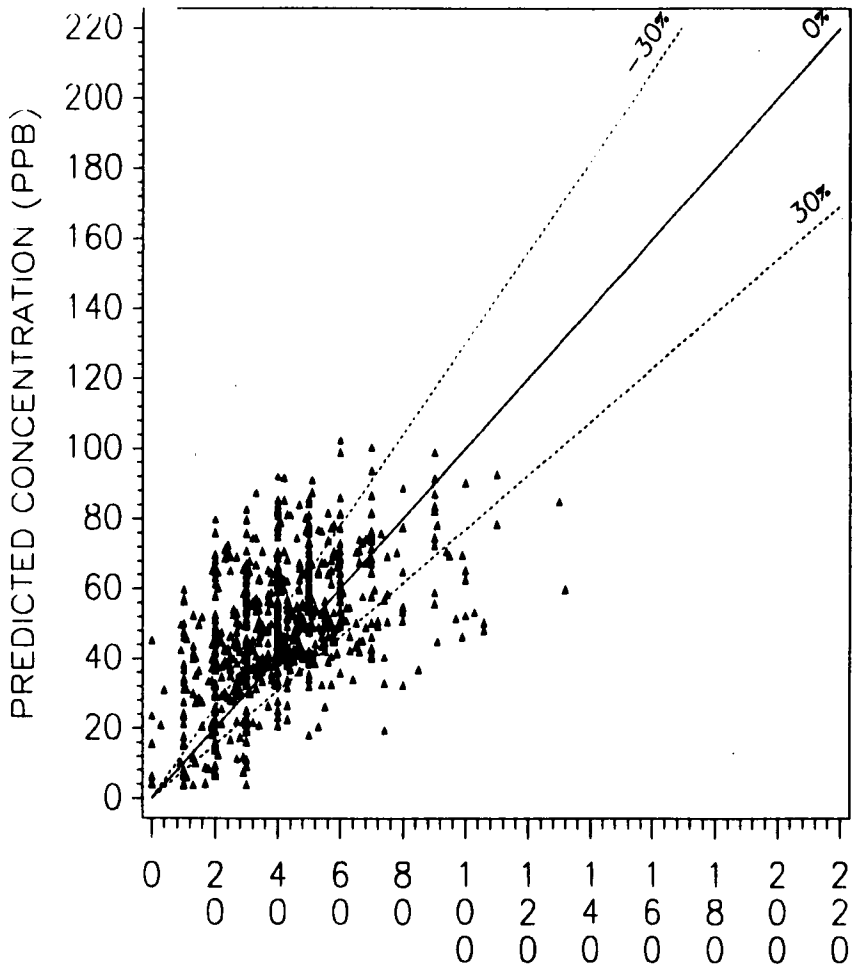

McIDAS
WT4CELL

SCATTER PLOT OF HOURLY O3 (PAIRED IN SPACE & TIME)

FOR MMS HOUSTON-GALVESTON, EPISODE #1

JULY 25 - AUGUST 6, 1988 (8 a.m. - 7 p.m.)

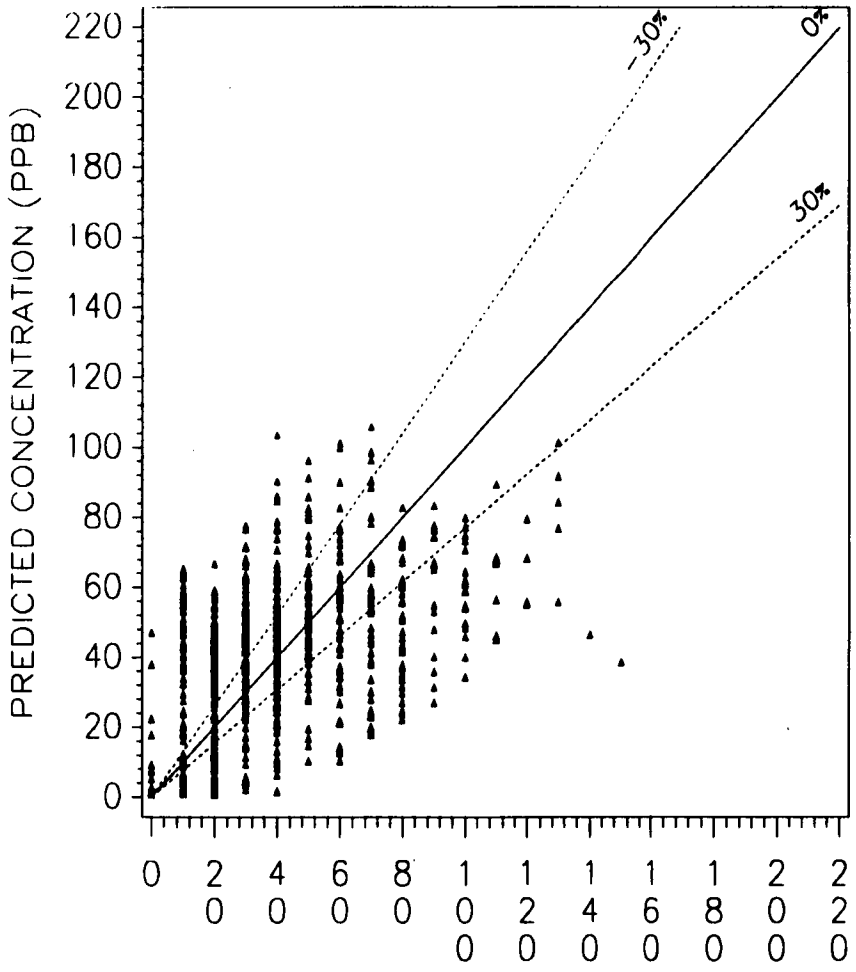

McIDAS
WT4CELL

SCATTER PLOT OF HOURLY O3 (PAIRED IN SPACE & TIME)

FOR MMS CORPUS CHRISTI, EPISODE #1

JULY 25 – AUGUST 6, 1988 (8 a.m. – 7 p.m.)

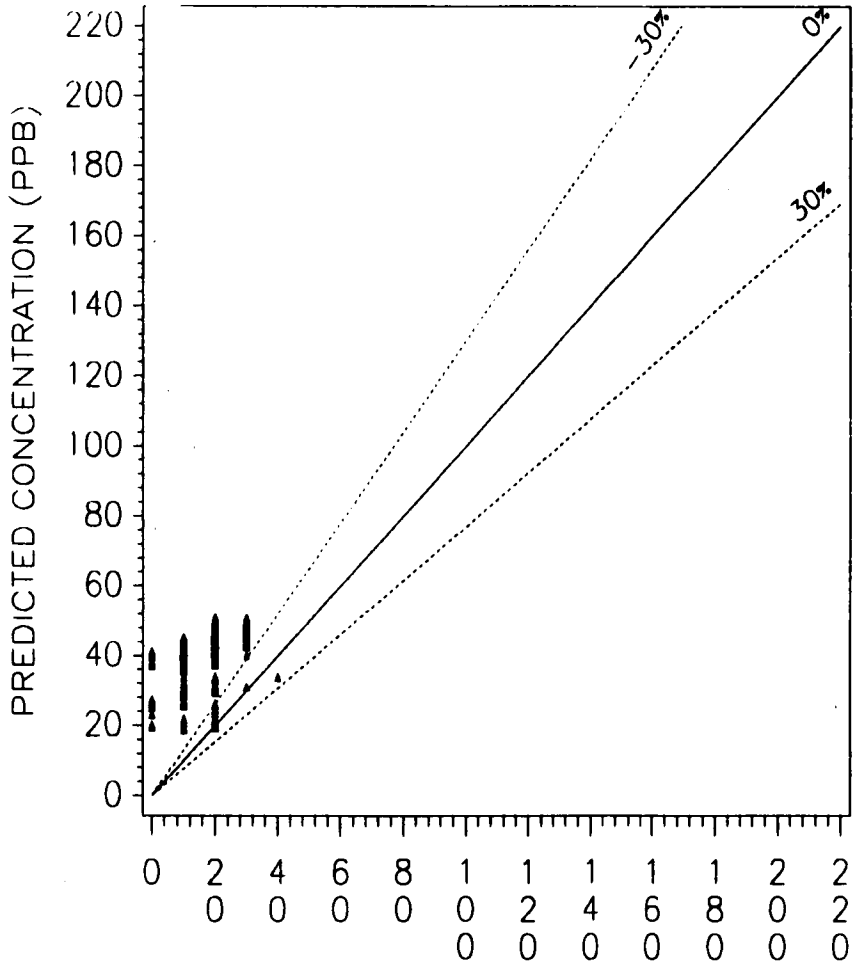

McIDAS
WT4CELL

2 (a). Quantile-Quantile Plots of Ozone Concentrations

For Episode #1, July 25 - August 6, 1988

QUANTILE – QUANTILE PLOT OF OZONE CONCENTRATIONS

FOR MMS BATON ROUGE–NEW ORLEANS

JULY 25 – AUGUST 6, 1988 (8 a.m. – 7 p.m.)

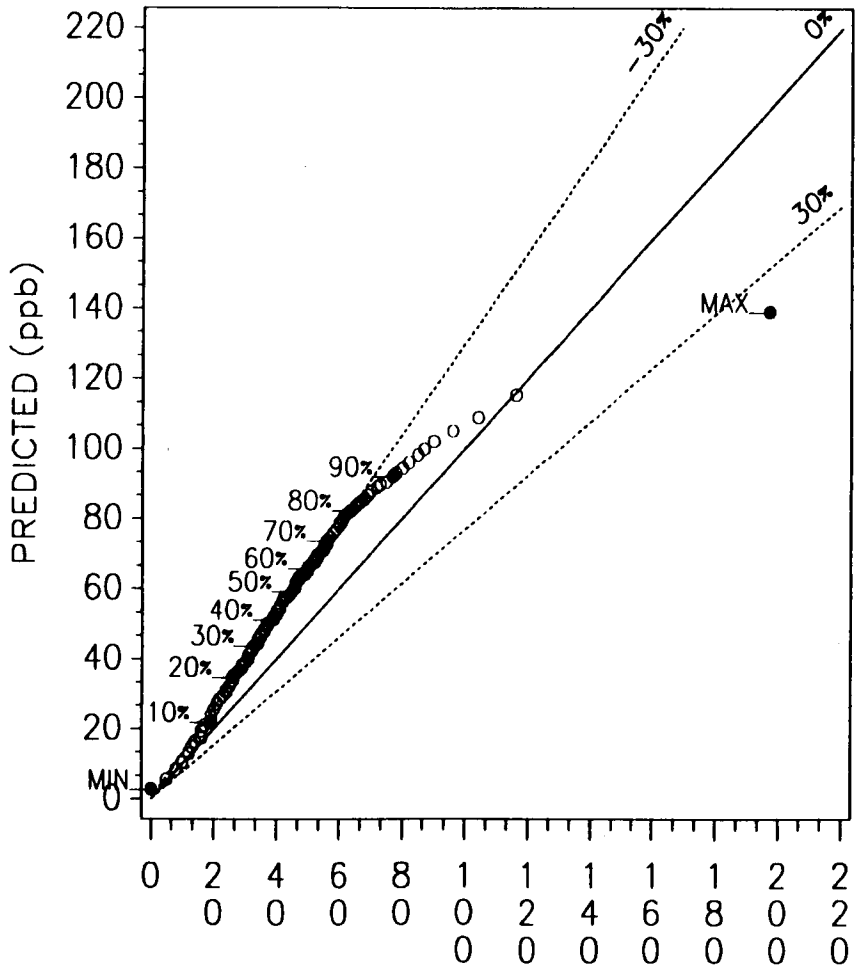

McIDAS
WT4CELL

QUANTILE – QUANTILE PLOT OF OZONE CONCENTRATIONS

FOR MMS BATON ROUGE I, EPISODE #1

JULY 25 – AUGUST 6, 1988 (8 a.m. – 7 p.m.)

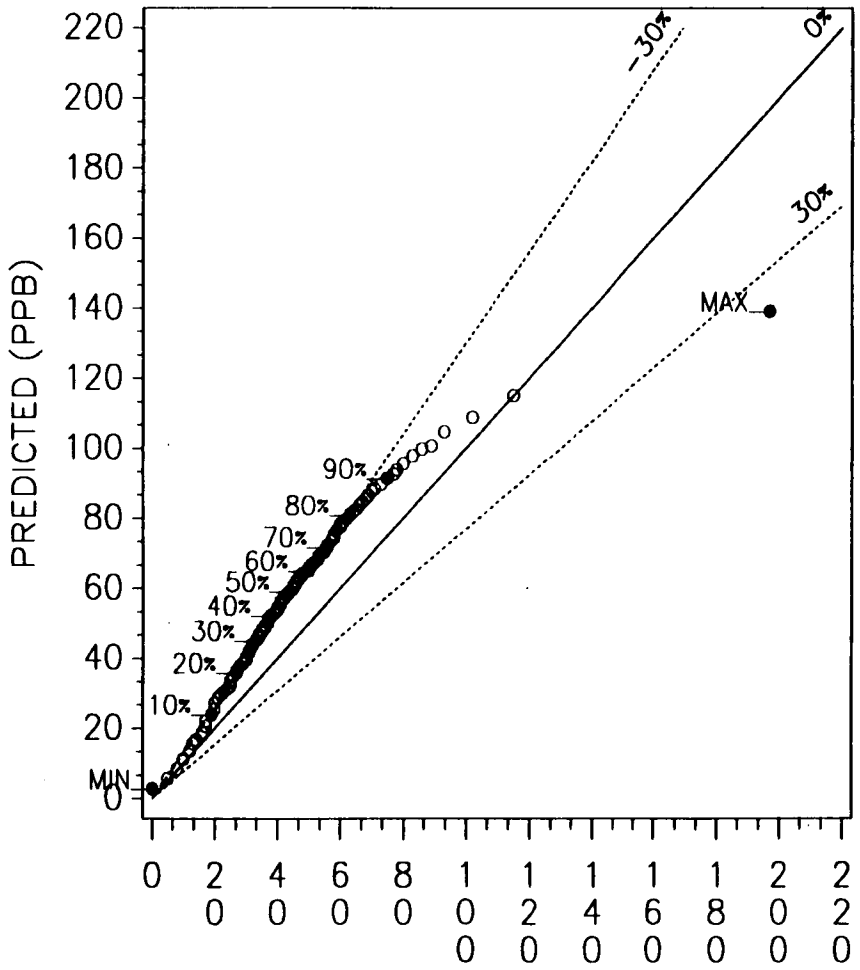

McIDAS
WT4CELL

QUANTILE – QUANTILE PLOT OF OZONE CONCENTRATIONS

FOR MMS LAKE CHARLES–BEAUMONT

JULY 25 – AUGUST 6, 1988 (8 a.m. – 7 p.m.)

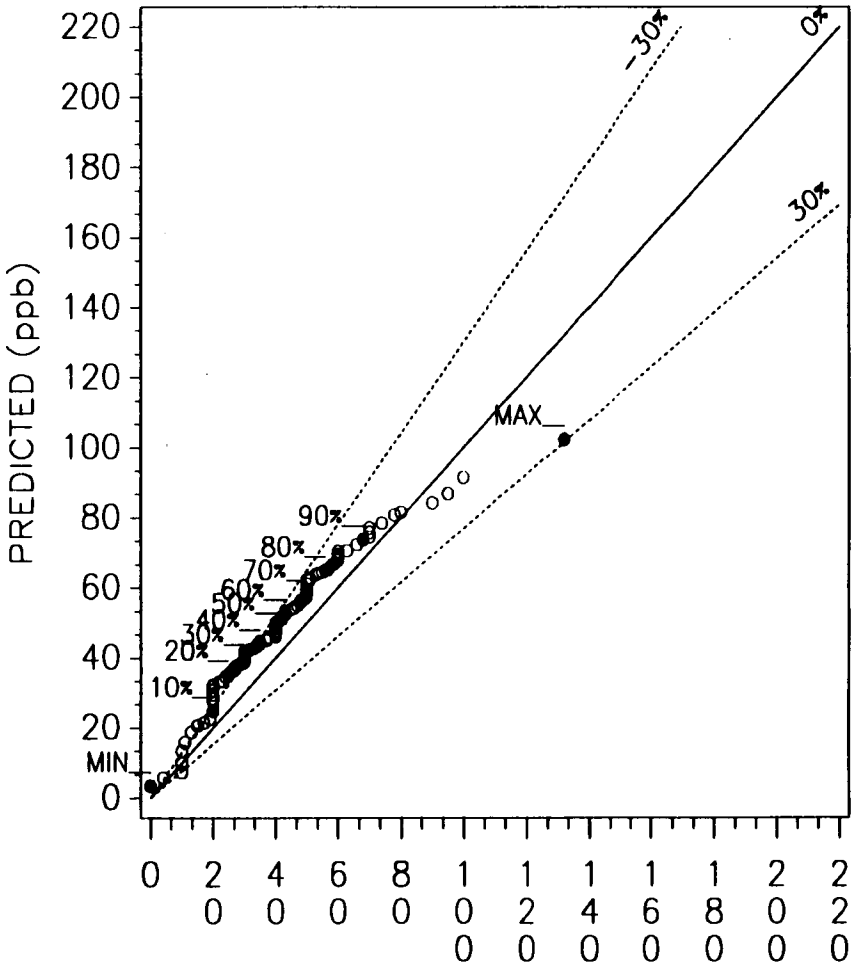

McIDAS
WT4CELL

QUANTILE – QUANTILE PLOT OF OZONE CONCENTRATIONS

FOR MMS HOUSTON–GALVESTON, EPISODE #1

JULY 25 – AUGUST 6, 1988 (8 a.m. – 7 p.m.)

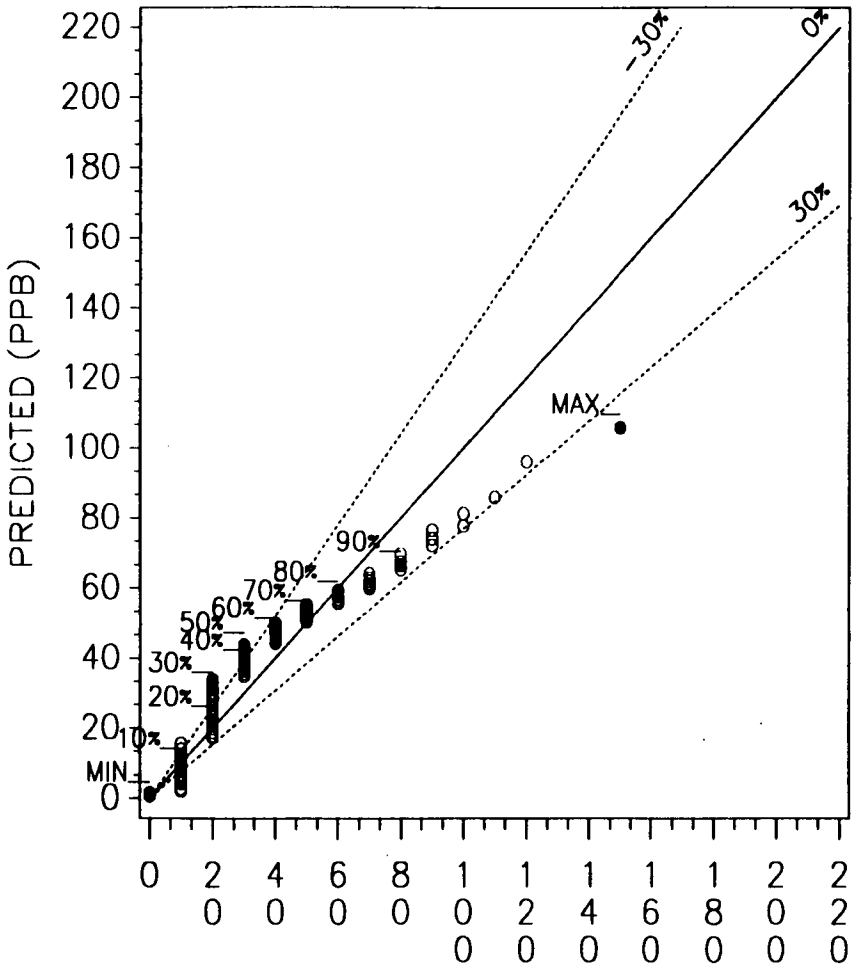

McIDAS
WT4CELL

QUANTILE – QUANTILE PLOT OF OZONE CONCENTRATIONS

FOR MMS CORPUS CHRISTI, EPISODE #1

JULY 25 – AUGUST 6, 1988 (8 a.m. – 7 p.m.)

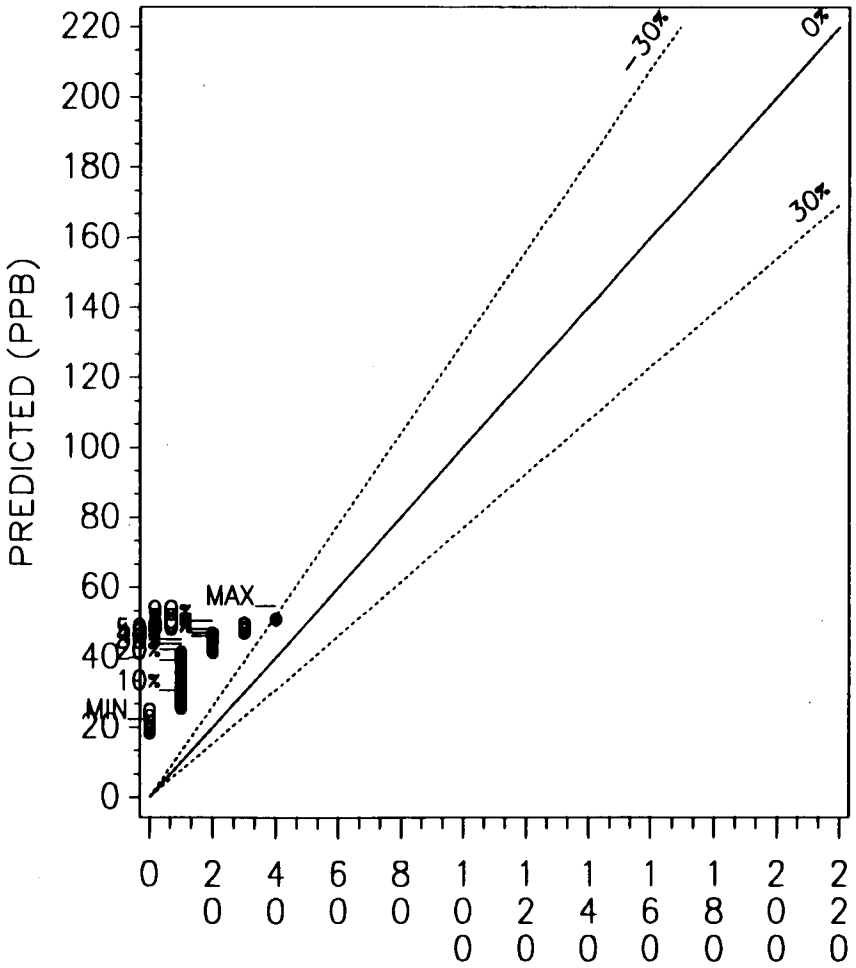

McIDAS
WT4CELL

3 (a). Time Series Plots of Maximum Hourly Ozone Concentrations

For Episode #1, July 25 - August 6, 1988

MAXIMUM HOURLY O3 CONCENTRATIONS
FOR MMS BATON ROUGE-NEW ORLEANS, EPISODE #1
JULY 25 – AUGUST 6, 1988

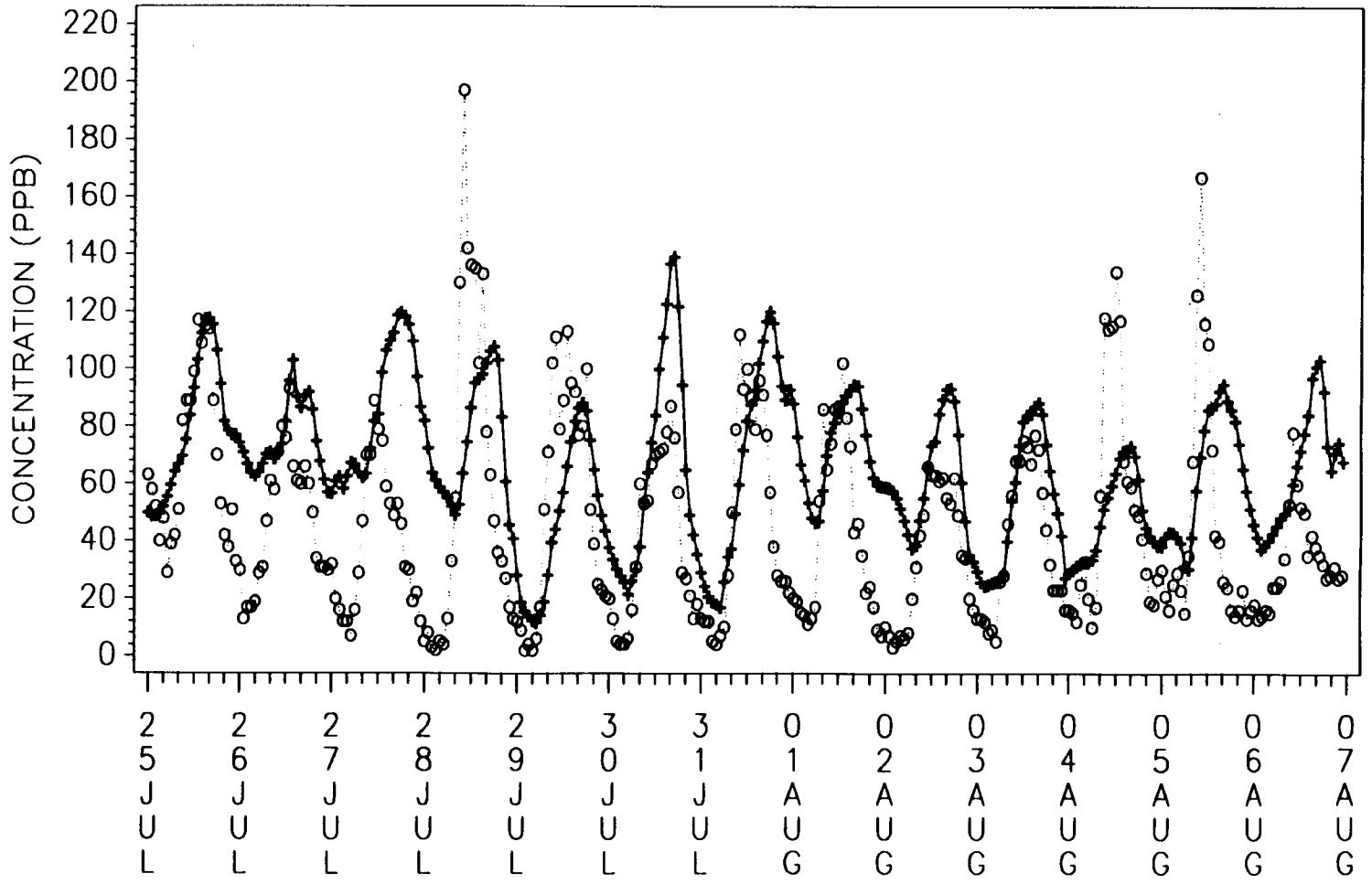

MAXIMUM HOURLY O3 CONCENTRATIONS
FOR MMS BATON ROUGE I, EPISODE #1
JULY 25 – AUGUST 6, 1988

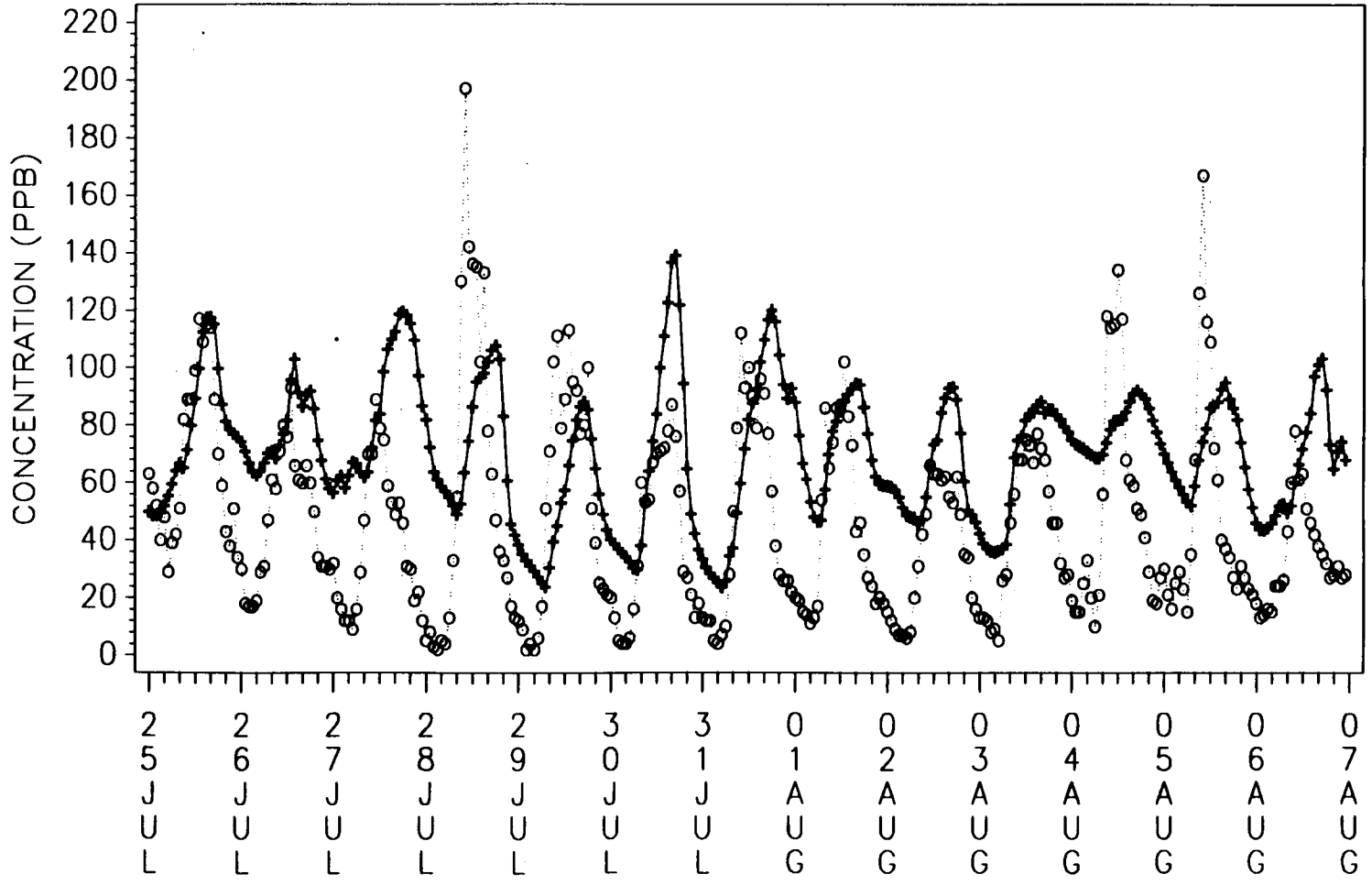

MAXIMUM HOURLY O3 CONCENTRATIONS
FOR MMS LAKE CHARLES–BEAUMONT, EPISODE #1
JULY 25 – AUGUST 6, 1988

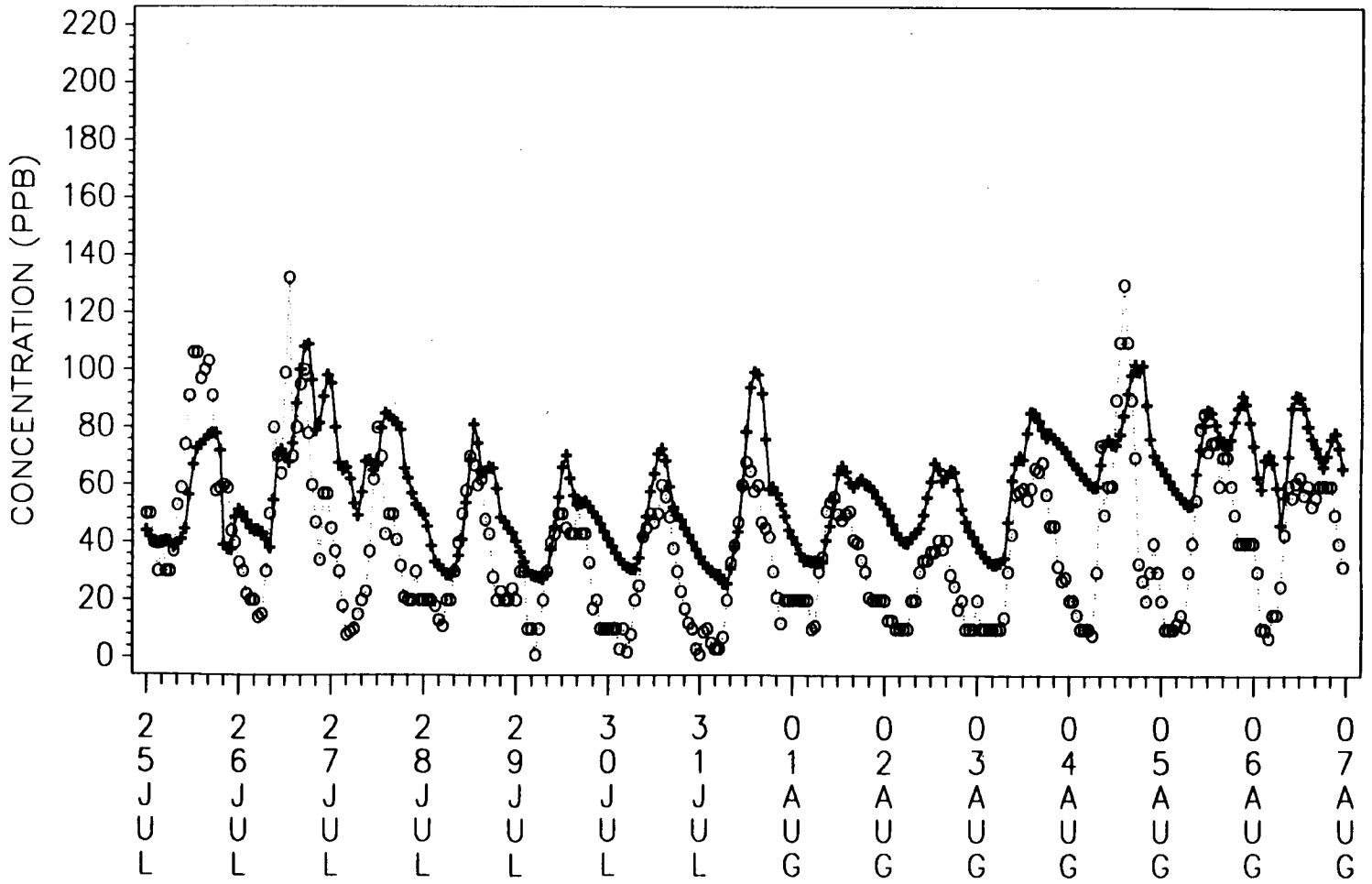

MAXIMUM HOURLY O3 CONCENTRATIONS
FOR MMS HOUSTON-GALVESTON, EPISODE #1
JULY 25 - AUGUST 6, 1988

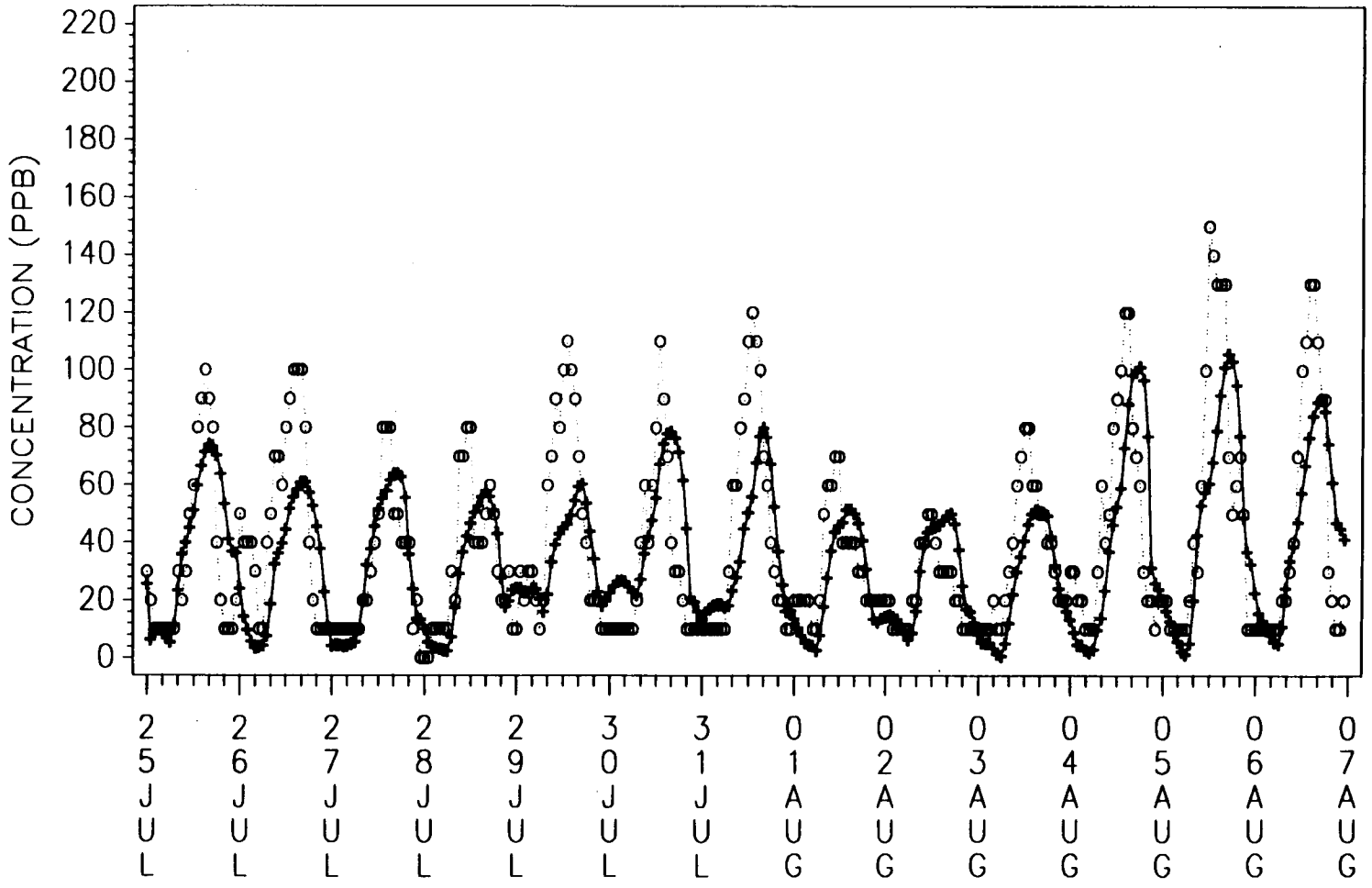

LEGEND: OBSERVED(o) PREDICTED(+)

McIDAS
WT4CELL

MAXIMUM HOURLY O3 CONCENTRATIONS
FOR MMS CORPUS CHRISTI, EPISODE #1
JULY 25 – AUGUST 6, 1988

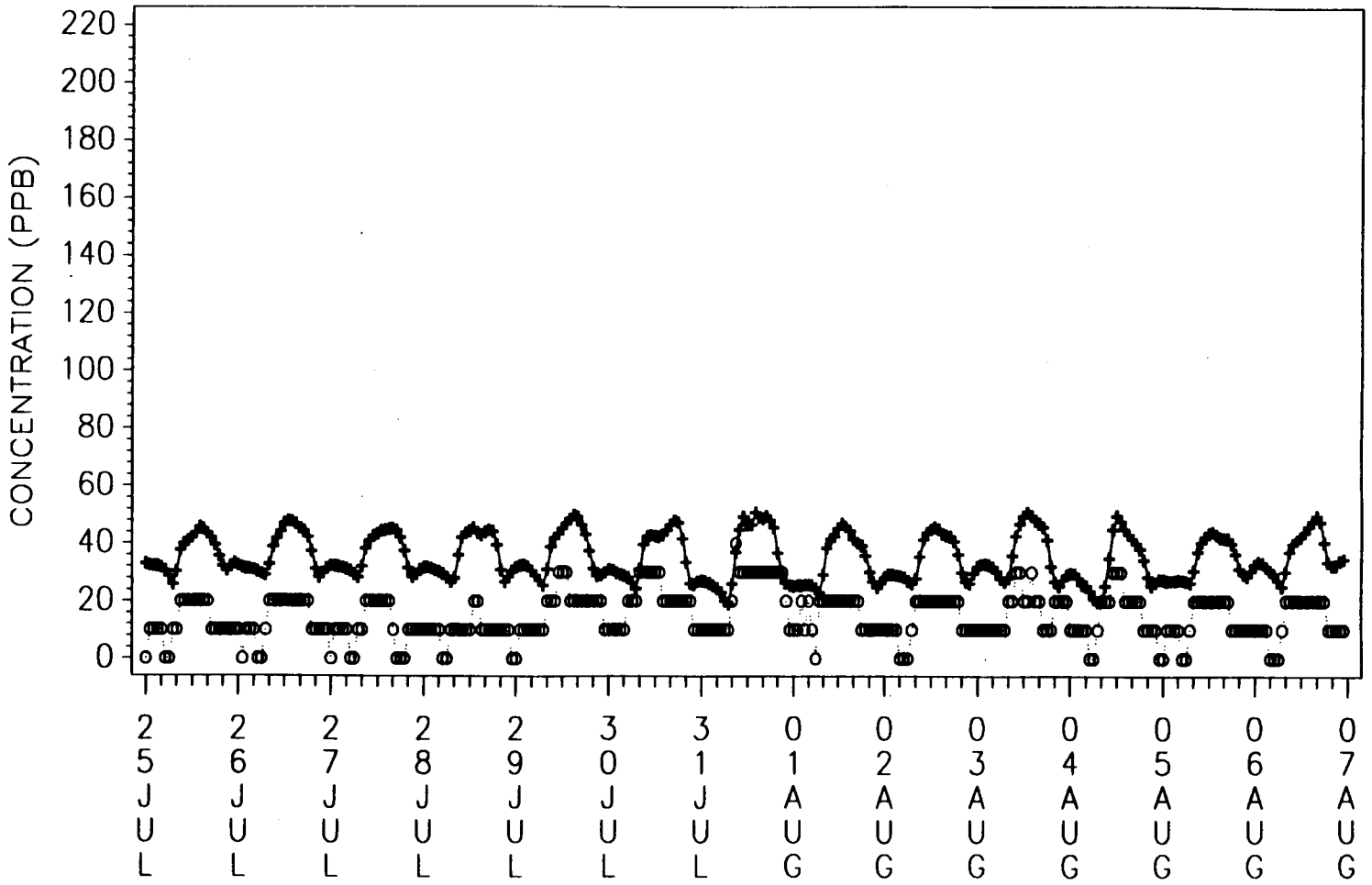

LEGEND: OBSERVED(o) PREDICTED(+)

McIDAS
WT4CELL

4 (a). Daily Box-Plots of Observed and Predicted Hourly Ozone

For Episode #1, July 25 - August 6, 1988

DAILY BOXPLOT OF OBSERVED AND PREDICTED HOURLY O3

FOR MMS BATON ROUGE–NEW ORLEANS, EPISODE #1

JULY 25 – AUGUST 6, 1988 (8 a.m. – 7 p.m.)

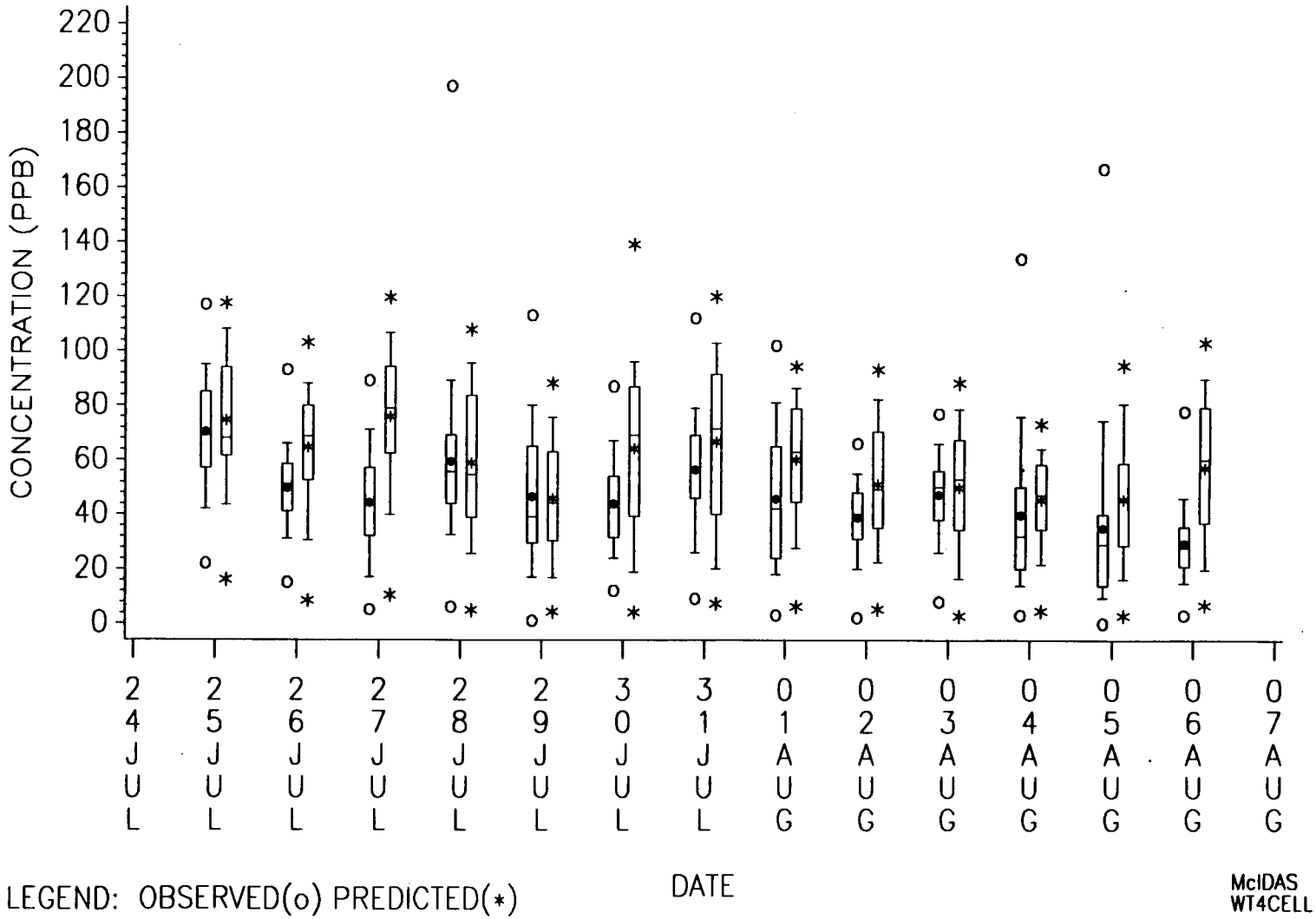

DAILY BOXPLOT OF OBSERVED AND PREDICTED HOURLY O3

FOR MMS BATON ROUGE I, EPISODE #1

JULY 25 – AUGUST 6, 1988 (8 a.m. – 7 p.m.)

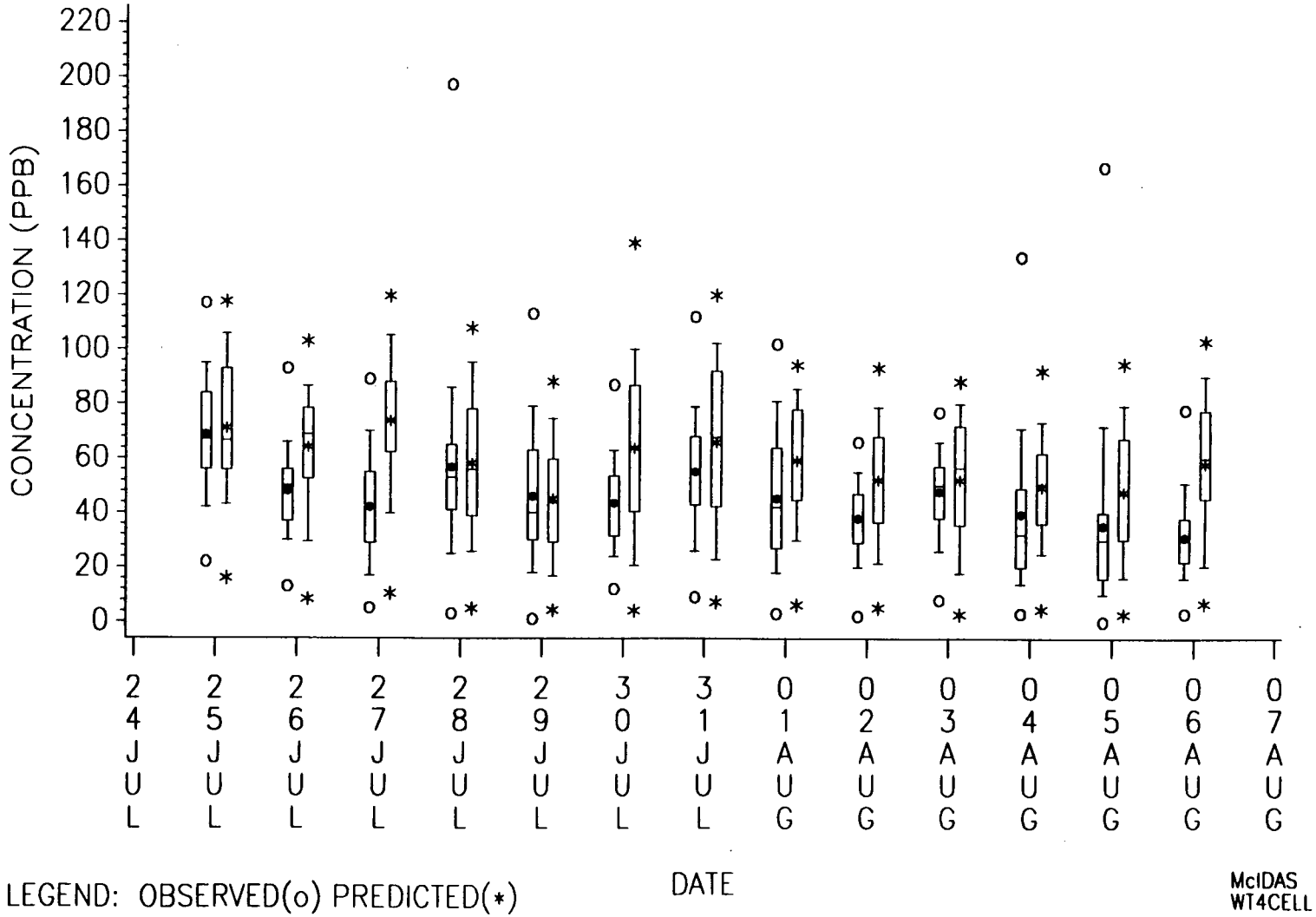

DAILY BOXPLOT OF OBSERVED AND PREDICTED HOURLY O3

FOR MMS LAKE CHARLES-BEAUMONT, EPISODE #1

JULY 25 - AUGUST 6, 1988 (8 a.m. - 7 p.m.)

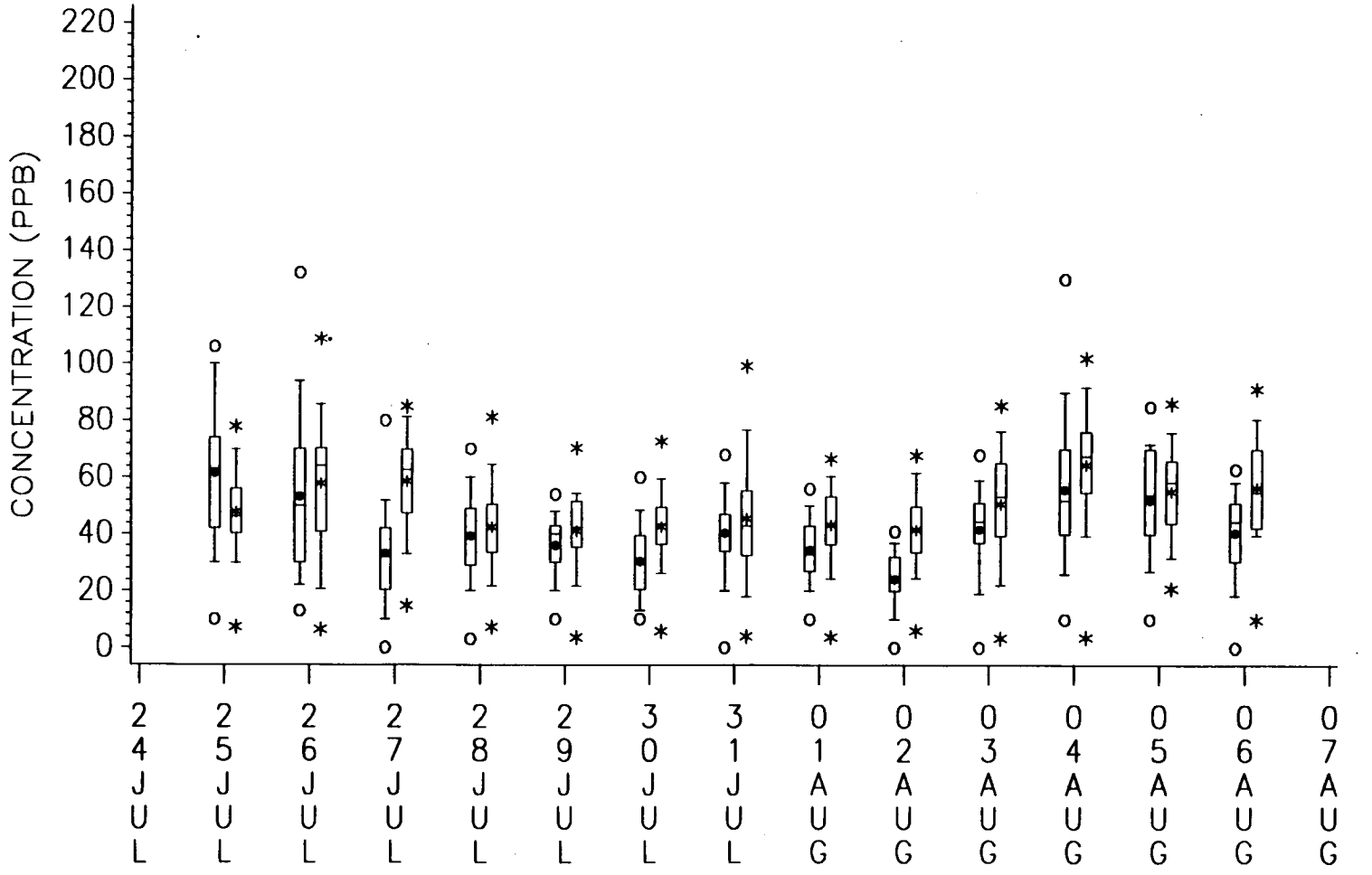

LEGEND: OBSERVED(o) PREDICTED(*)

McIDAS WT4CELL

DAILY BOXPLOT OF OBSERVED AND PREDICTED HOURLY O3

FOR MMS HOUSTON-GALVESTON, EPISODE #1

JULY 25 - AUGUST 6, 1988 (8 a.m. - 7 p.m.)

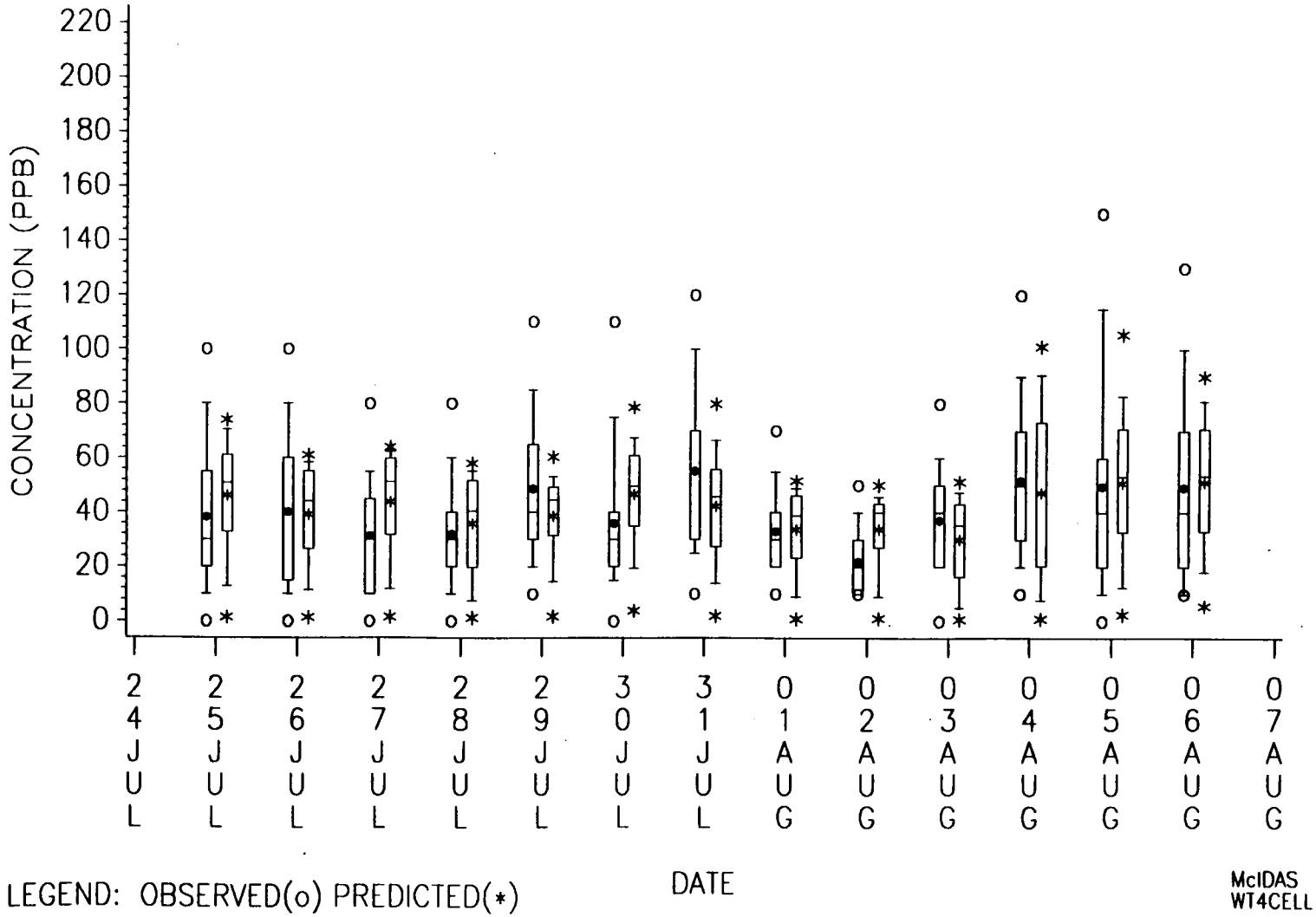

DAILY BOXPLOT OF OBSERVED AND PREDICTED HOURLY O3

FOR MMS CORPUS CHRISTI, EPISODE #1

JULY 25 – AUGUST 6, 1988 (8 a.m. – 7 p.m.)

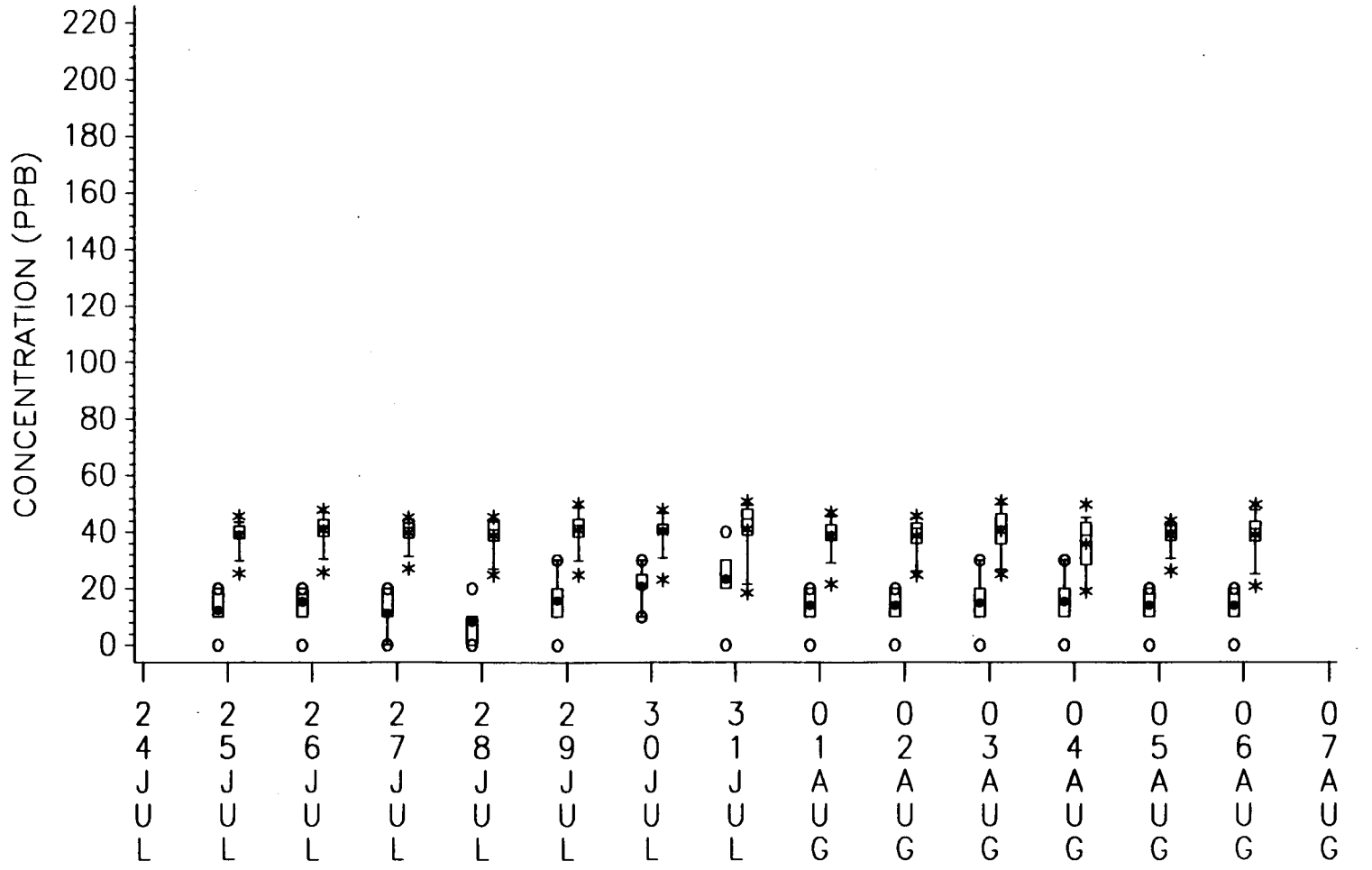

5 (a). Box-Plots of Bias (Obs.-Pred.),

For Episode #1, July 25 - August 6, 1988

BOX–PLOT OF BIAS(OBS–PRED) BY DAY
FOR MMS BATON ROUGE–NEW ORLEANS, EPISODE #1
JULY 25 – AUGUST 6, 1988 (8 a.m. – 7 p.m.)

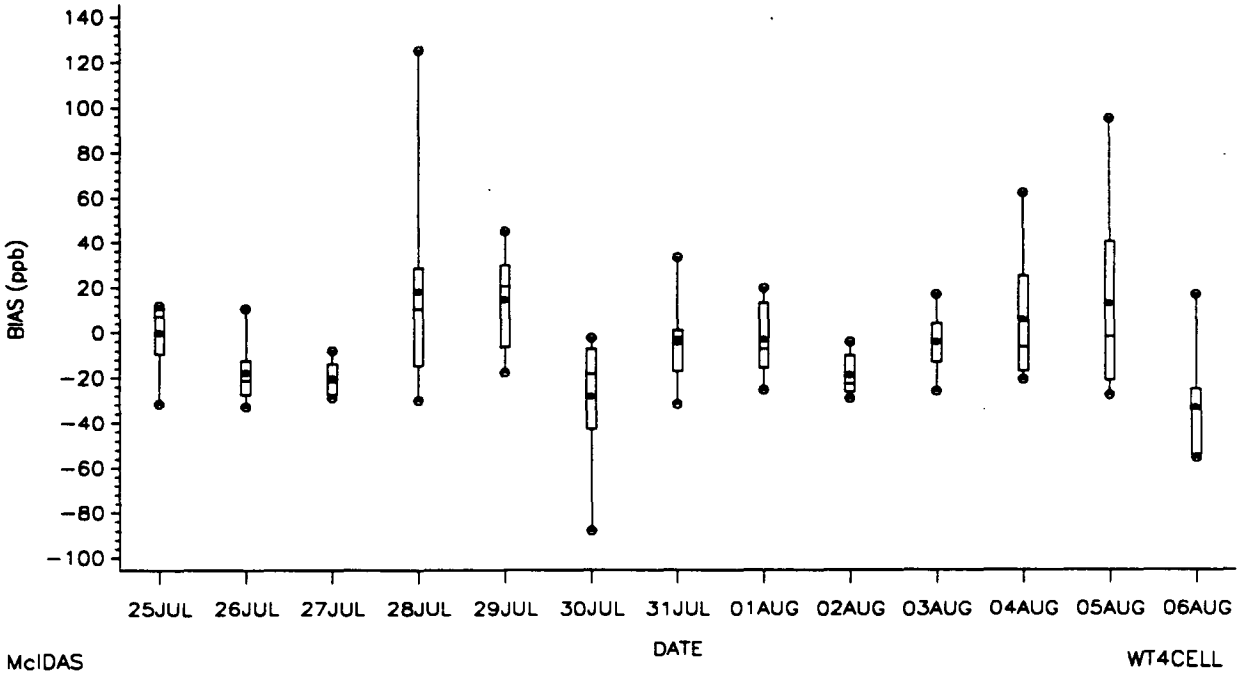

McIDAS WT4CELL

BOX–PLOT OF BIAS(OBS–PRED) BY O3 CONCENTRATION
FOR MMS BATON ROUGE–NEW ORLEANS, EPISODE #1
JULY 25 – AUGUST 6, 1988 (8 a.m. – 7 p.m.)

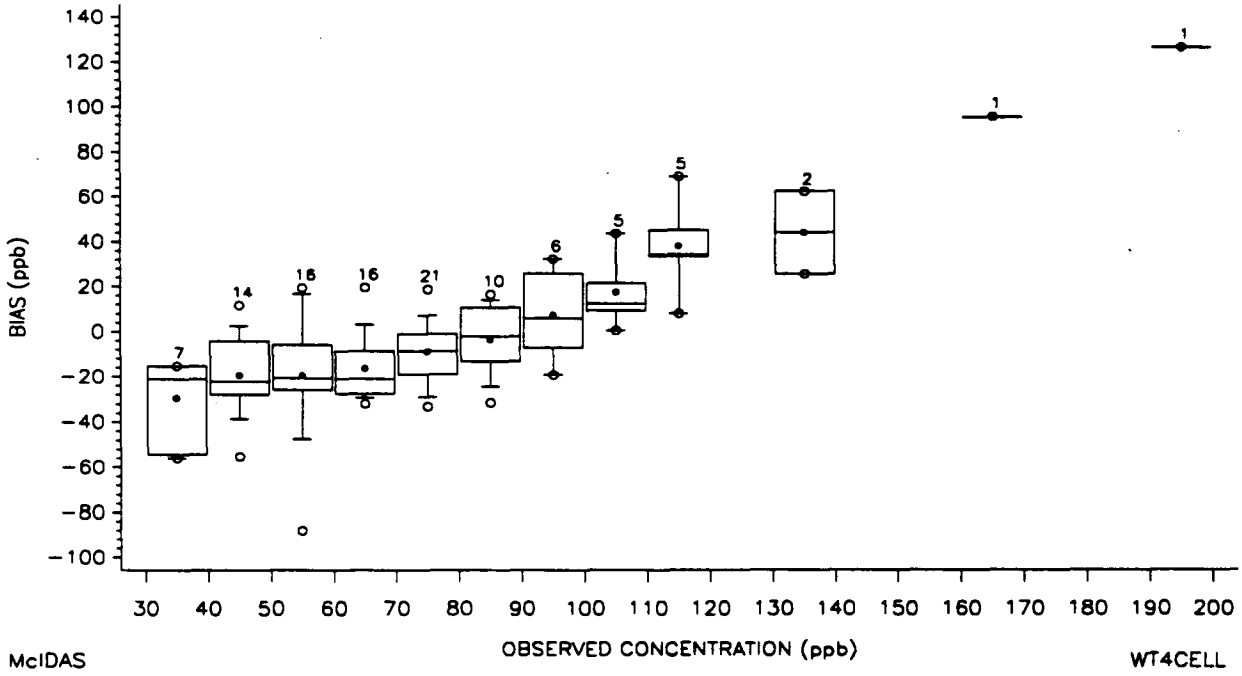

McIDAS WT4CELL

BOX–PLOT OF BIAS(OBS–PRED) BY DAY
FOR MMS BATON ROUGE I, EPISODE #1
JULY 25 – AUGUST 6, 1988 (8 a.m. – 7 p.m.)

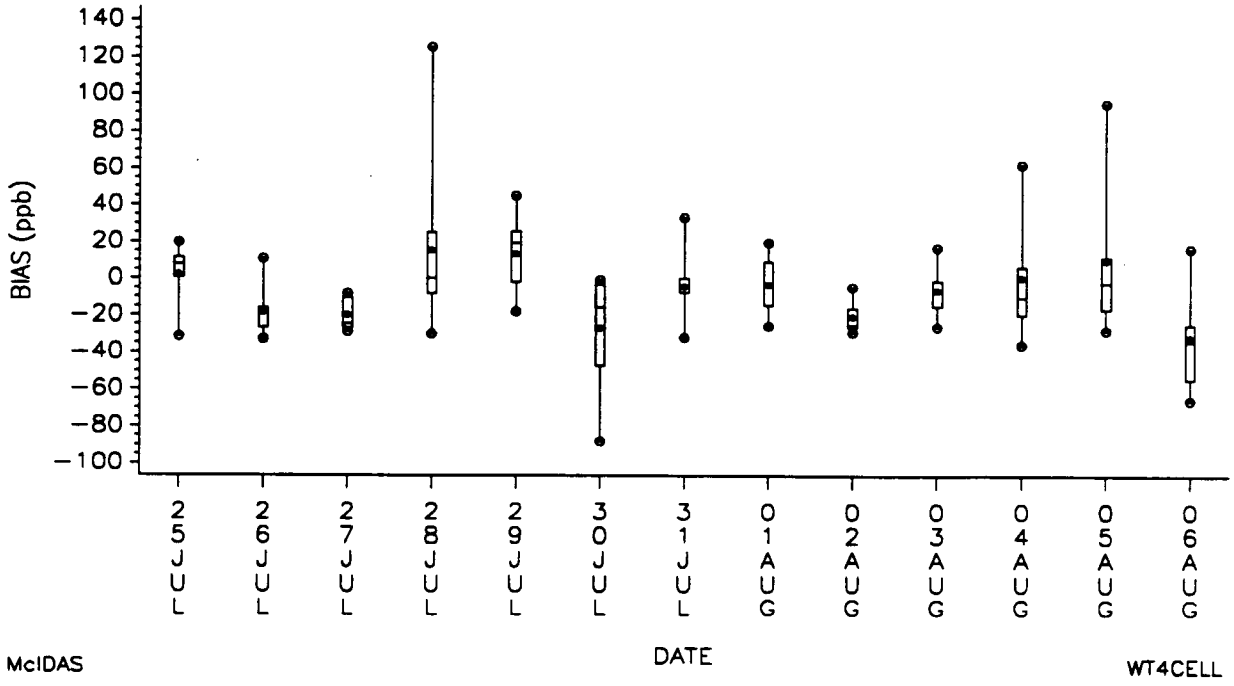

McIDAS WT4CELL

BOX–PLOT OF BIAS(OBS–PRED) BY O3 CONCENTRATION
FOR MMS BATON ROUGE I, EPISODE #1
JULY 25 – AUGUST 6, 1988 (8 a.m. – 7 p.m.)

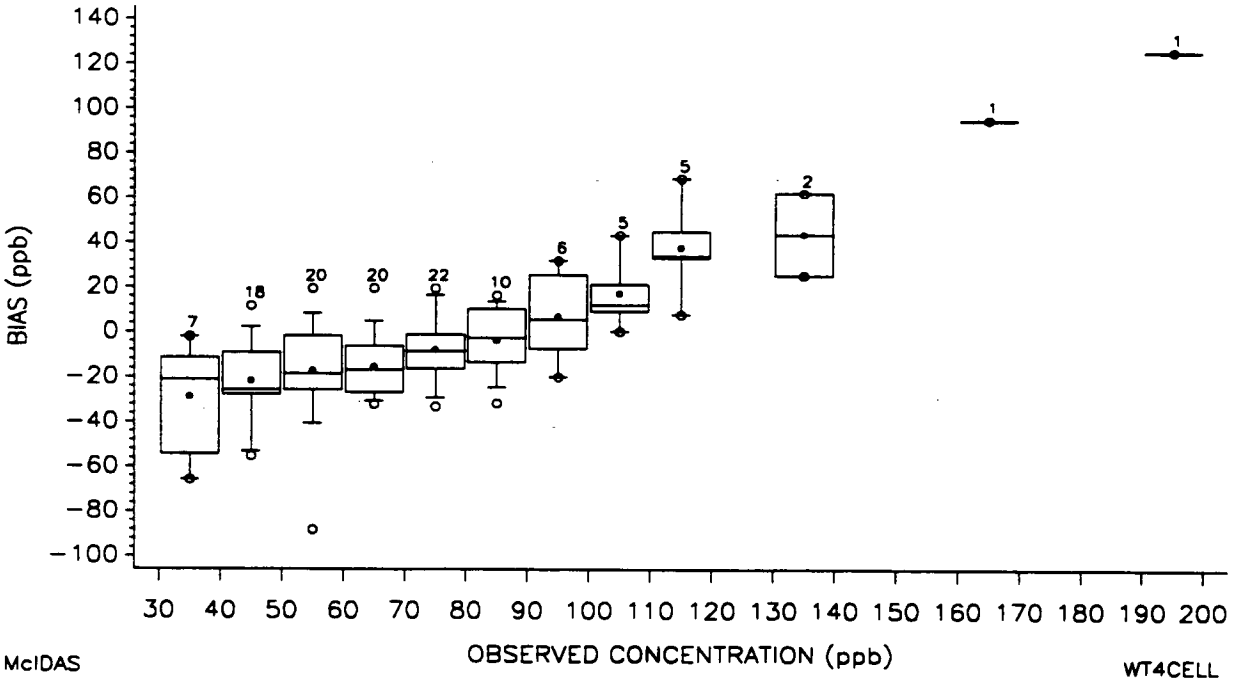

McIDAS WT4CELL

BOX–PLOT OF BIAS(OBS–PRED) BY DAY
FOR MMS LAKE CHARLES–BEAUMONT, EPISODE #1
JULY 25 – AUGUST 6, 1988 (8 a.m. – 7 p.m.)

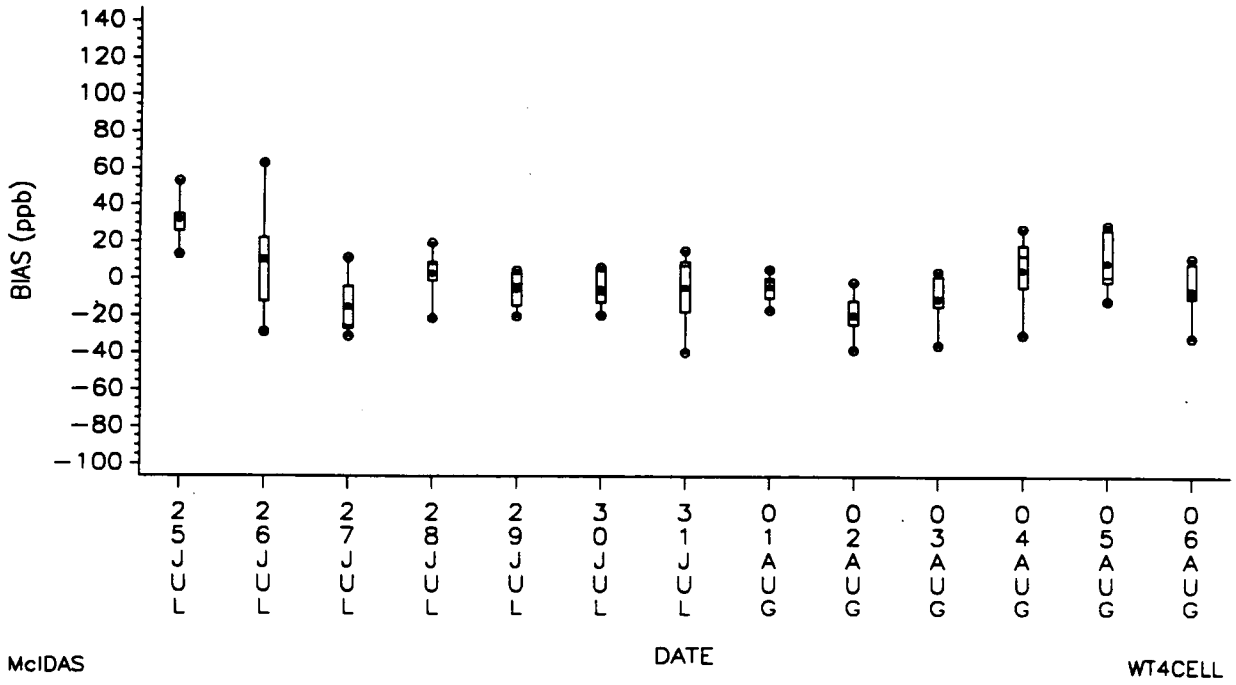

McIDAS WT4CELL

BOX–PLOT OF BIAS(OBS–PRED) BY O3 CONCENTRATION
FOR MMS LAKE CHARLES–BEAUMONT, EPISODE #1
JULY 25 – AUGUST 6, 1988 (8 a.m. – 7 p.m.)

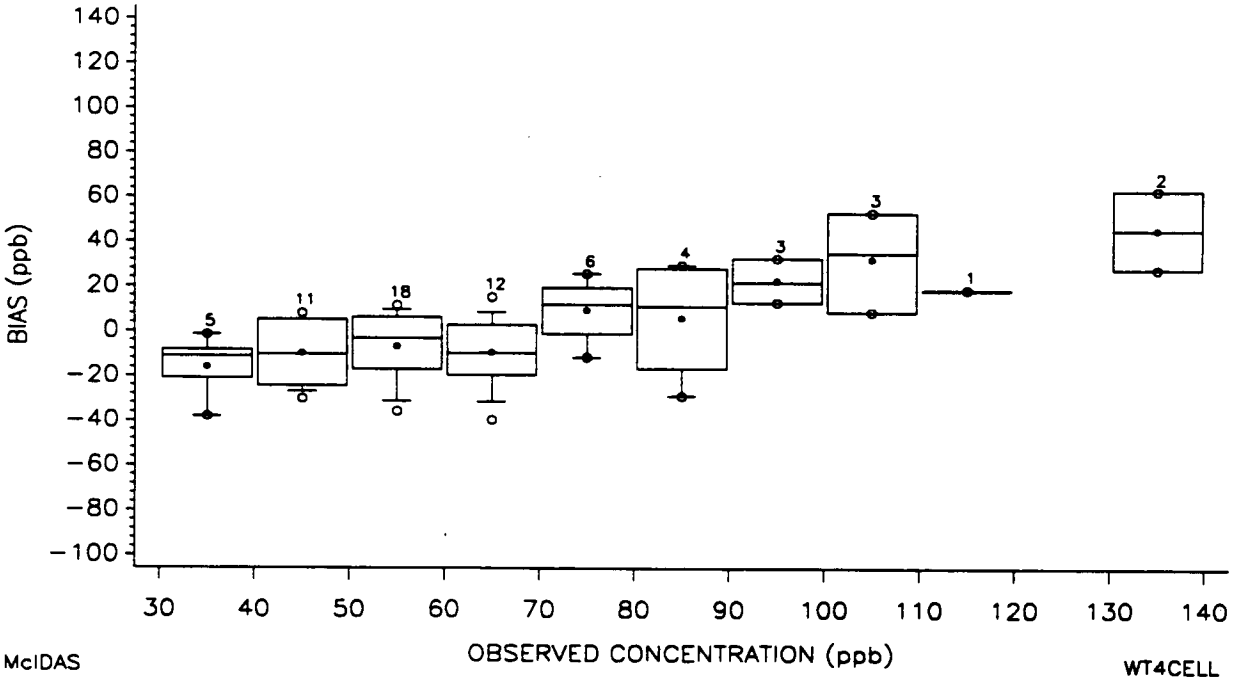

McIDAS WT4CELL

BOX–PLOT OF BIAS(OBS–PRED) BY DAY
FOR MMS HOUSTON–GALVESTON, EPISODE #1
JULY 25 – AUGUST 6, 1988 (8 a.m. – 7 p.m.)

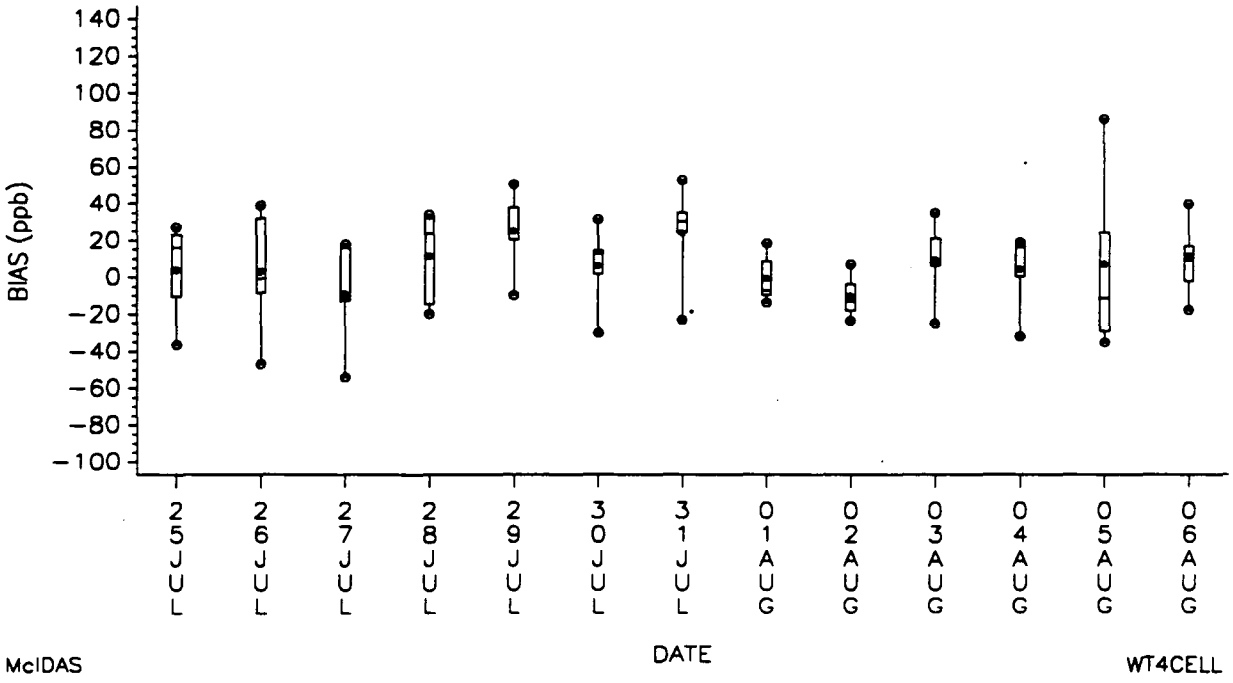

McIDAS WT4CELL

BOX–PLOT OF BIAS(OBS–PRED) BY O3 CONCENTRATION
FOR MMS HOUSTON–GALVESTON, EPISODE #1
JULY 25 – AUGUST 6, 1988 (8 a.m. – 7 p.m.)

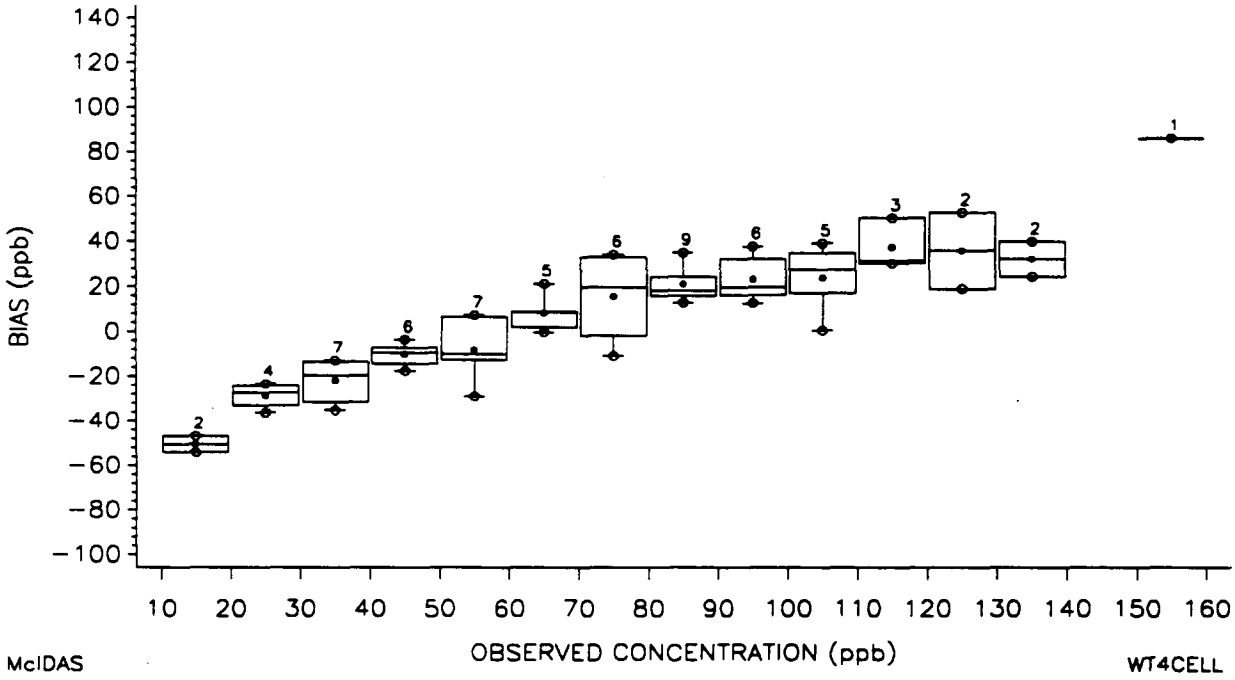

McIDAS WT4CELL

BOX-PLOT OF BIAS(OBS-PRED) BY DAY
FOR MMS CORPUS CHRISTI, EPISODE #1
JULY 25 - AUGUST 6, 1988 (8 a.m. - 7 p.m.)

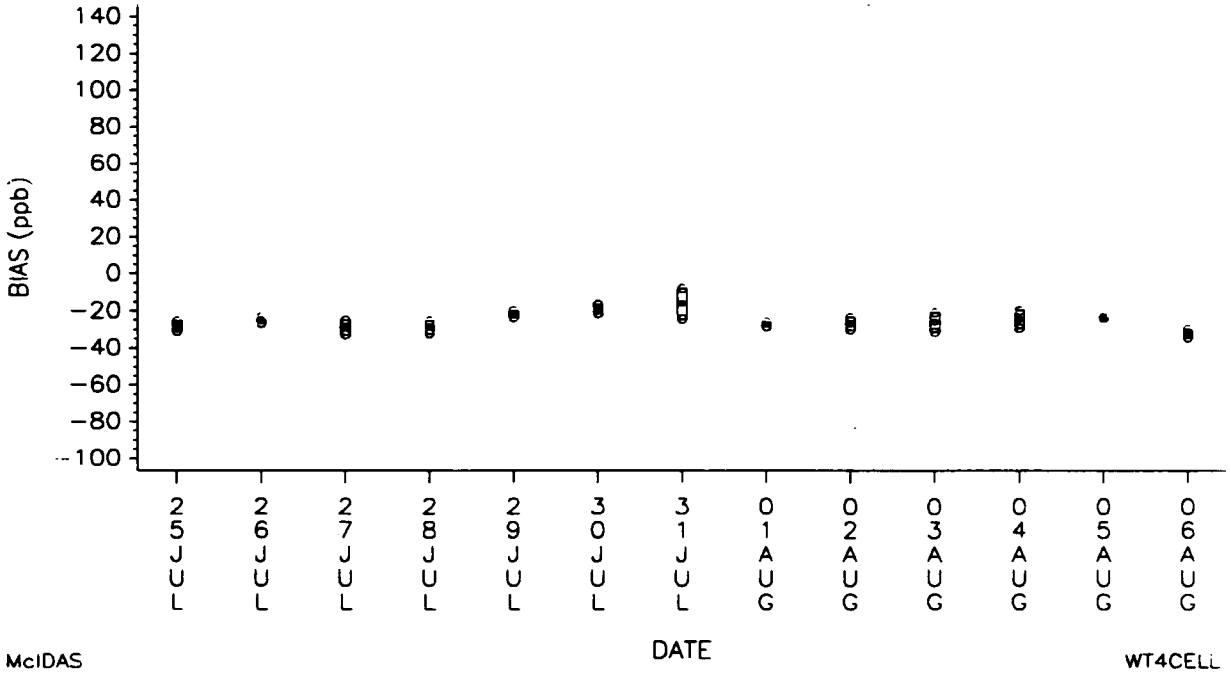

McIDAS WT4CELL

BOX-PLOT OF BIAS(OBS-PRED) BY O3 CONCENTRATION
FOR MMS CORPUS CHRISTI, EPISODE #1
JULY 25 - AUGUST 6, 1988 (8 a.m. - 7 p.m.)

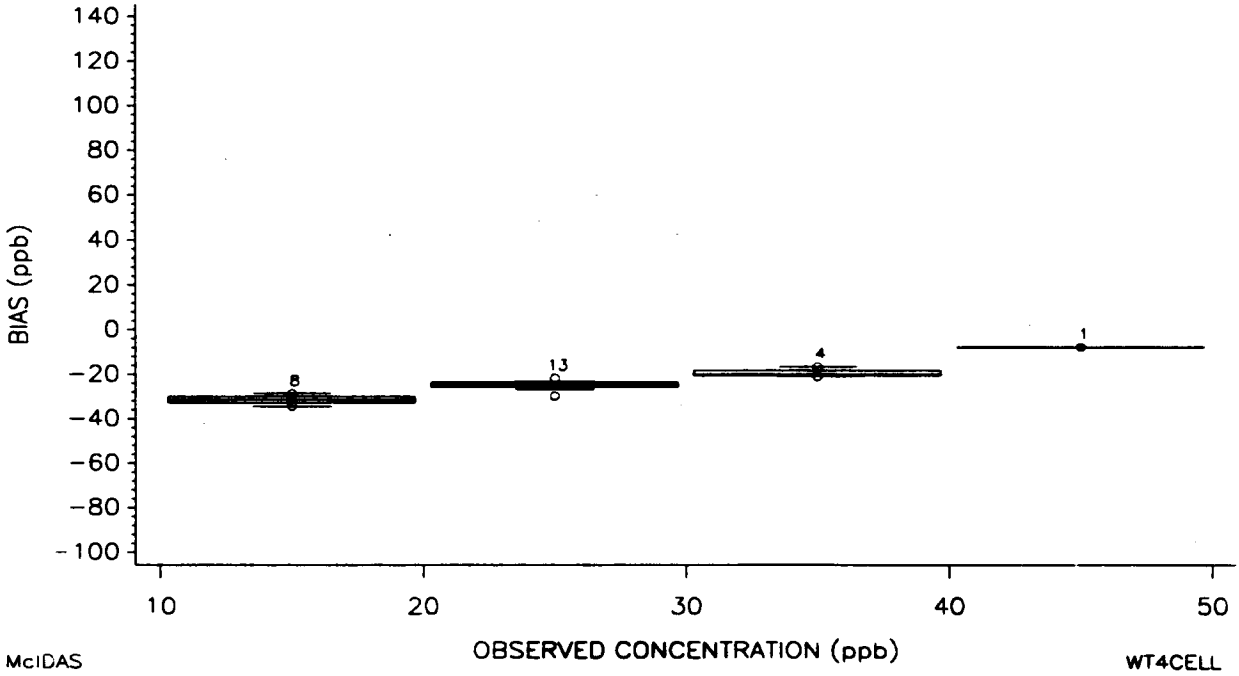

McIDAS WT4CELL

6 (a). Box-Plots of Normalized Bias,

For Episode #1, July 25 - August 6, 1988

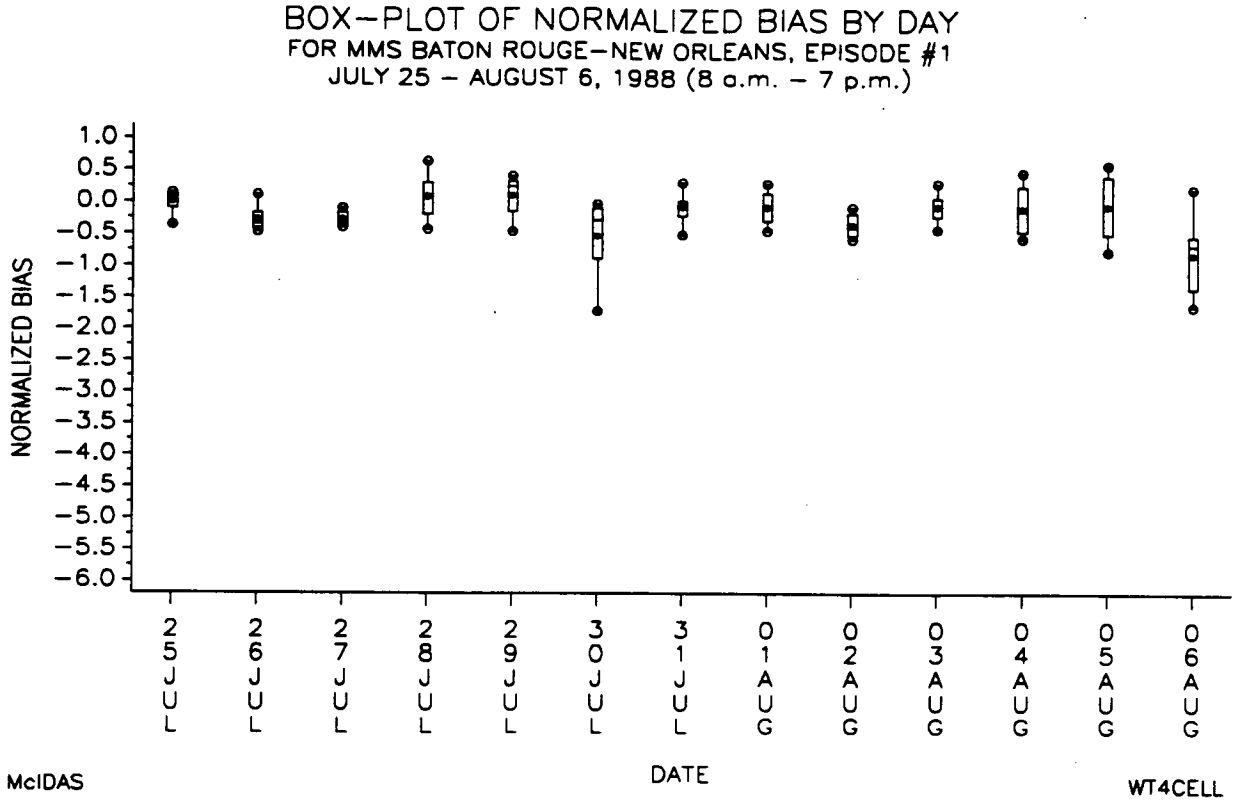
BOX–PLOT OF NORMALIZED BIAS BY DAY
FOR MMS BATON ROUGE–NEW ORLEANS, EPISODE #1
JULY 25 – AUGUST 6, 1988 (8 a.m. – 7 p.m.)
NORMALIZED BIAS
1.0
0.5
0.0
−0.5
−1.0
−1.5
−2.0
−2.5
−3.0
−3.5
−4.0
−4.5
−5.0
−5.5
−6.0
25JUL
26JUL
27JUL
28JUL
29JUL
30JUL
31JUL
01AUG
02AUG
03AUG
04AUG
05AUG
06AUG
DATE
McIDAS
WT4CELL

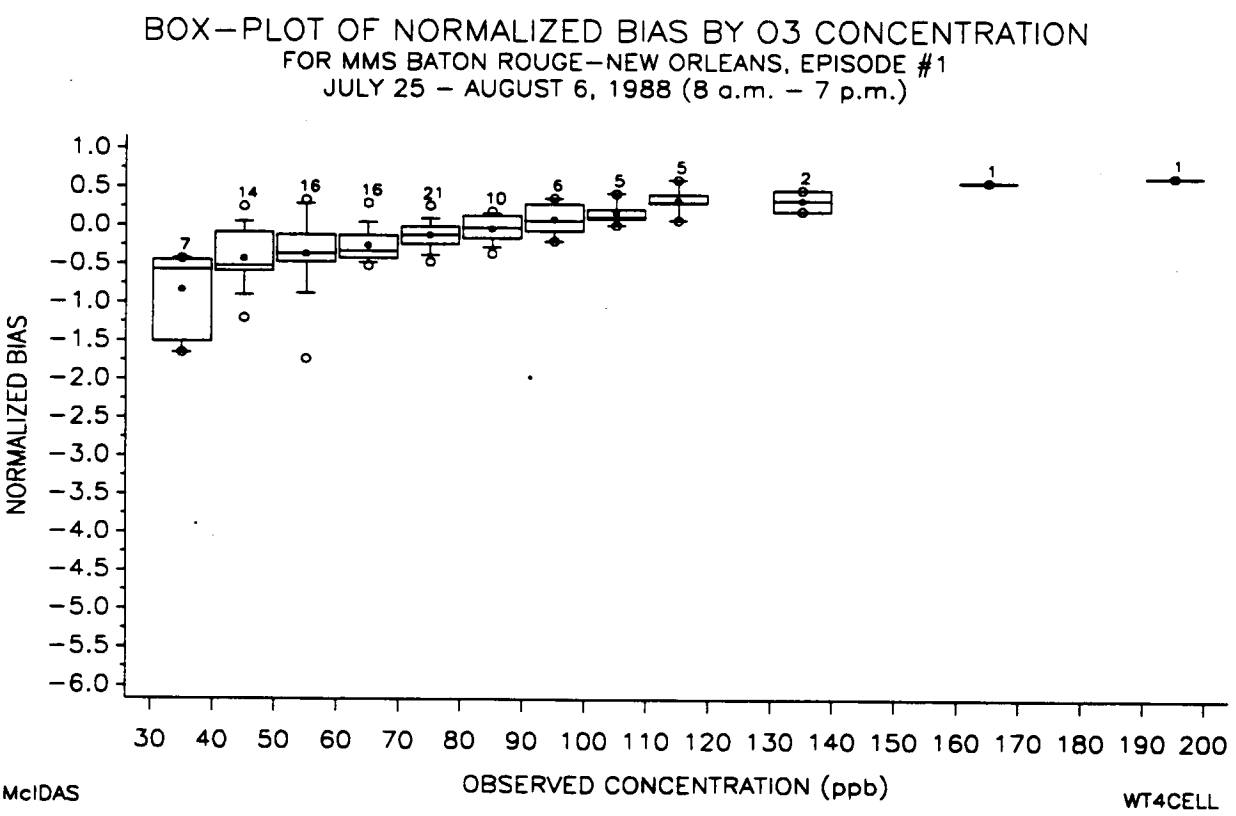
BOX–PLOT OF NORMALIZED BIAS BY O3 CONCENTRATION
FOR MMS BATON ROUGE–NEW ORLEANS, EPISODE #1
JULY 25 – AUGUST 6, 1988 (8 a.m. – 7 p.m.)
NORMALIZED BIAS
1.0
0.5
0.0
−0.5
−1.0
−1.5
−2.0
−2.5
−3.0
−3.5
−4.0
−4.5
−5.0
−5.5
−6.0
7
14
16
16
21
10
6
5
5
2
1
1
30 40 50 60 70 80 90 100 110 120 130 140 150 160 170 180 190 200
OBSERVED CONCENTRATION (ppb)
McIDAS
WT4CELL

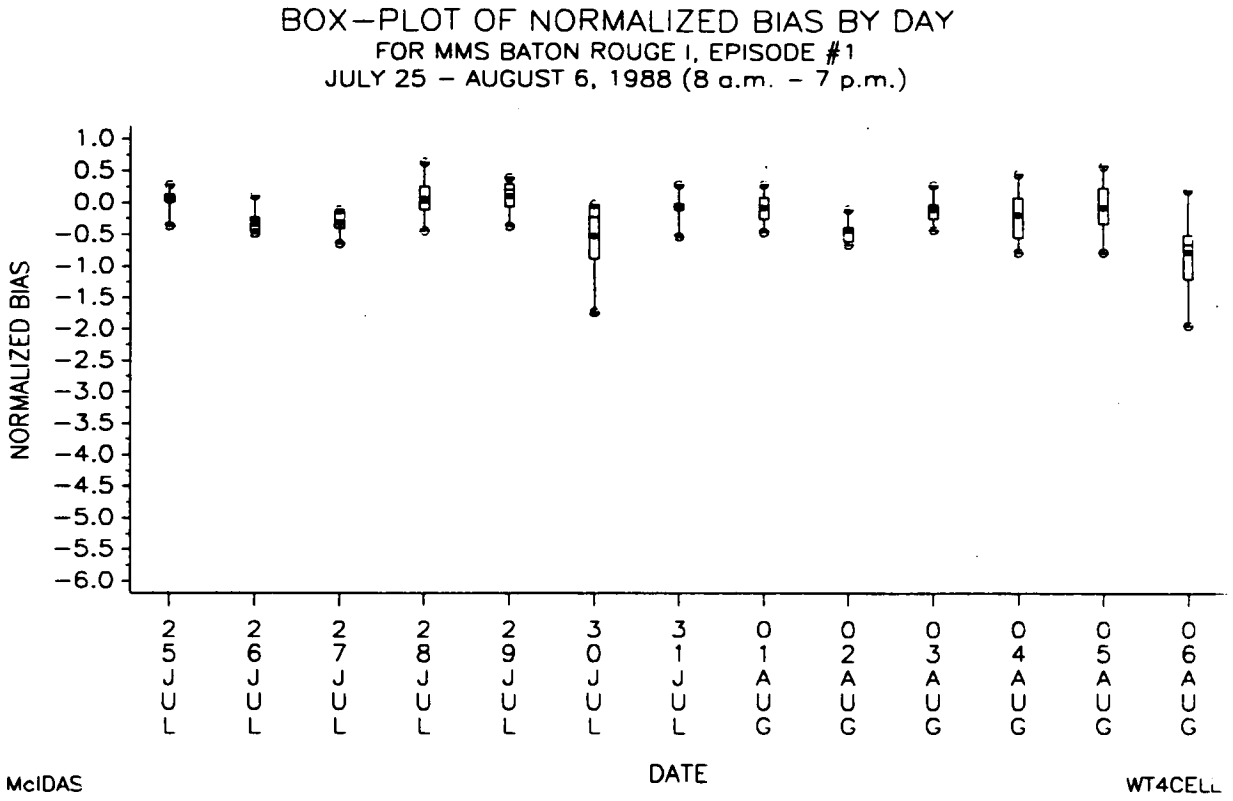
BOX–PLOT OF NORMALIZED BIAS BY DAY
FOR MMS BATON ROUGE I, EPISODE #1
JULY 25 – AUGUST 6, 1988 (8 a.m. – 7 p.m.)
NORMALIZED BIAS
1.0
0.5
0.0
-0.5
-1.0
-1.5
-2.0
-2.5
-3.0
-3.5
-4.0
-4.5
-5.0
-5.5
-6.0
25 JUL
26 JUL
27 JUL
28 JUL
29 JUL
30 JUL
31 JUL
01 AUG
02 AUG
03 AUG
04 AUG
05 AUG
06 AUG
DATE
McIDAS
WT4CELL

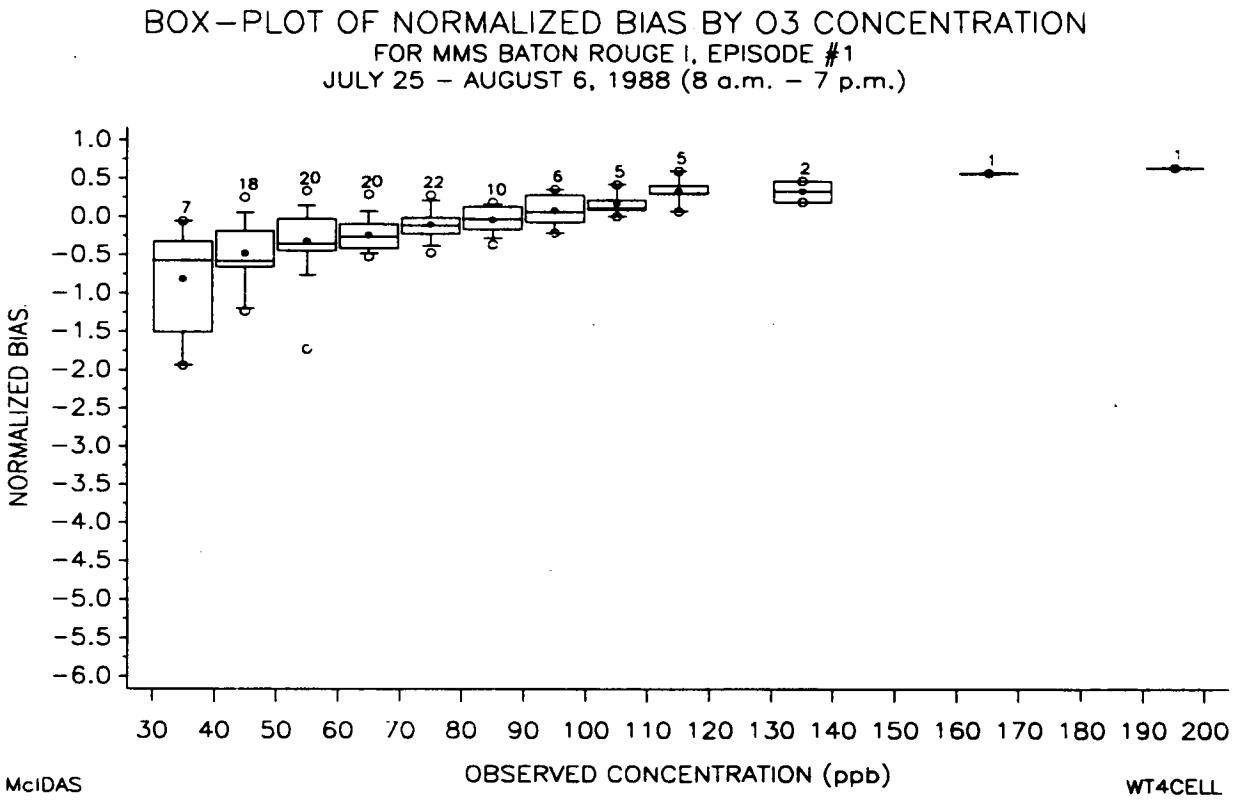
BOX–PLOT OF NORMALIZED BIAS BY O3 CONCENTRATION
FOR MMS BATON ROUGE I, EPISODE #1
JULY 25 – AUGUST 6, 1988 (8 a.m. – 7 p.m.)
NORMALIZED BIAS
1.0
0.5
0.0
-0.5
-1.0
-1.5
-2.0
-2.5
-3.0
-3.5
-4.0
-4.5
-5.0
-5.5
-6.0
7
18
20
20
22
10
6
5
5
2
1
1
c
30 40 50 60 70 80 90 100 110 120 130 140 150 160 170 180 190 200
OBSERVED CONCENTRATION (ppb)
McIDAS
WT4CELL

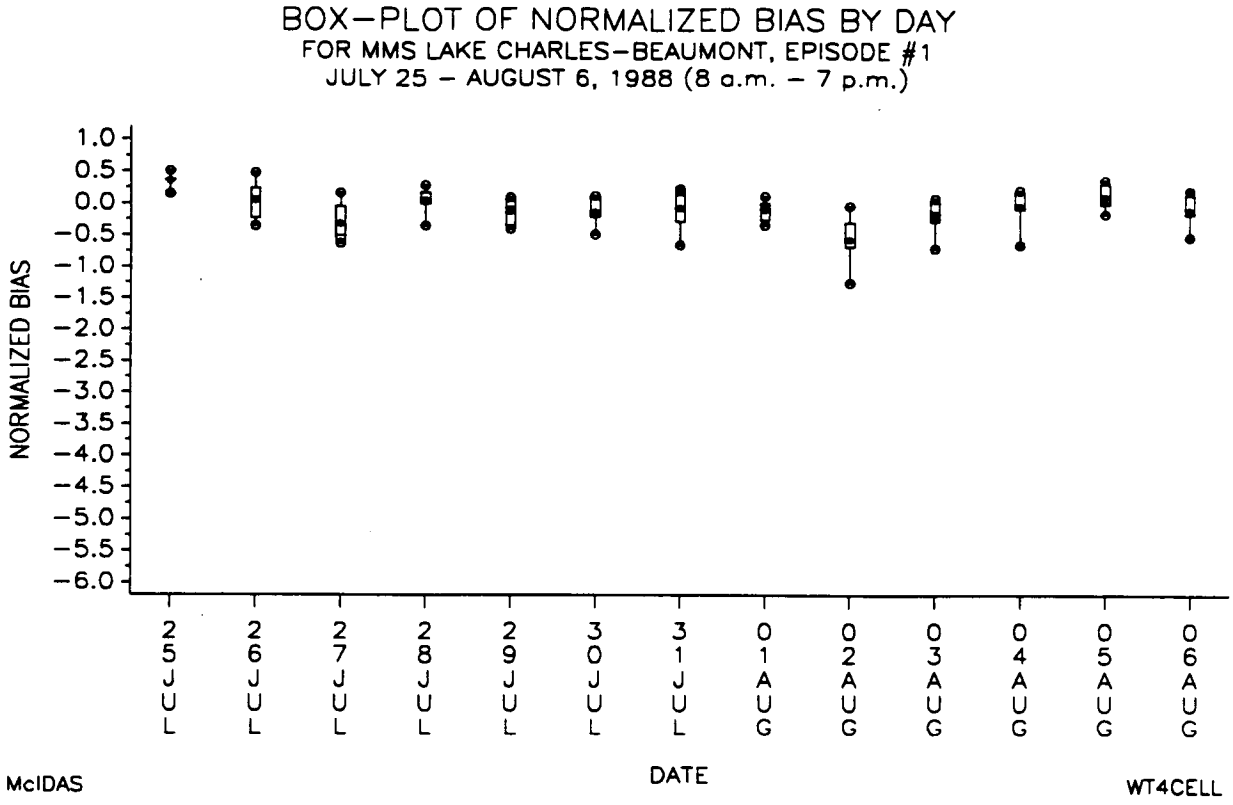
BOX–PLOT OF NORMALIZED BIAS BY DAY
FOR MMS LAKE CHARLES–BEAUMONT, EPISODE #1
JULY 25 – AUGUST 6, 1988 (8 a.m. – 7 p.m.)
NORMALIZED BIAS
1.0
0.5
0.0
−0.5
−1.0
−1.5
−2.0
−2.5
−3.0
−3.5
−4.0
−4.5
−5.0
−5.5
−6.0
25 JUL
26 JUL
27 JUL
28 JUL
29 JUL
30 JUL
31 JUL
01 AUG
02 AUG
03 AUG
04 AUG
05 AUG
06 AUG
DATE
McIDAS
WT4CELL

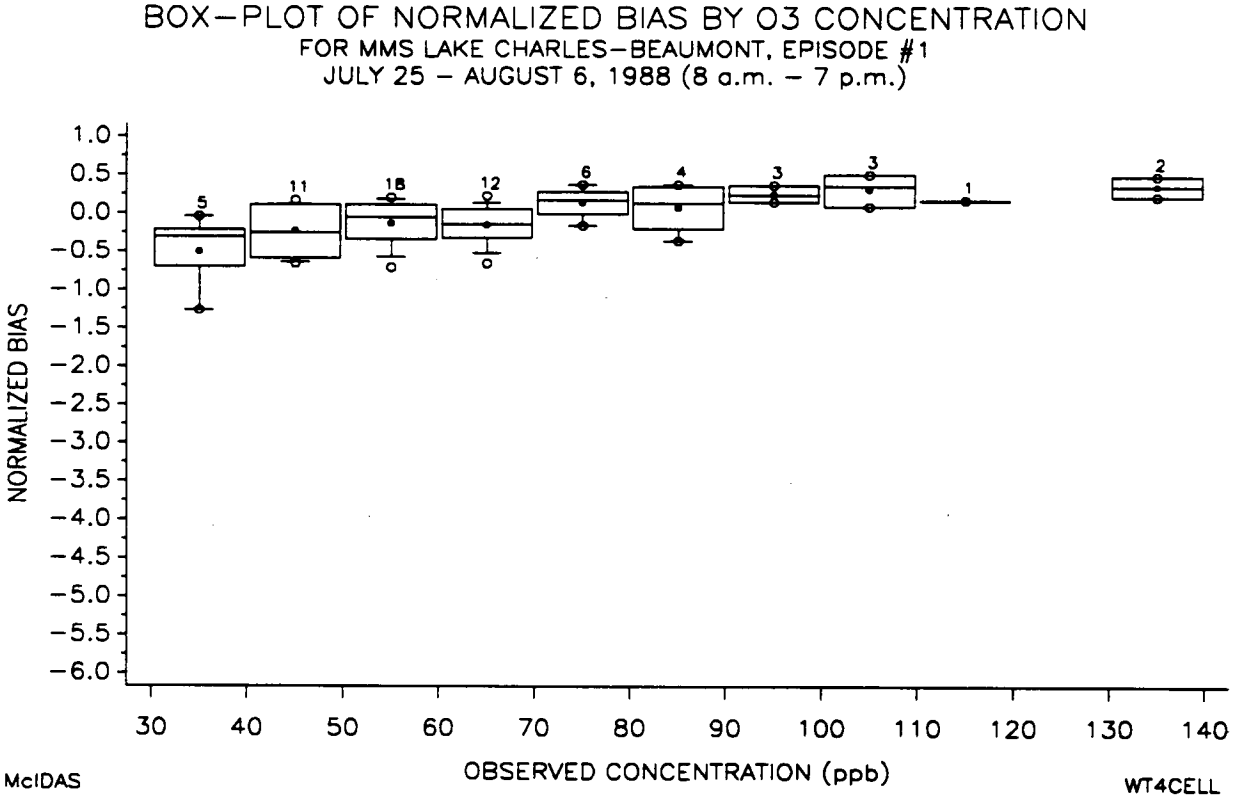
BOX–PLOT OF NORMALIZED BIAS BY O3 CONCENTRATION
FOR MMS LAKE CHARLES–BEAUMONT, EPISODE #1
JULY 25 – AUGUST 6, 1988 (8 a.m. – 7 p.m.)
NORMALIZED BIAS
1.0
0.5
0.0
−0.5
−1.0
−1.5
−2.0
−2.5
−3.0
−3.5
−4.0
−4.5
−5.0
−5.5
−6.0
5
11
18
12
6
4
3
3
1
2
30
40
50
60
70
80
90
100
110
120
130
140
OBSERVED CONCENTRATION (ppb)
McIDAS
WT4CELL

BOX–PLOT OF NORMALIZED BIAS BY DAY
FOR MMS HOUSTON–GALVESTON, EPISODE #1
JULY 25 – AUGUST 6, 1988 (8 a.m. – 7 p.m.)

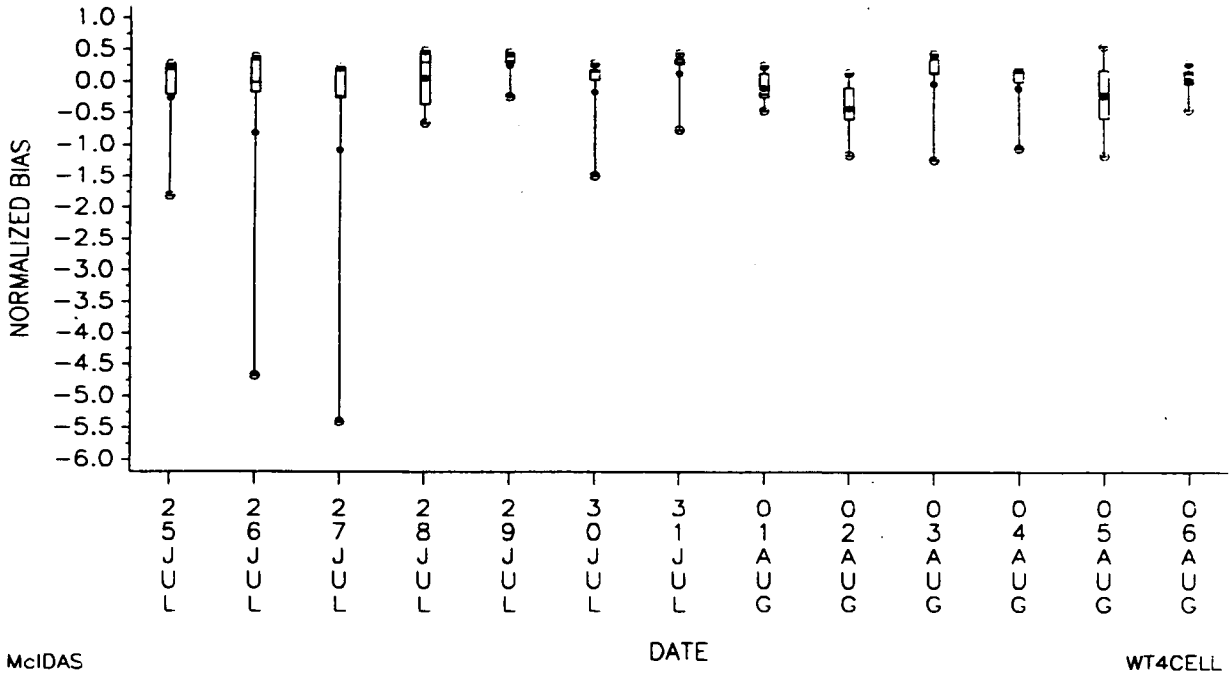

McIDAS WT4CELL

BOX–PLOT OF NORMALIZED BIAS BY O3 CONCENTRATION
FOR MMS HOUSTON–GALVESTON, EPISODE #1
JULY 25 – AUGUST 6, 1988 (8 a.m. – 7 p.m.)

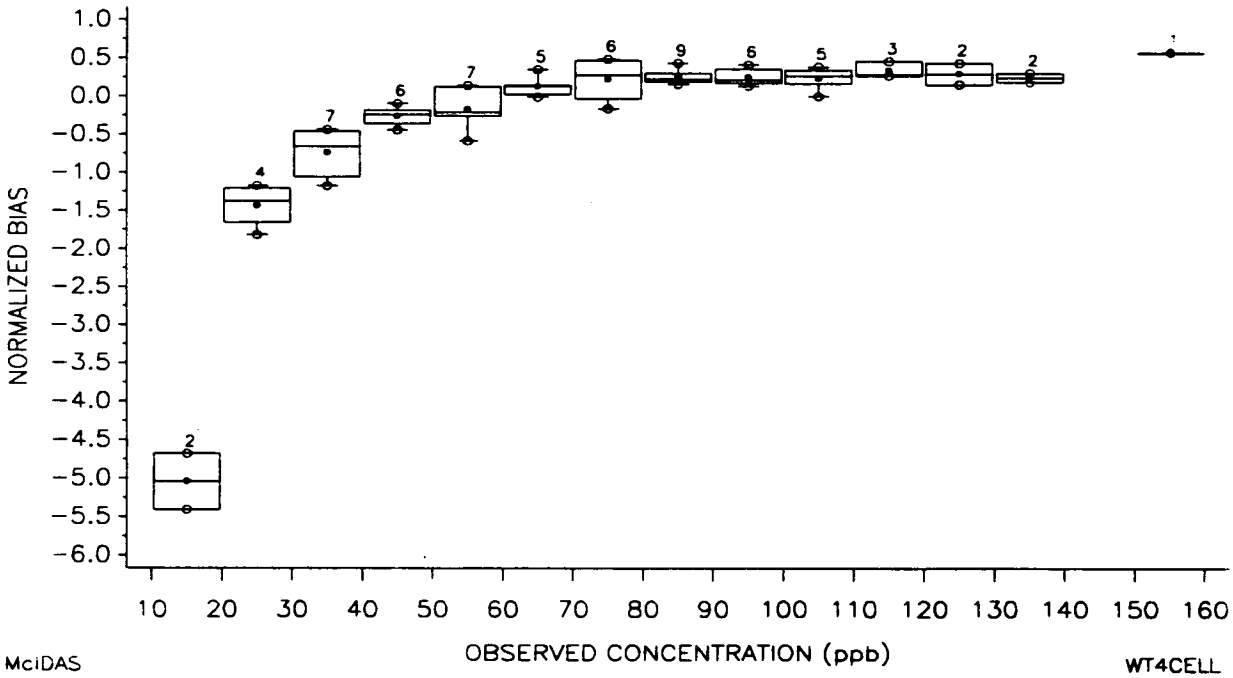

McIDAS WT4CELL

BOX–PLOT OF NORMALIZED BIAS BY DAY
FOR MMS CORPUS CHRISTI, EPISODE #1
JULY 25 – AUGUST 6, 1988 (8 a.m. – 7 p.m.)

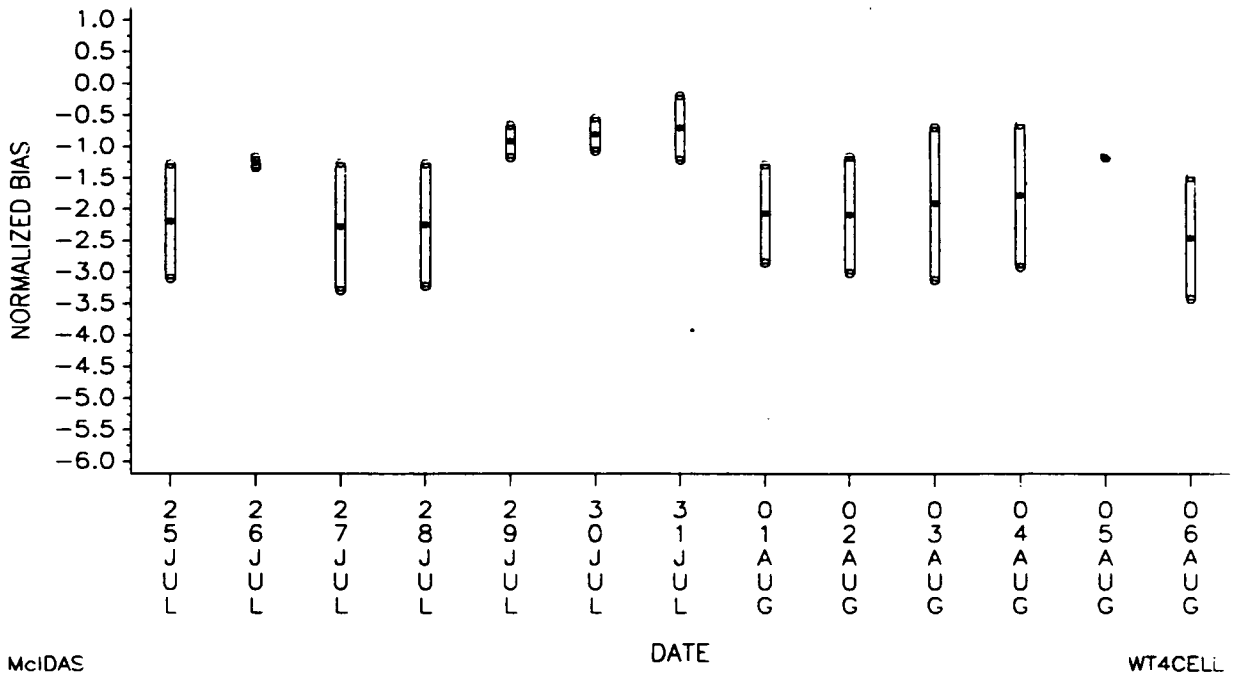

BOX–PLOT OF NORMALIZED BIAS BY O3 CONCENTRATION
FOR MMS CORPUS CHRISTI, EPISODE #1
JULY 25 – AUGUST 6, 1988 (8 a.m. – 7 p.m.)

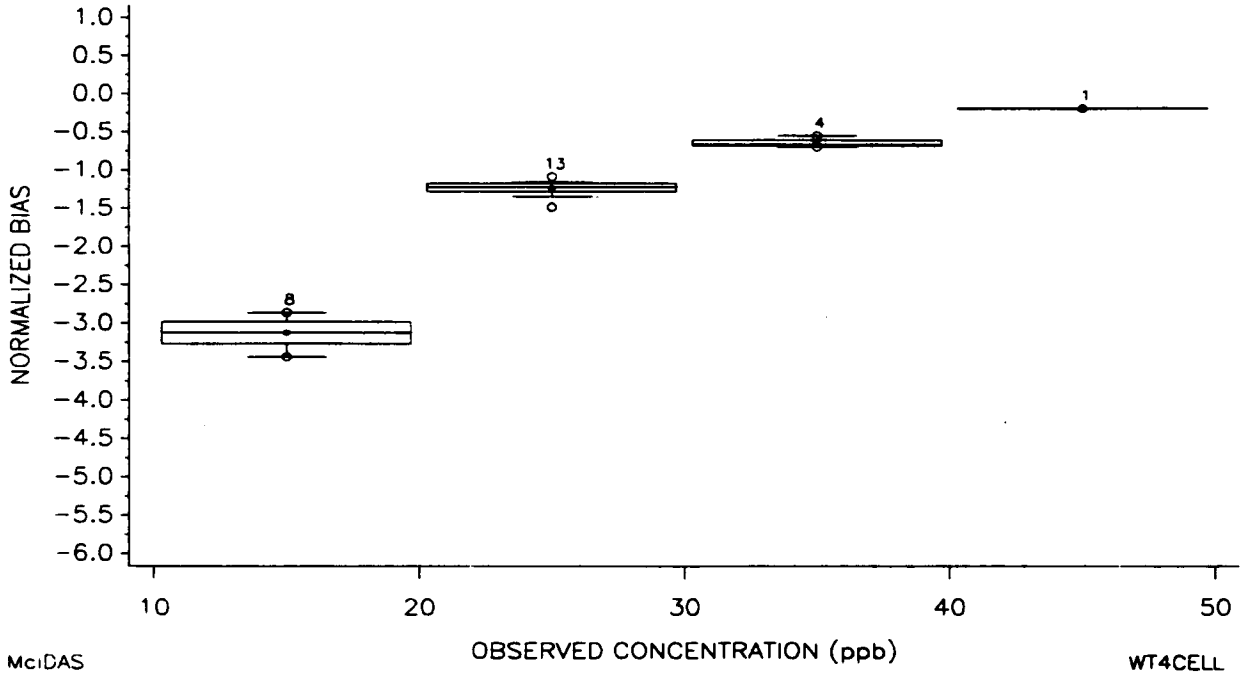

7 (a). Box-Plots of Normalized Gross Error,

For Episode #1, July 25 - August 6, 1988

BOX–PLOT OF NORMALIZED GROSS ERROR BY DAY
FOR MMS BATON ROUGE–NEW ORLEANS, EPISODE #1
JULY 25 – AUGUST 6, 1988 (8 a.m. – 7 p.m.)

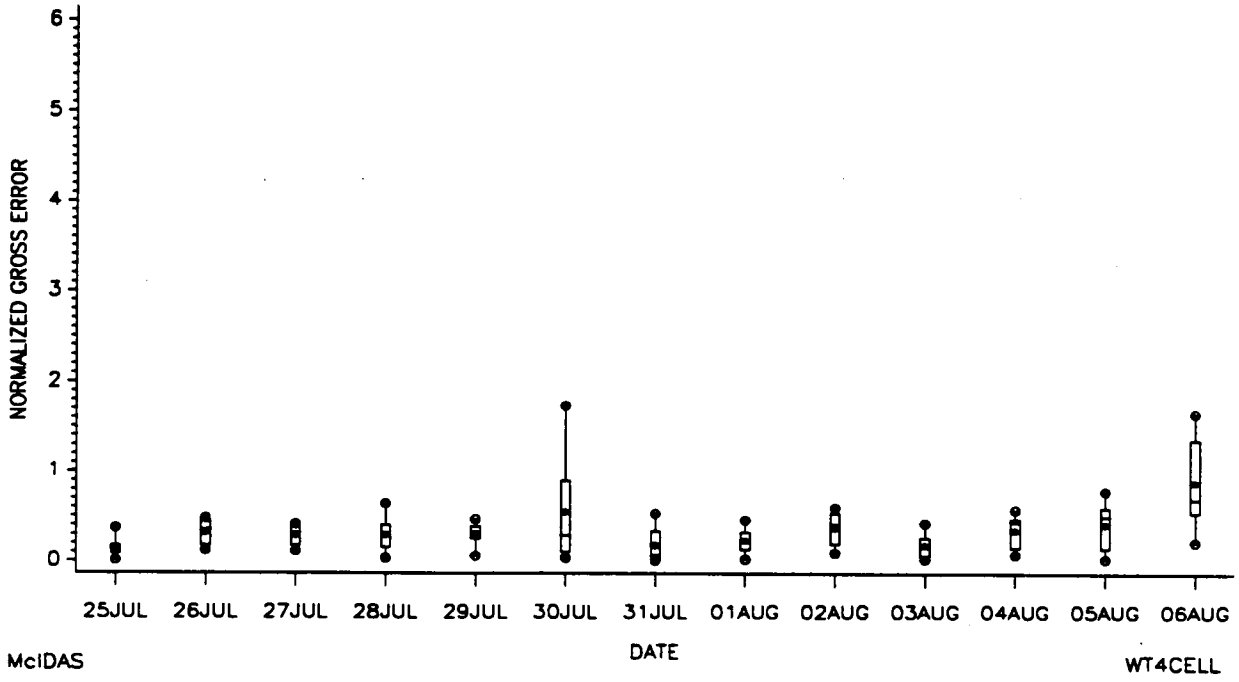

BOX–PLOT OF NORMALIZED GROSS ERROR BY O3 CONCENTRATION
FOR MMS BATON ROUGE–NEW ORLEANS, EPISODE #1
JULY 25 – AUGUST 6, 1988 (8 a.m. – 7 p.m.)

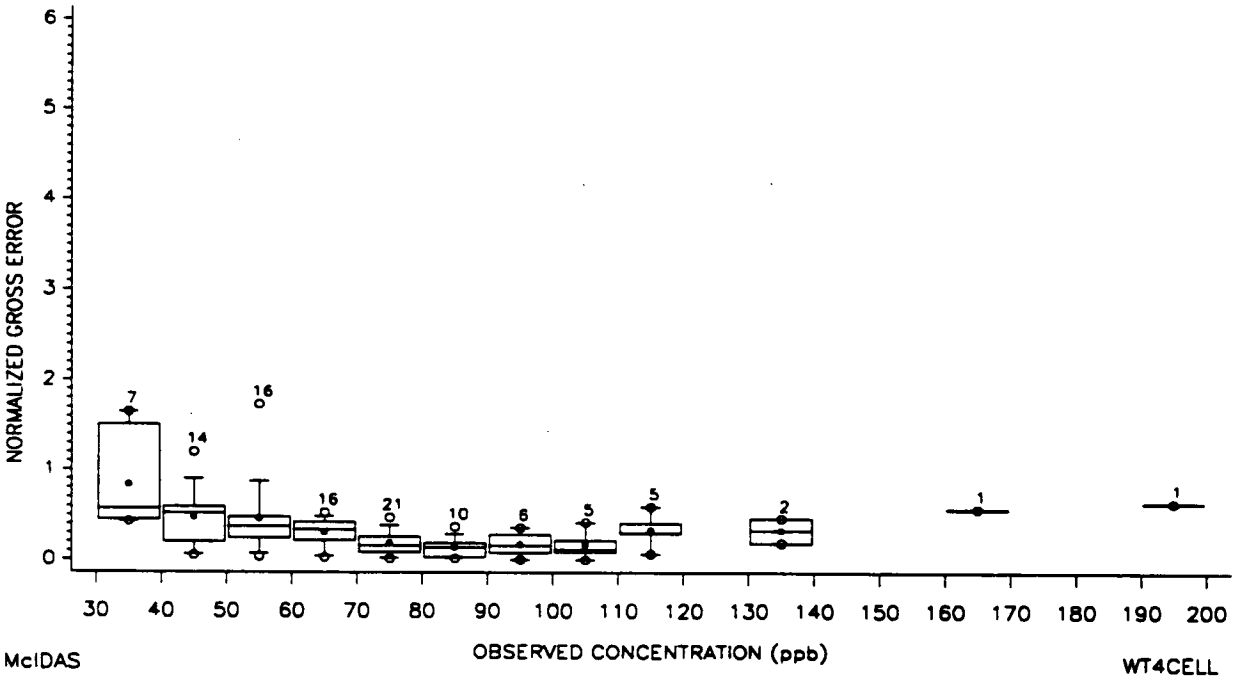

BOX–PLOT OF NORMALIZED GROSS ERROR BY DAY
FOR MMS BATON ROUGE I, EPISODE #1
JULY 25 – AUGUST 6, 1988 (8 a.m. – 7 p.m.)

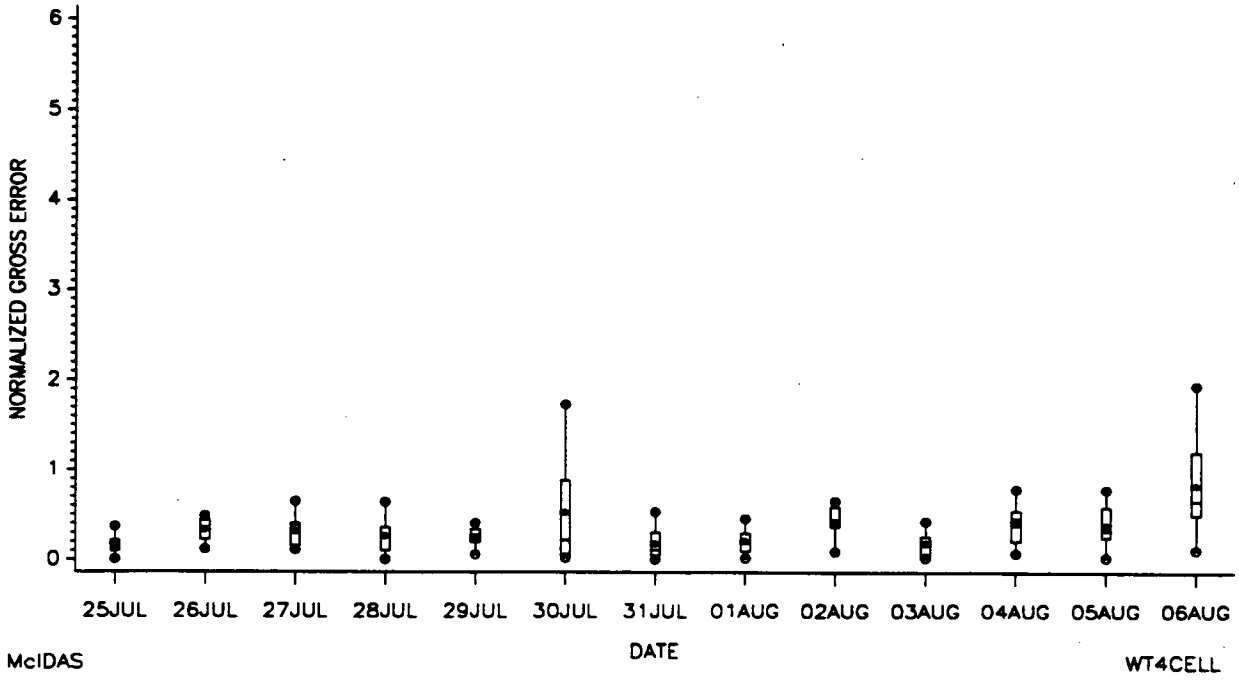

BOX–PLOT OF NORMALIZED GROSS ERROR BY O3 CONCENTRATION
FOR MMS BATON ROUGE I, EPISODE #1
JULY 25 – AUGUST 6, 1988 (8 a.m. – 7 p.m.)

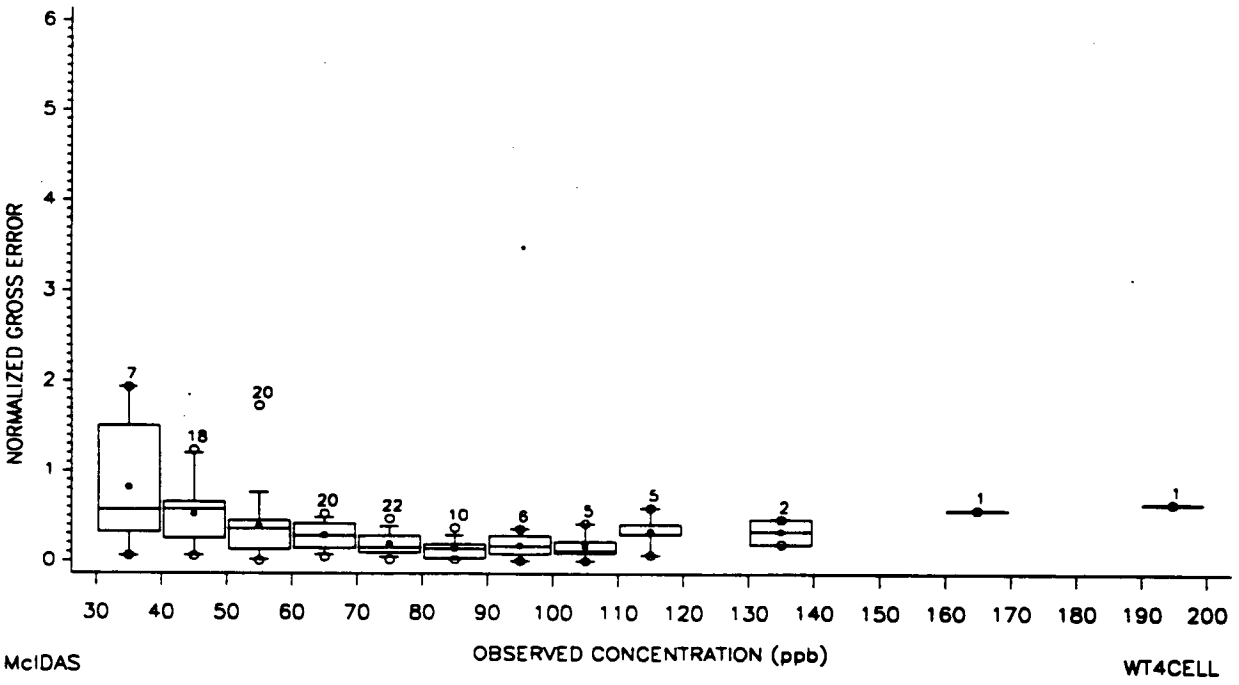

BOX–PLOT OF NORMALIZED GROSS ERROR BY DAY
FOR MMS LAKE CHARLES–BEAUMONT, EPISODE #1
JULY 25 – AUGUST 6, 1988 (8 a.m. – 7 p.m.)

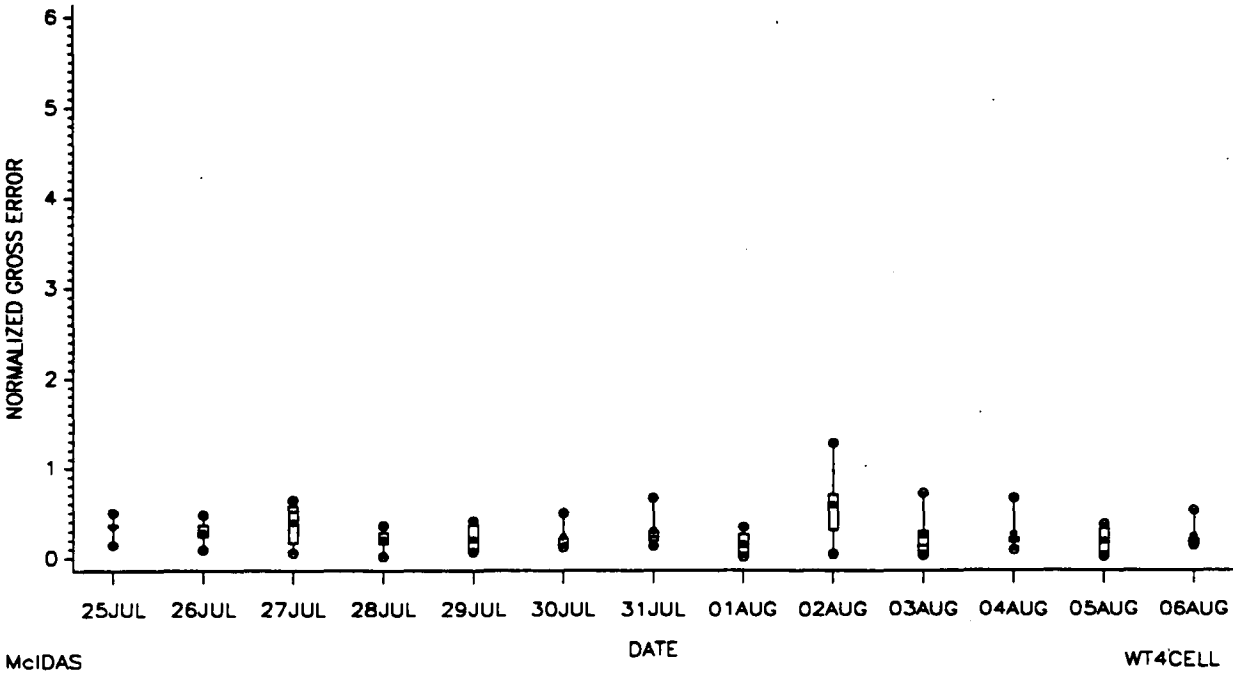

BOX–PLOT OF NORMALIZED GROSS ERROR BY O3 CONCENTRATION
FOR MMS LAKE CHARLES–BEAUMONT, EPISODE #1
JULY 25 – AUGUST 6, 1988 (8 a.m. – 7 p.m.)

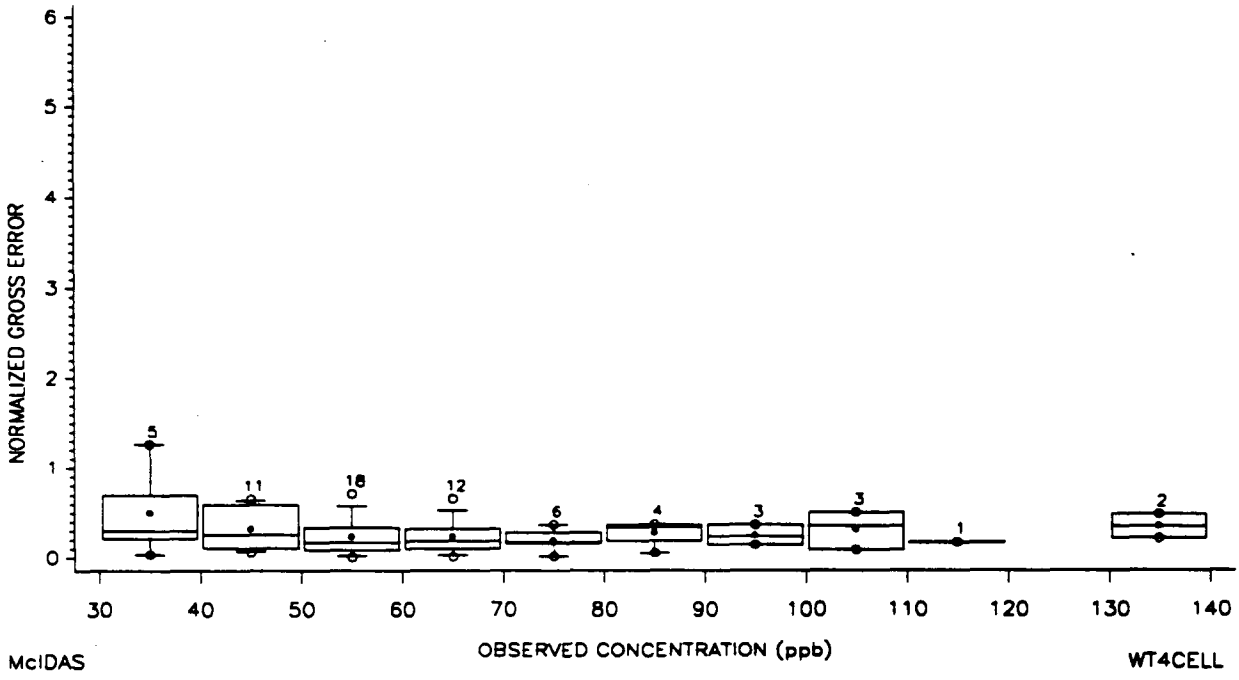

BOX–PLOT OF NORMALIZED GROSS ERROR BY DAY
FOR MMS HOUSTON–GALVESTON, EPISODE #1
JULY 25 – AUGUST 6, 1988 (8 a.m. – 7 p.m.)

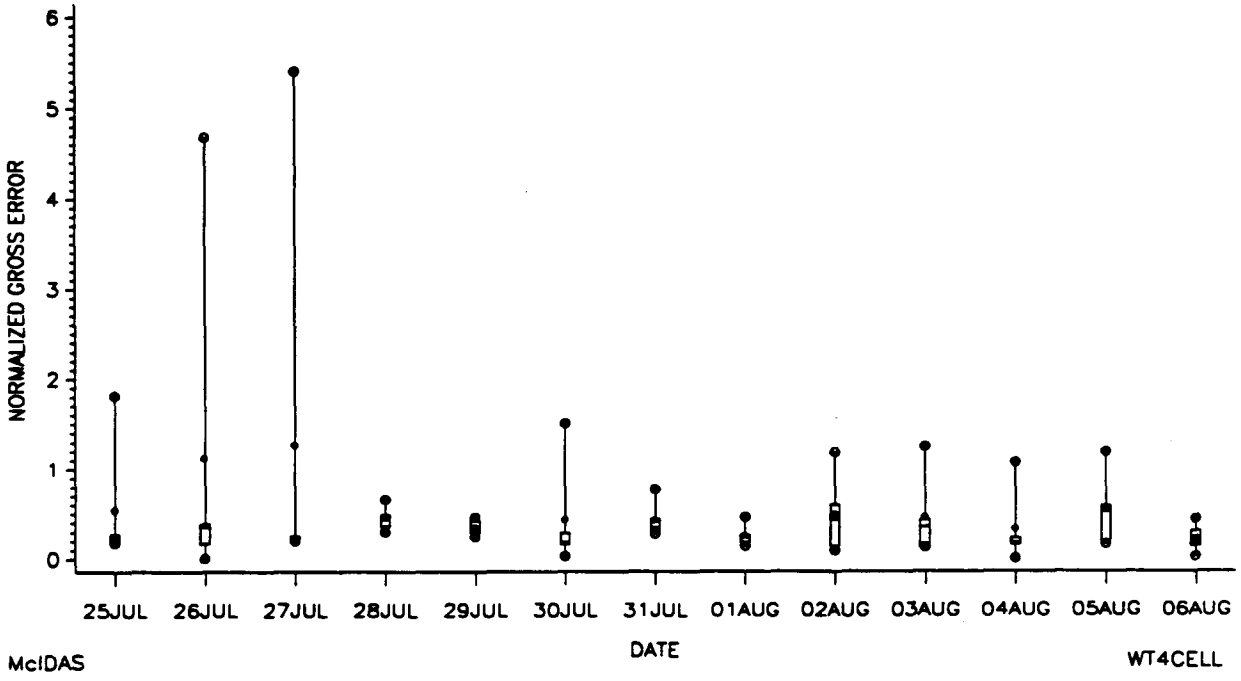

BOX–PLOT OF NORMALIZED GROSS ERROR BY O3 CONCENTRATION
FOR MMS HOUSTON–GALVESTON, EPISODE #1
JULY 25 – AUGUST 6, 1988 (8 a.m. – 7 p.m.)

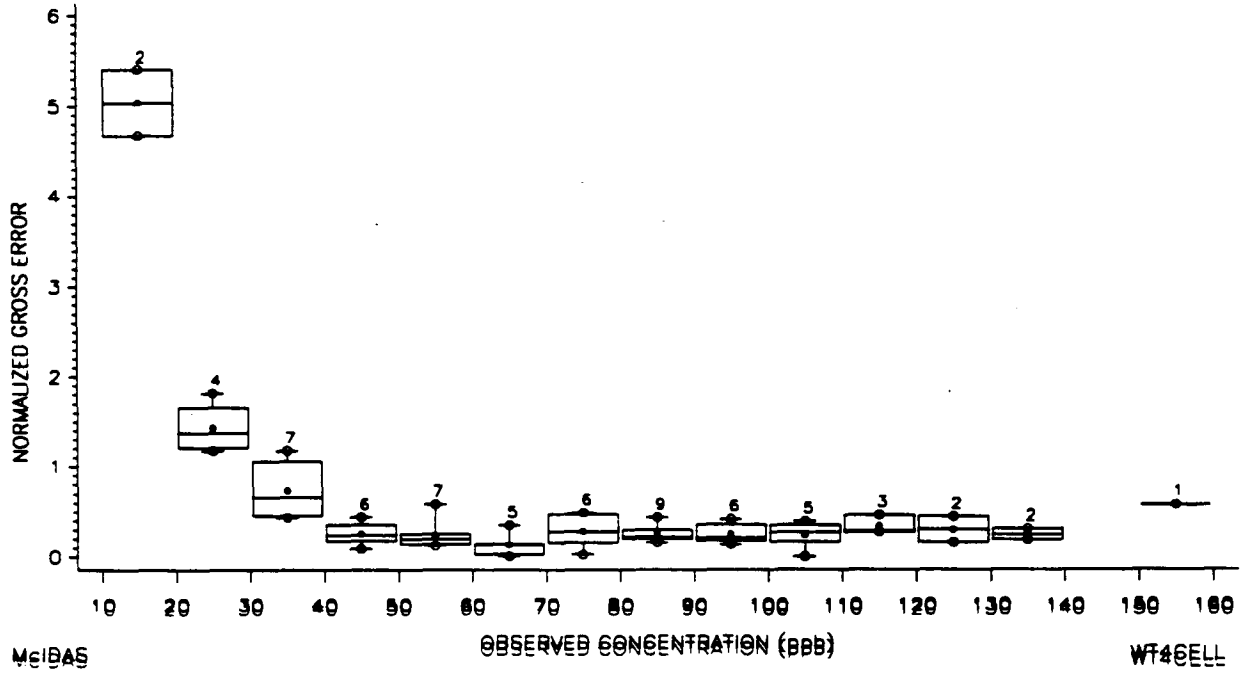

BOX–PLOT OF NORMALIZED GROSS ERROR BY DAY
FOR MMS CORPUS CHRISTI, EPISODE #1
JULY 25 – AUGUST 6, 1988 (8 a.m. – 7 p.m.)

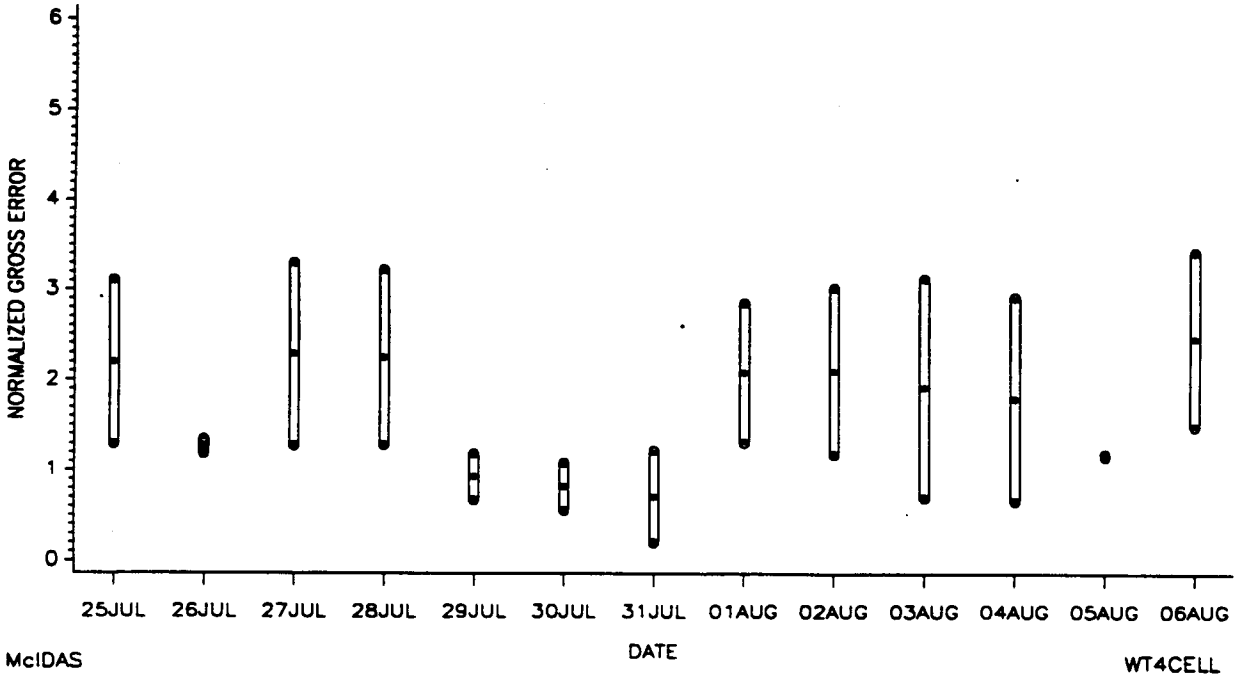

BOX–PLOT OF NORMALIZED GROSS ERROR BY O3 CONCENTRATION
FOR MMS CORPUS CHRISTI, EPISODE #1
JULY 25 – AUGUST 6, 1988 (8 a.m. – 7 p.m.)

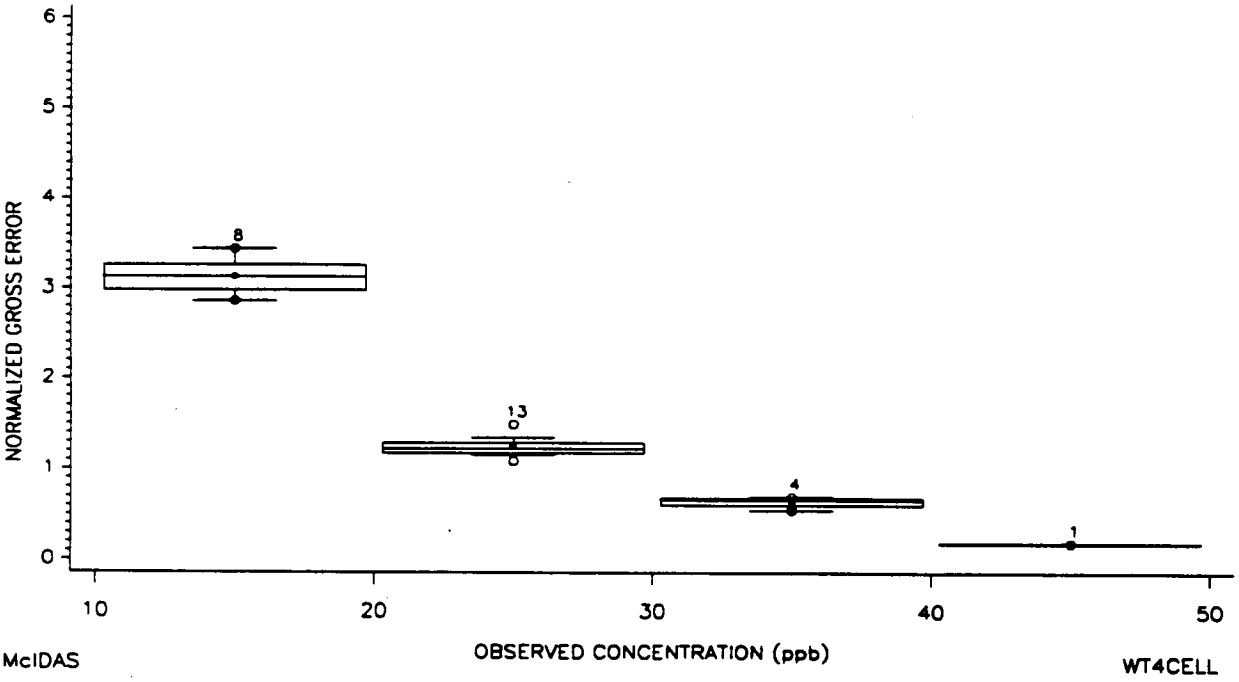

8 (a). Plots of Daily Paired Accuracy by Subregion,

For Episode #1, July 25 - August 6, 1988

DAILY PAIRED ACCURACY BY SUBREGION

FOR EPISODE #1

JULY 25 – AUGUST 6, 1988 (8 a.m. – 7 p.m.)

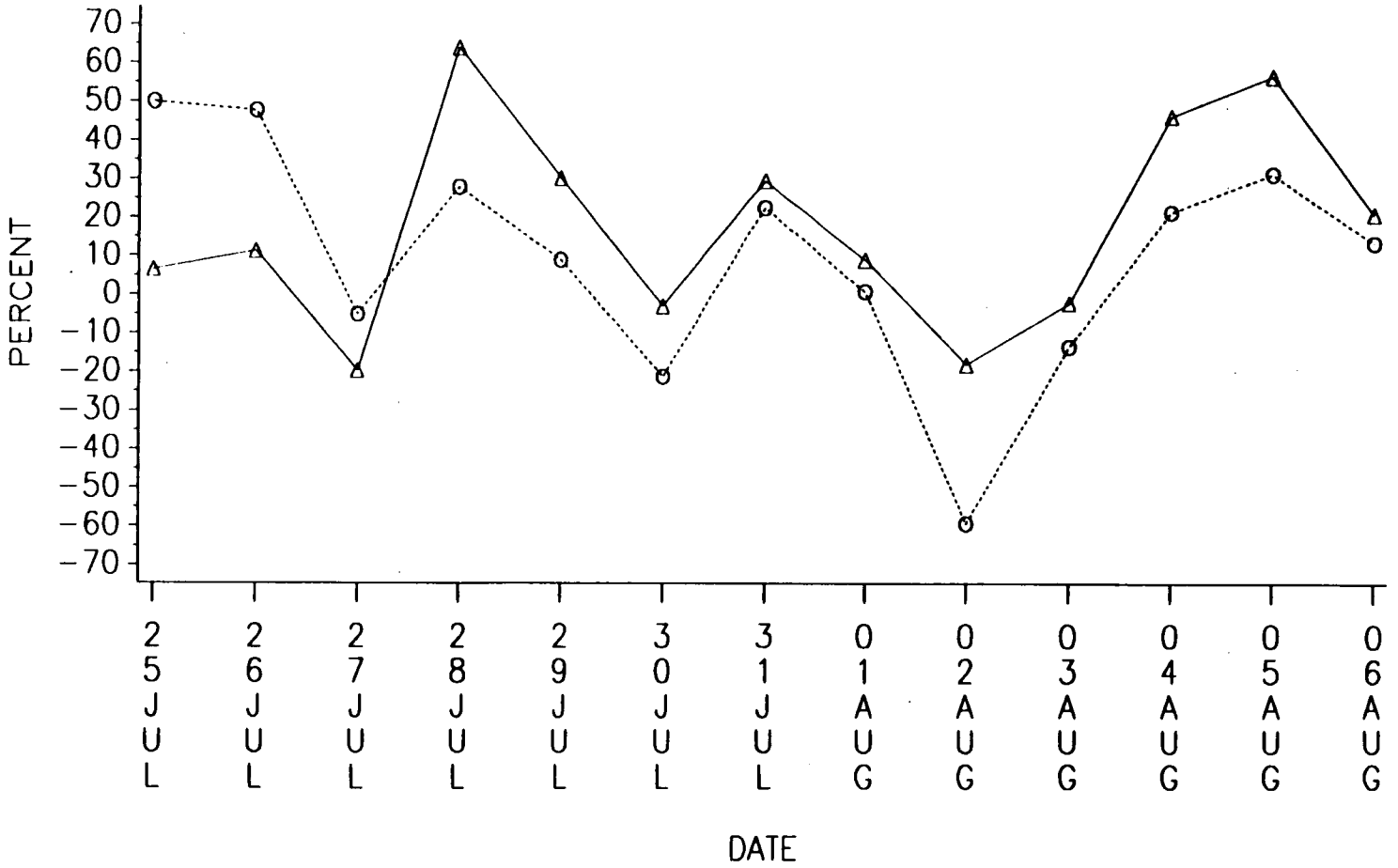

McIDAS
WT4CELL

DAILY PAIRED ACCURACY BY SUBREGION

FOR EPISODE #1

JULY 25 – AUGUST 6, 1988 (8 a.m. – 7 p.m.)

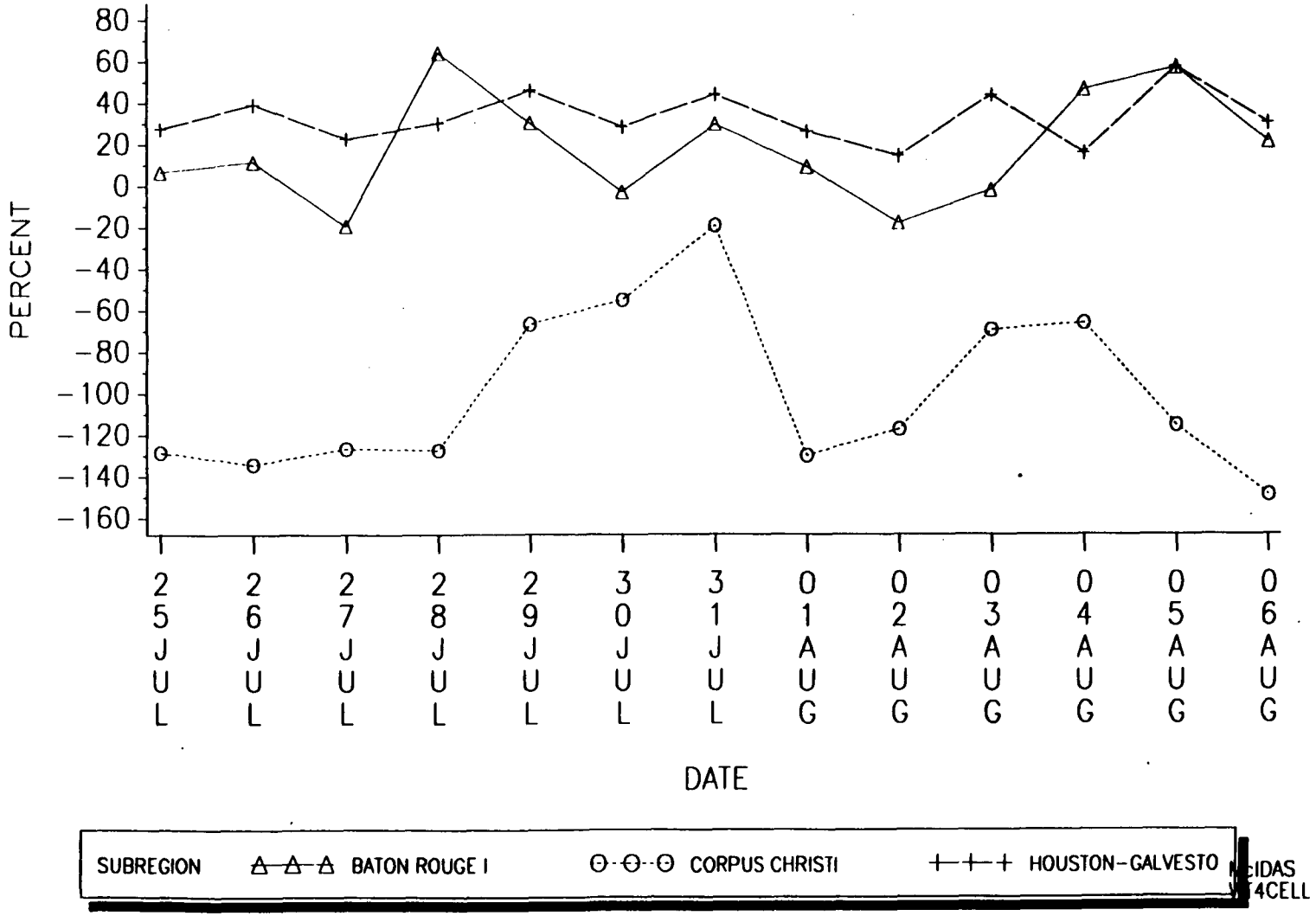

9 (a). Plots of Daily Unpaired Accuracy by Subregion.

For Episode #1, July 25 - August 6, 1988

DAILY UNPAIRED ACCURACY BY SUBREGION

FOR EPISODE #1

JULY 25 – AUGUST 6, 1988 (8 a.m. – 7 p.m.)

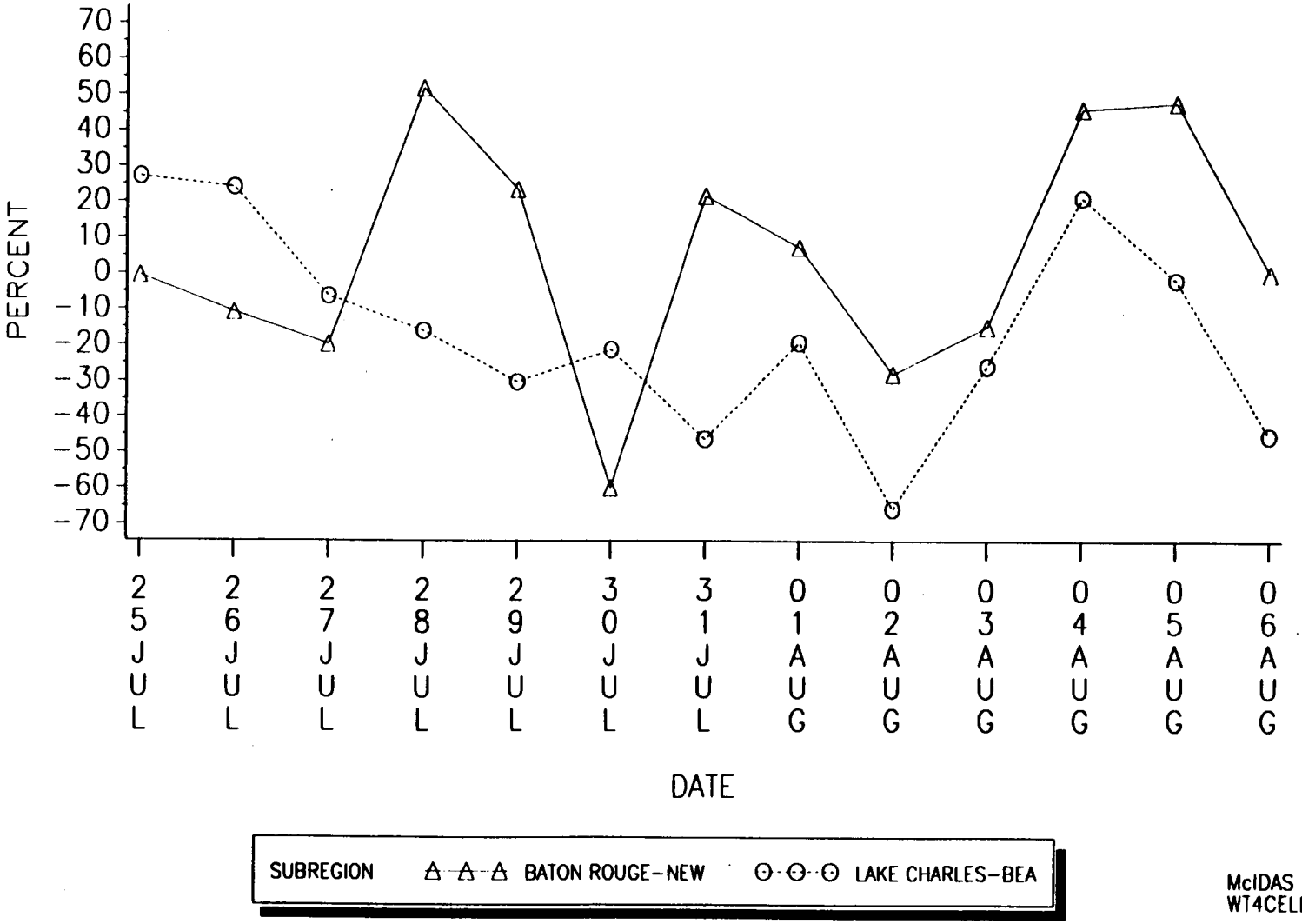

McIDAS
WT4CELL

DAILY UNPAIRED ACCURACY BY SUBREGION

FOR EPISODE #1

JULY 25 – AUGUST 6, 1988 (8 a.m. – 7 p.m.)

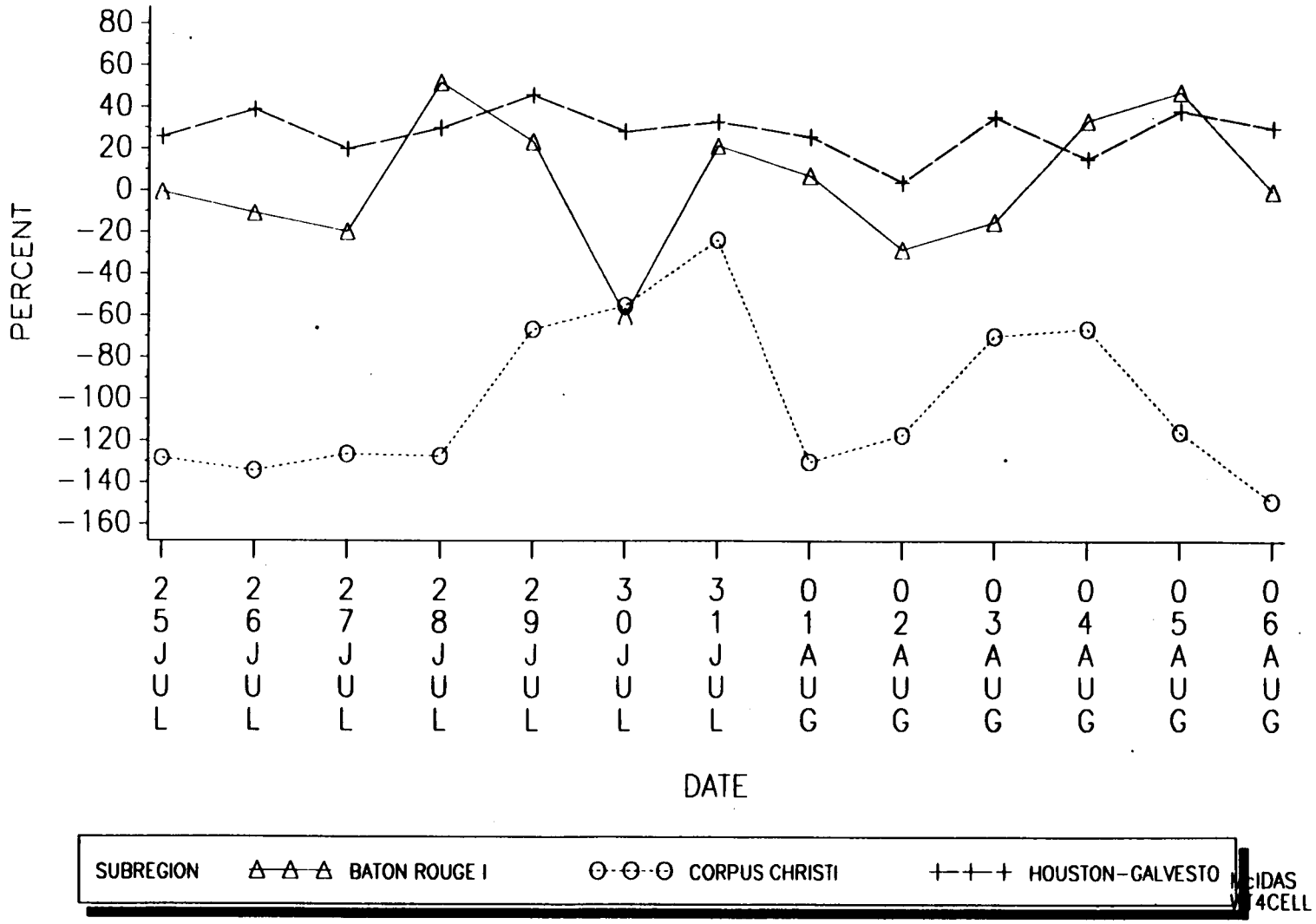

1 (b). Scatter Plots of Hourly Ozone (Paired in Spaced & Time)

For Episode #2, July 26 - July 31, 1990

SCATTER PLOT OF HOURLY O3 (PAIRED IN SPACE & TIME)

FOR BATON ROUGE-NEW ORLEANS, EPISODE #2

JULY 26-31, 1992 (8 a.m. - 7 p.m.)

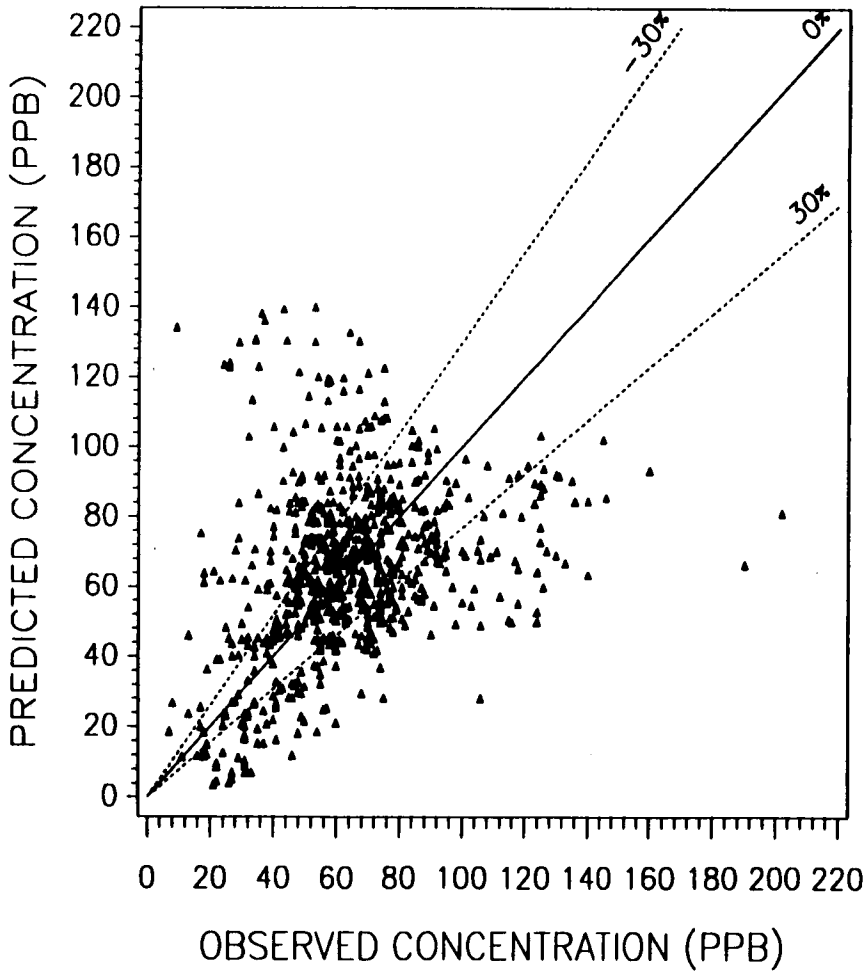

McIDAS
WT4CELL

SCATTER PLOT OF HOURLY O3 (PAIRED IN SPACE & TIME)

BATON ROUGE I, EPISODE #2

JULY 26–31, 1990 (8 a.m. – 7 p.m.)

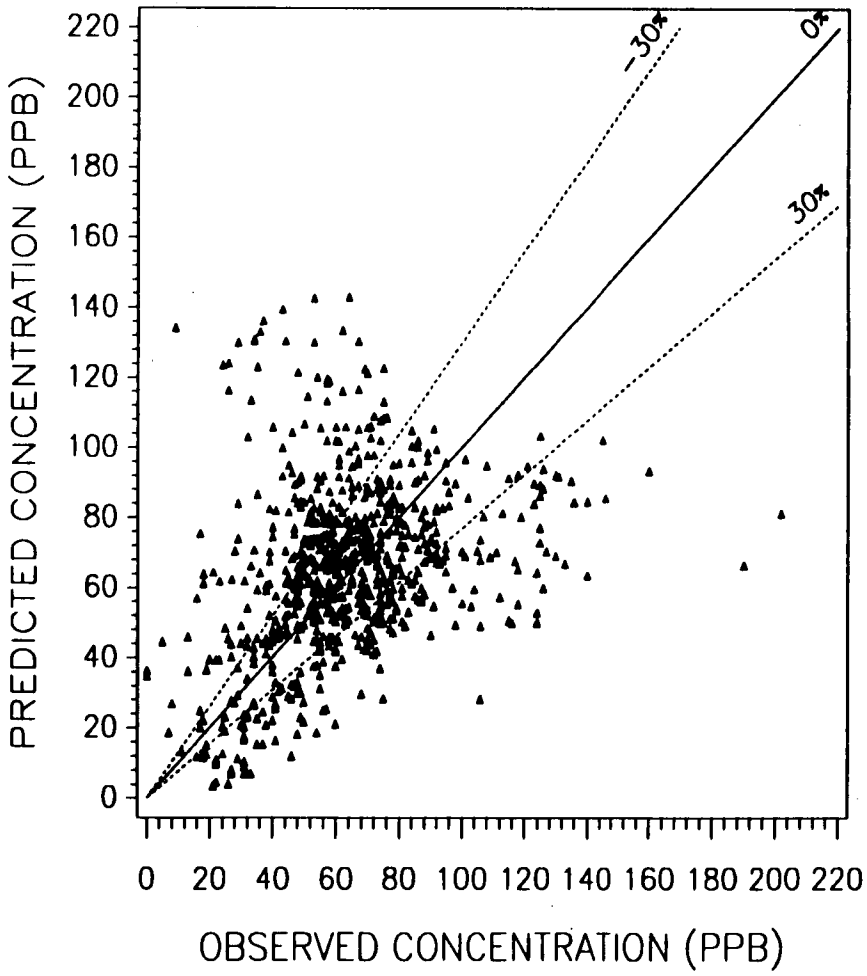

McIDAS
WT4CELL

SCATTER PLOT OF HOURLY O3 (PAIRED IN SPACE & TIME)
FOR LAKE CHARLES–BEAUMONT, EPISODE #2
JULY 26–31, 1992 (8 a.m. – 7 p.m.)

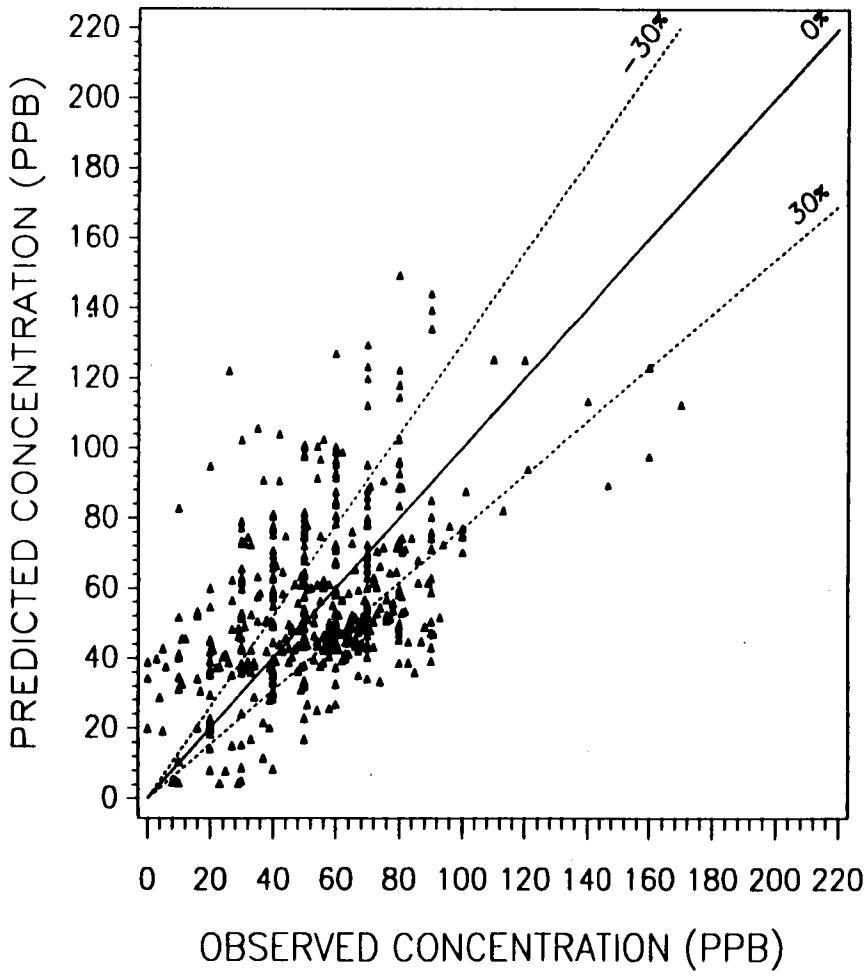

McIDAS
WT4CELL

SCATTER PLOT OF HOURLY O3 (PAIRED IN SPACE & TIME)

HOUSTON-GALVESTON, EPISODE #2

JULY 26-31, 1990 (8 a.m. - 7 p.m.)

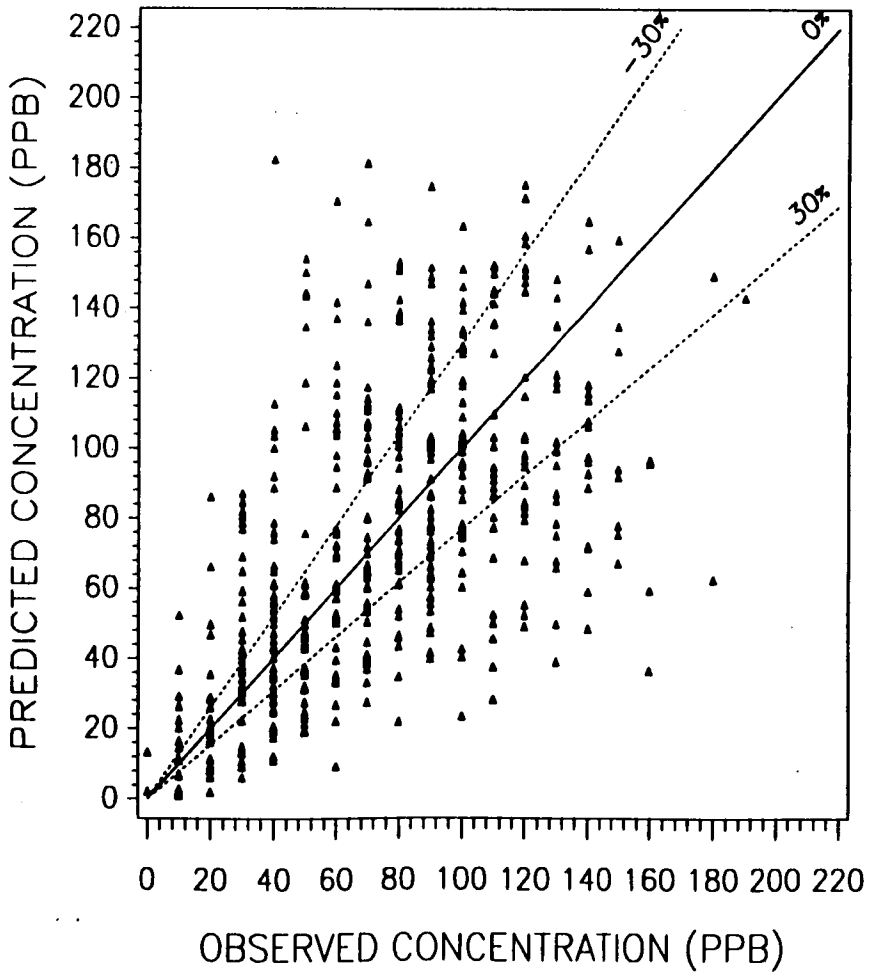

McIDAS
WT4CELL

SCATTER PLOT OF HOURLY O3 (PAIRED IN SPACE & TIME)

CORPUS CHRISTI, EPISODE #2

JULY 26-31, 1990 (8 a.m. - 7 p.m.)

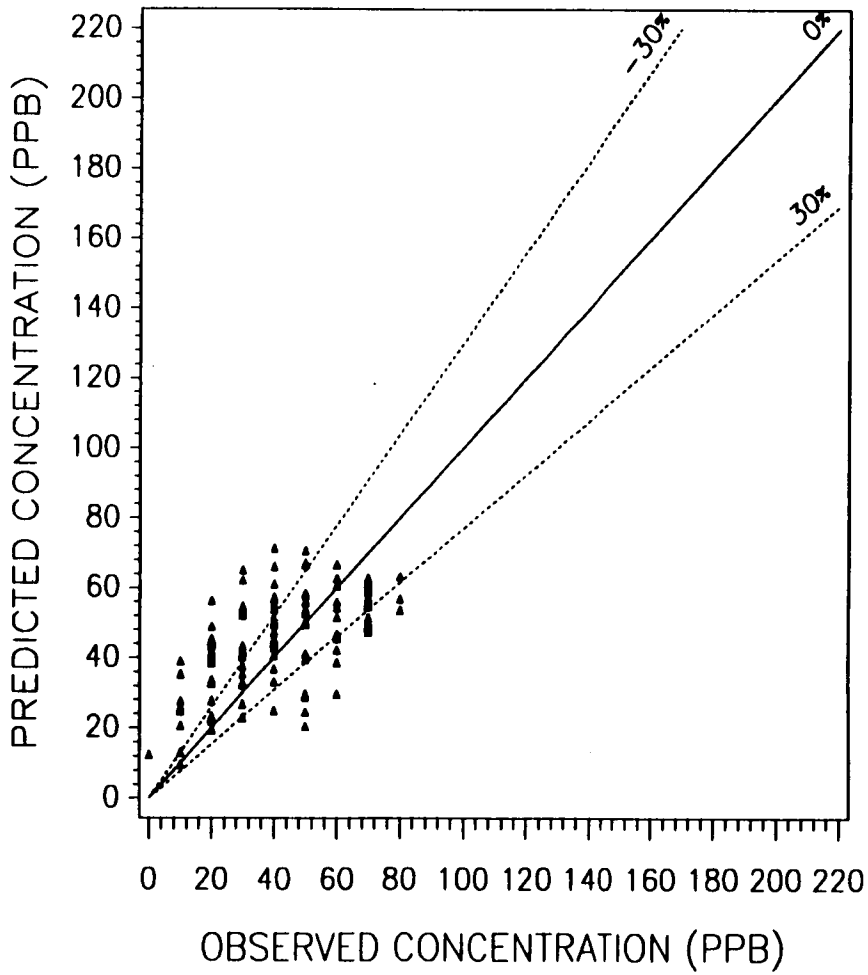

McIDAS
WT4CELL

2 (b). Quantile-Quantile Plots of Ozone Concentrations

For Episode #2, July 26 - July 31, 1990

QUANTILE – QUANTILE PLOT OF OZONE CONCENTRATIONS
FOR BATON ROUGE–NEW ORLEANS, EPISODE #2
JULY 26–31, 1990 (8 a.m. – 7 p.m.)

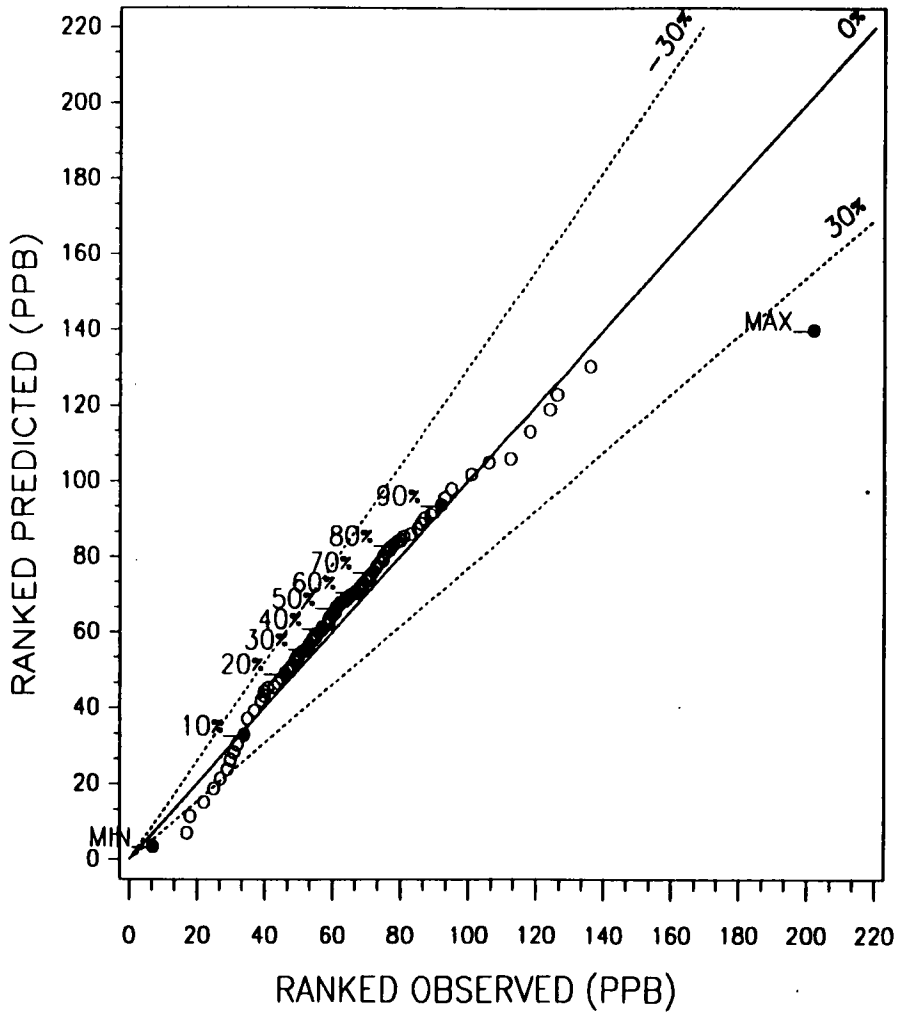

McIDAS
WT4CELL

QUANTILE – QUANTILE PLOT OF OZONE CONCENTRATIONS

FOR BATON ROUGE I, EPISODE #2

JULY 26–31, 1990 (8 a.m. – 7 p.m.)

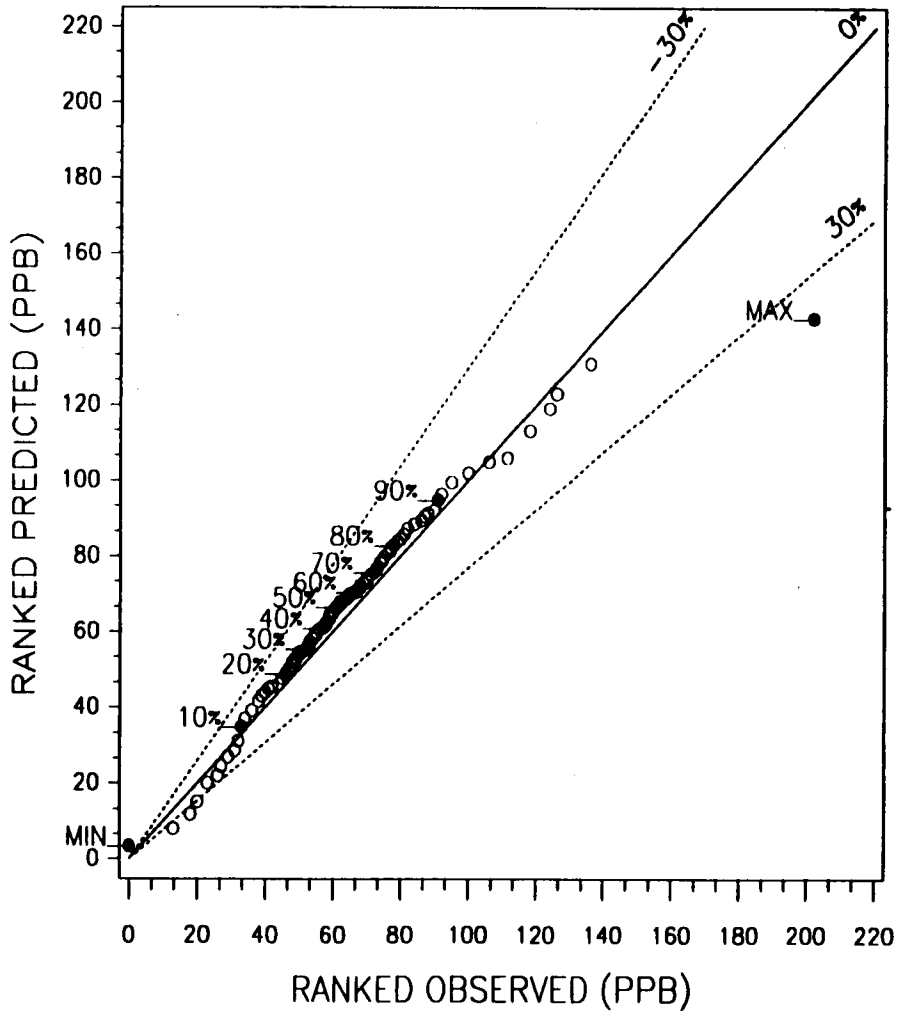

McIDAS
WT4CELL

QUANTILE – QUANTILE PLOT OF OZONE CONCENTRATIONS
FOR LAKE CHARLES–BEAUMONT, EPISODE #2
JULY 26–31, 1990 (8 a.m. – 7 p.m.)

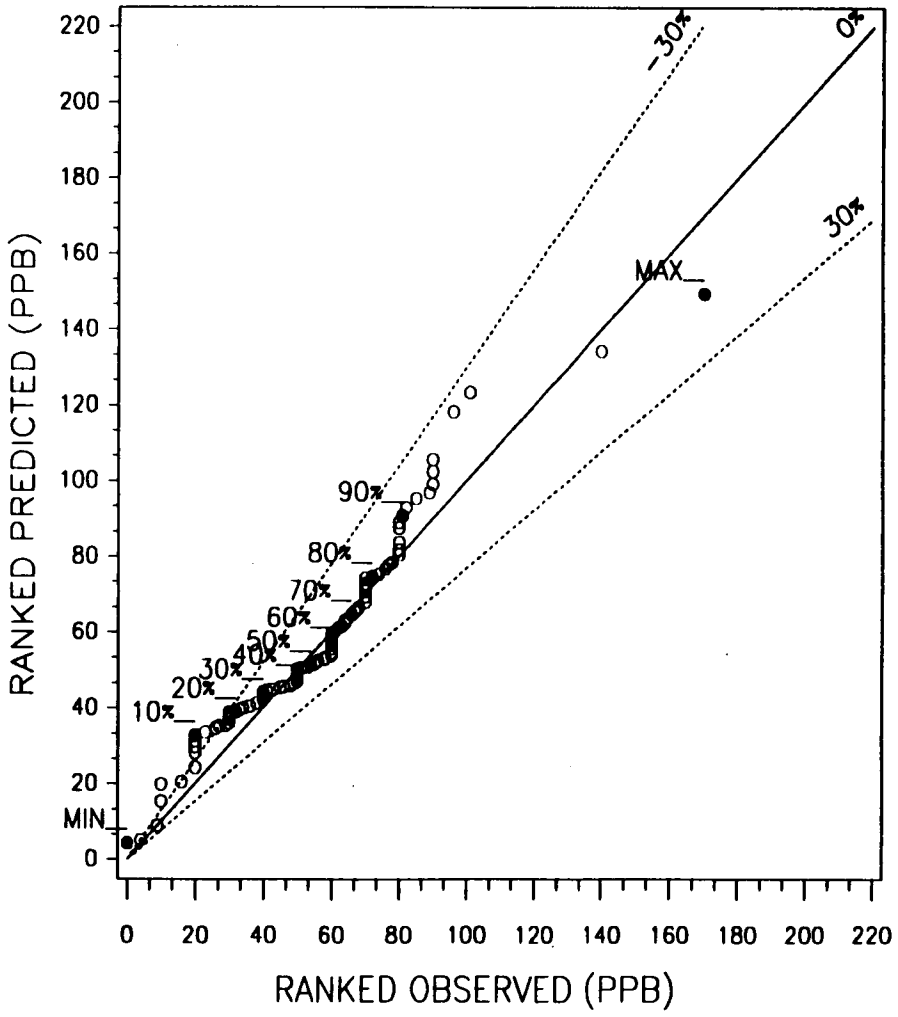

McIDAS
WT4CELL

QUANTILE – QUANTILE PLOT OF OZONE CONCENTRATIONS
FOR HOUSTON–GALVESTON, EPISODE #2
JULY 26–31, 1990 (8 a.m. – 7 p.m.)

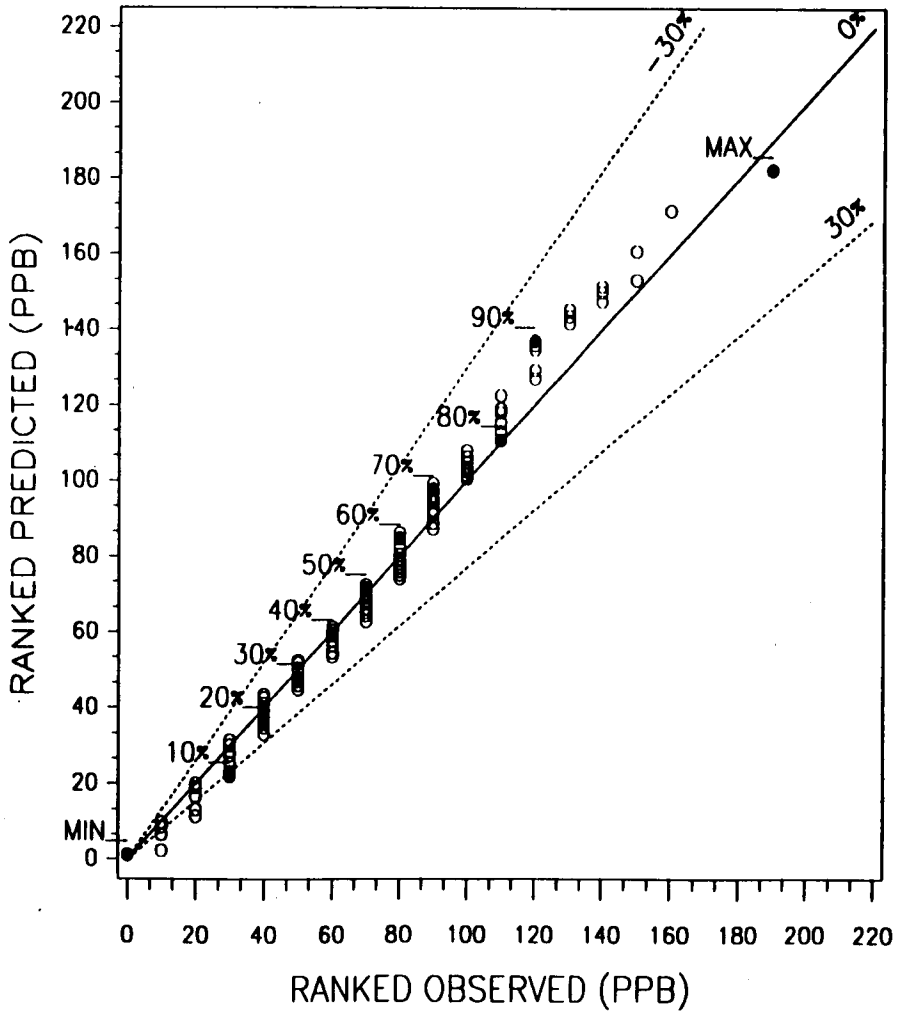

McIDAS
WT4CELL

QUANTILE – QUANTILE PLOT OF OZONE CONCENTRATIONS
FOR CORPUS CHRISTI, EPISODE #2
JULY 26–31, 1990 (8 a.m. – 7 p.m.)

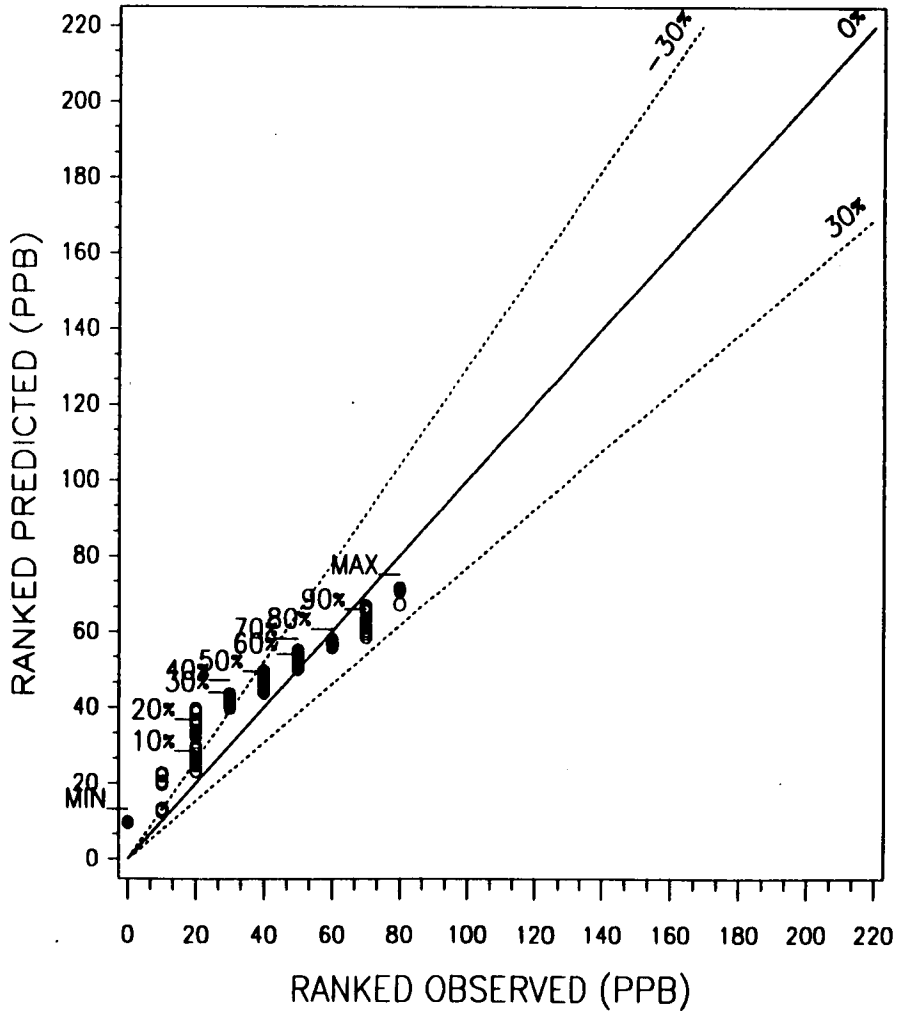

McIDAS
WT4CELL

3 (b). Time Series Plots of Maximum Hourly Ozone Concentrations

For Episode #2, July 26 - July 31, 1990

MAXIMUM HOURLY O3 CONCENTRATIONS
FOR MMS BATON ROUGE-NEW ORLEANS, EPISODE #2
JULY 26-31, 1990

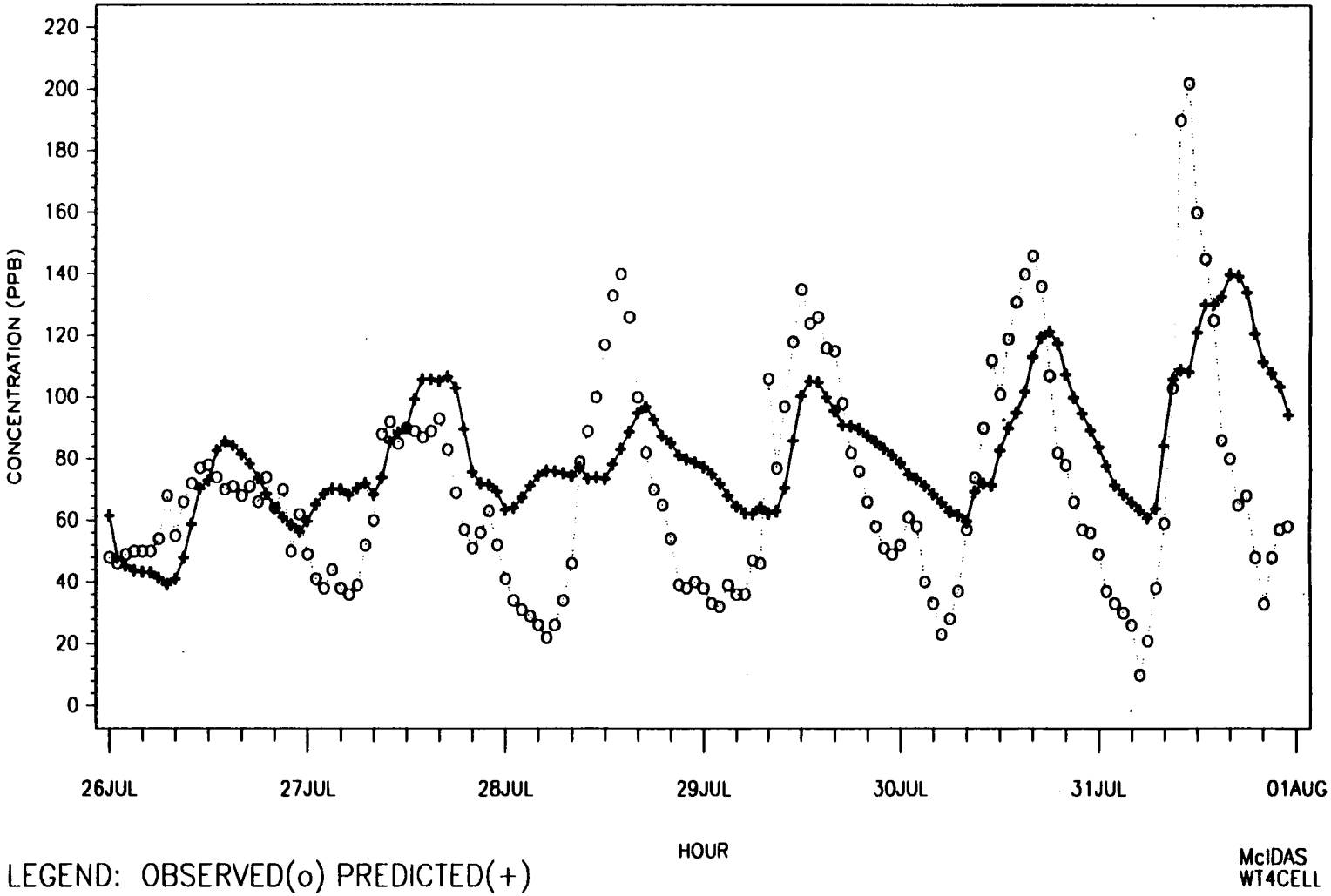

LEGEND: OBSERVED(o) PREDICTED(+)

MAXIMUM HOURLY O3 CONCENTRATIONS
FOR MMS BATON ROUGE I, EPISODE #2
JULY 26-31, 1990

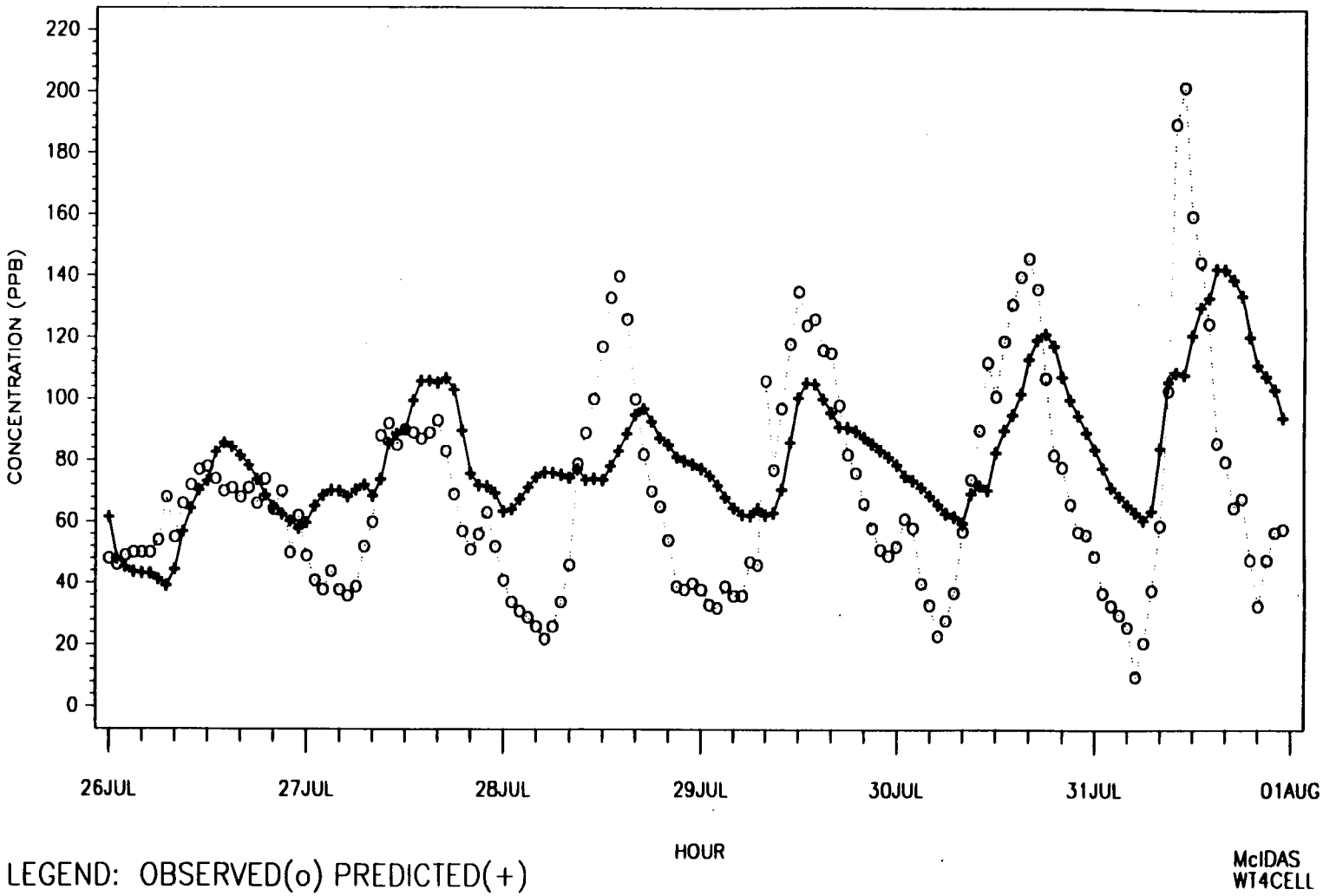

LEGEND: OBSERVED(o) PREDICTED(+)

MAXIMUM HOURLY O3 CONCENTRATIONS
FOR MMS LAKE CHARLES-BEAUMONT, EPISODE #2
JULY 26-31, 1990

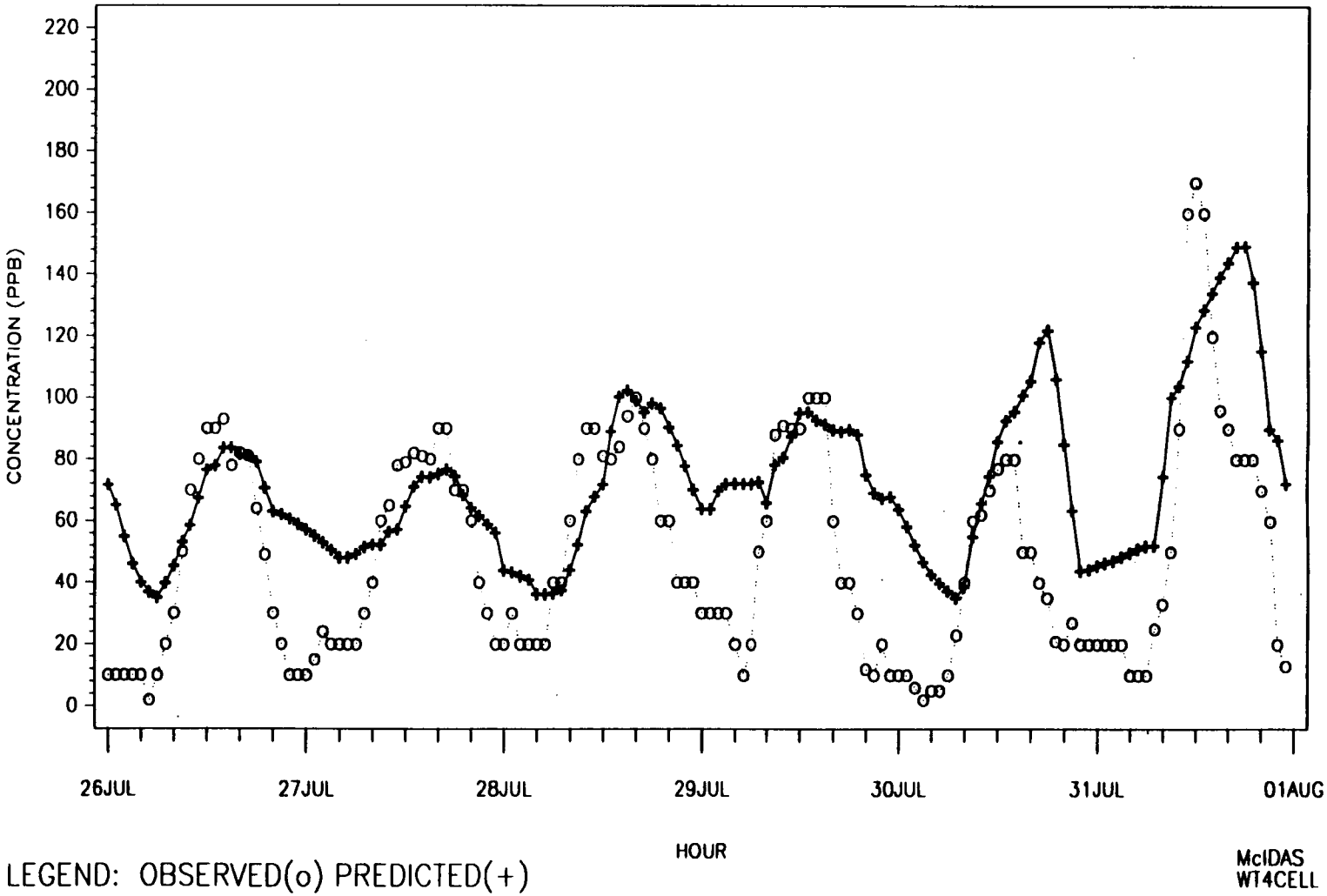

LEGEND: OBSERVED(o) PREDICTED(+)

MAXIMUM HOURLY O3 CONCENTRATIONS
FOR MMS HOUSTON-GALVESTON, EPISODE #2
JULY 26-31, 1990

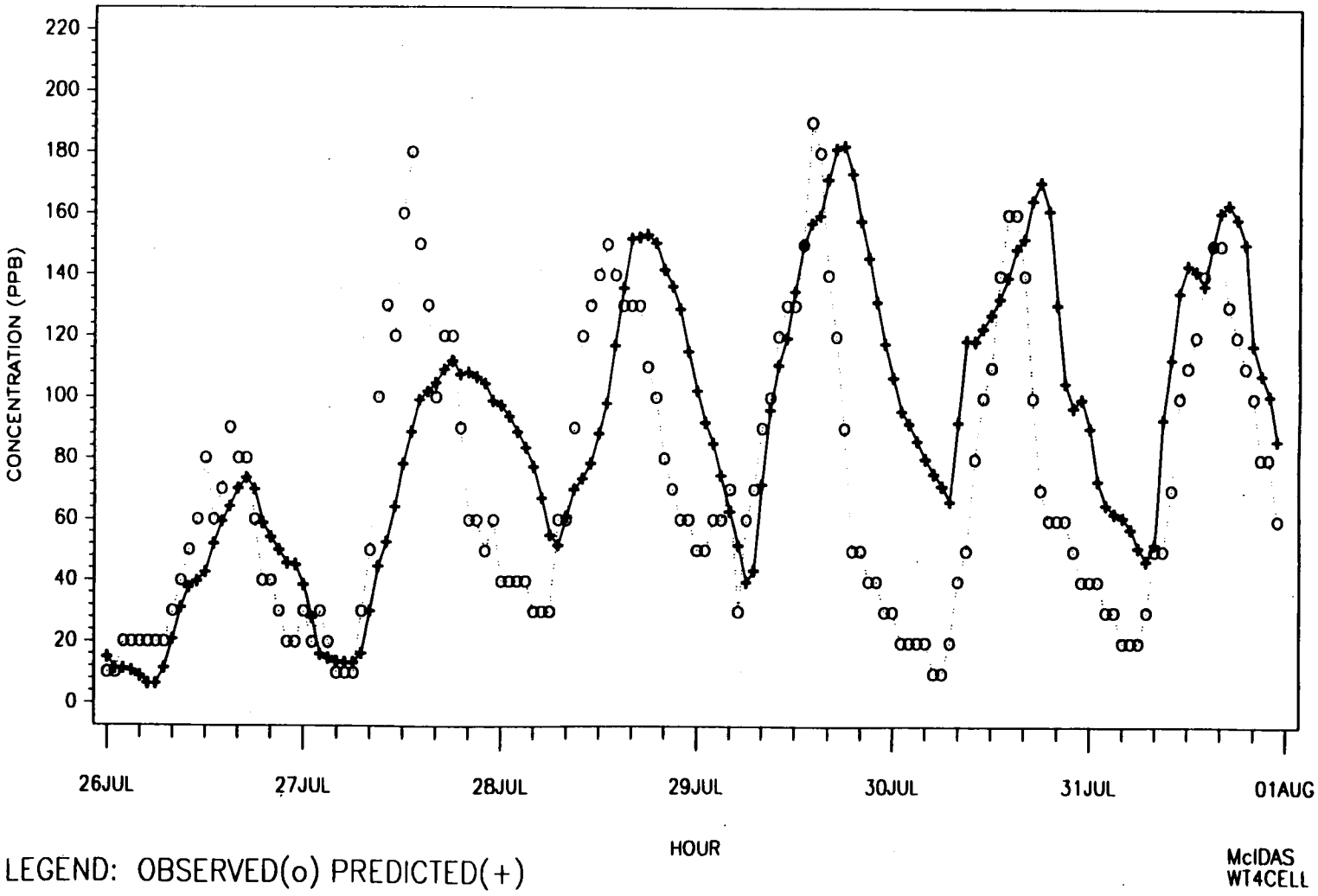

LEGEND: OBSERVED(o) PREDICTED(+)

McIDAS
WT4CELL

MAXIMUM HOURLY O3 CONCENTRATIONS
FOR MMS CORPUS CHRISTI, EPISODE #2
JULY 26–31, 1990

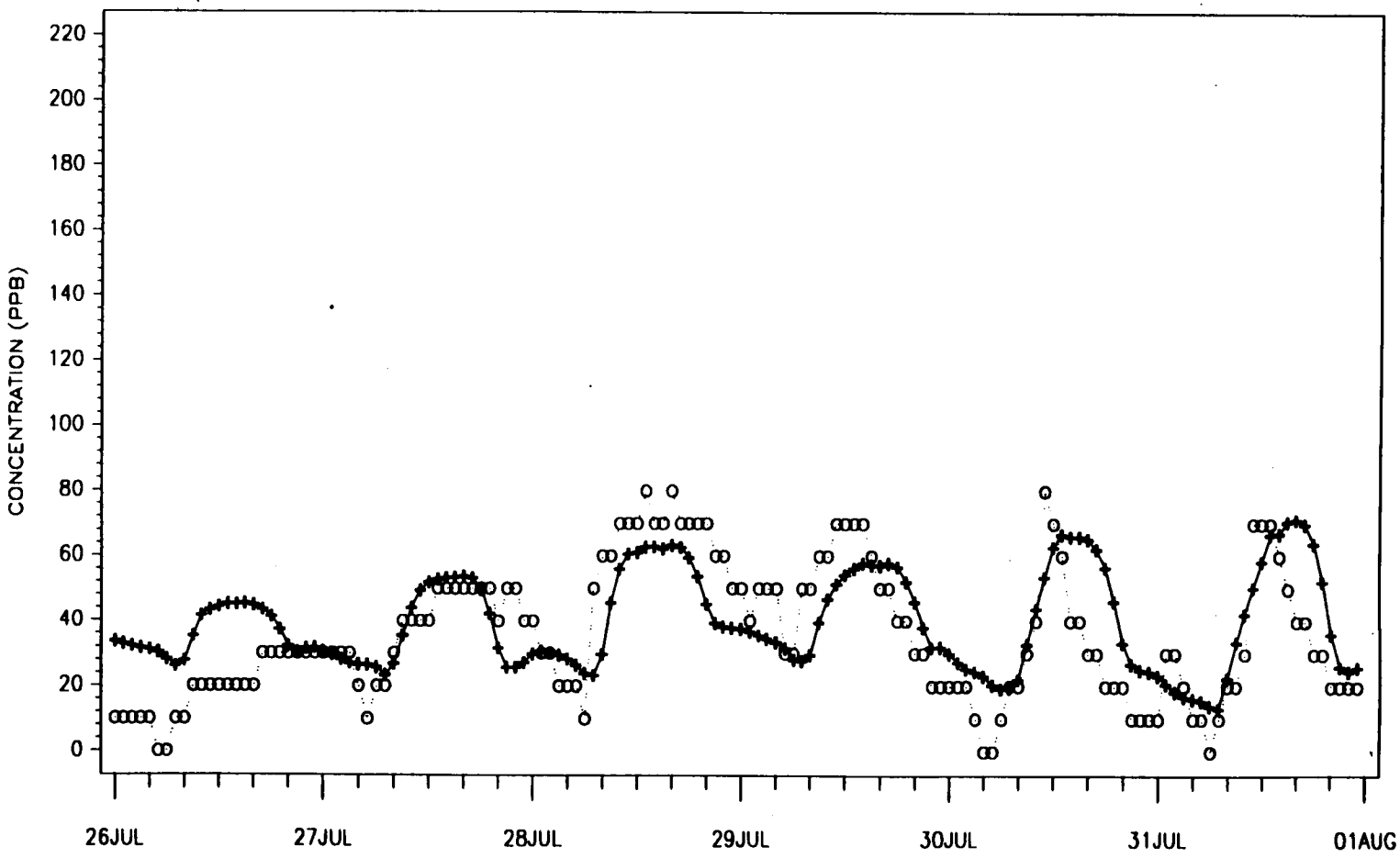

LEGEND: OBSERVED(o) PREDICTED(+)

McIDAS
WT4CELL

4 (b). Daily Box-Plots of Observed and Predicted Hourly Ozone

For Episode #2, July 26 - July 31, 1990

DAILY BOXPLOT OF OBSERVED AND PREDICTED HOURLY O3
FOR BATON ROUGE-NEW ORLEANS, EPISODE #2
JULY 26-31, 1990 (8 a.m. - 7 p.m.)

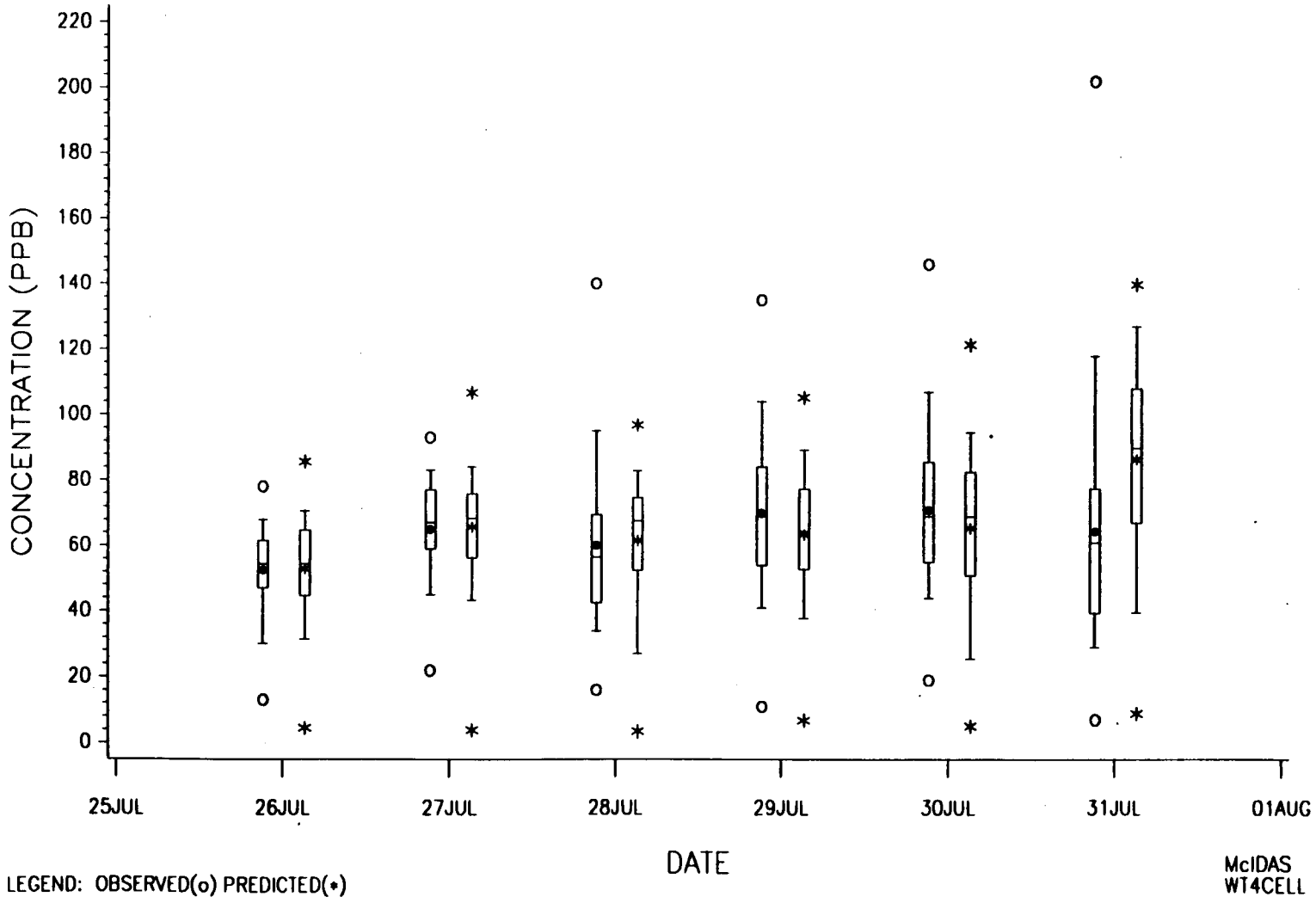

DAILY BOXPLOT OF OBSERVED AND PREDICTED HOURLY O3
FOR BATON ROUGE I, EPISODE #2
JULY 26–31, 1990 (8 a.m. – 7 p.m.)

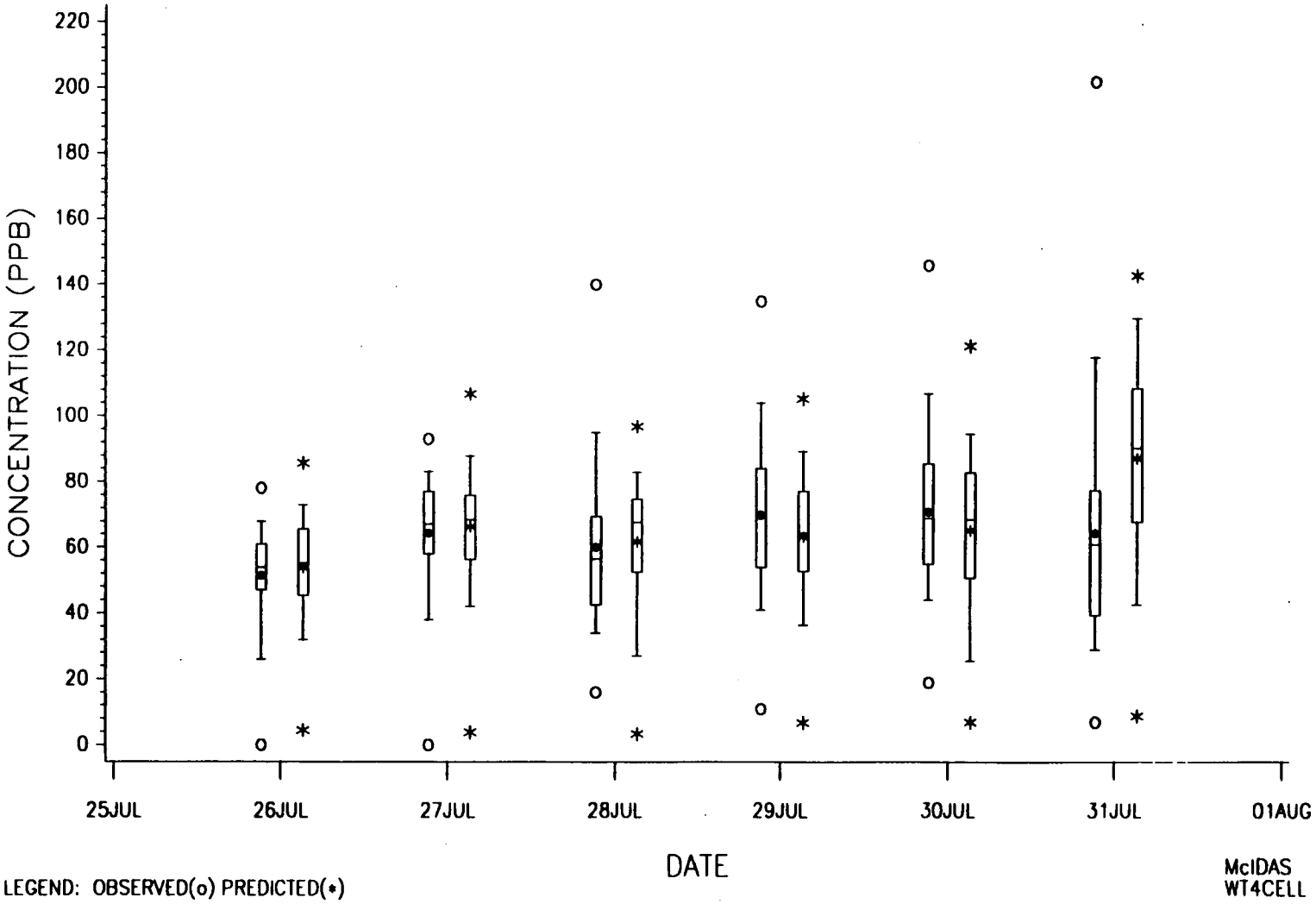

DAILY BOXPLOT OF OBSERVED AND PREDICTED HOURLY O3
FOR LAKE CHARLES-BEAUMONT, EPISODE #2
JULY 26-31, 1990 (8 a.m. - 7 p.m.)

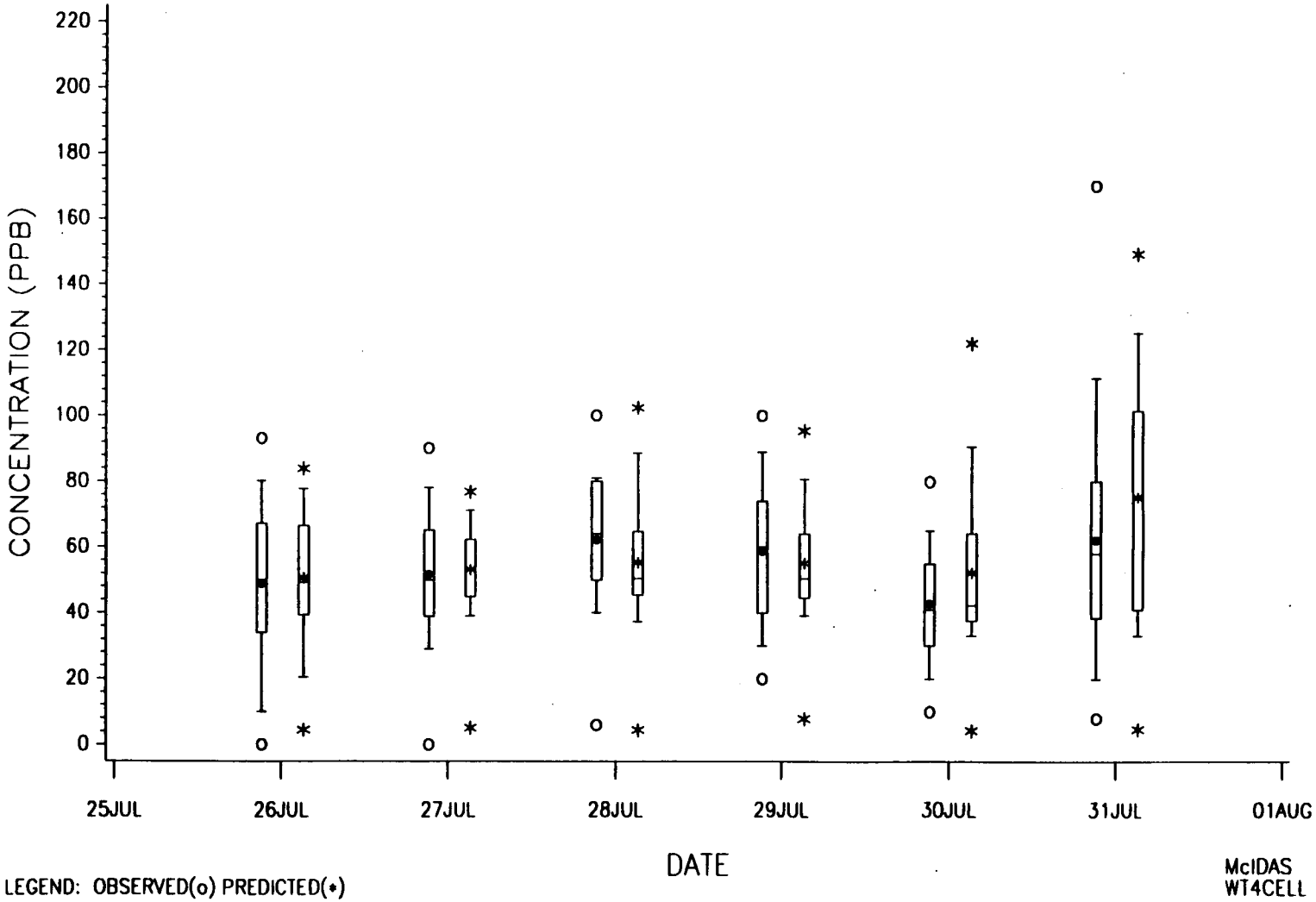

DAILY BOXPLOT OF OBSERVED AND PREDICTED HOURLY O3
FOR HOUSTON–GALVESTON, EPISODE #2
JULY 26–31, 1990 (8 a.m. – 7 p.m.)

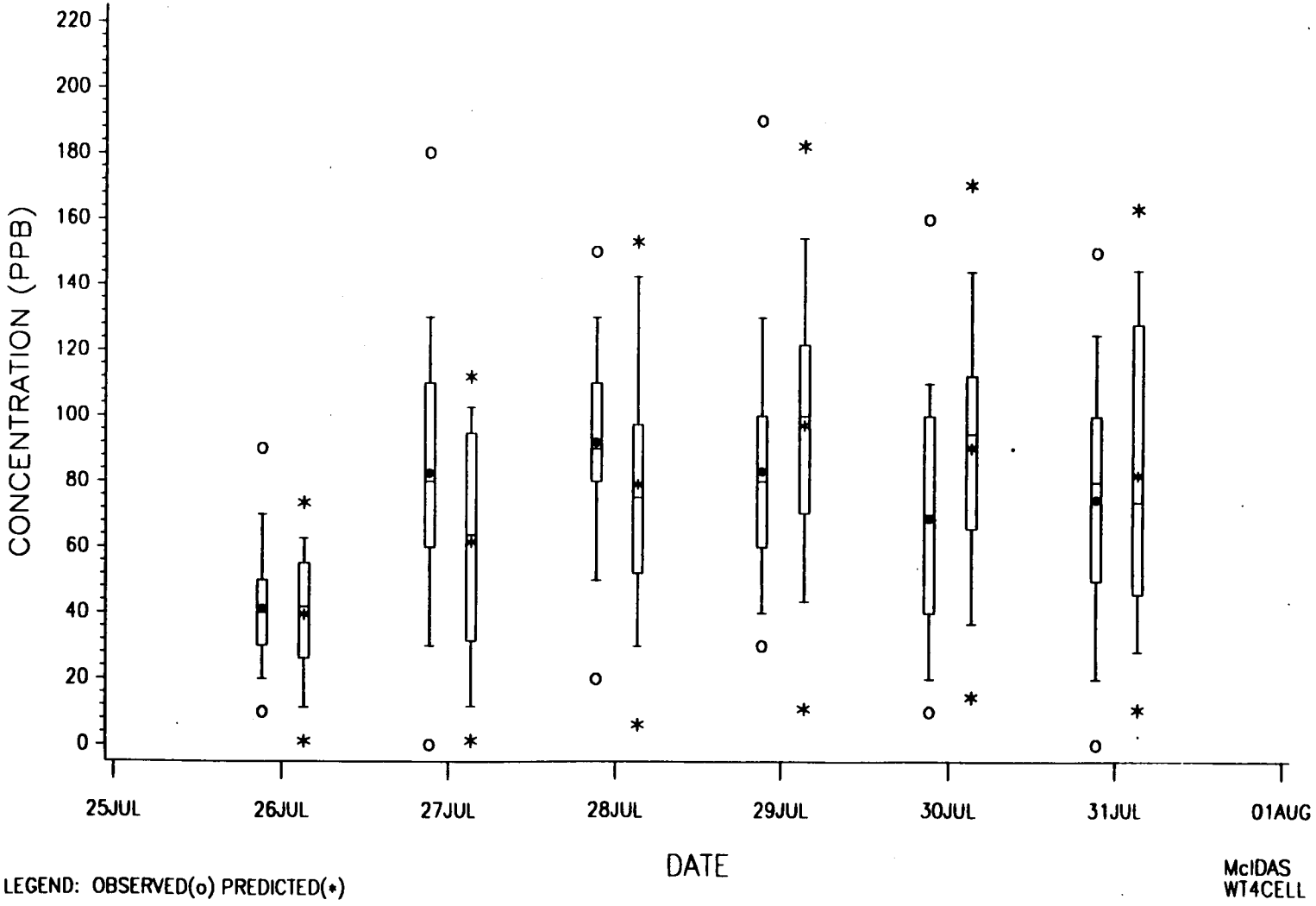

DAILY BOXPLOT OF OBSERVED AND PREDICTED HOURLY O3
FOR CORPUS CHRISTI, EPISODE #2
JULY 26-31, 1990 (8 a.m. - 7 p.m.)

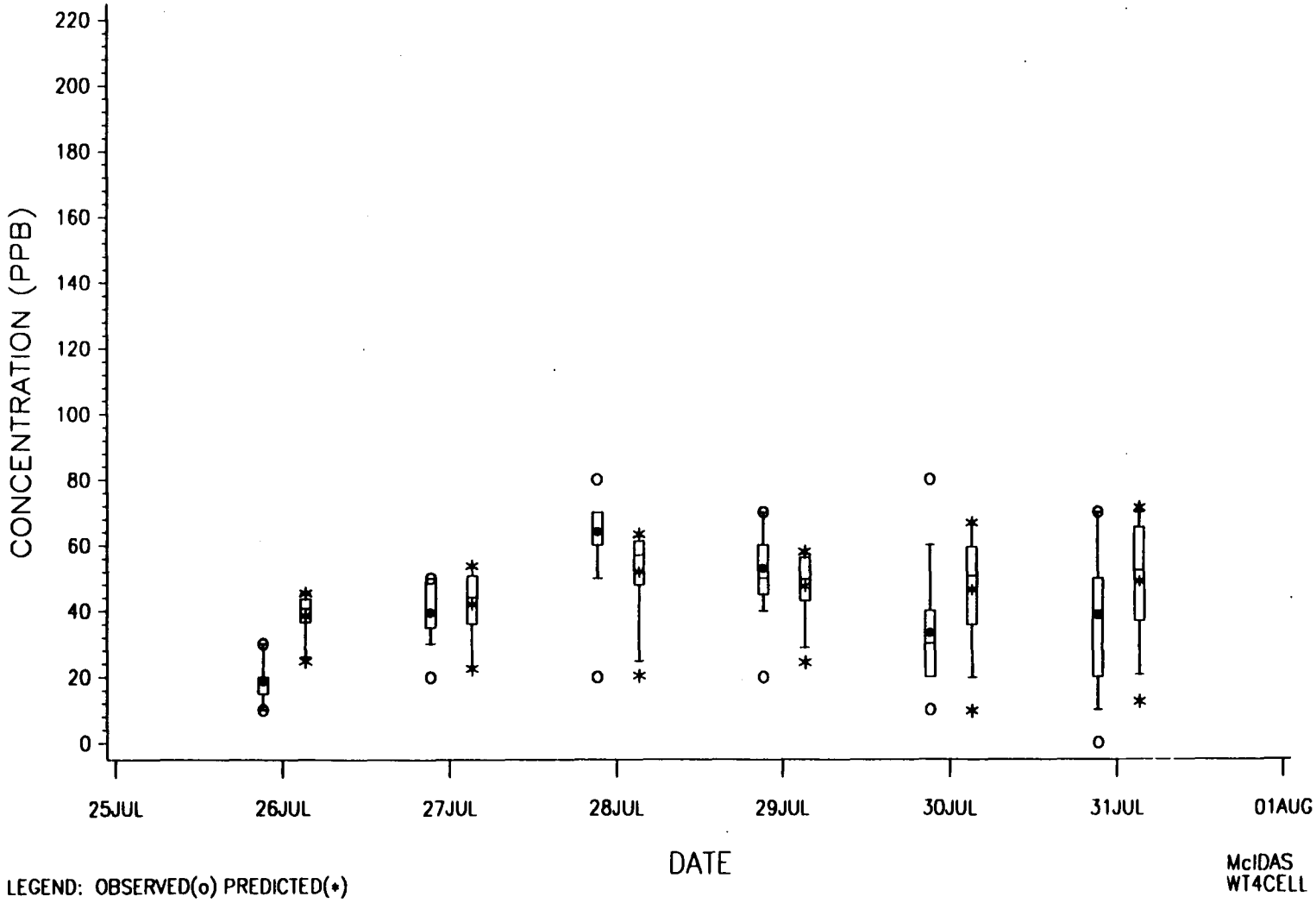

LEGEND: OBSERVED(o) PREDICTED(*)

5 (b). Box-Plots of Bias (Obs.-Pred.),

For Episode #2, July 26 - July 31, 1990

BOX–PLOT OF BIAS(OBS–PRED) BY DAY
FOR BATON ROUGE–NEW ORLEANS, EPISODE #2
JULY 26–31, 1990 (8 a.m. – 7 p.m.)

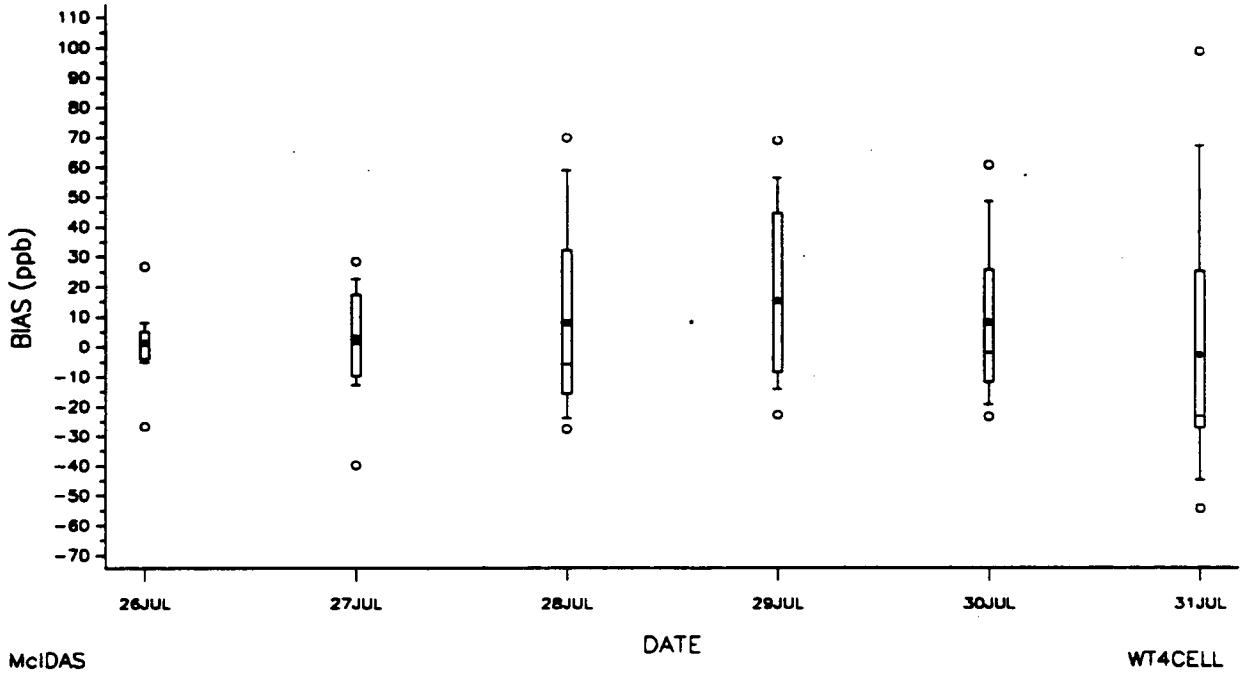

McIDAS WT4CELL

BOX–PLOT OF BIAS(OBS–PRED) BY O3 CONCENTRATION
FOR BATON ROUGE–NEW ORLEANS, EPISODE #2
JULY 26–31, 1990 (8 a.m. – 7 p.m.)

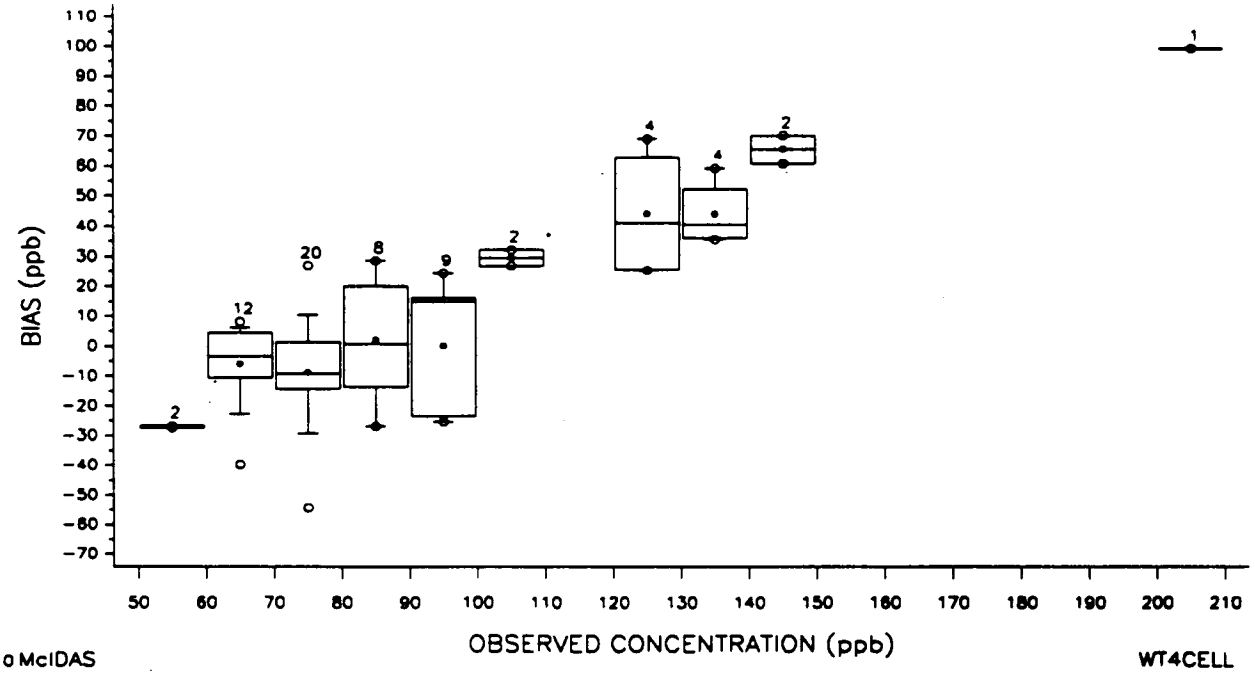

o McIDAS WT4CELL

BOX–PLOT OF BIAS(OBS–PRED) BY DAY
FOR BATON ROUGE I, EPISODE #2
JULY 26–31, 1990 (8 a.m. – 7 p.m.)

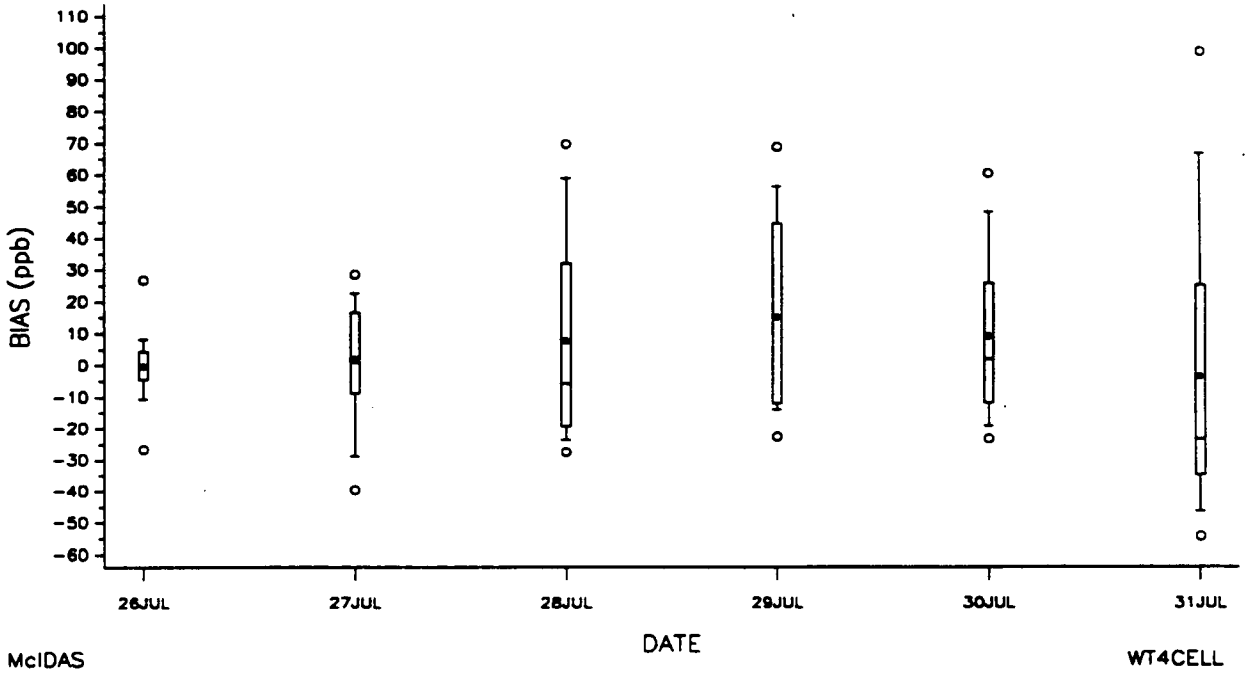

BOX–PLOT OF BIAS(OBS–PRED) BY O3 CONCENTRATION
FOR BATON ROUGE I, EPISODE #2
JULY 26–31, 1990 (8 a.m. – 7 p.m.)

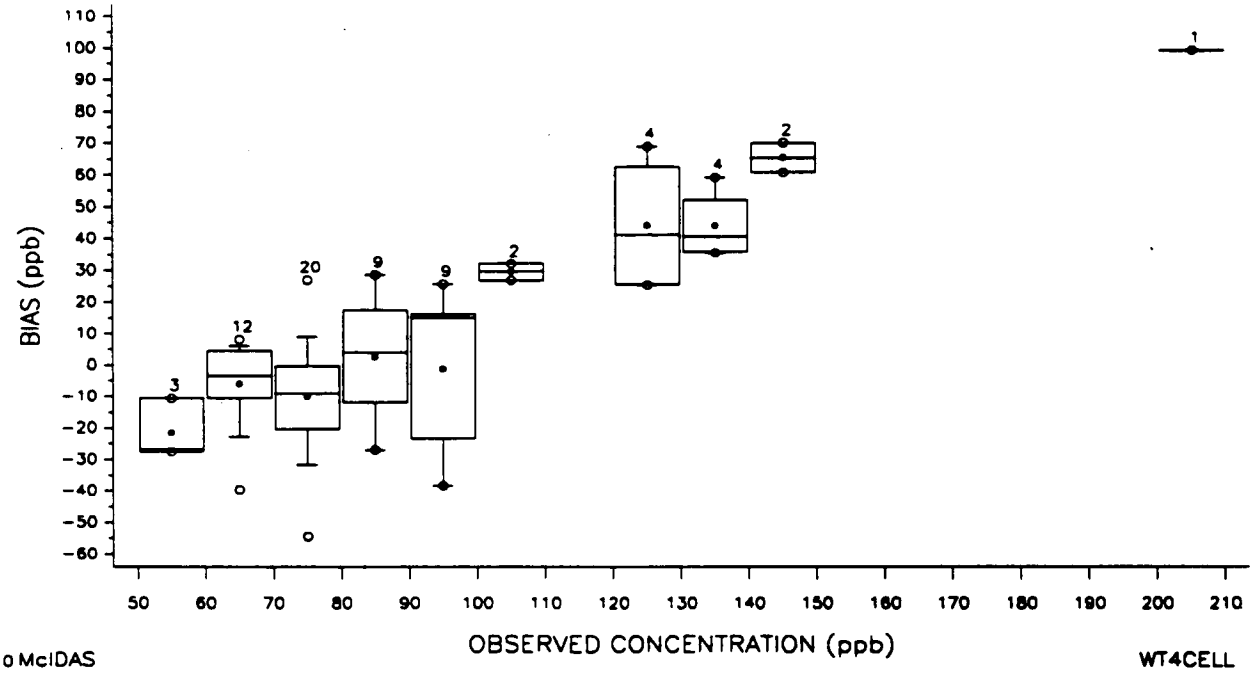

BOX–PLOT OF BIAS(OBS–PRED) BY DAY
FOR LAKE CHARLES–BEAUMONT, EPISODE #2
JULY 26–31, 1990 (8 a.m. – 7 p.m.)

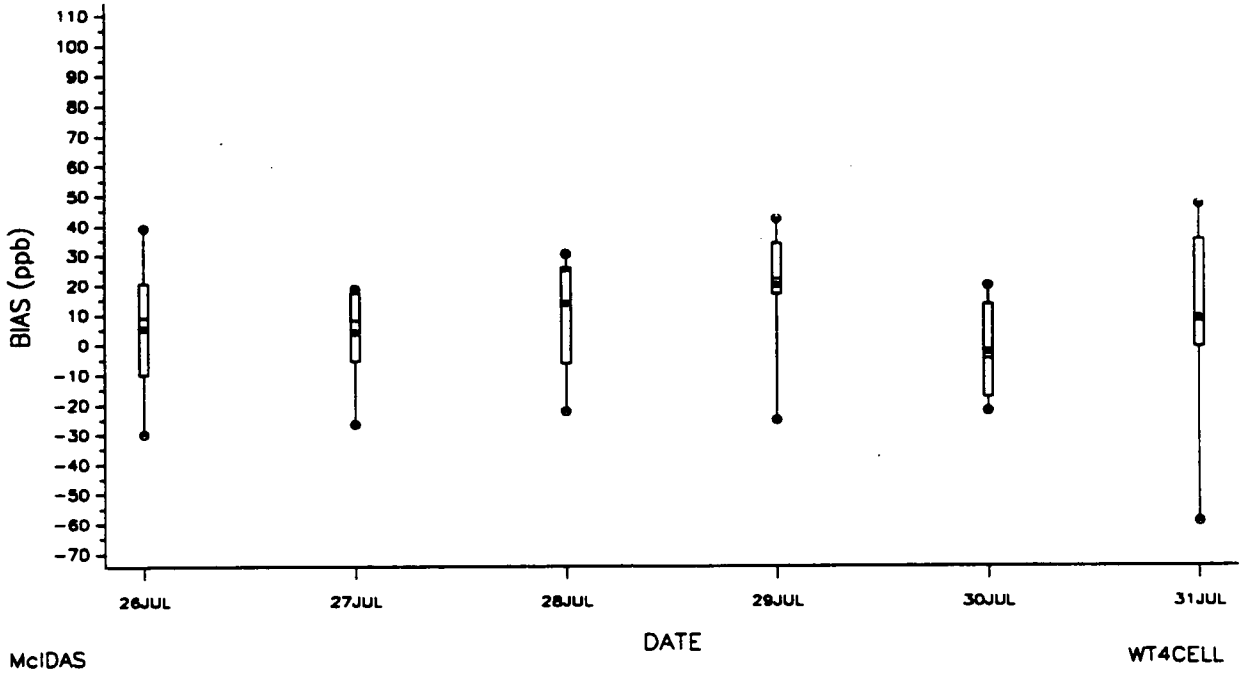

McIDAS WT4CELL

BOX–PLOT OF BIAS(OBS–PRED) BY O3 CONCENTRATION
FOR LAKE CHARLES–BEAUMONT, EPISODE #2
JULY 26–31, 1990 (8 a.m. – 7 p.m.)

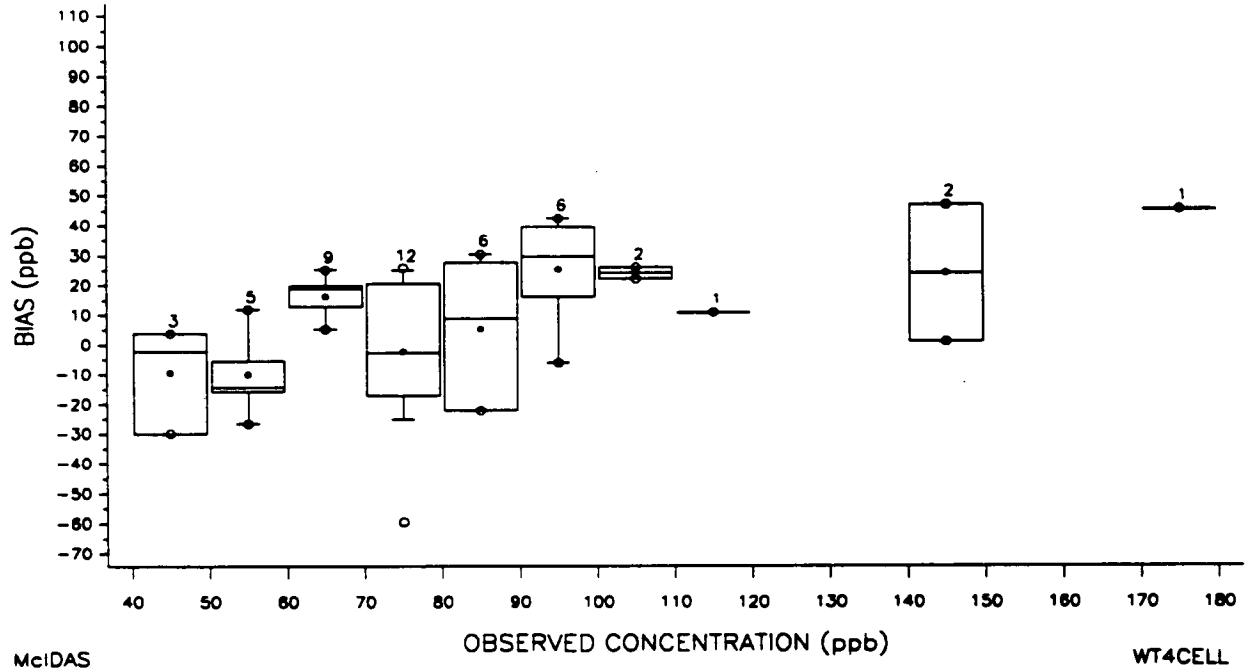

McIDAS WT4CELL

BOX–PLOT OF BIAS(OBS–PRED) BY DAY
FOR HOUSTON–GALVESTON, EPISODE #2
JULY 26–31, 1990 (8 a.m. – 7 p.m.)

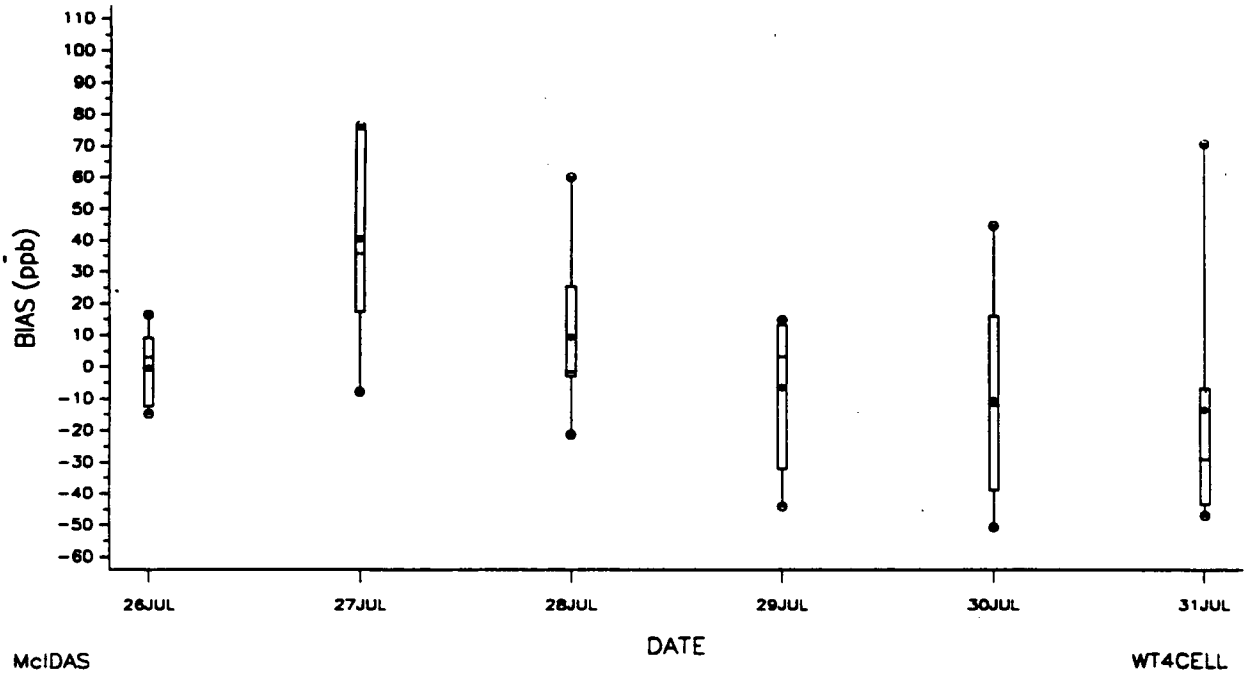

McIDAS WT4CELL

BOX–PLOT OF BIAS(OBS–PRED) BY O3 CONCENTRATION
FOR HOUSTON–GALVESTON, EPISODE #2
JULY 26–31, 1990 (8 a.m. – 7 p.m.)

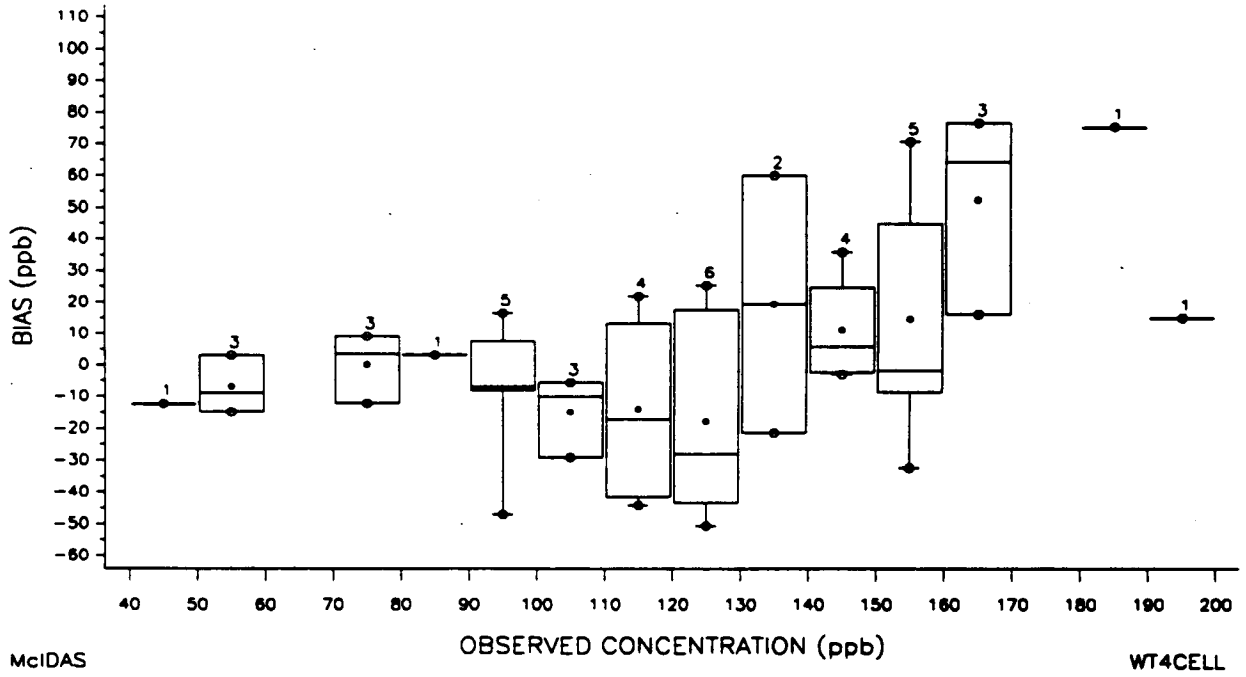

McIDAS WT4CELL

BOX–PLOT OF BIAS(OBS–PRED) BY DAY
FOR CORPUS CHRISTI, EPISODE #2
JULY 26–31, 1990 (8 a.m. – 7 p.m.)

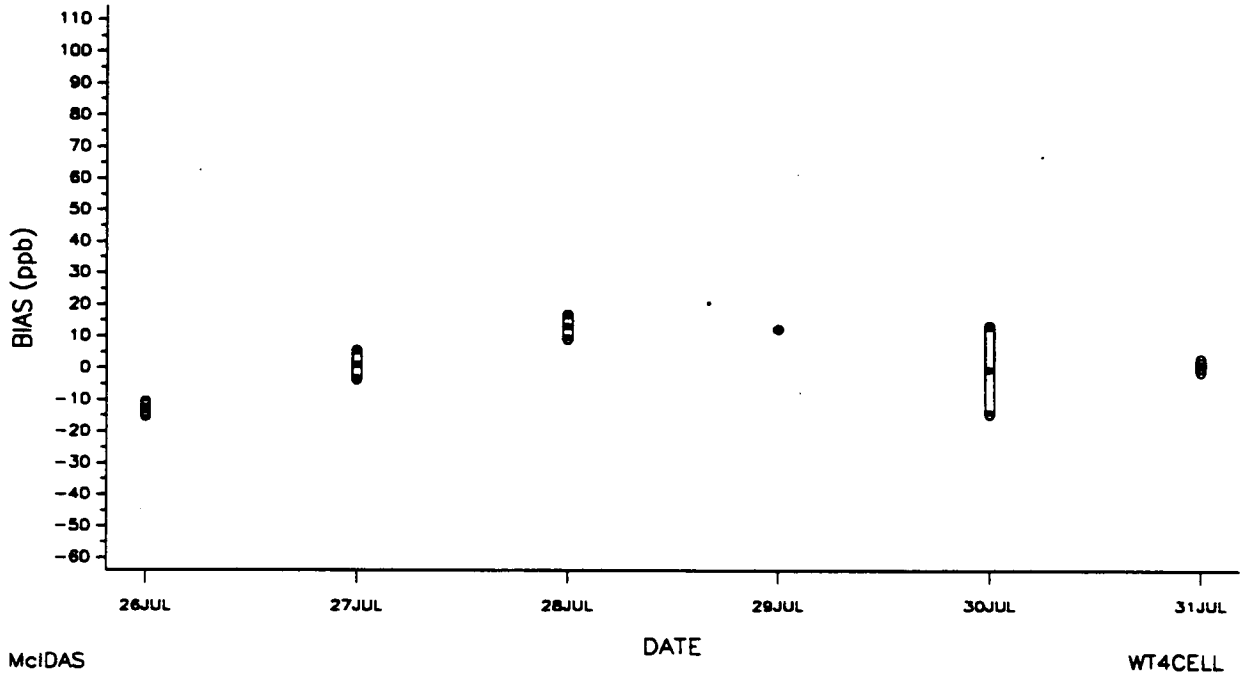

BOX–PLOT OF BIAS(OBS–PRED) BY O3 CONCENTRATION
FOR CORPUS CHRISTI, EPISODE #2
JULY 26–31, 1990 (8 a.m. – 7 p.m.)

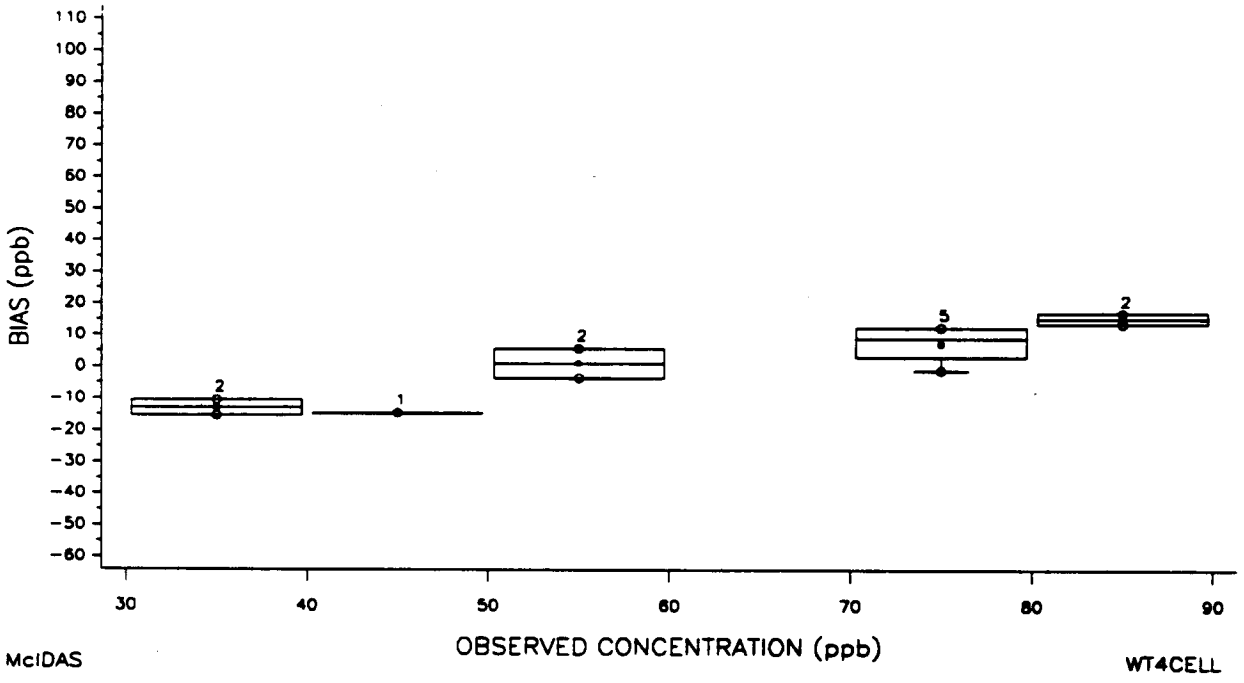

6 (b). Box-Plots of Normalized Bias,

For Episode #2, July 26 - July 31, 1990

BOX–PLOT OF NORMALIZED BIAS BY DAY
FOR MMS BATON ROUGE–NEW ORLEANS, EPISODE #2
JULY 26–31, 1990 (8 a.m. – 7 p.m.)

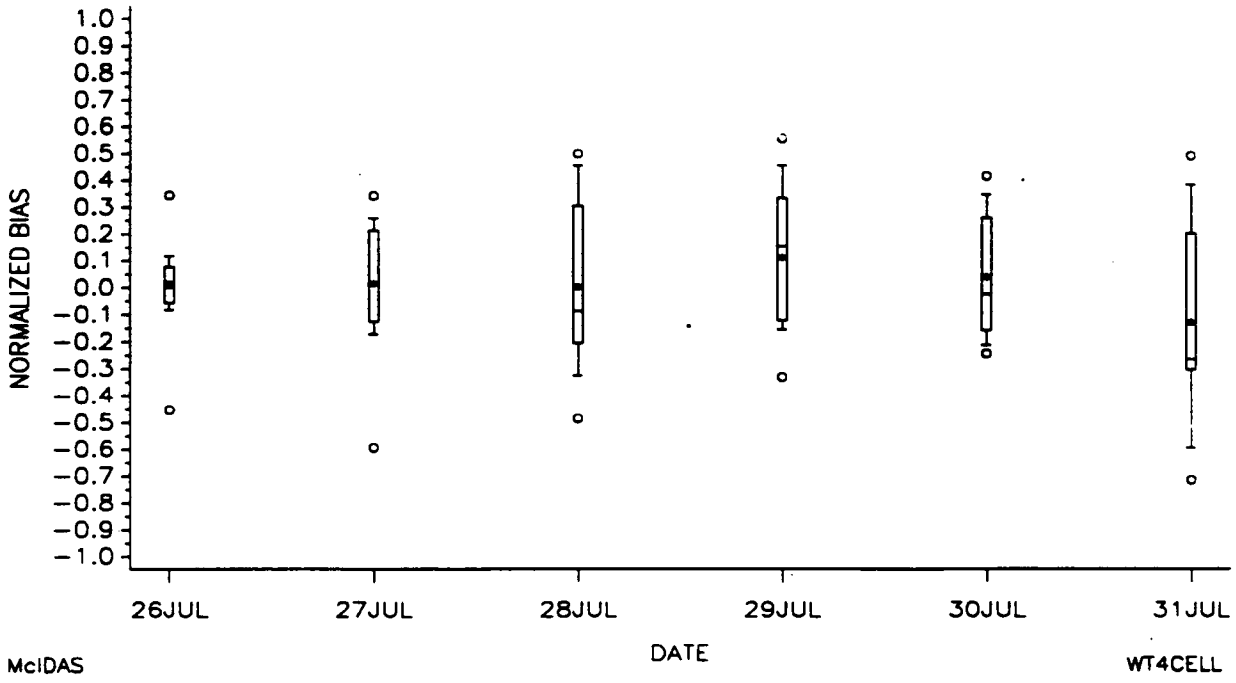

BOX–PLOT OF NORMALIZED BIAS BY O3 CONCENTRATION
FOR MMS BATON ROUGE–NEW ORLEANS, EPISODE #2
JULY 26–31, 1990 (8 a.m. – 7 p.m.)

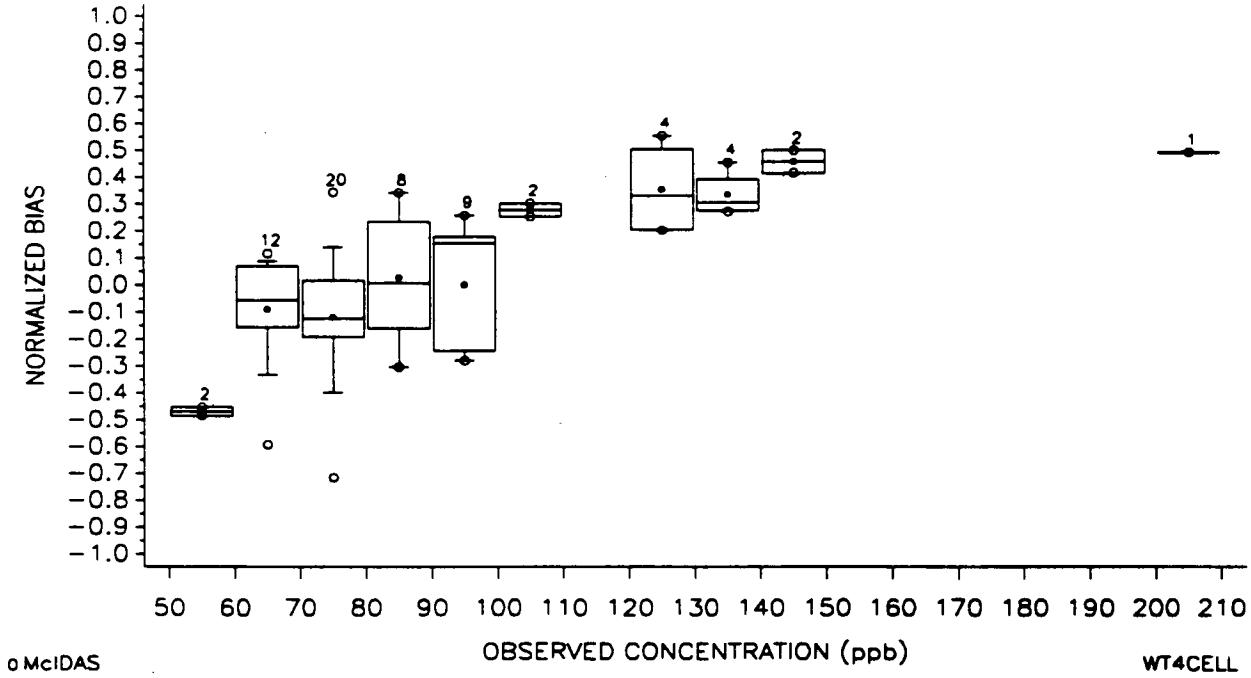

BOX–PLOT OF NORMALIZED BIAS BY DAY
FOR MMS BATON ROUGE I, EPISODE #2
JULY 26–31, 1990 (8 a.m. – 7 p.m.)

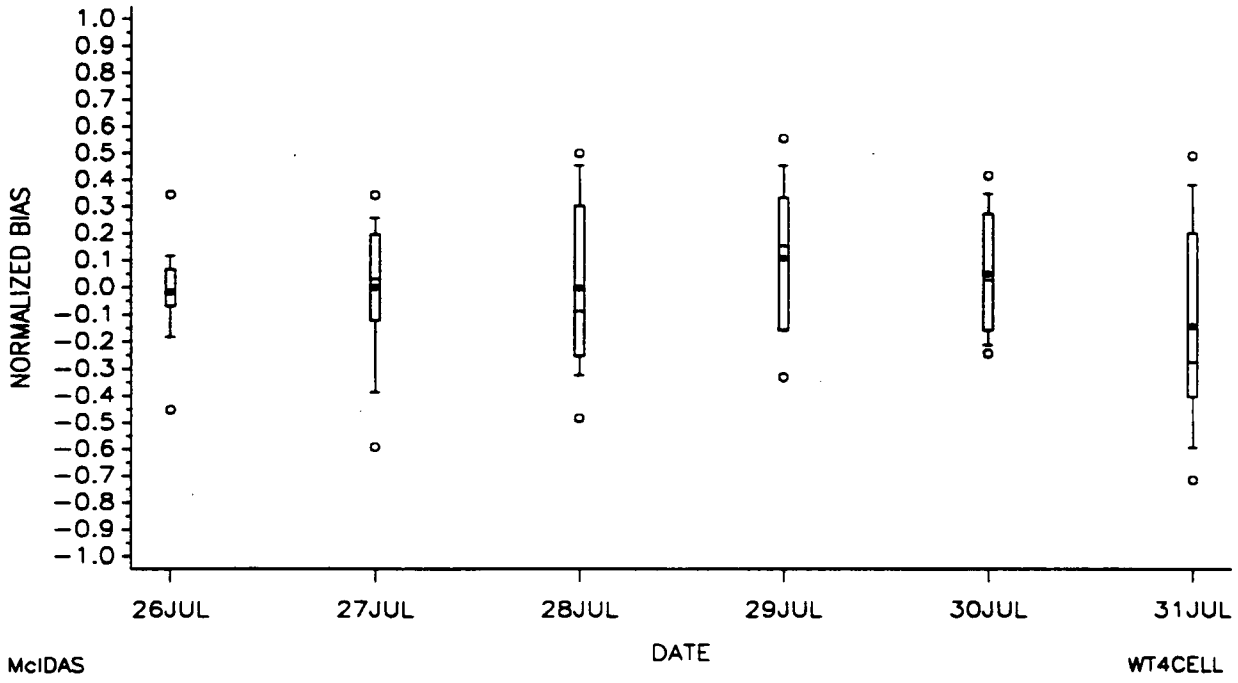

BOX–PLOT OF NORMALIZED BIAS BY O3 CONCENTRATION
FOR MMS BATON ROUGE I, EPISODE #2
JULY 26–31, 1990 (8 a.m. – 7 p.m.)

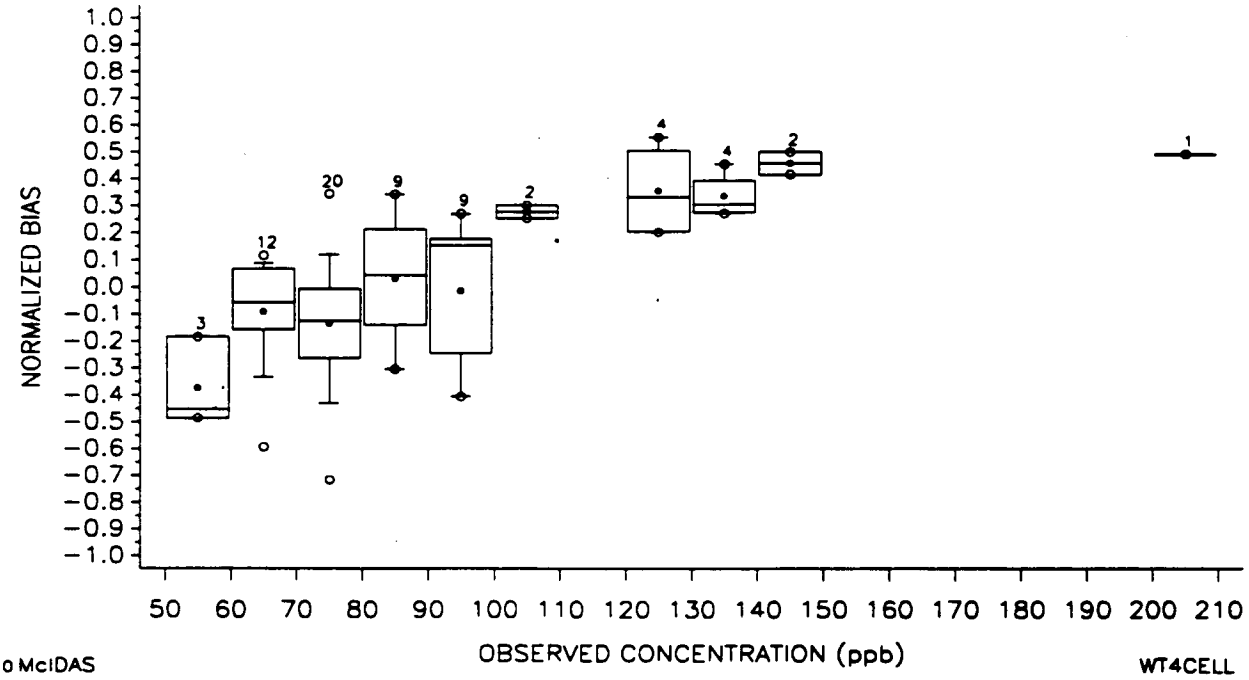

BOX–PLOT OF NORMALIZED BIAS BY DAY
FOR MMS LAKE CHARLES–BEAUMONT, EPISODE #2
JULY 26–31, 1990 (8 a.m. – 7 p.m.)

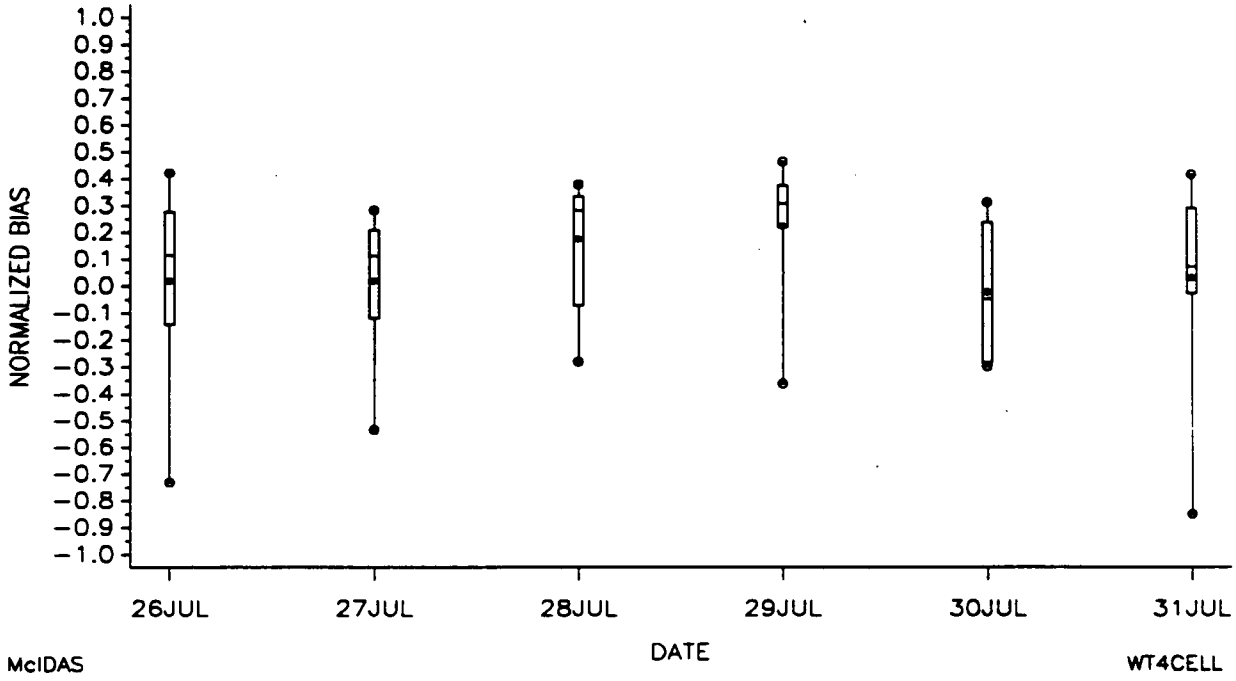

BOX–PLOT OF NORMALIZED BIAS BY O3 CONCENTRATION
FOR MMS LAKE CHARLES–BEAUMONT, EPISODE #2
JULY 26–31, 1990 (8 a.m. – 7 p.m.)

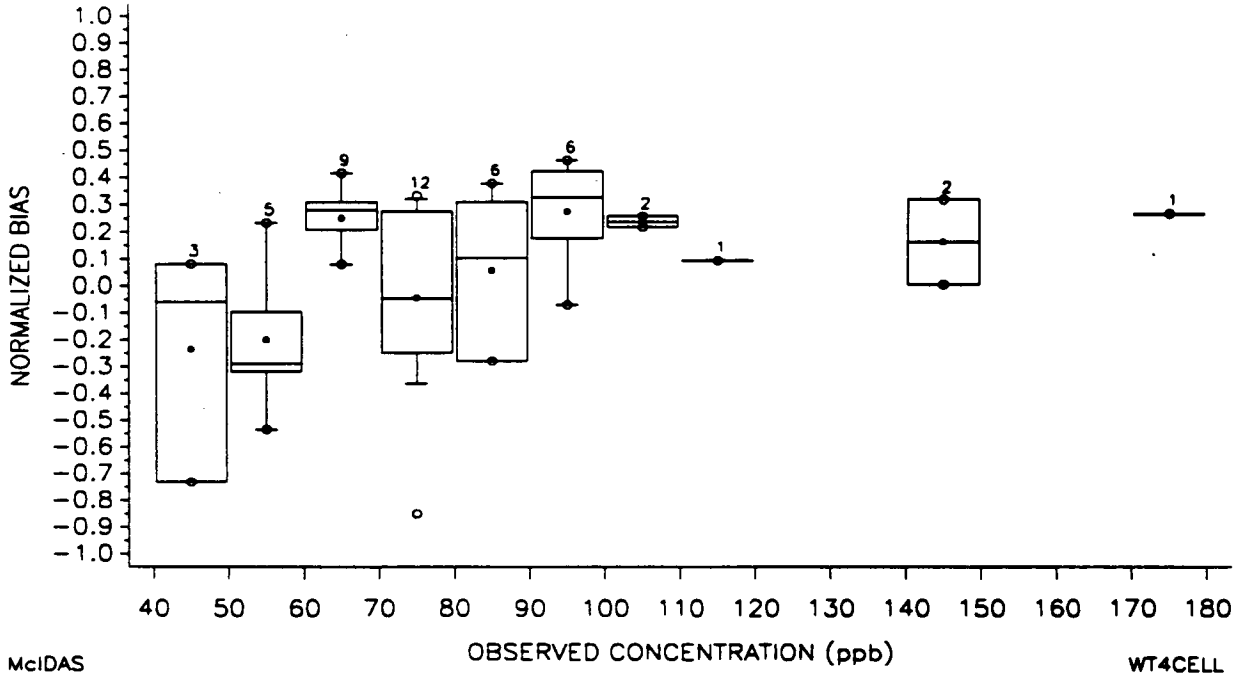

BOX–PLOT OF NORMALIZED BIAS BY DAY
FOR MMS HOUSTON–GALVESTON, EPISODE #2
JULY 26–31, 1990 (8 a.m. – 7 p.m.)

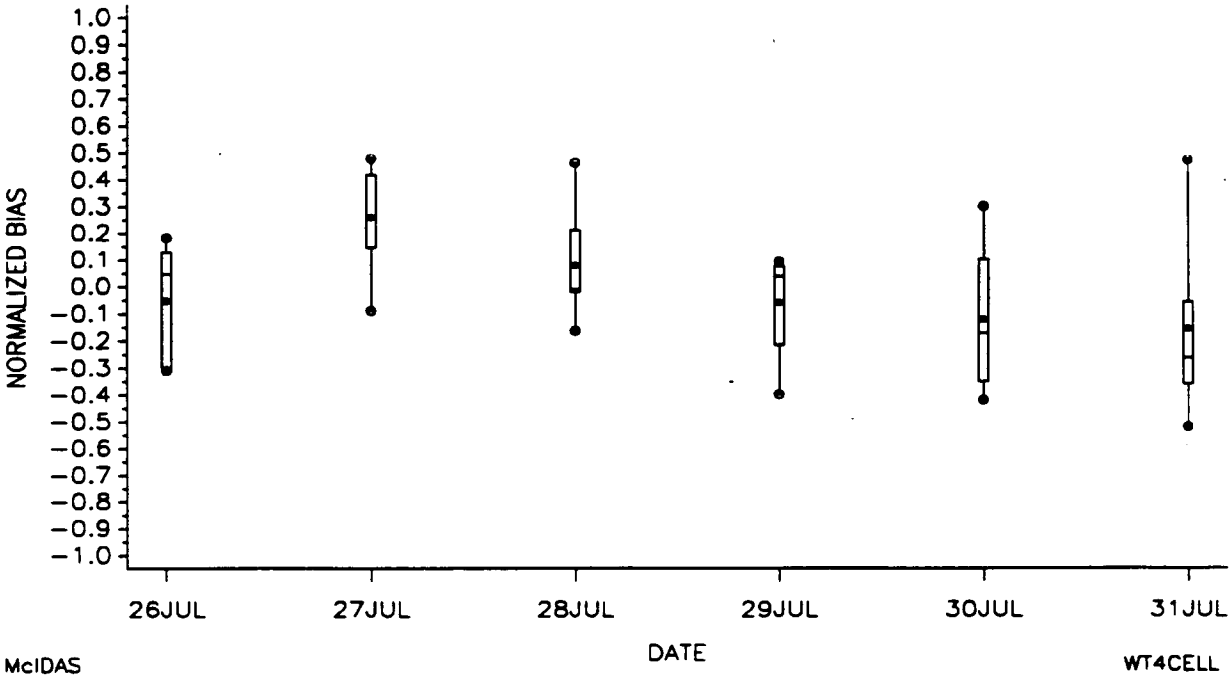

BOX–PLOT OF NORMALIZED BIAS BY O3 CONCENTRATION
FOR MMS HOUSTON–GALVESTON, EPISODE #2
JULY 26–31, 1990 (8 a.m. – 7 p.m.)

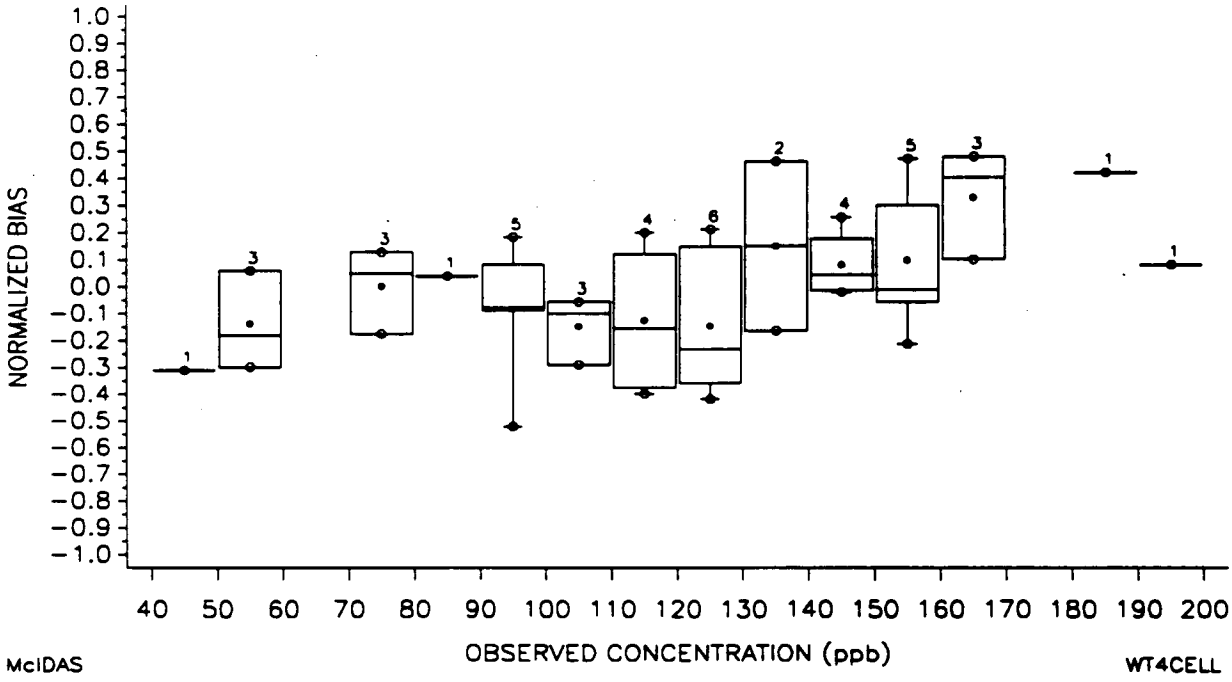

BOX–PLOT OF NORMALIZED BIAS BY DAY
FOR MMS CORPUS CHRISTI, EPISODE #2
JULY 26–31, 1990 (8 a.m. – 7 p.m.)

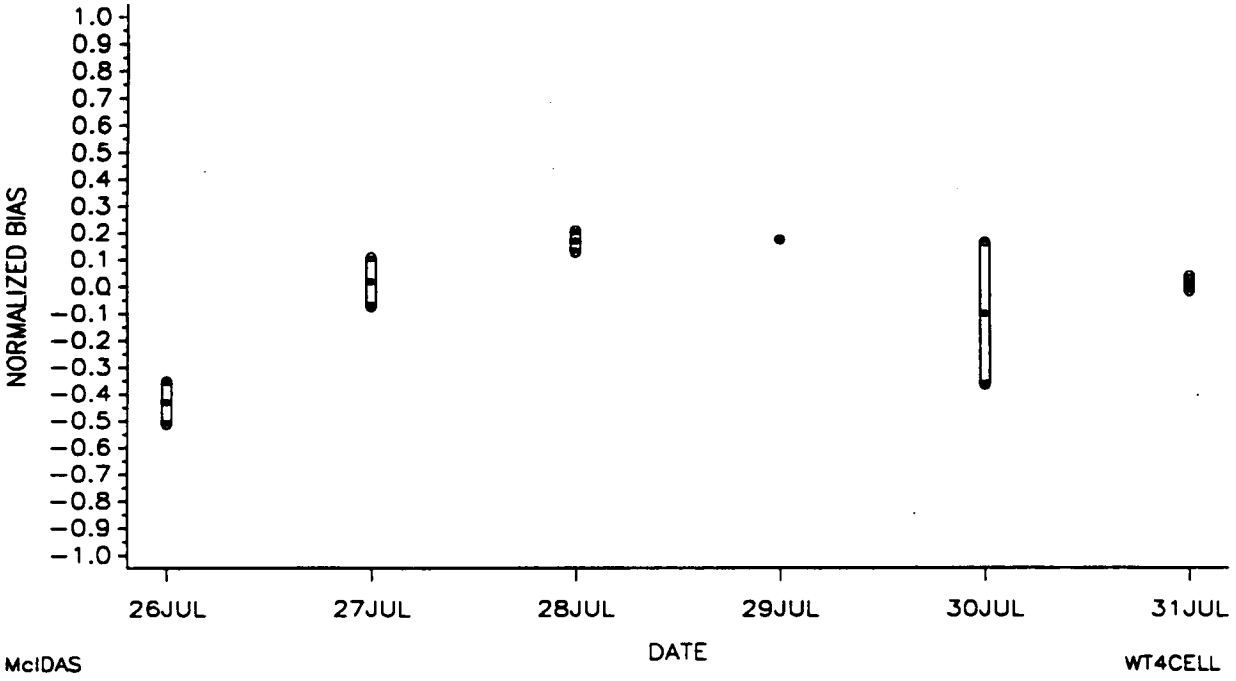

BOX–PLOT OF NORMALIZED BIAS BY O3 CONCENTRATION
FOR MMS CORPUS CHRISTI, EPISODE #2
JULY 26–31, 1990 (8 a.m. – 7 p.m.)

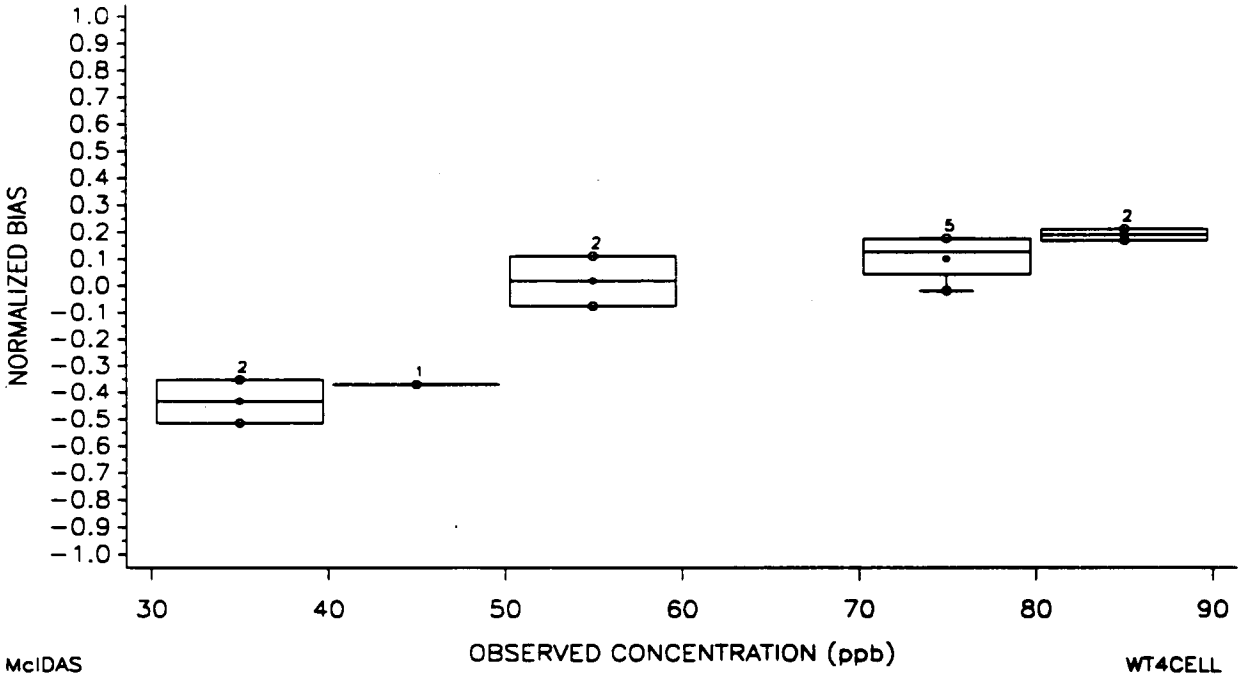

7 (b). Box-Plots of Normalized Gross Error,

For Episode #2, July 26 - July 31, 1990

BOX–PLOT OF NORMALIZED GROSS ERROR BY DAY
FOR MMS BATON ROUGE–NEW ORLEANS, EPISODE #2
JULY 26 – 31, 1990 (8 a.m. – 7 p.m.)

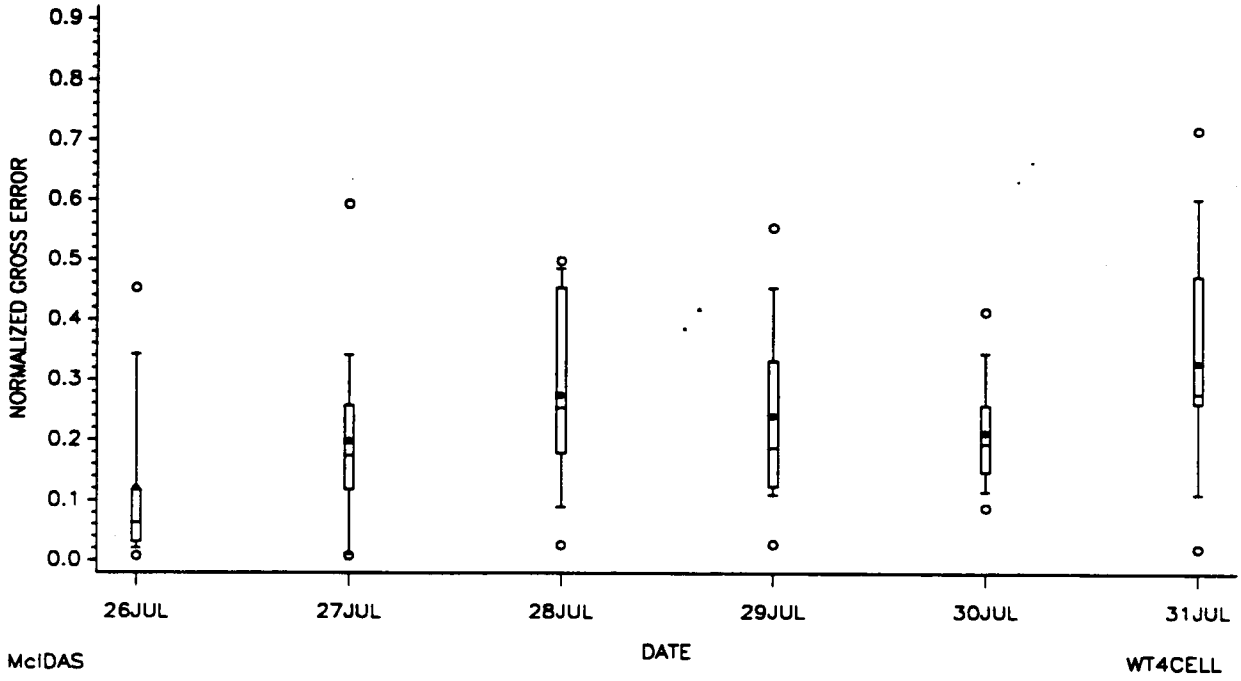

BOX–PLOT OF NORMALIZED GROSS ERROR BY O3 CONCENTRATION
FOR MMS BATON ROUGE–NEW ORLEANS, EPISODE #2
JULY 26 – 31, 1990 (8 a.m. – 7 p.m.)

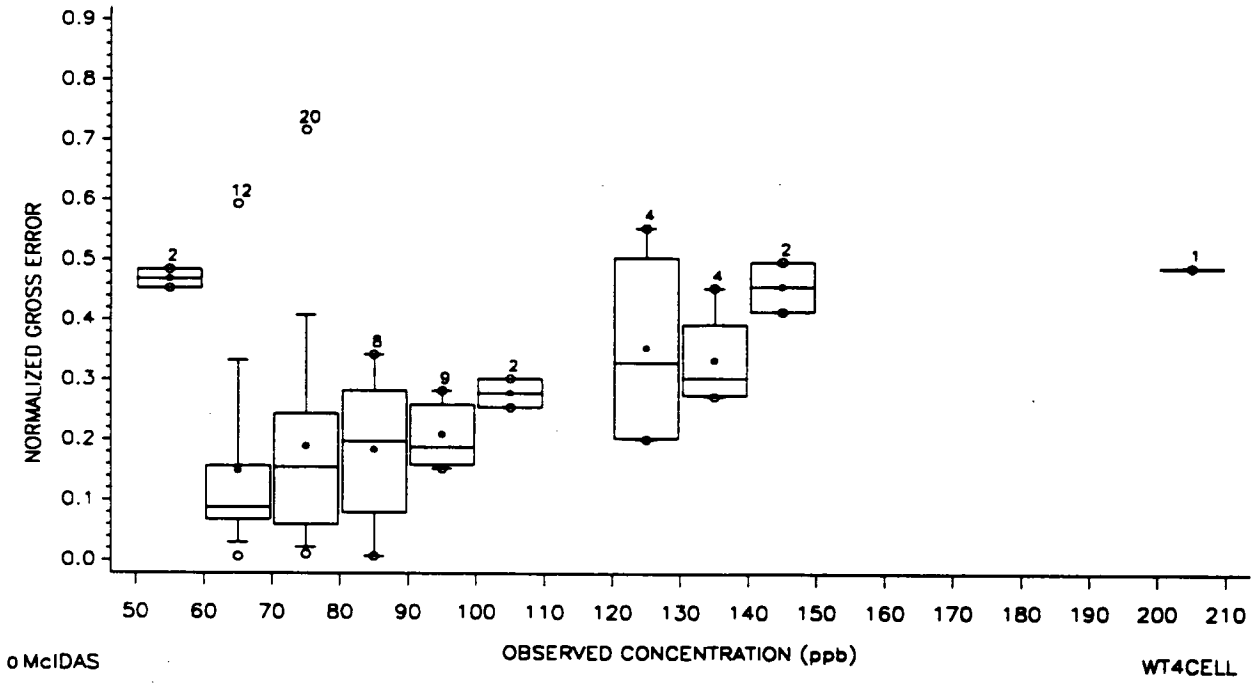

BOX–PLOT OF NORMALIZED GROSS ERROR BY DAY
FOR MMS BATON ROUGE I, EPISODE #2
JULY 26 – 31, 1990 (8 a.m. – 7 p.m.)

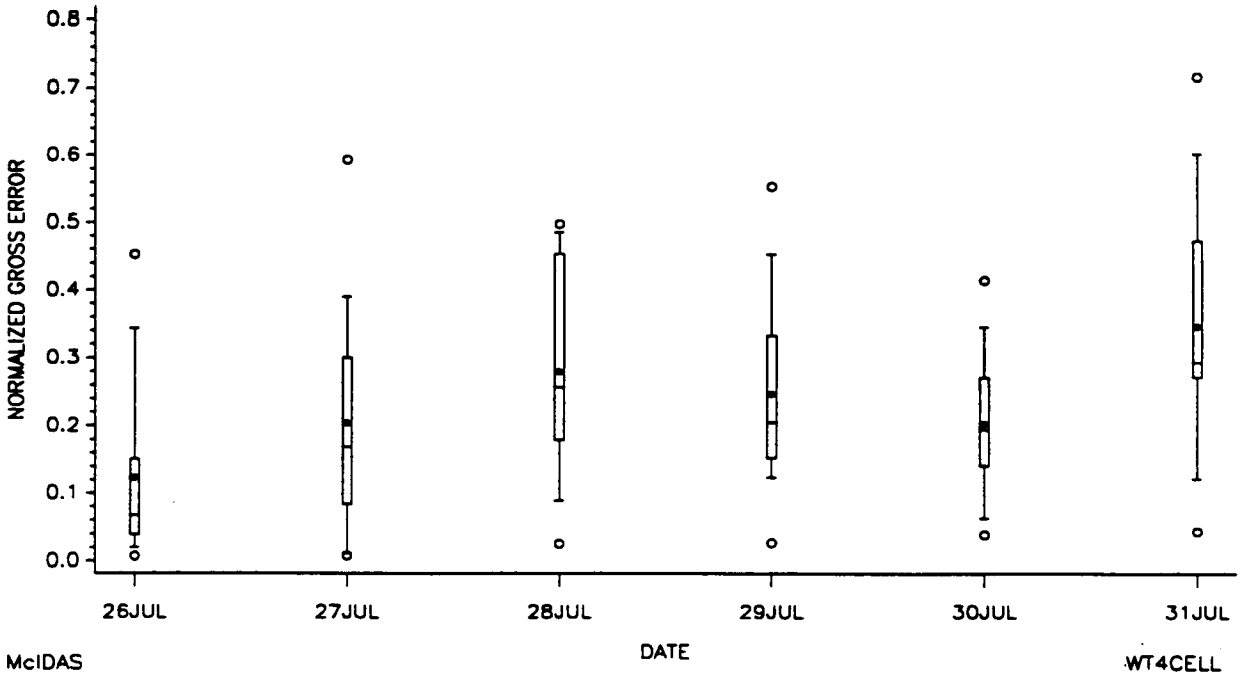

BOX–PLOT OF NORMALIZED GROSS ERROR BY O3 CONCENTRATION
FOR MMS BATON ROUGE I, EPISODE #2
JULY 26 – 31, 1990 (8 a.m. – 7 p.m.)

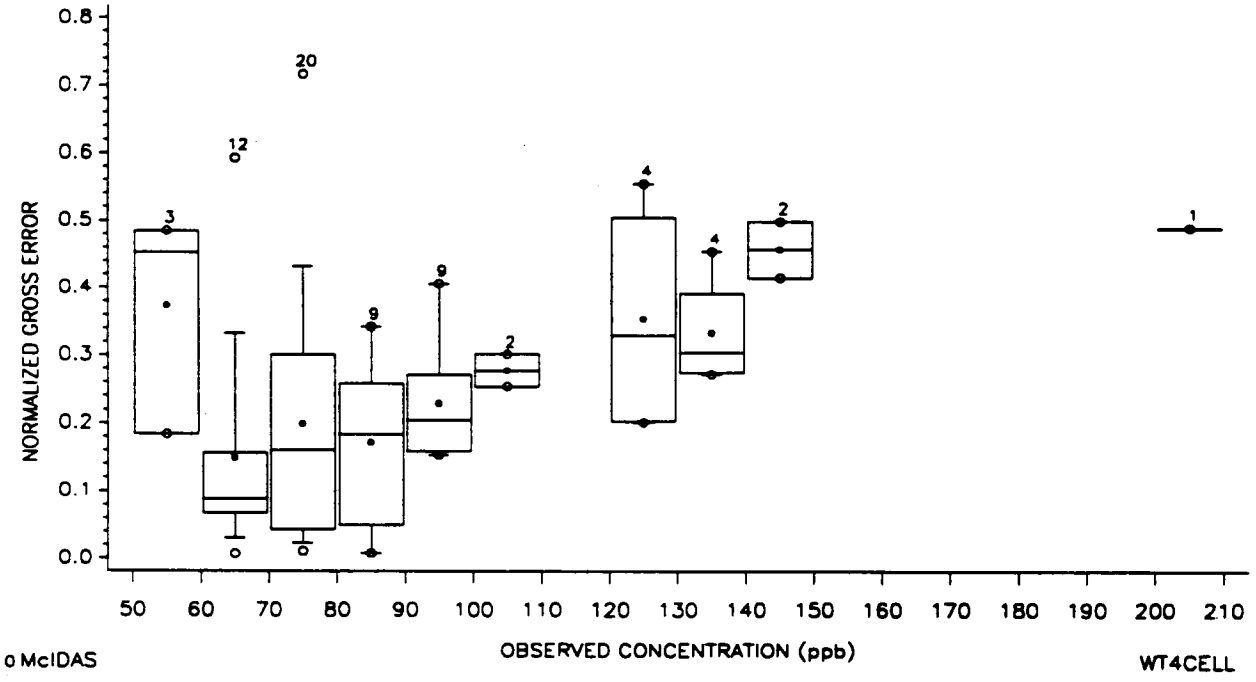

BOX–PLOT OF NORMALIZED GROSS ERROR BY DAY
FOR MMS LAKE CHARLES–BEAUMONT, EPISODE #2
JULY 26 – 31, 1990 (8 a.m. – 7 p.m.)

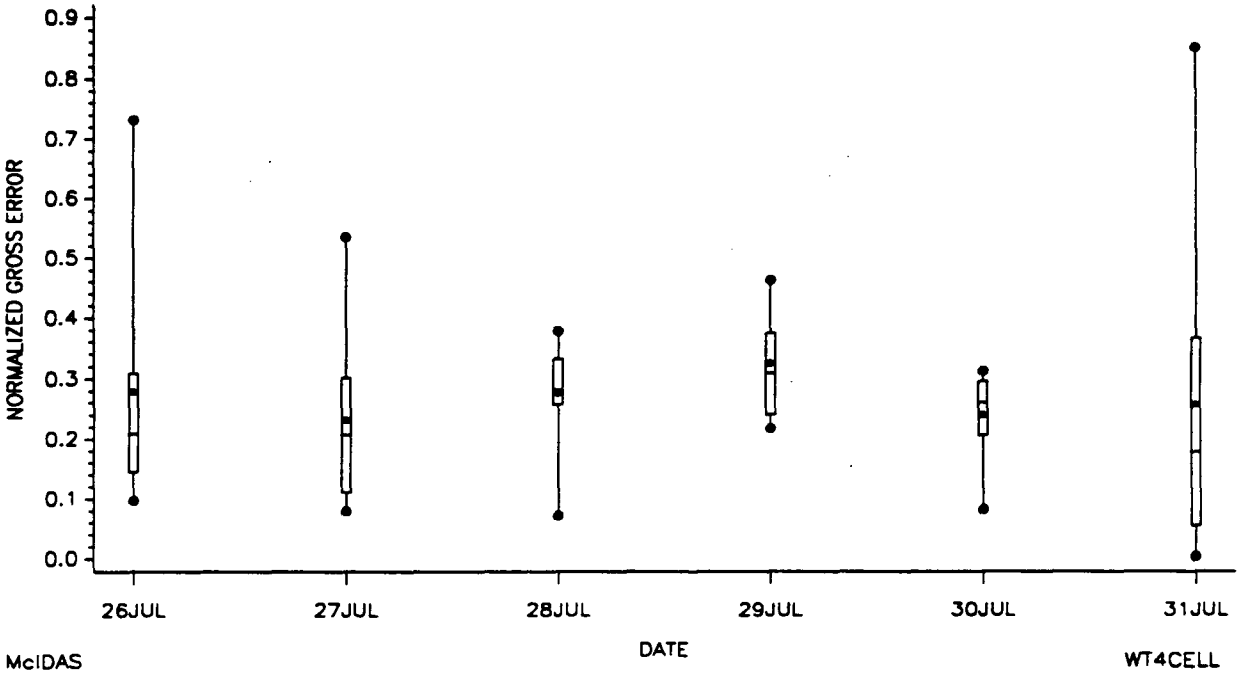

BOX–PLOT OF NORMALIZED GROSS ERROR BY O3 CONCENTRATION
FOR MMS LAKE CHARLES–BEAUMONT, EPISODE #2
JULY 26 – 31, 1990 (8 a.m. – 7 p.m.)

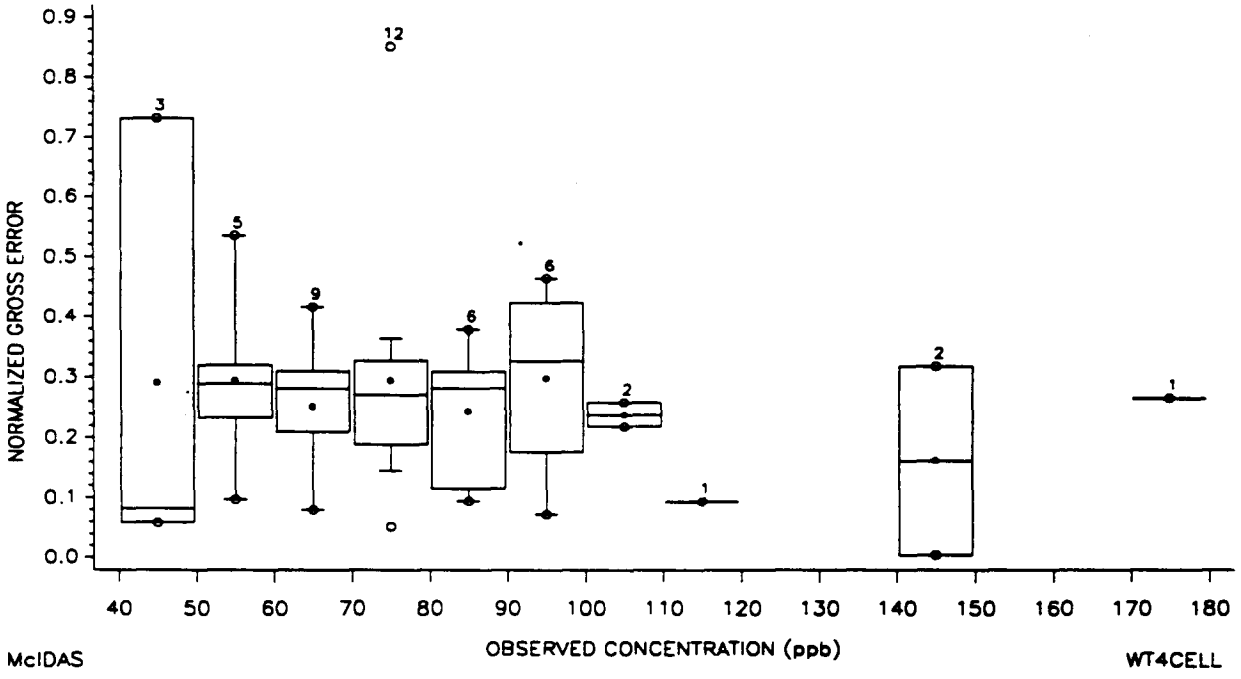

BOX–PLOT OF NORMALIZED GROSS ERROR BY DAY
FOR MMS HOUSTON–GALVESTON, EPISODE #2
JULY 26 – 31, 1990 (8 a.m. – 7 p.m.)

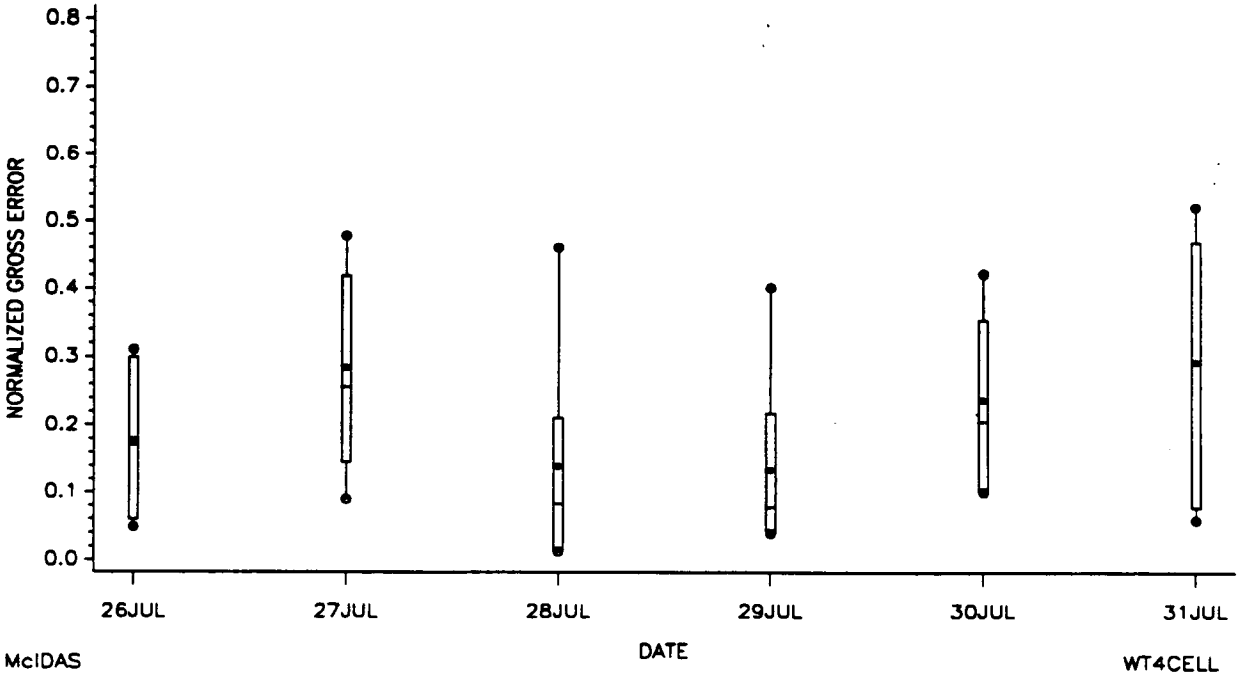

BOX–PLOT OF NORMALIZED GROSS ERROR BY O3 CONCENTRATION
FOR MMS HOUSTON–GALVESTON, EPISODE #2
JULY 26 – 31, 1990 (8 a.m. – 7 p.m.)

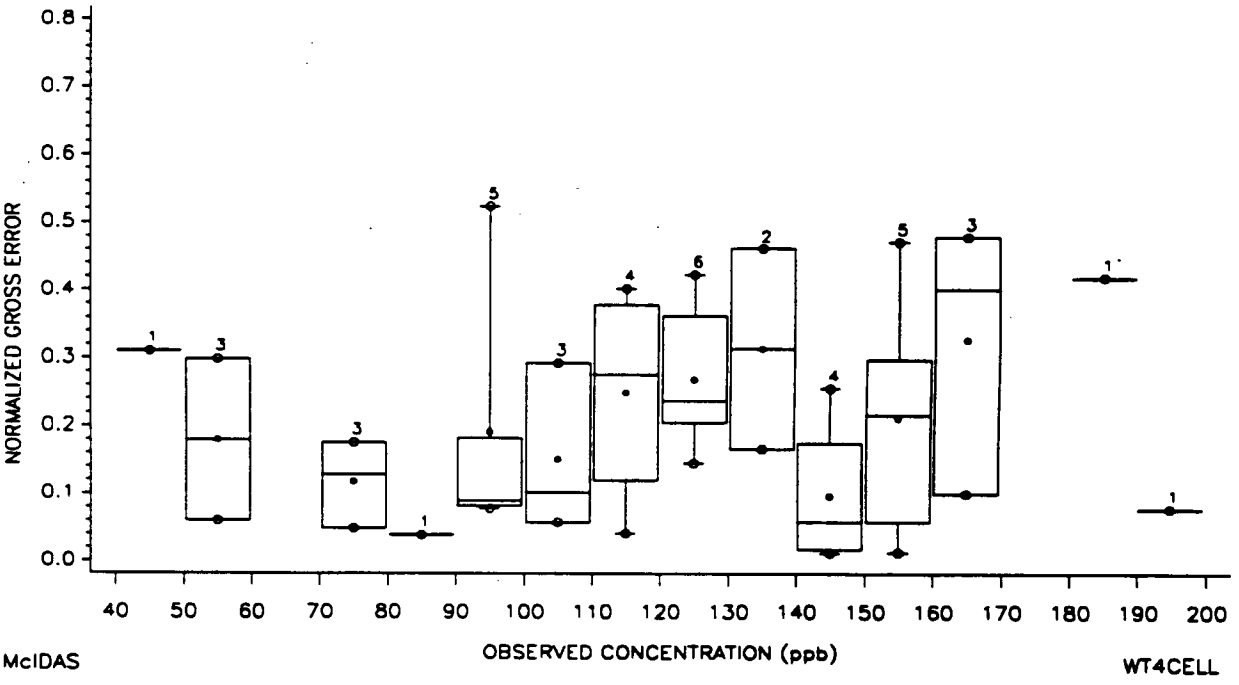

BOX–PLOT OF NORMALIZED GROSS ERROR BY DAY
FOR MMS CORPUS CHRISTI, EPISODE #2
JULY 26 – 31, 1990 (8 a.m. – 7 p.m.)

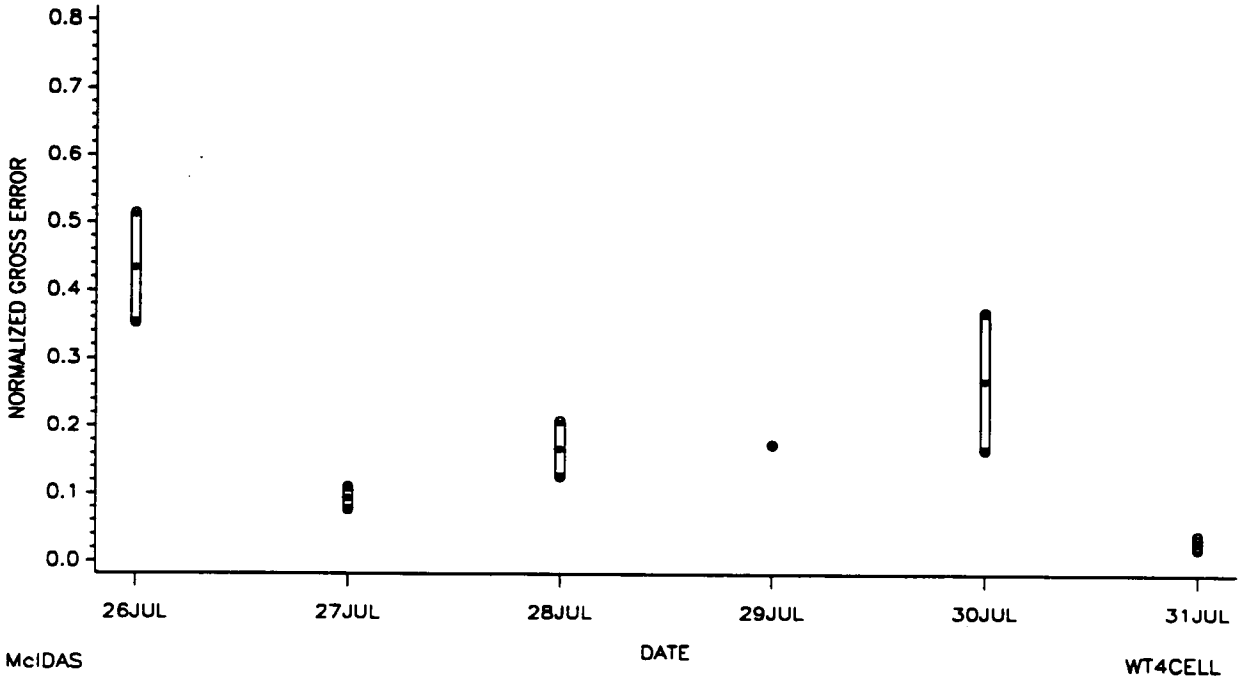

BOX–PLOT OF NORMALIZED GROSS ERROR BY O3 CONCENTRATION
FOR MMS CORPUS CHRISTI, EPISODE #2
JULY 26 – 31, 1990 (8 a.m. – 7 p.m.)

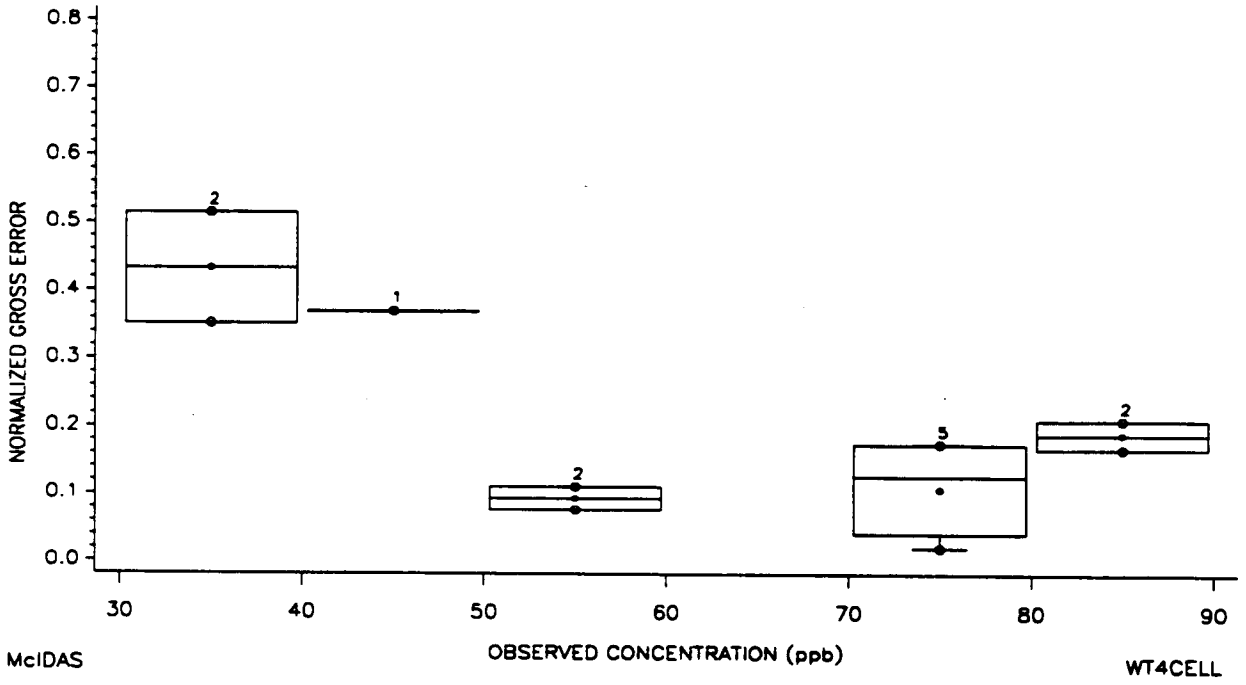

8 (b). Plots of Daily Paired Accuracy by Subregion,

For Episode #2, July 26 - July 31, 1990

DAILY PAIRED ACCURACY BY SUBREGION
FOR EPISODE #2
JULY 26–31, 1990 (8 a.m. – 7 p.m.)

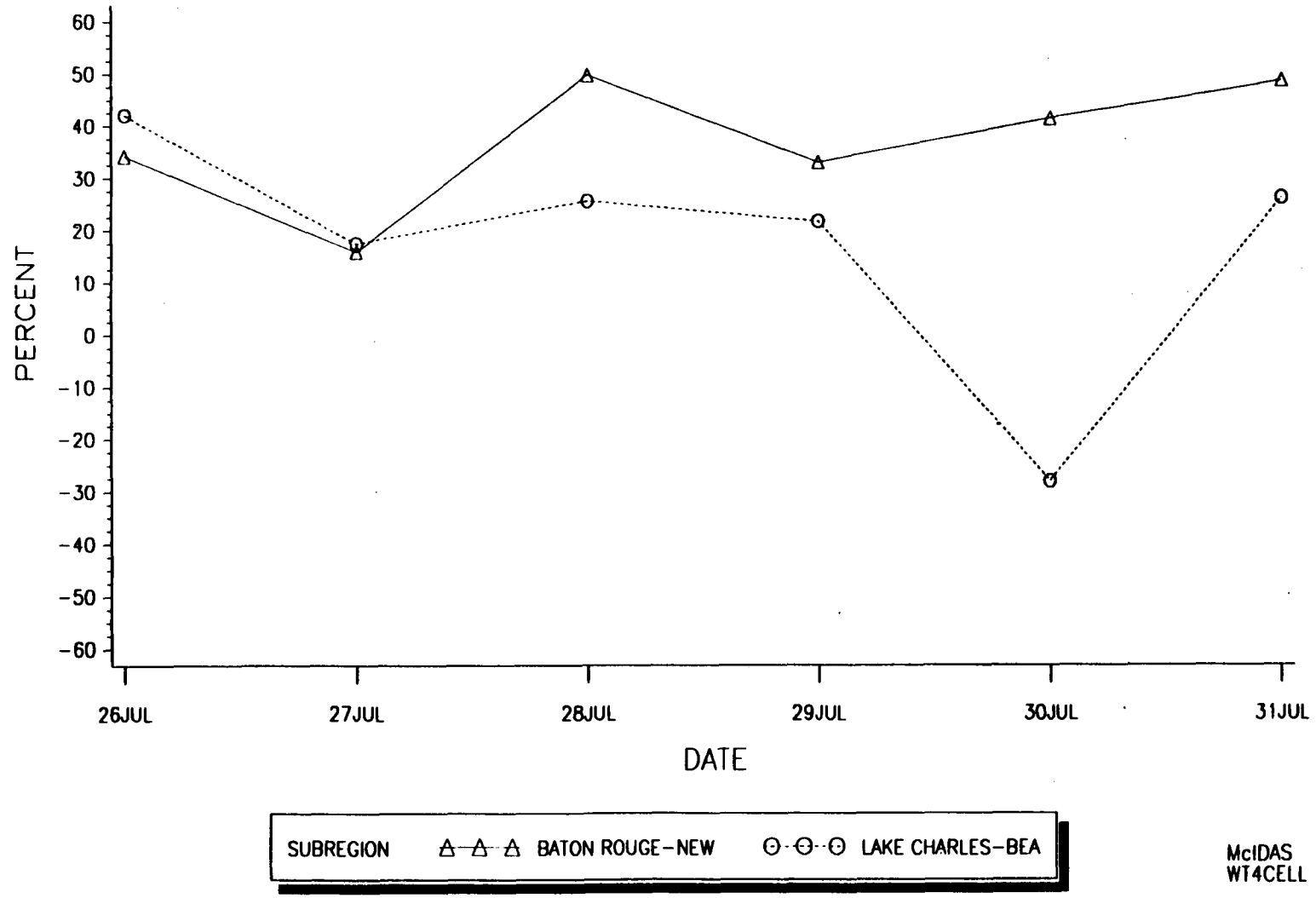

DAILY PAIRED ACCURACY BY SUBREGION
FOR EPISODE #2
JULY 26–31, 1990 (8 a.m. – 7 p.m.)

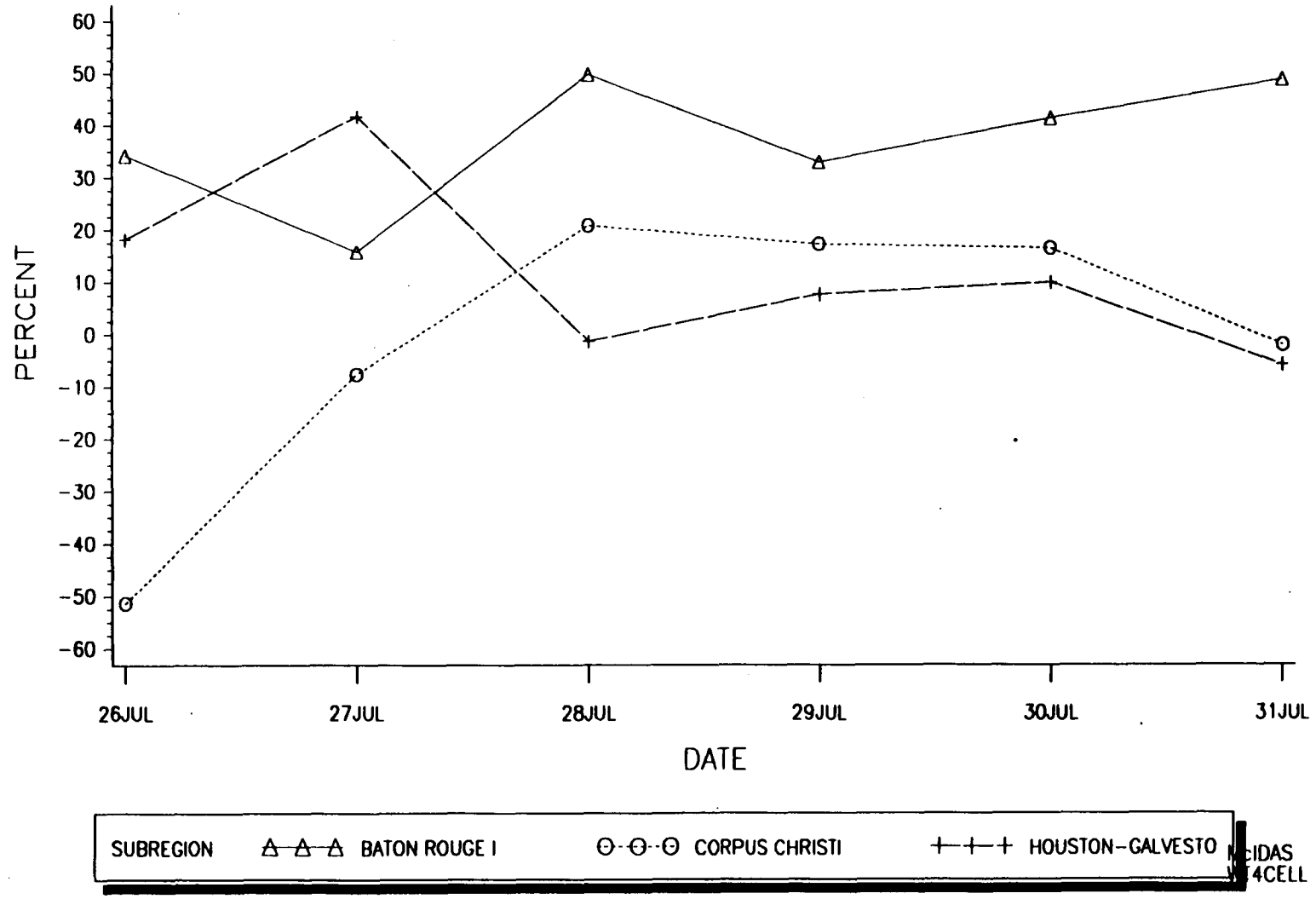

9 (b). Plots of Daily Unpaired Accuracy by Subregion.

For Episode #2, July 26 - July 31, 1990

DAILY UNPAIRED ACCURACY BY SUBREGION
FOR EPISODE #2
JULY 26–31, 1990 (8 a.m. – 7 p.m.)

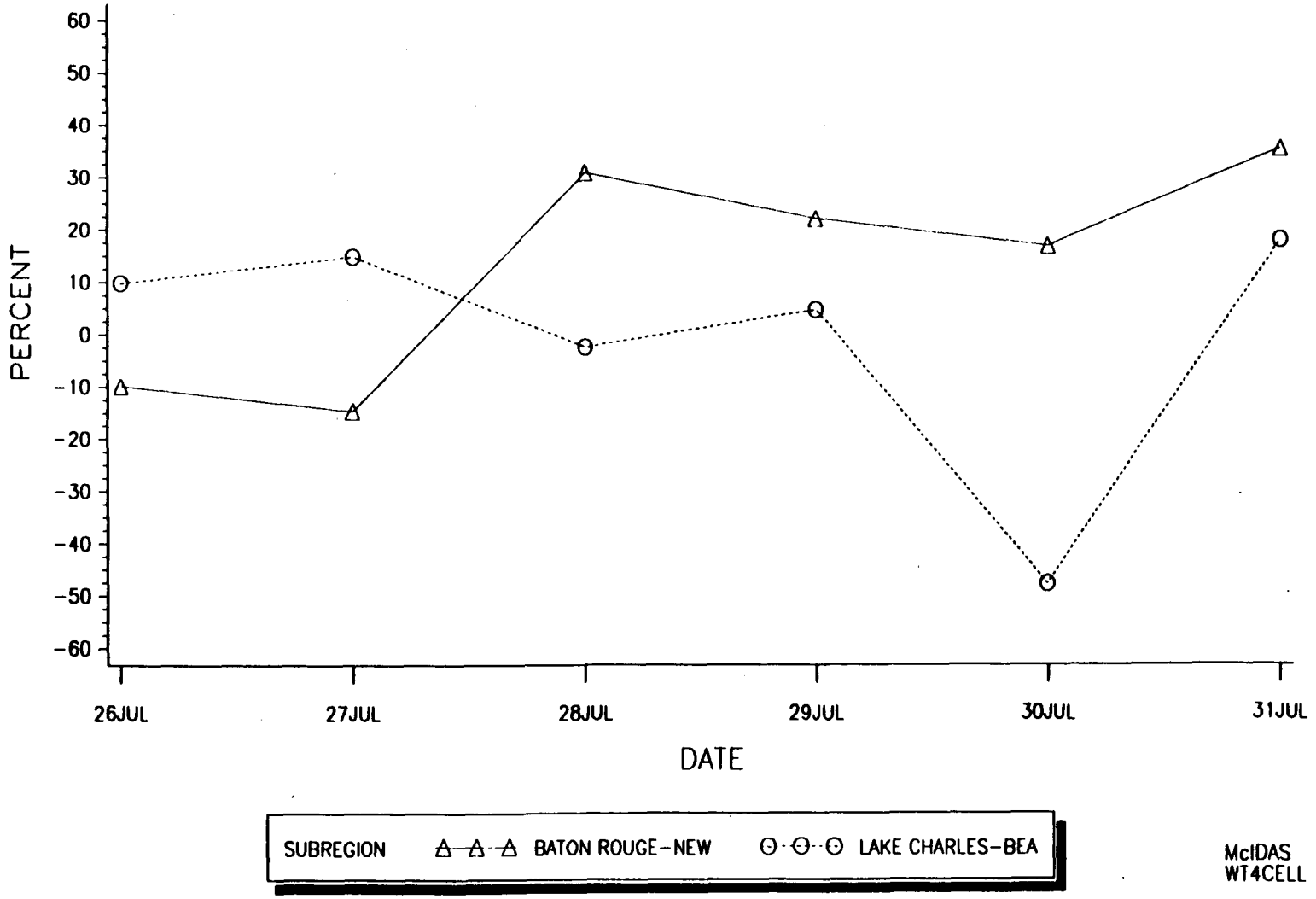

DAILY UNPAIRED ACCURACY BY SUBREGION
FOR EPISODE #2
JULY 26-31, 1990 (8 a.m. - 7 p.m.)

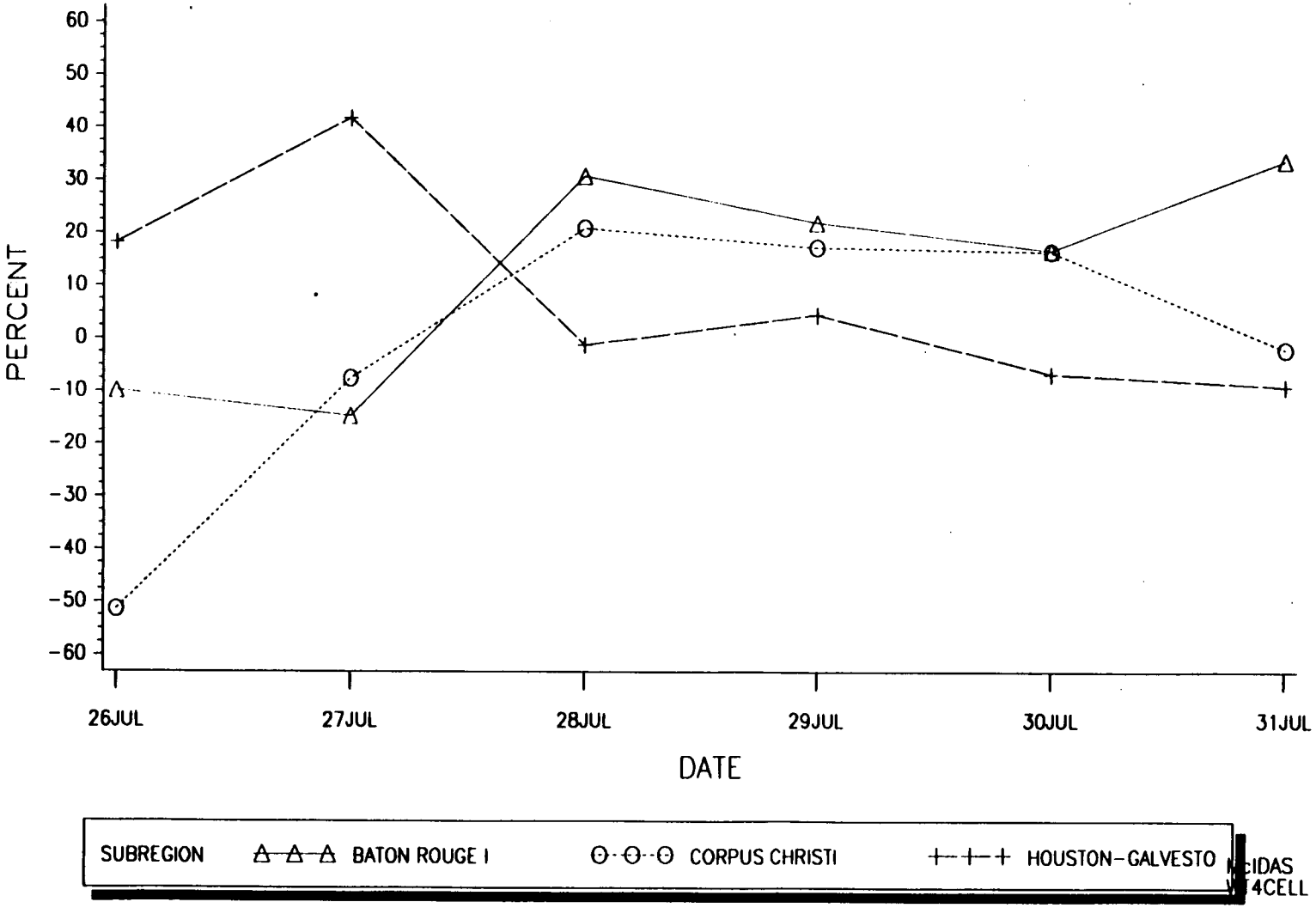

APPENDIX B

PERFORMANCE MEASURE FORMULATIONS

This appendix provides information on the notation, formulas, and statistical terminology, as discussed in Section 5 of the text and Appendix A. For reasons discussed in Section 5 of the text, only the daytime (8 a.m. - 7 p.m.) data (predictions and observations) are used in model performance evaluation for this study.

PERFORMANCE MEASURE FORMULATION

1. Spatially-Paired Peak Prediction Accuracy (A_s)

$$A_s = \frac{c_o(x,t) - c_p(x,T)}{c_o(x,t)} \times 100\%$$

where

A_s = paired highest-prediction accuracy (quantifies the difference between the magnitude of the highest[1] 1-hour observed value and the spatially paired highest 1-hour predicted value in a time window of +/- 3 hours of the observed maximum)

$c_o(x,t)$ = maximum 1-hour observed concentration over all hours between 8 a.m. and 7 p.m. and monitoring stations

$c_p(x,T)$ = maximum 1-hour predicted concentration over a time window +/- 3 hours of the observed maximum and paired surface grid squares

[1]"Highest" refers to the maximum 1-hour concentration across all daytime (8 a.m. - 7 p.m.) hours and monitoring stations.

2. Unpaired Highest-Prediction Accuracy (A_u)

$$A_u = \frac{c_o(x,t) - c_p(X,T)}{c_o(x,t)} \times 100\%$$

where

A_u = unpaired highest-prediction accuracy (quantifies the difference between the magnitude of the highest[2] 1-hour observed value and the highest 1-hour predicted value

$c_o(x,t)$ = maximum 1-hour observed concentration over all hours between 8 a.m. and 7 p.m. and monitoring stations

$c_p(X,T)$ = maximum 1-hour predicted concentration over a time window +/- 3 hours of the observed maximum and all surface grid squares

[2]"Highest" refers to the maximum 1-hour concentration across all daytime (8 a.m. - 7 p.m.) hours and monitoring stations.

3. Mean Bias of All Pairs (D)

$$D = \frac{1}{N_T} \sum_{i=1}^{N} \sum_{j=1}^{H_i} [c_o(i,j) - c_p(i,j)]$$

where

D = non-normalized bias from all hourly prediction-observation pairs

N = number of monitoring stations

H_i = number of hourly prediction-observation pairs for monitoring station i

N_T = total number of station-hours

$$= \sum_{i=1}^{N} H_i$$

$c_o(i,j)$ = observed value at monitoring station i for hour j

$c_p(i,j)$[3] = weighted predicted value at paired four grids of monitoring station i for hour j

[3]Predicted value derived from weighted average of the predicted value at the four grid cells nearest to station i for the given hour j. The pairing aggregation of the "predicted" with the "observed" monitoring data is described in Appendix C.

4. Normalized Bias (D^*)

$$D^* = \frac{1}{N_T} \sum_{i=1}^{N} \sum_{j=1}^{H_i} \frac{c_o(i,j) - c_p(i,j)}{c_o(i,j)}$$

where

D^*	=	normalized bias obtained from all hourly prediction-observation pairs
N	=	number of monitoring stations
H_i	=	number of hourly prediction-observation pairs for monitoring station i
N_T	=	total number of station-hours (defined previously)
$c_o(i,j)$	=	observed value at monitoring station i for hour j
$c_p(i,j)$[4]	=	predicted value at monitoring station i for hour j

[4]Predicted value derived from weighted average of the four grid cells nearest to station *i* for the given hour.

5. Normalized Gross Error of All Pairs (E_d^*)

$$E_d^* = \frac{1}{N_T} \sum_{i=1}^{N} \sum_{j=1}^{H_i} \frac{|c_o(i,j) - c_p(i,j)|}{c_o(i,j)}$$

where

E_d^*	=	normalized gross error for all hourly prediction-observation pairs
N_T	=	total number of station hours (defined previously)
N	=	number of monitoring stations
H_i	=	number of hourly prediction-observation pairs for monitoring station i
$c_o(i,j)$	=	observed value at monitoring station i for hour j
$c_p(i,j)$[5]	=	predicted value at monitoring station i for hour j

[5]Predicted value derived from weighted average of the predicted values at the four grid cells nearest to station *i* for the given hour *j*.

6. Fractional Bias for Peak Concentration

The fractional bias is calculated for both the mean and standard deviation of peak ozone values, as follows:

$$F_m = 2 \times \frac{(m_o - m_p)}{(m_o + m_p)}$$

$$F_s = 2 \times \frac{(s_o - s_p)}{(s_o + s_p)}$$

where

F_m = fractional bias of means

F_s = fractional bias of standard deviation

m_o = mean maximum observed concentration

m_p = mean peak predicted concentration

s_o = standard deviation of peak observed concentrations

s_p = standard deviation of peak predicted concentrations

The means and standard deviations of predicted and observed concentrations are determined by each of two methods:

Peak station values:

$C_o(i,.)$ = maximum observed concentration at monitoring station i across all hours

$C_p(i,.)$[6] = maximum predicted concentration at monitoring station i across all hours

where i = 1,...,N monitoring stations

Peak hourly values:

$C_o(.,j)$ = maximum observed concentration at hour j across all monitoring stations

$C_p(.,j)$[7] = maximum predicted concentration at hour j across all monitoring stations

where j = 1,...,H hours

The fractional bias of the mean and standard deviation varies from -2 to +2. Negative values indicate overprediction and positive values indicate underprediction.

[6]Predicted value derived from weighted average of the predicted values at the four grid cells nearest to the station i across all hours.

[7]Predicted value derived from the maximum four-cell-weighted-average value of spatially paired grid cells at all stations for the given hour j. The spatial pairing is described in Appendix C.

APPENDIX C

ALGORITHMS FOR CELL-AGGREGATION

APPENDIX C

ALGORITHMS FOR CELL-AGGREGATION

C.1 DISTANCE-WEIGHTED ALGORITHM

The algorithm applies to both the distance-weighted, four-cell and the distance-weighted, nine-cell aggregation method. The algorithm calculates an average concentration that is weighted according to the squared inverse of the distance from the monitor to the center of each cell. Therefore, the predicted concentrations of the cell centers that are closer to the monitor are given greater weight than the values of the cell centers that are farther from the monitor. The formula for this algorithm is:

$$AV = \sum \frac{PR}{D^2} \div \sum \frac{1}{D^2}$$

where PR is the predicted concentration for each cell and D is the distance from cell center to monitor.

C.2 FOUR-CELL ALGORITHM

The distance-weighted four cell approach uses the following algorithm to select a square of four cells; then, it applies the distance-weighted algorithm described in C.1 to arrive at a unique aggregation method.

The four-cell algorithm first determines which quadrant of cell 5 the monitor occupies. Next, it selects the three cells adjacent to that quadrant to complete a square of four cells. This process is illustrated in Figure C-1.

If the monitor is in the northwest quadrant of cell 5, then cells 5, 4, 7, and 8 are selected. If the monitor is in the northeast quadrant of cell 5, then cells 5, 6, 8, and 9 are selected. If the monitor is in the southwest quadrant of cell 5, then cells 5, 1, 2, and 4 are selected. If the monitor is in the southeast quadrant of cell 5, then cells 5, 2, 3, and 6 are selected.

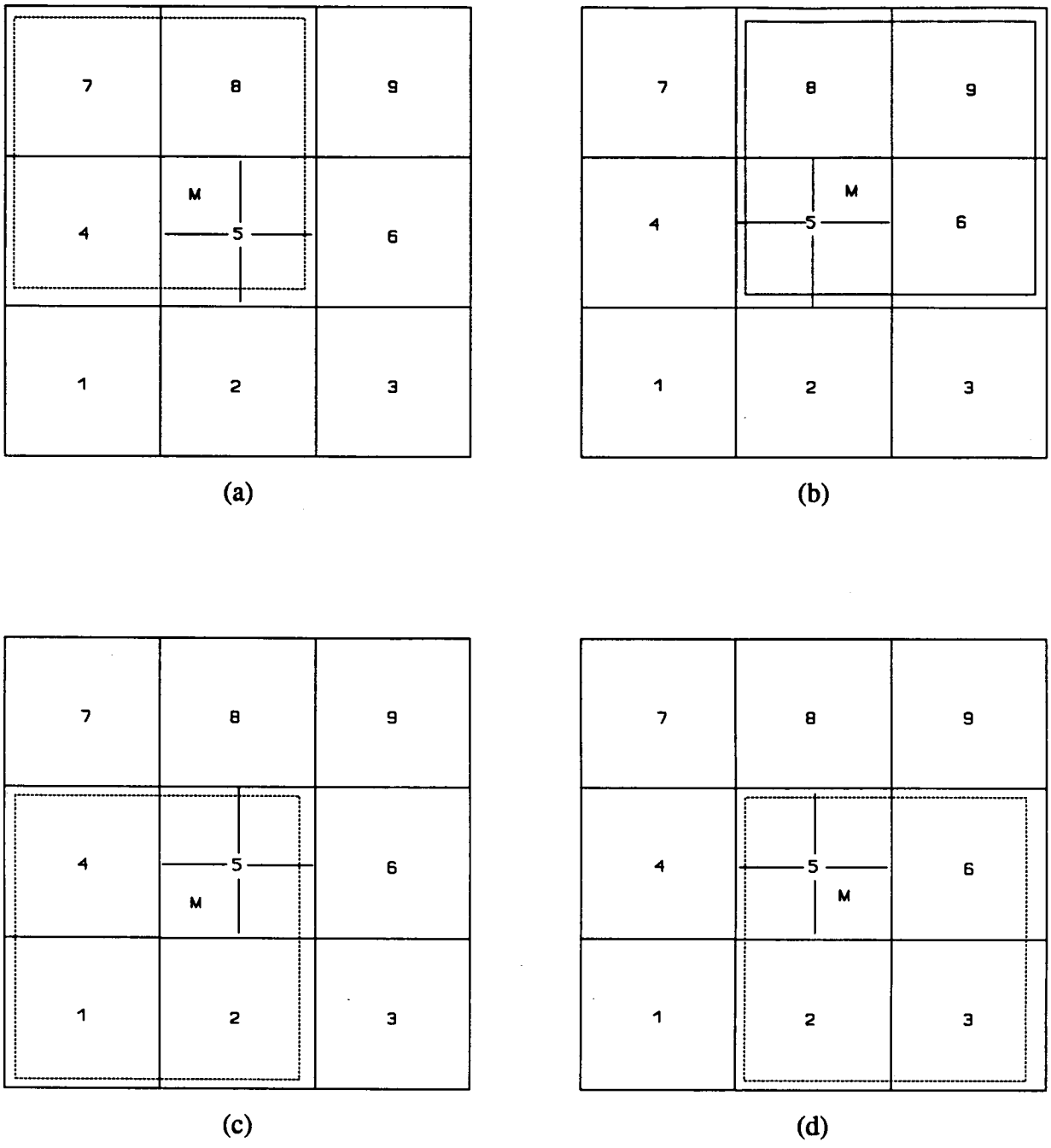

Figure C-1. The square of four cells.
(a) Monitor in northwest quadrant of cell 5.
(b) Monitor in northeast quadrant of cell 5.
(c) Monitor in southwest quadrant of cell 5.
(d) Monitor in southeast quadrant of cell 5.

APPENDIX D

EPISODIC AND DAILY VALUE PLOTS OF PREDICTED OZONE DIFFERENCES BETWEEN THE SCENARIOS AND BASE CASE (units: ppb)

Episodic Ozone Concentration Difference
Between Without OCS Emissions and Base Case
For Episode #1, July 25, 1988 - August 6, 1988

Difference: MMS Base Without OCS - MMS Base
Episode Maximum Ozone, Layer 1 – July 25 – July 31, 1988

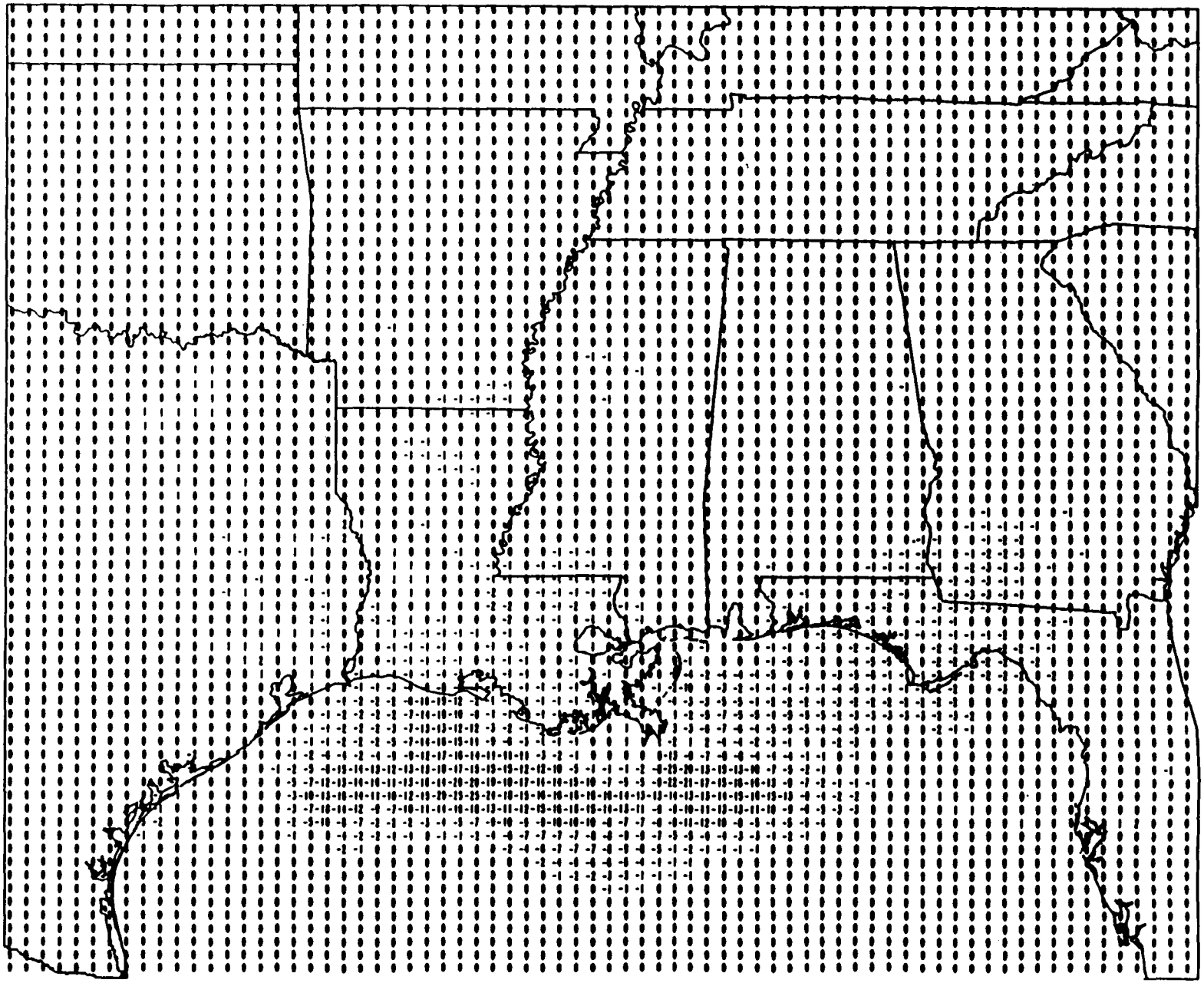

Difference: MMS Base Without OCS - MMS Base
Episode Maximum Ozone, Layer 1 – August 1 – August 6, 1988

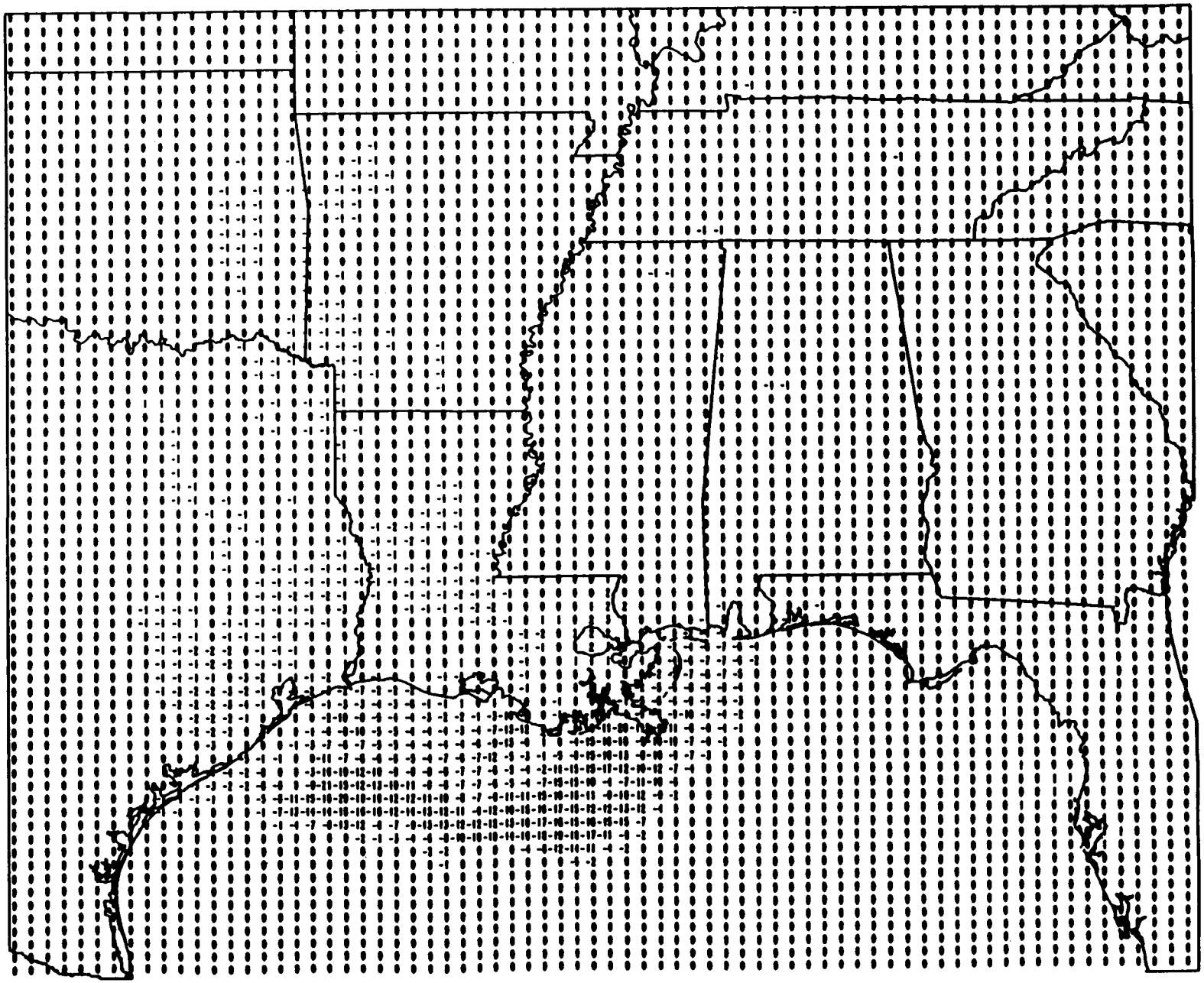

Daily Ozone Concentration Difference
Between Without OCS Emissions and Base Case
For Episode #1, July 25, 1988 - August 6, 1988

Difference: MMS Base Without OCS - MMS Base
Daily Maximum Ozone, Layer 1 – JULY 25, 1988

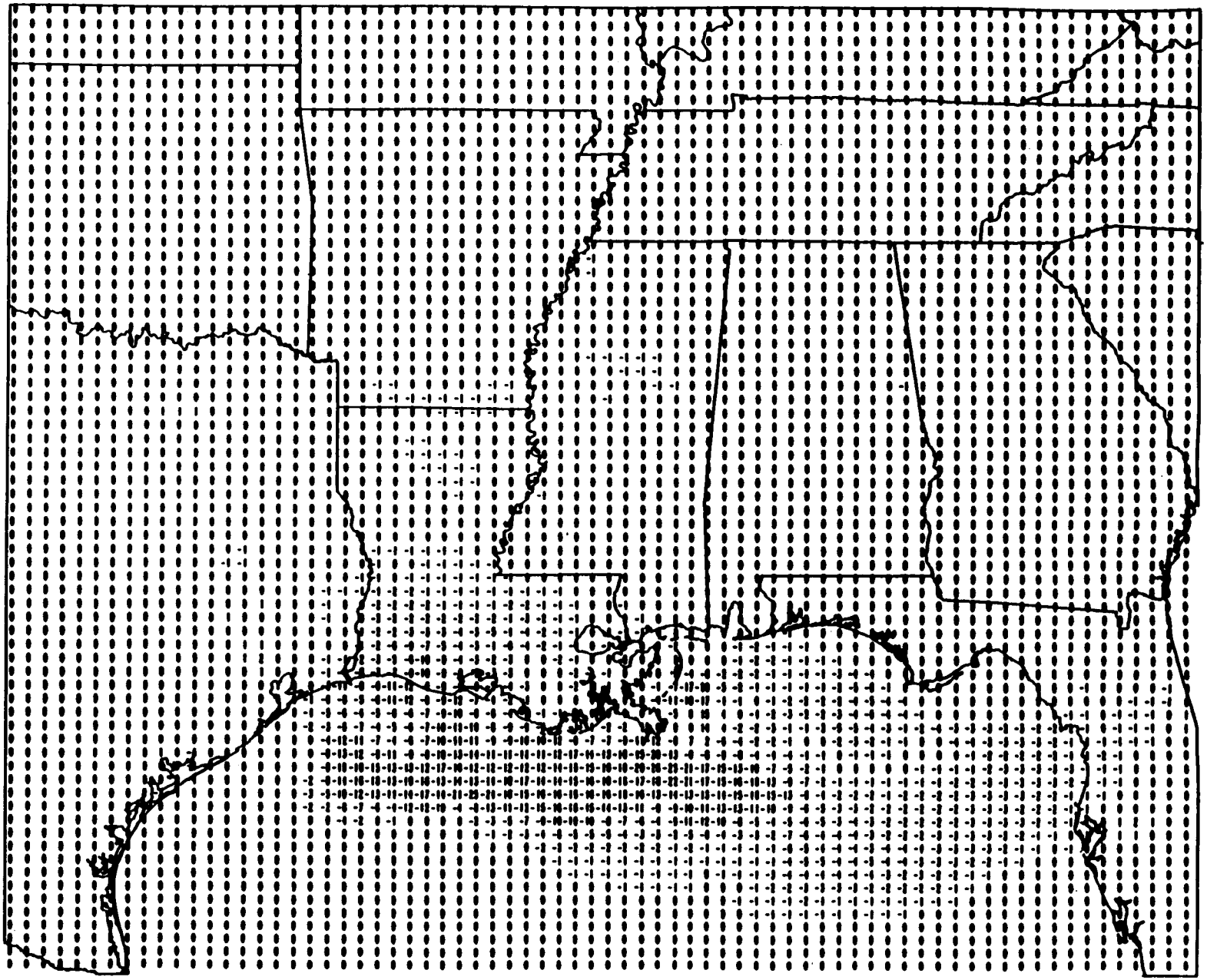

Difference: MMS Base Without OCS - MMS Base
Daily Maximum Ozone, Layer 1 – JULY 26, 1988

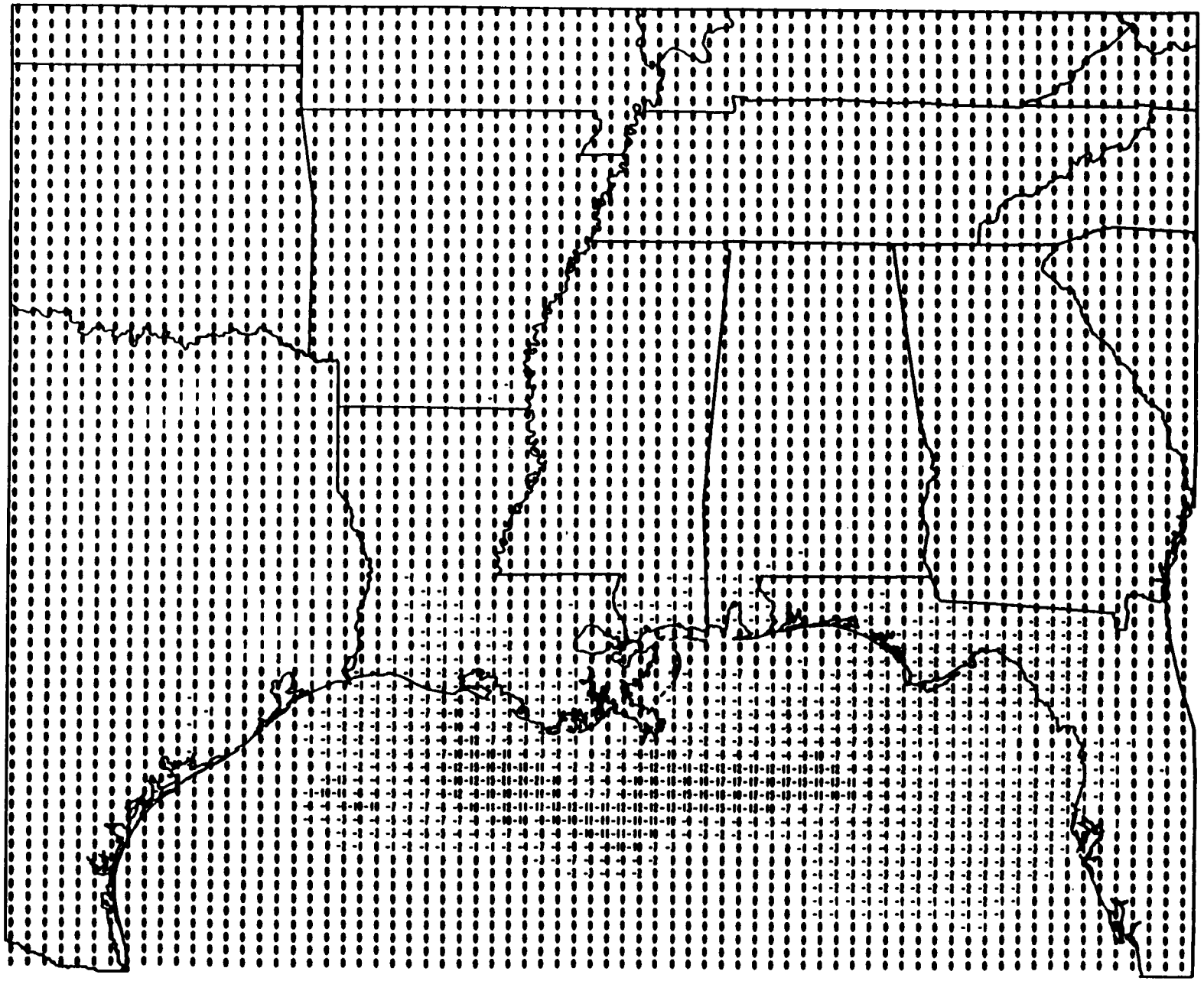

Difference: MMS Base Without OCS - MMS Base
Daily Maximum Ozone, Layer 1 – JULY 27, 1988

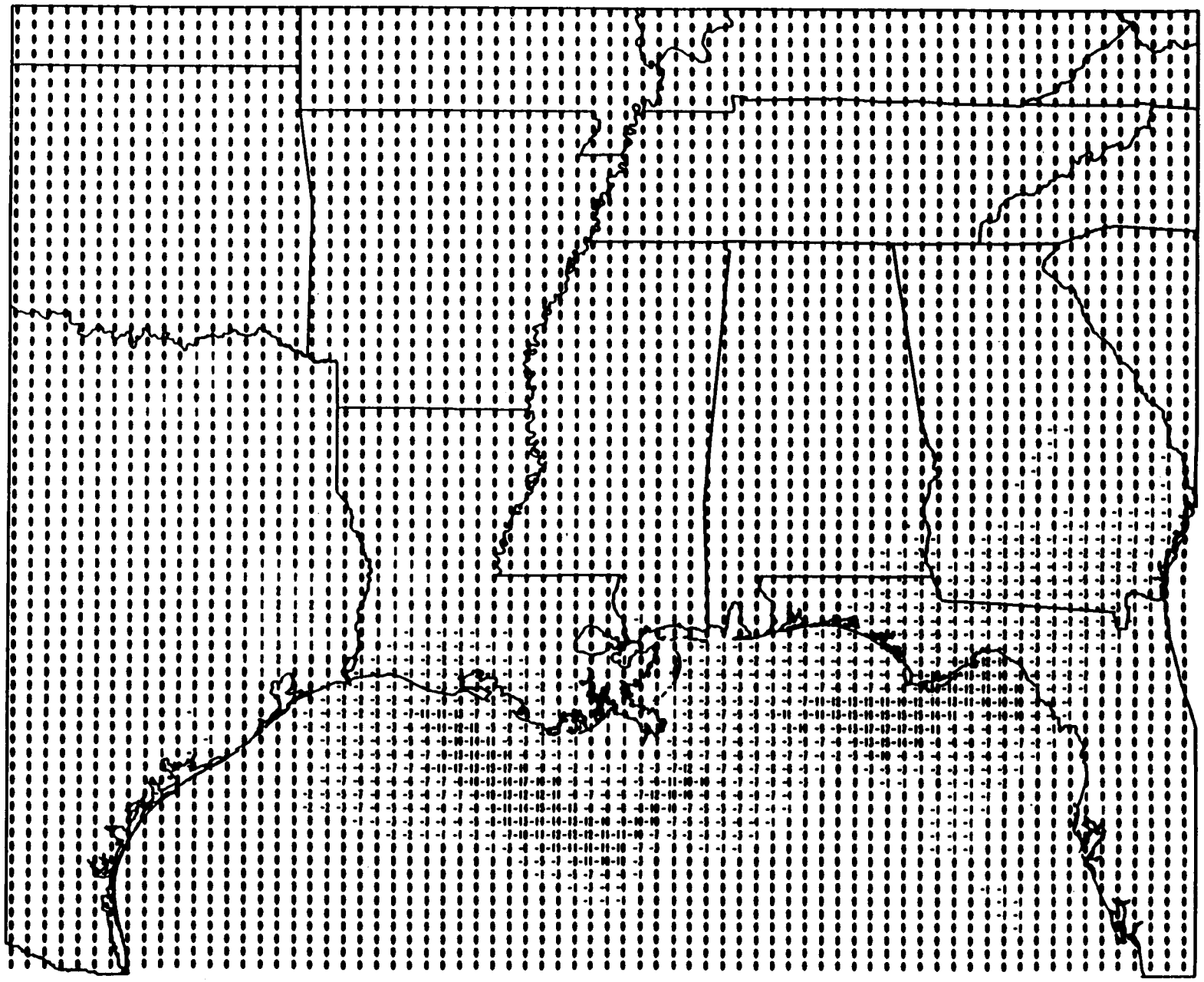

Difference: MMS Base Without OCS - MMS Base
Daily Maximum Ozone, Layer 1 – JULY 28, 1988

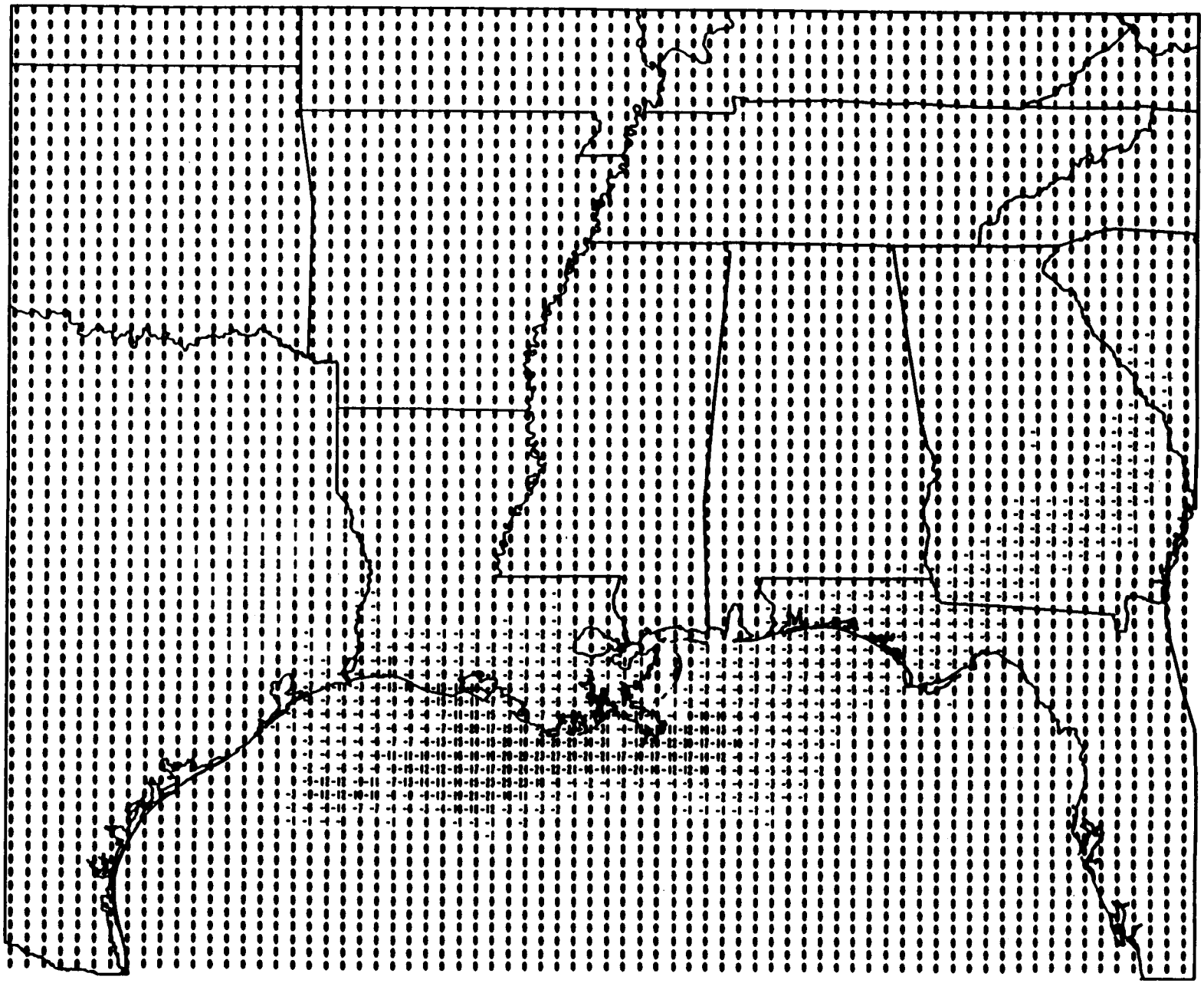

Difference: MMS Base Without OCS - MMS Base
Daily Maximum Ozone, Layer 1 – JULY 29, 1988

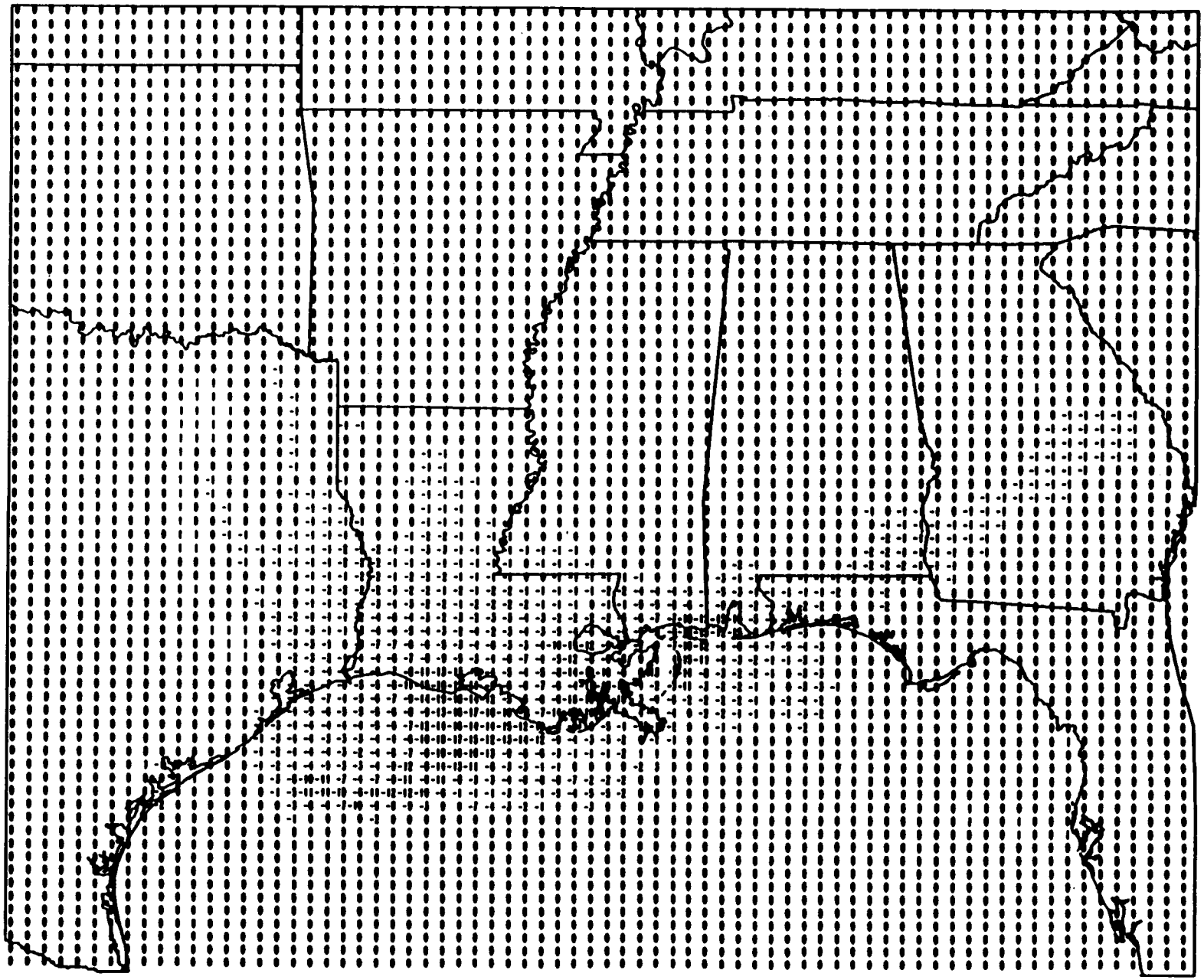

Difference: MMS Base Without OCS - MMS Base
Daily Maximum Ozone, Layer 1 – JULY 30, 1988

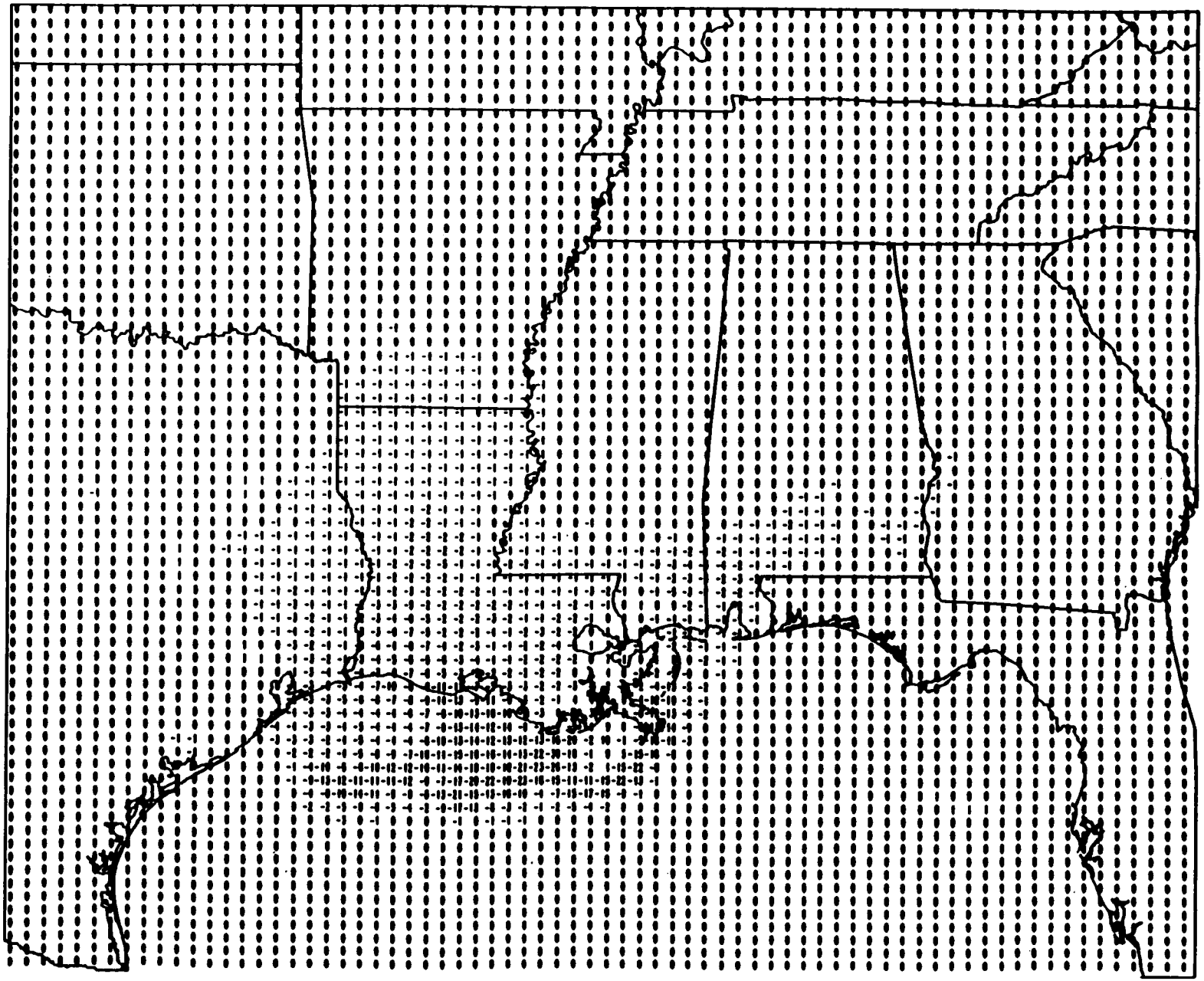

Difference: MMS Base Without OCS - MMS Base
Daily Maximum Ozone, Layer 1 – JULY 31, 1988

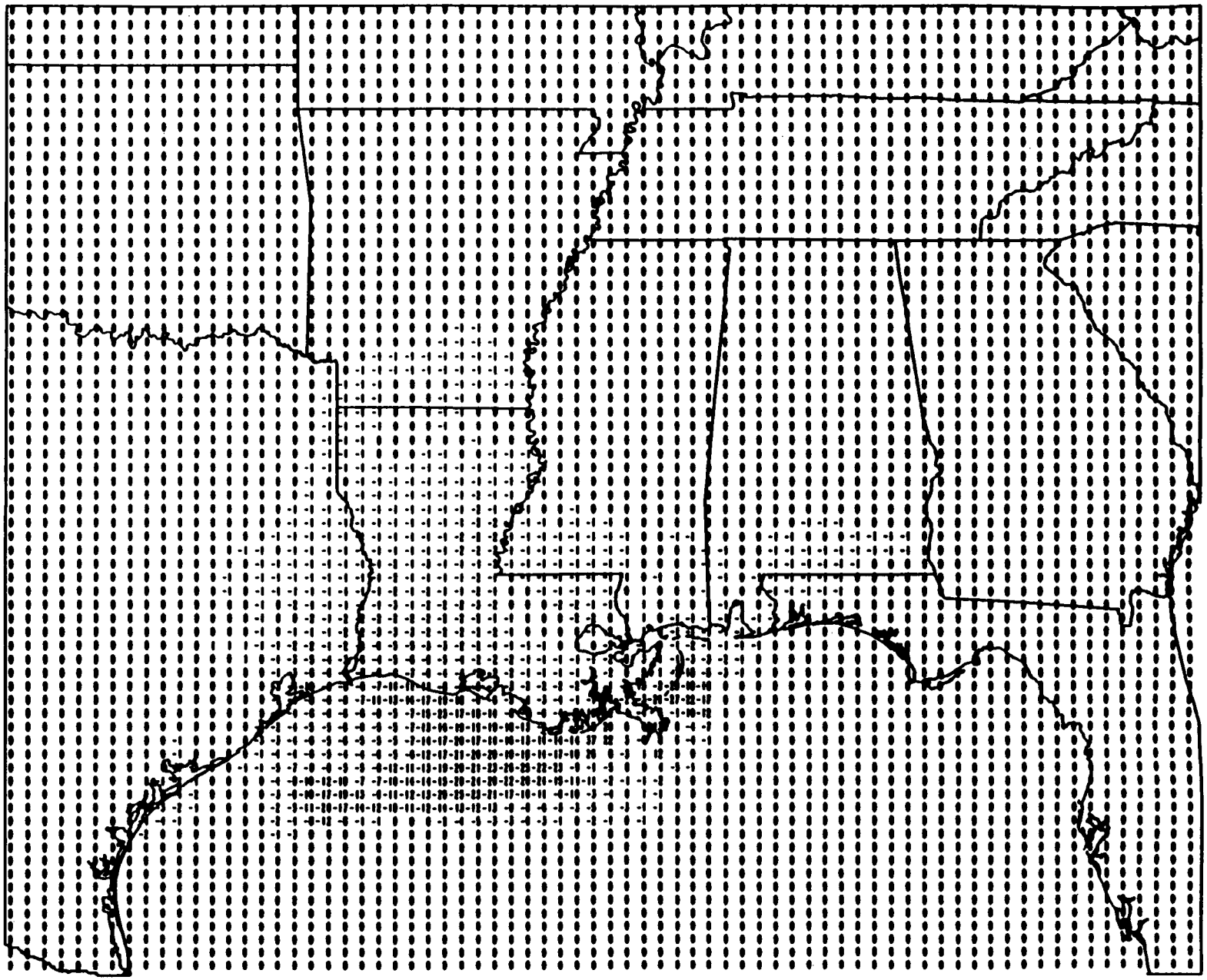

Difference: MMS Base Without OCS - MMS Base
Daily Maximum Ozone, Layer 1 – AUGUST 1, 1988

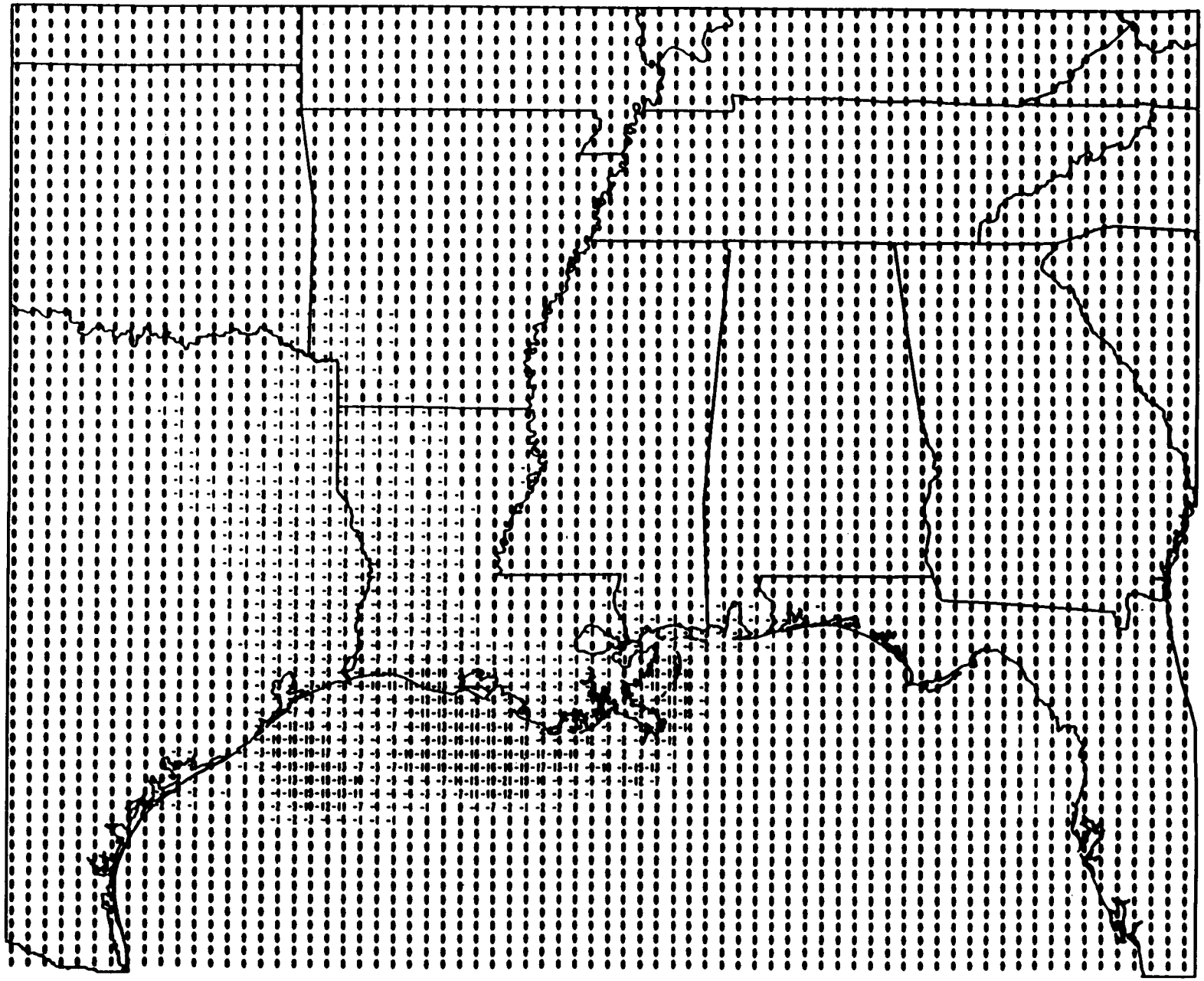

Difference: MMS Base Without OCS - MMS Base
Daily Maximum Ozone, Layer 1 – AUGUST 2, 1988

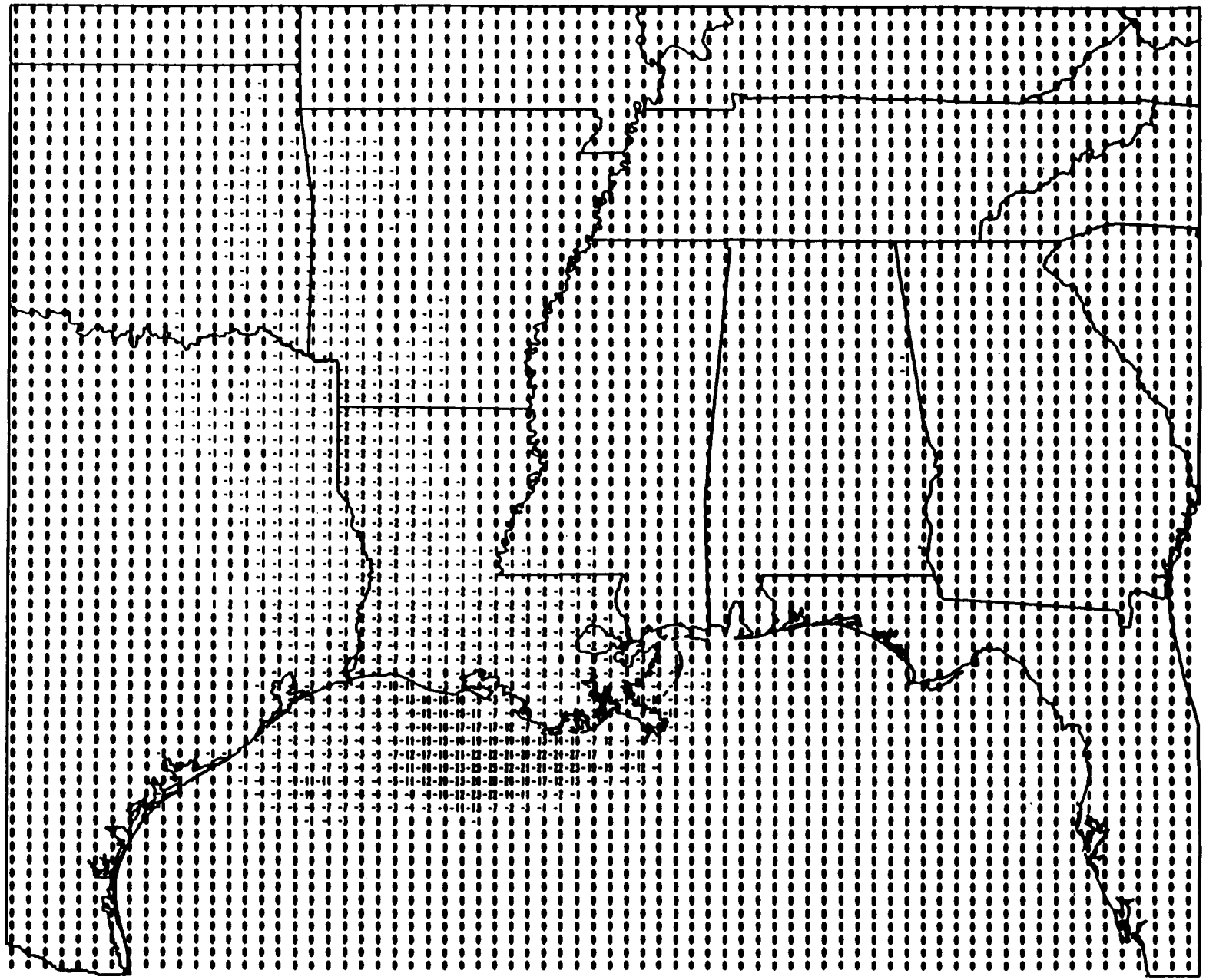

Difference: MMS Base Without OCS - MMS Base
Daily Maximum Ozone, Layer 1 – AUGUST 3, 1988

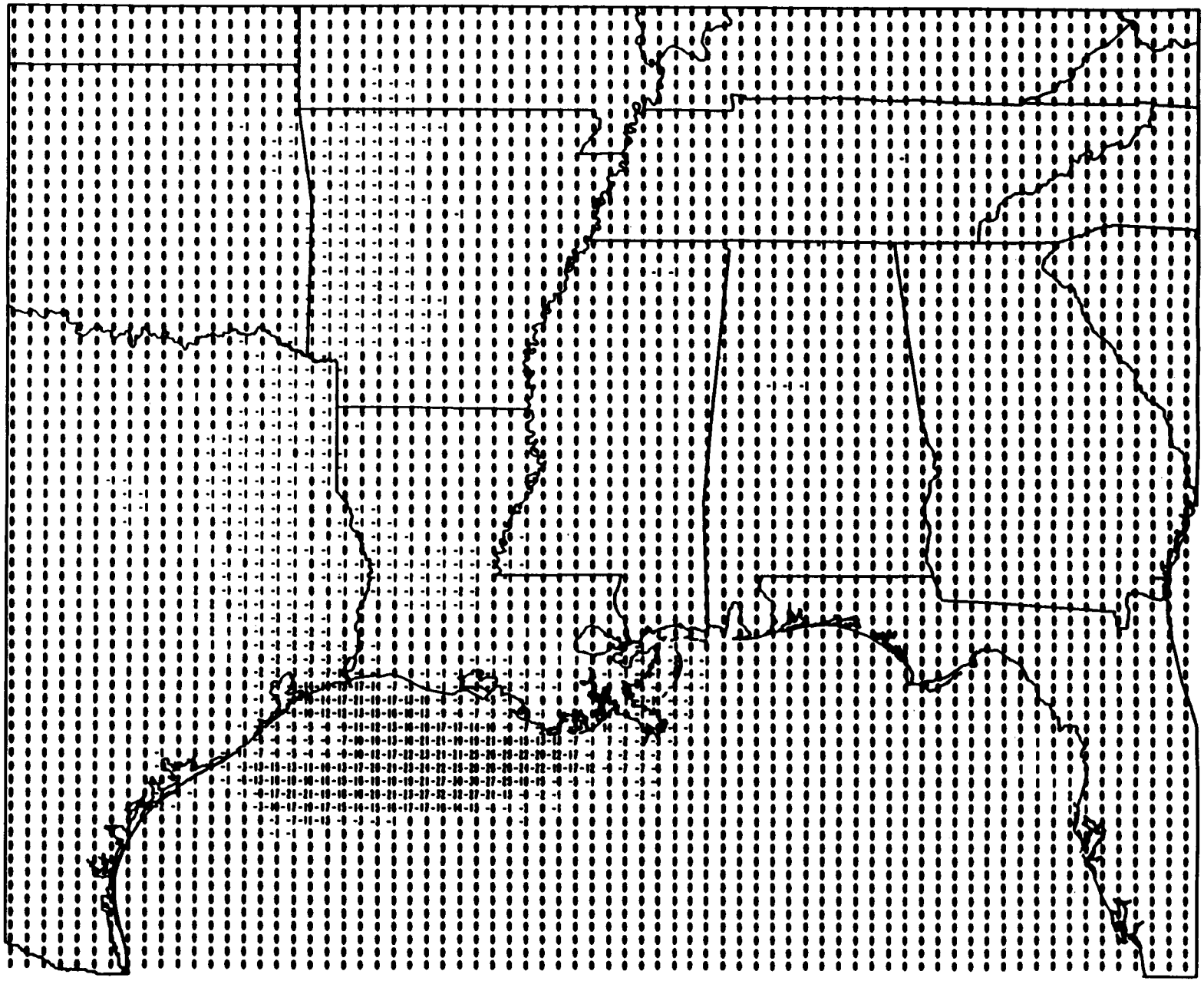

Difference: MMS Base Without OCS - MMS Base
Daily Maximum Ozone, Layer 1 – AUGUST 4, 1988

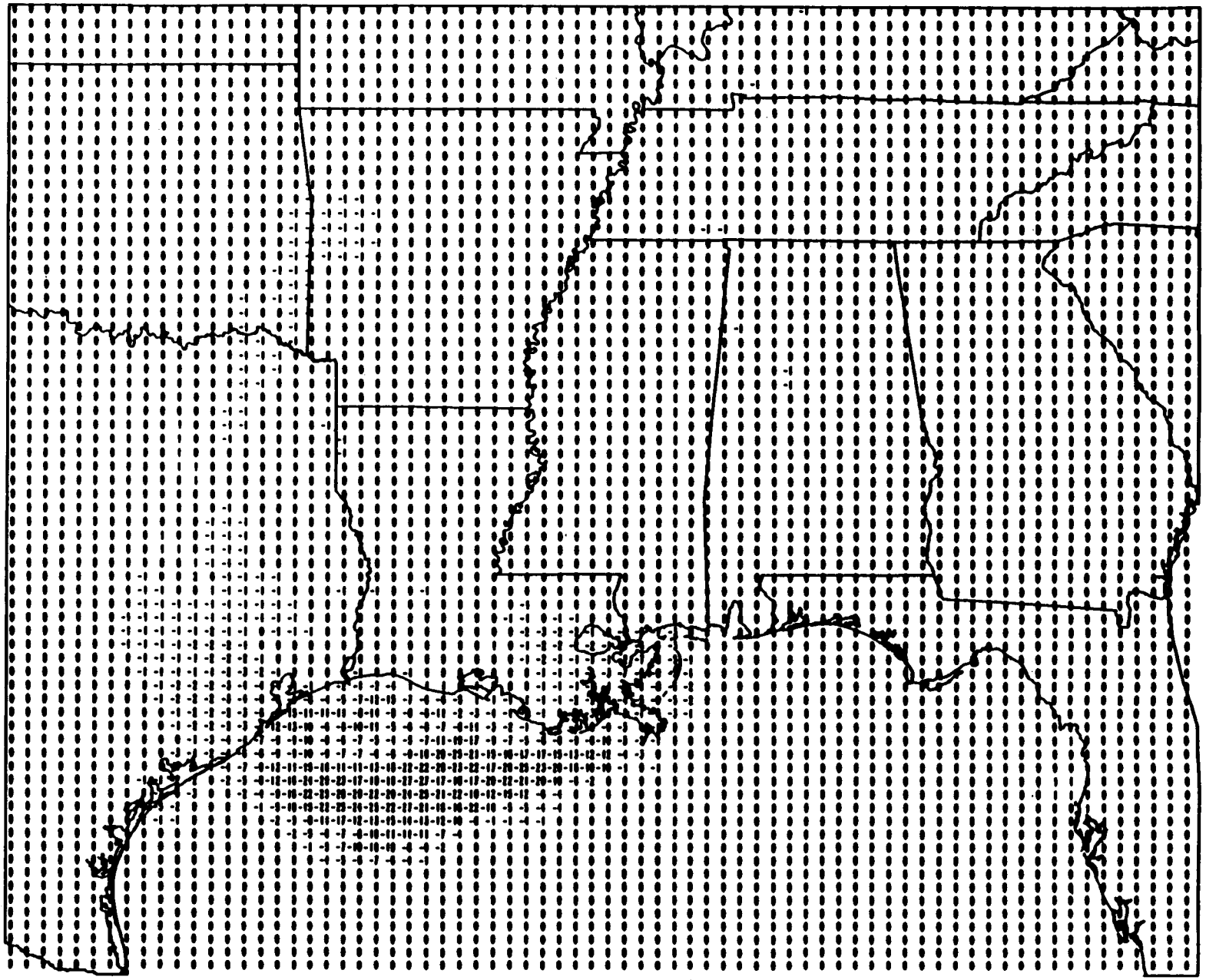

Difference: MMS Base Without OCS - MMS Base
Daily Maximum Ozone, Layer 1 – AUGUST 5, 1988

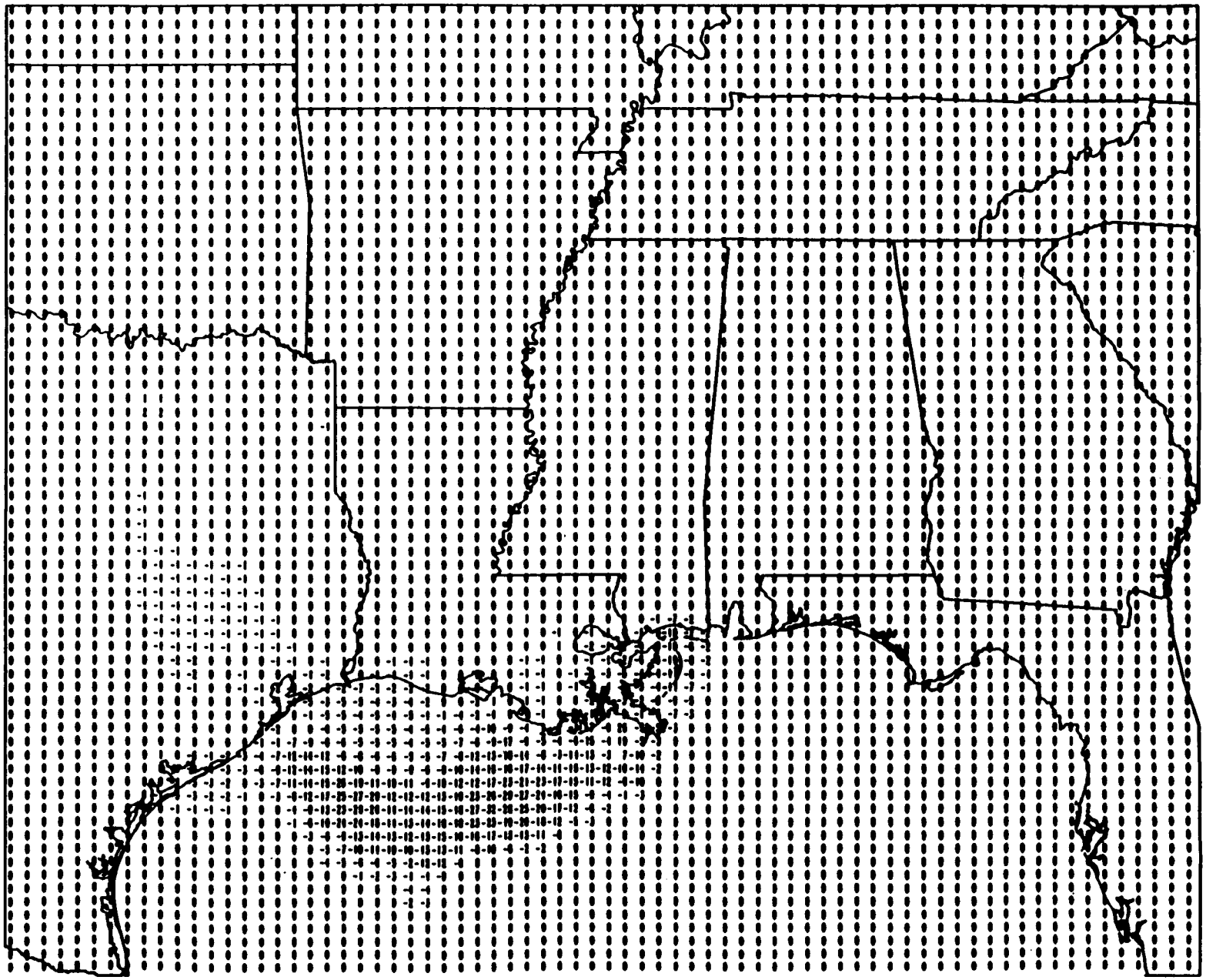

Difference: MMS Base Without OCS - MMS Base
Daily Maximum Ozone, Layer 1 – AUGUST 6, 1988

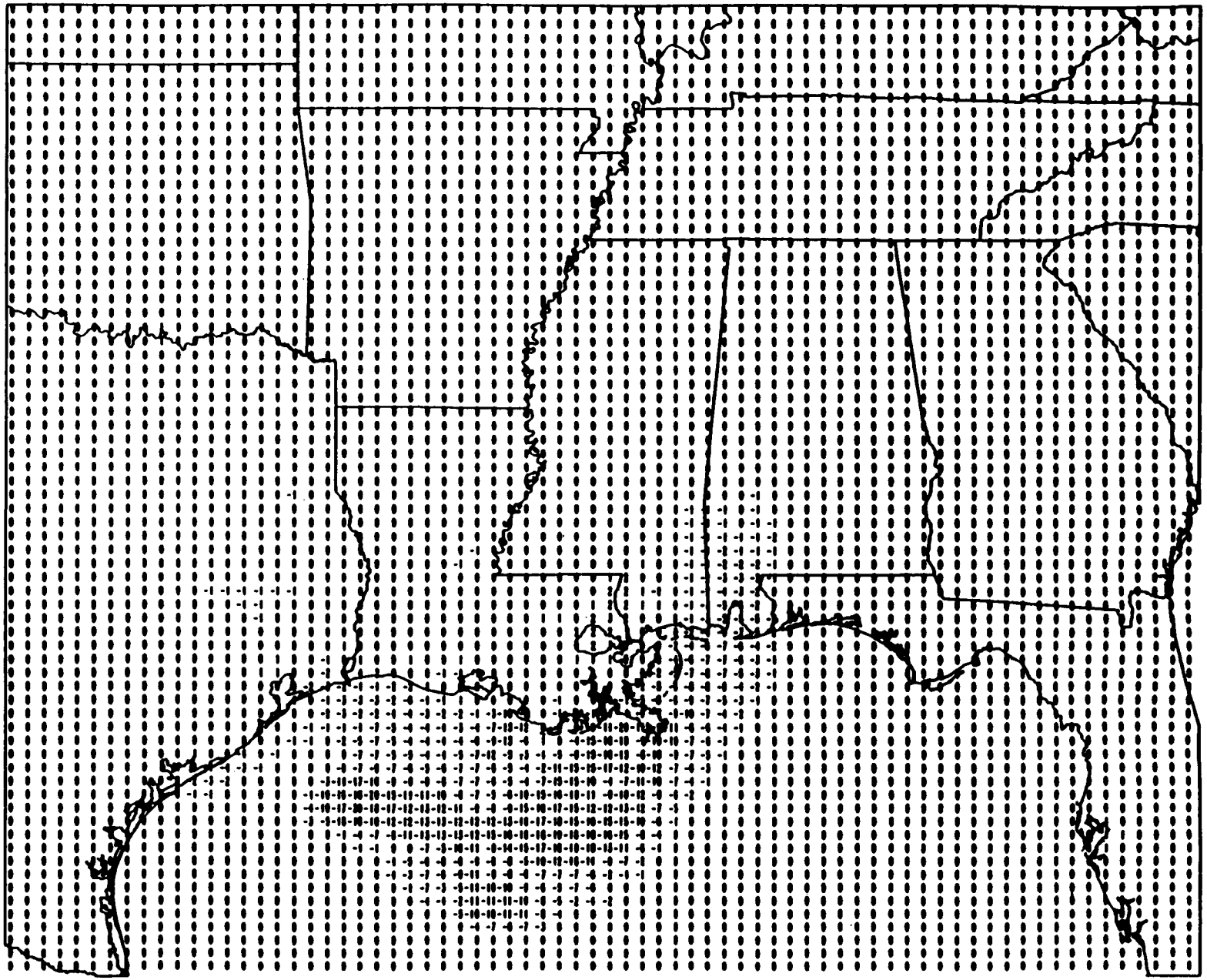

Episodic Ozone Concentration Difference
Between Double OCS Emissions and Base Case
For Episode #1, July 25, 1988 - August 6, 1988

Difference: MMS Base With Double OCS - MMS Base
Episode Maximum Ozone, Layer 1 – July 25 – July 31, 1988

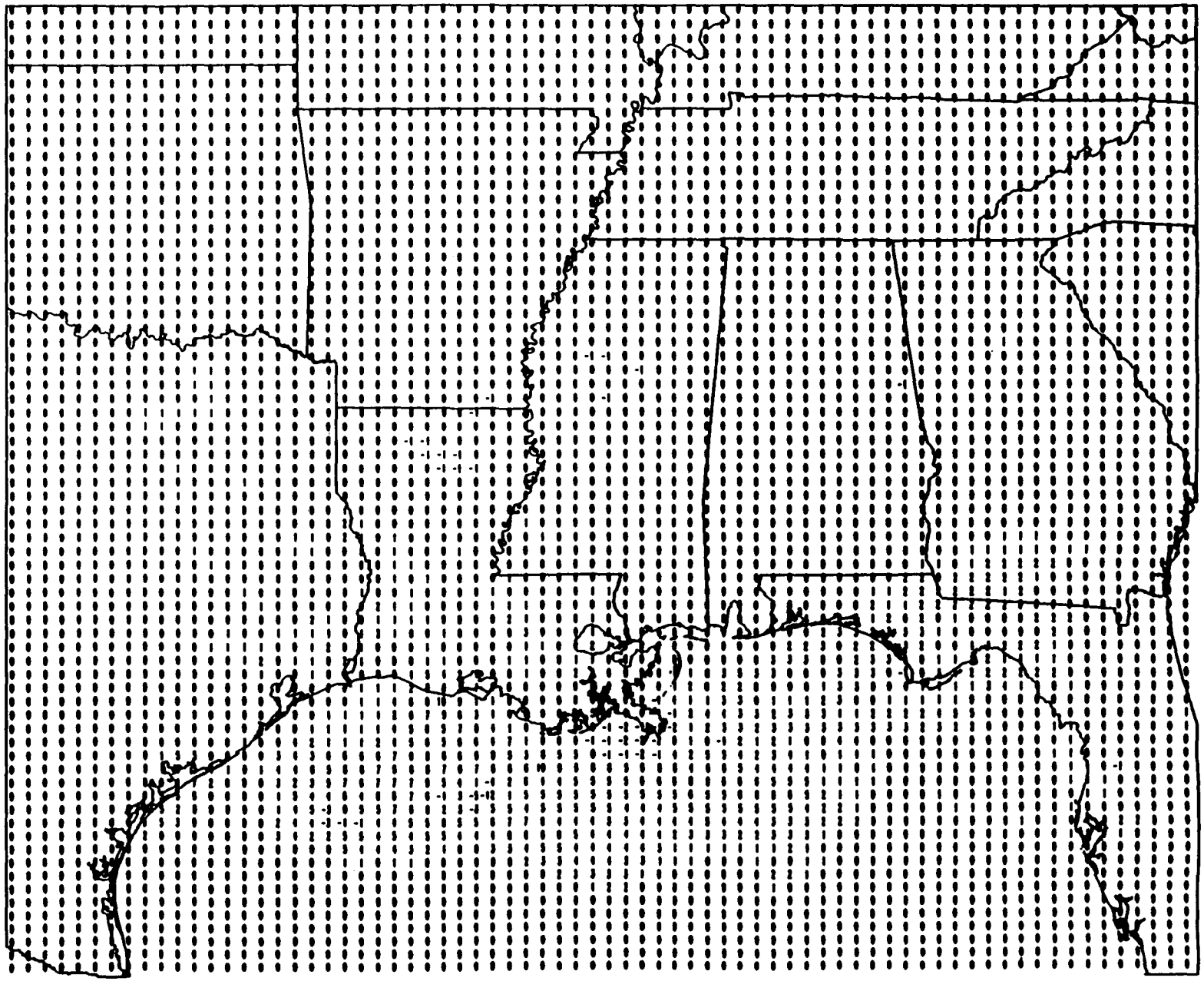

Difference: MMS Base With Double OCS - MMS Base
Episode Maximum Ozone, Layer 1 – August 1 – August 6, 1988

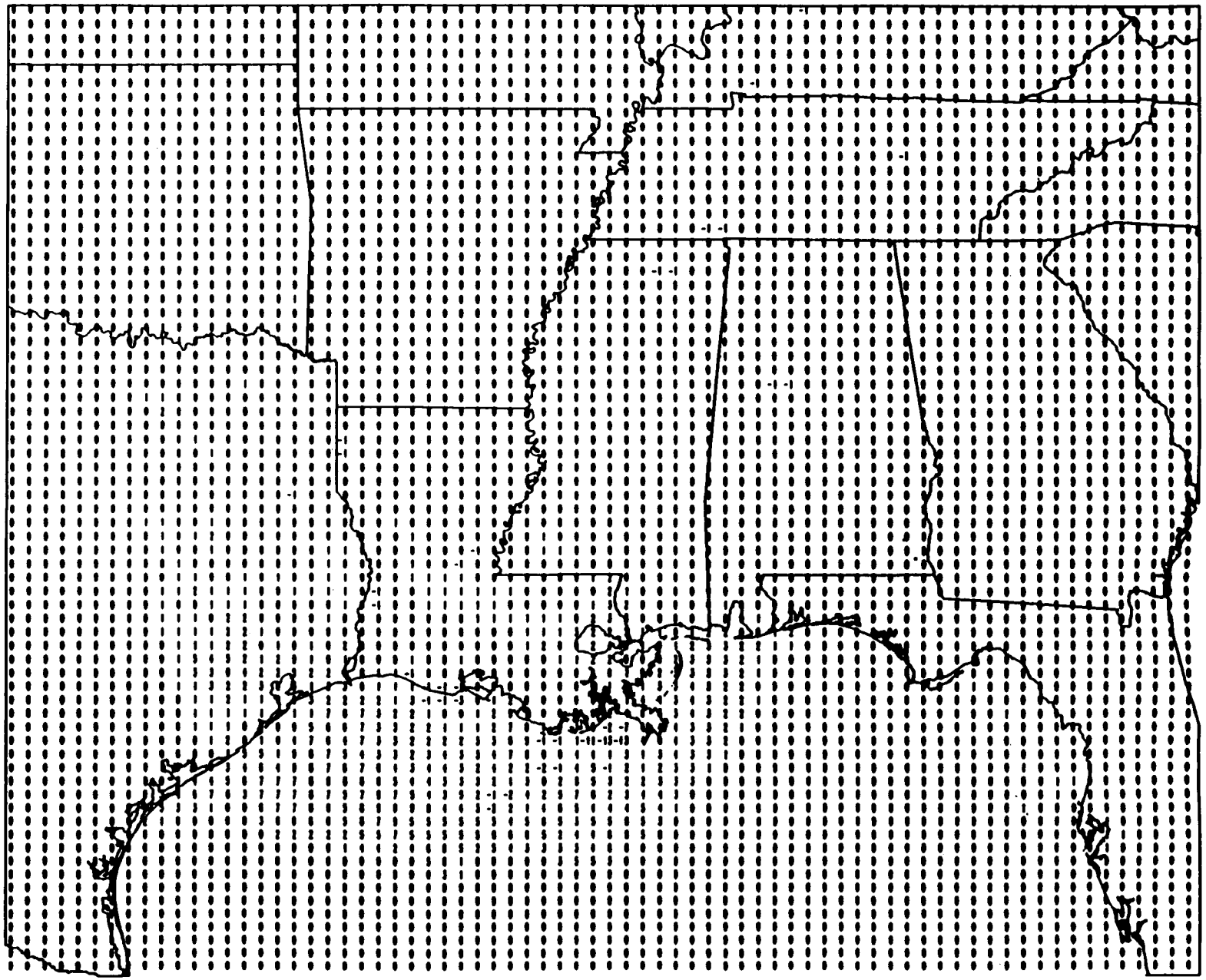

Daily Ozone Concentration Difference
Between Double OCS Emissions and Base Case
For Episode #1, July 25, 1988 - August 6, 1988

Difference: MMS Base With Double OCS - MMS Base
Daily Maximum Ozone, Layer 1 – JULY 25, 1988

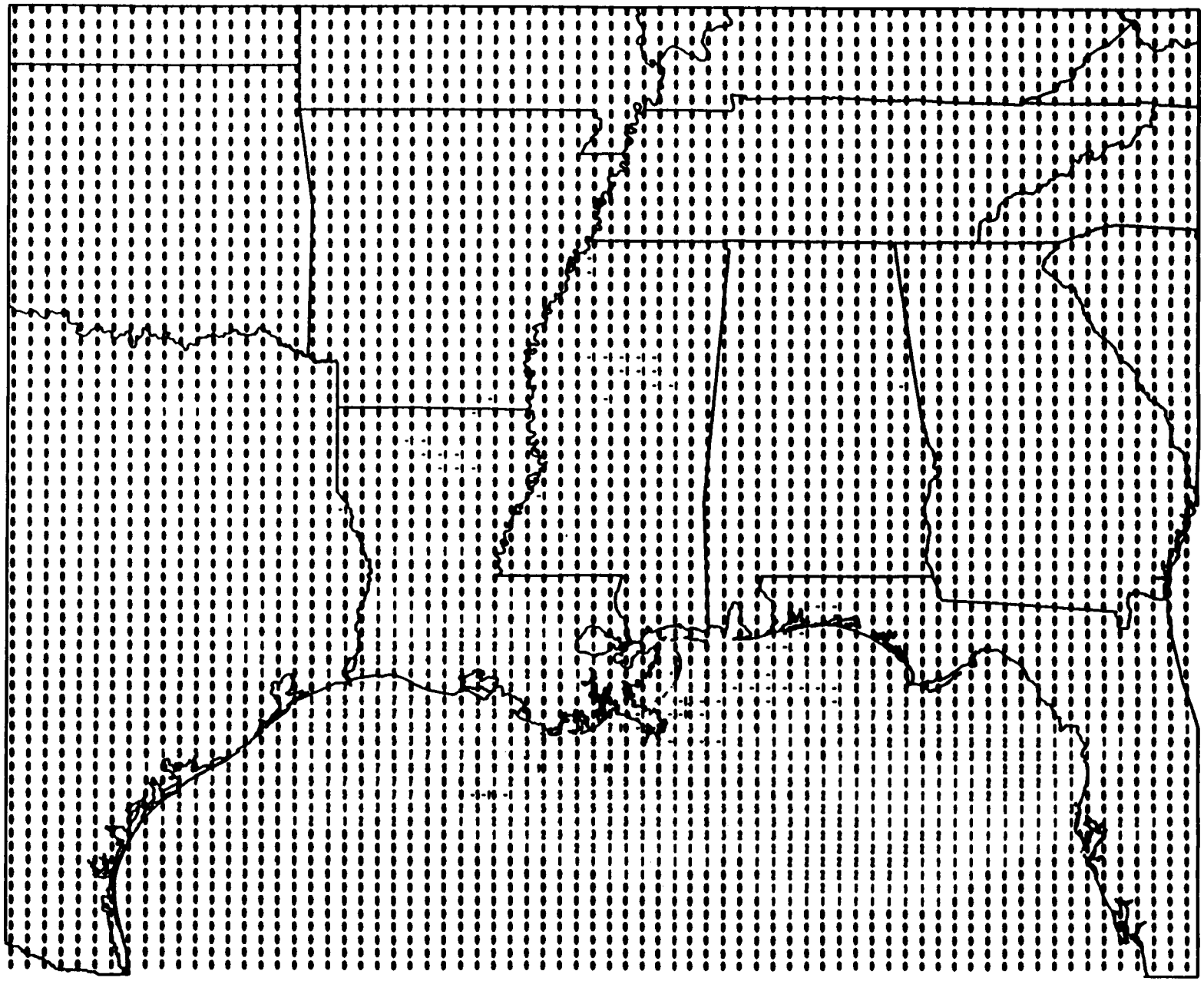

Difference: MMS Base With Double OCS - MMS Base
Daily Maximum Ozone, Layer 1 – JULY 26, 1988

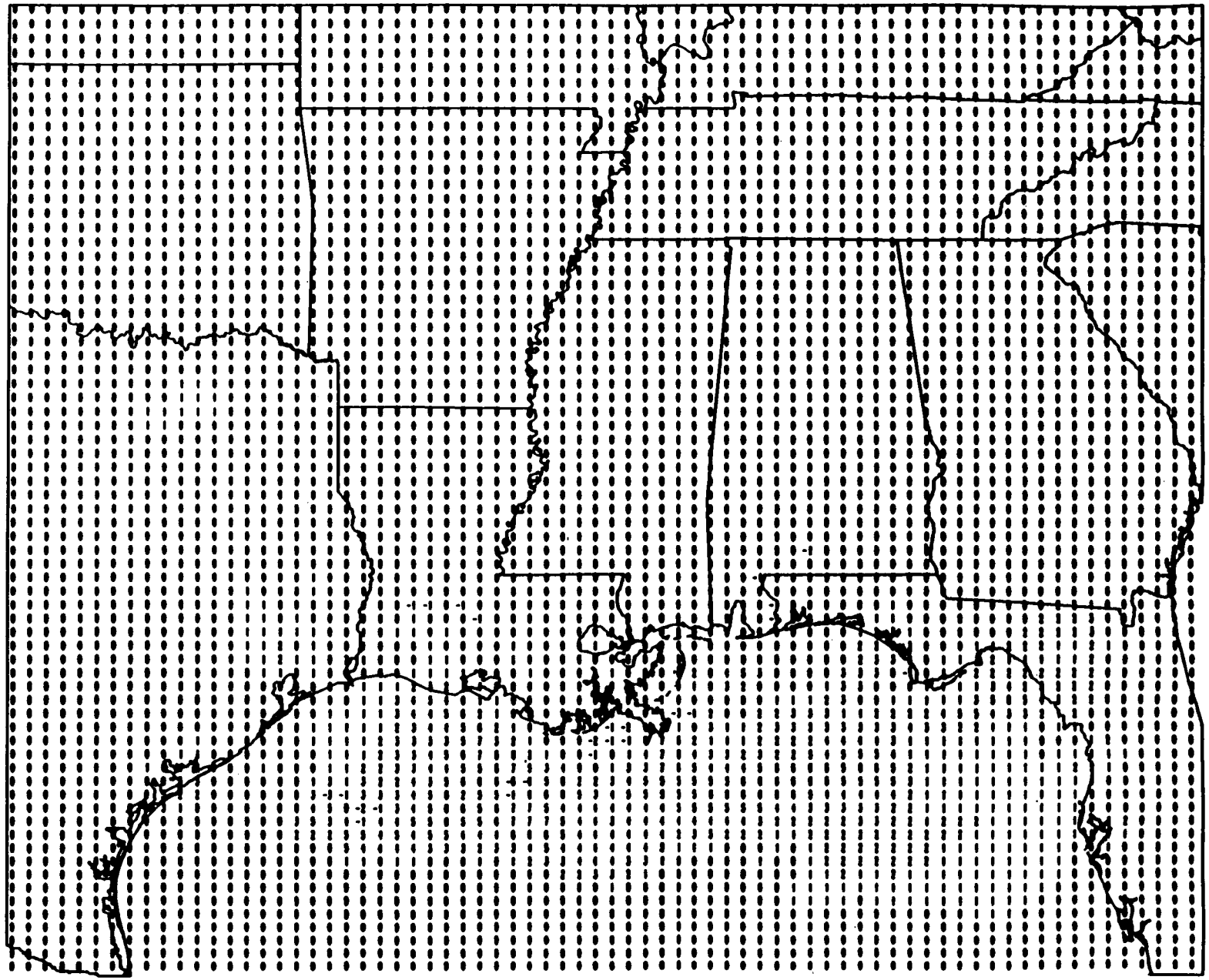

Difference: MMS Base With Double OCS - MMS Base
Daily Maximum Ozone, Layer 1 – JULY 27, 1988

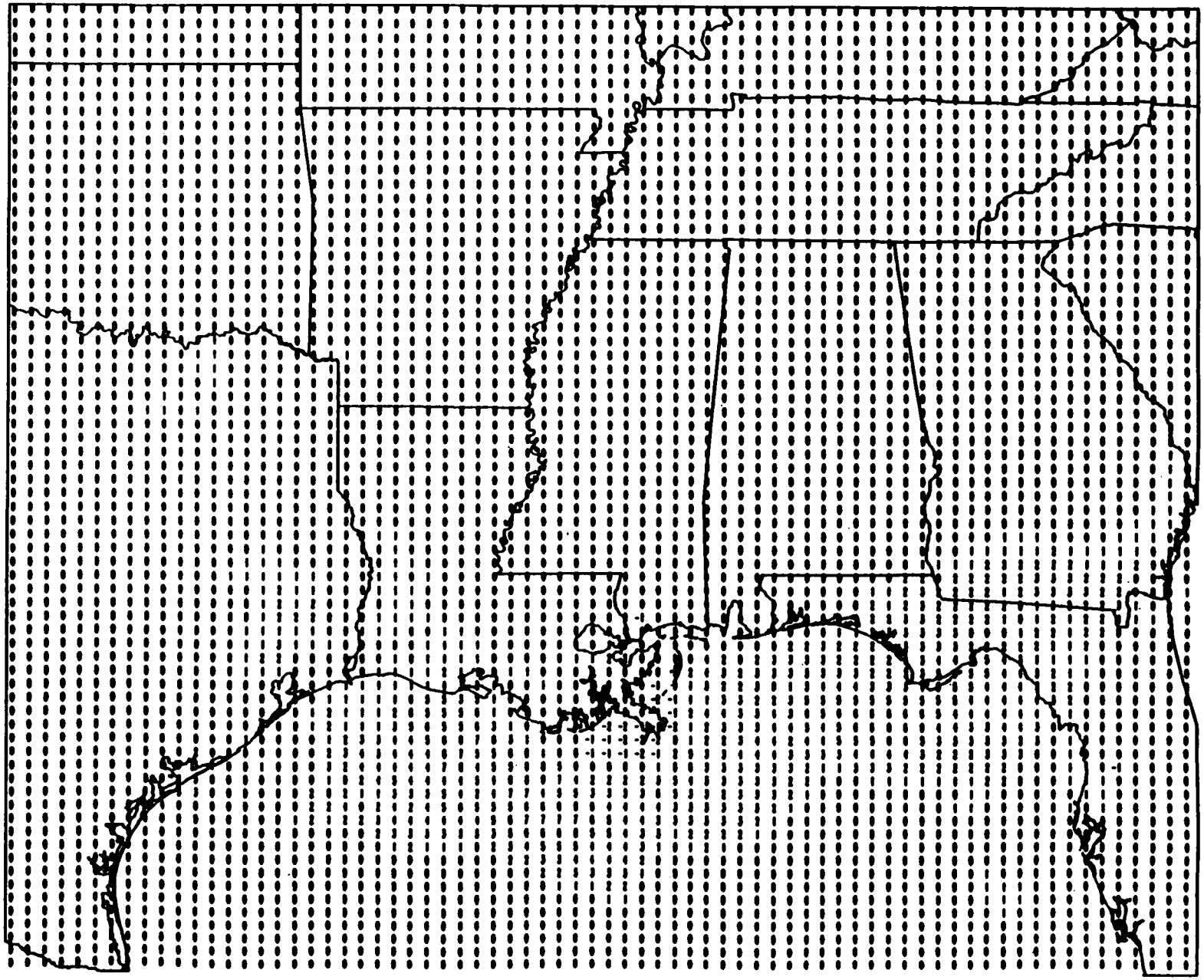

Difference: MMS Base With Double OCS - MMS Base
Daily Maximum Ozone, Layer 1 – JULY 28, 1988

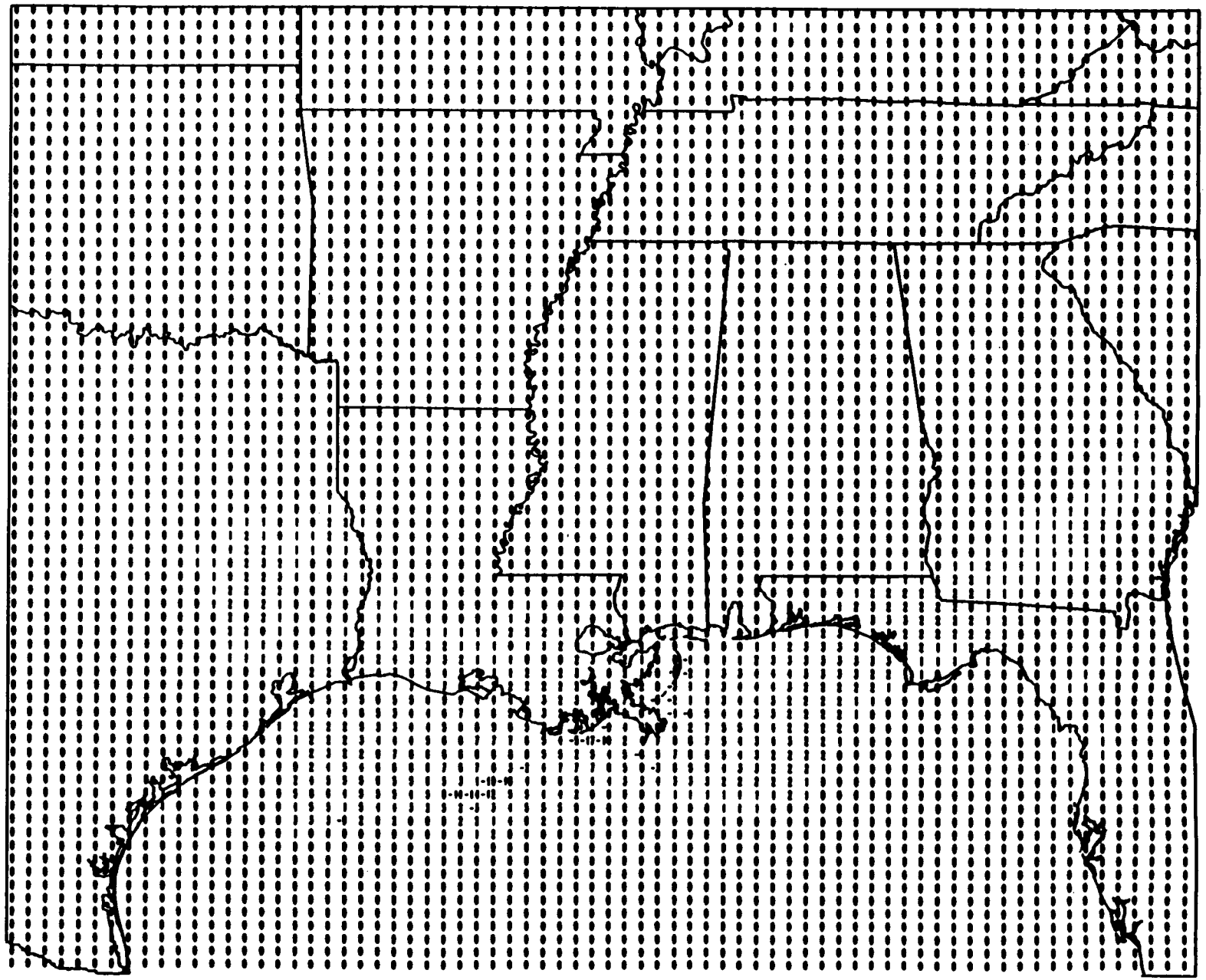

Difference: MMS Base With Double OCS - MMS Base
Daily Maximum Ozone, Layer 1 – JULY 29, 1988

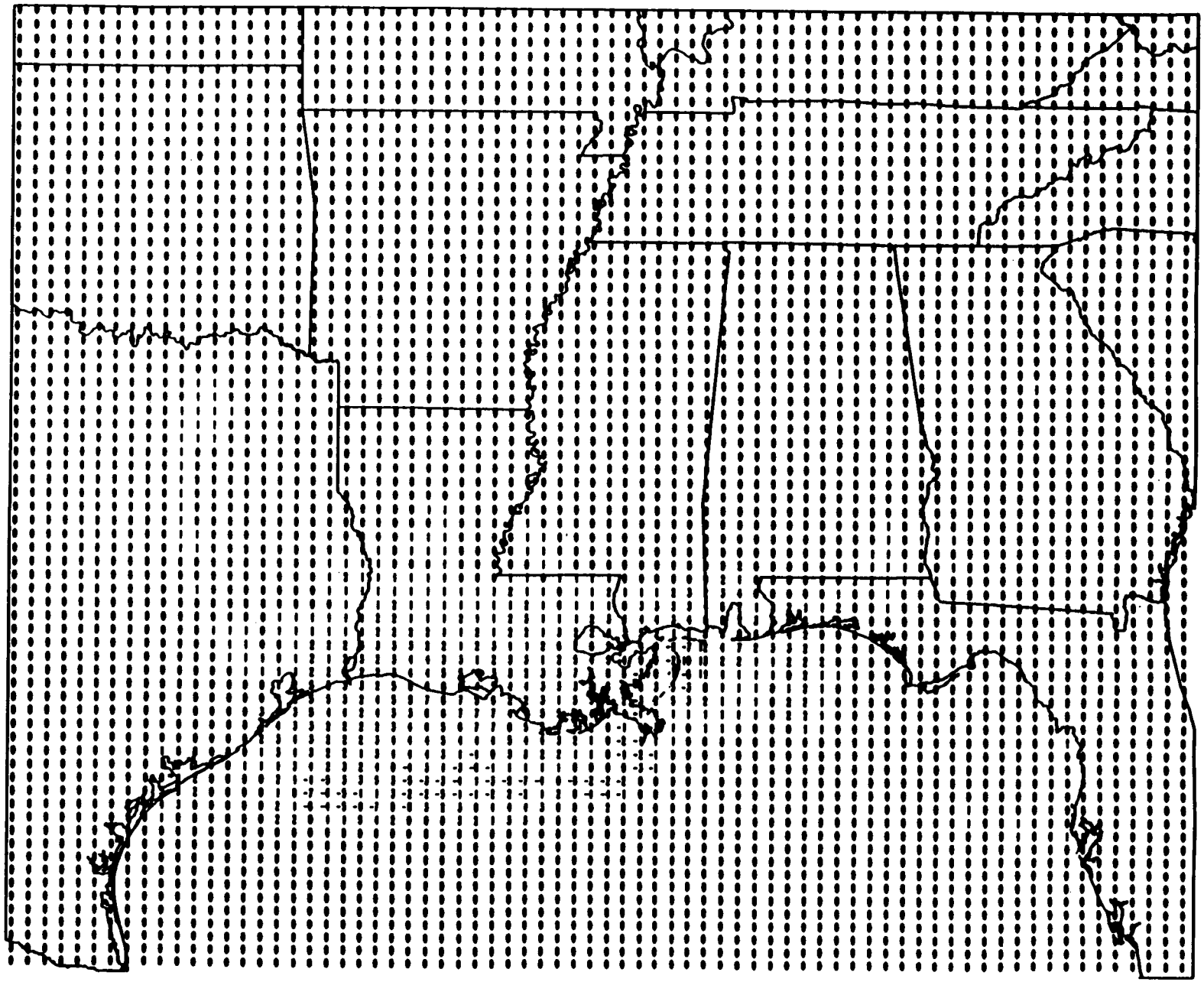

Difference: MMS Base With Double OCS - MMS Base
Daily Maximum Ozone, Layer 1 – JULY 30, 1988

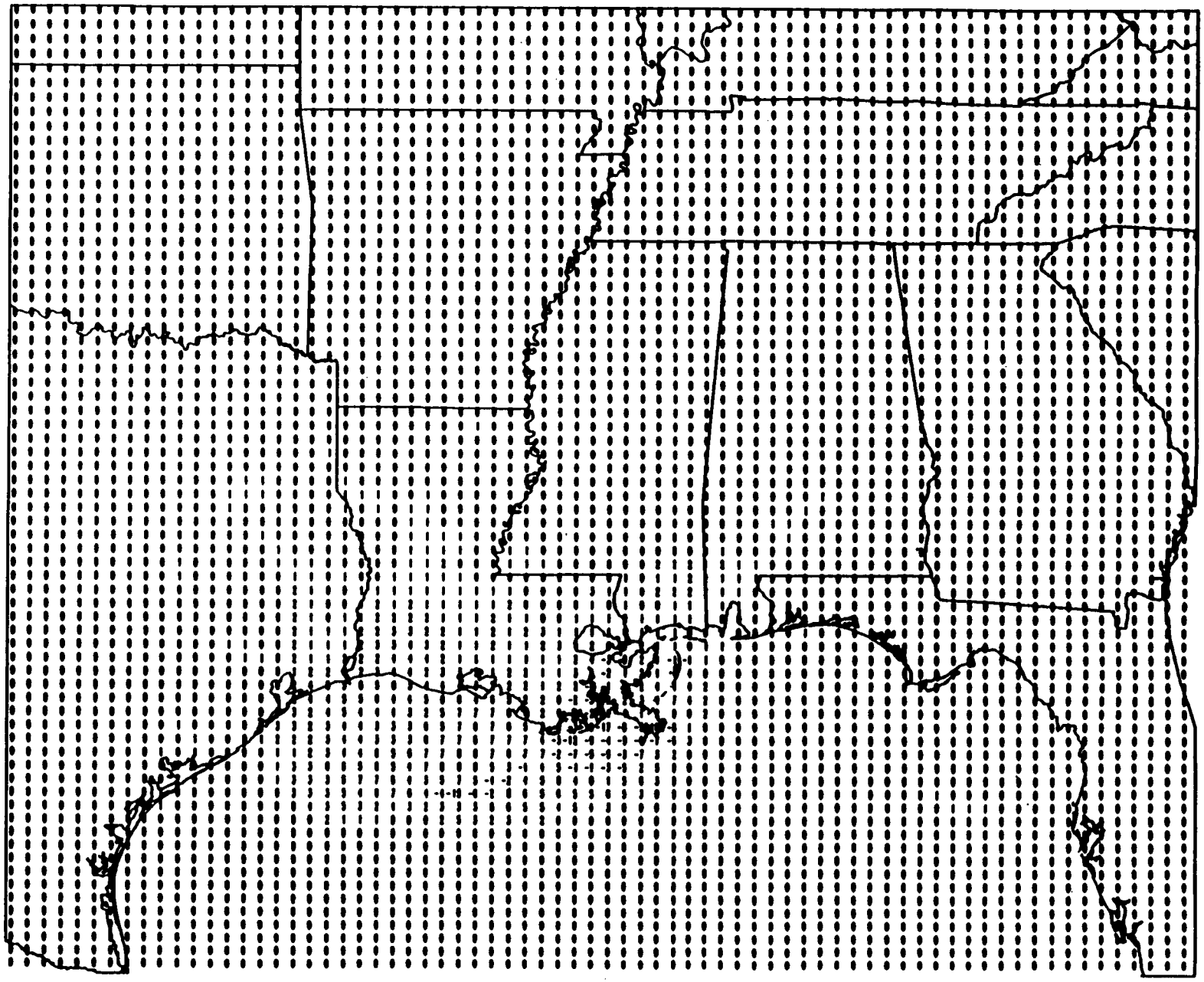

Difference: MMS Base With Double OCS - MMS Base
Daily Maximum Ozone, Layer 1 – JULY 31, 1988

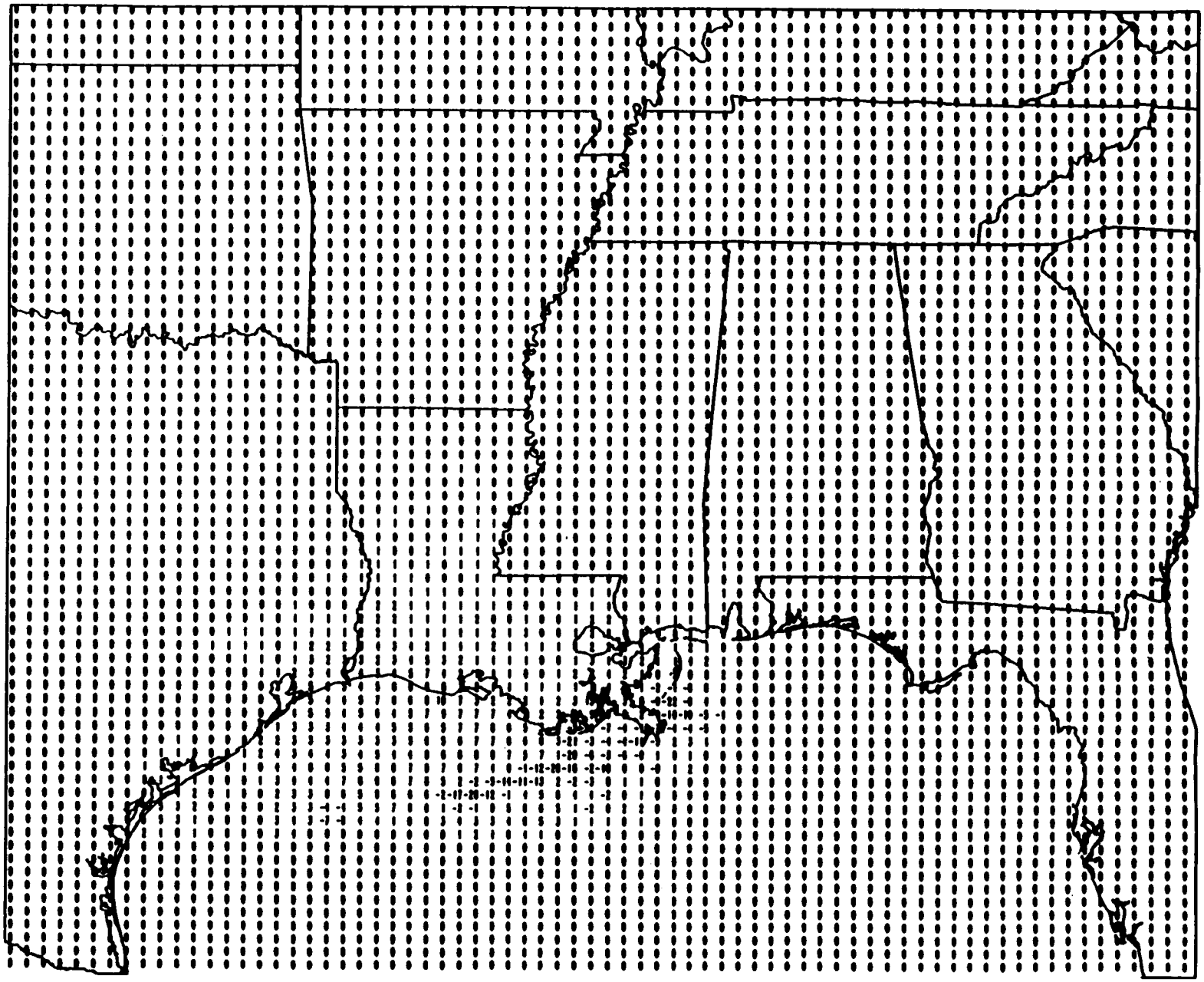

Difference: MMS Base With Double OCS - MMS Base
Daily Maximum Ozone, Layer 1 – AUGUST 1, 1988

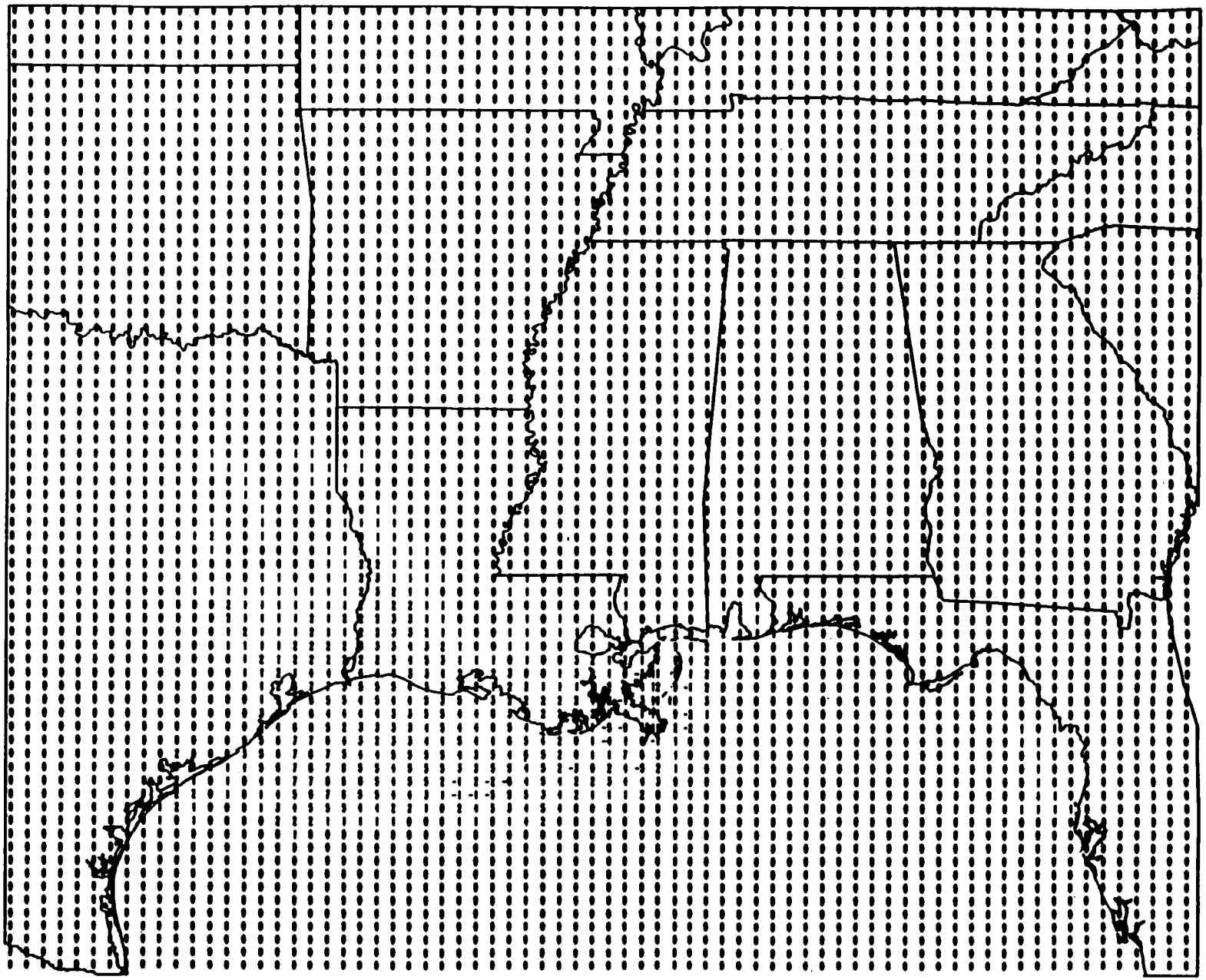

Difference: MMS Base With Double OCS - MMS Base
Daily Maximum Ozone, Layer 1 – AUGUST 2, 1988

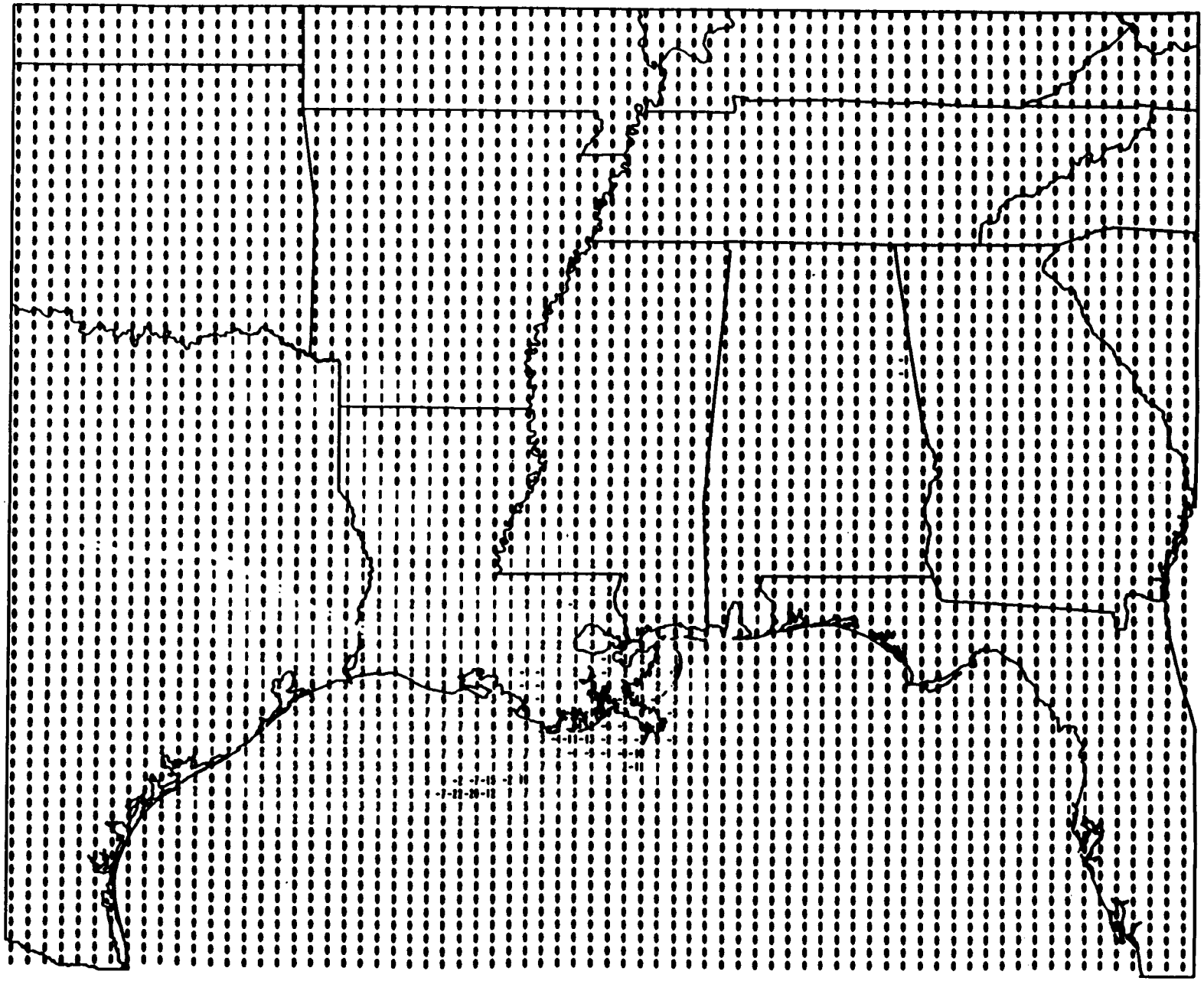

Difference: MMS Base With Double OCS - MMS Base
Daily Maximum Ozone, Layer 1 – AUGUST 3, 1988

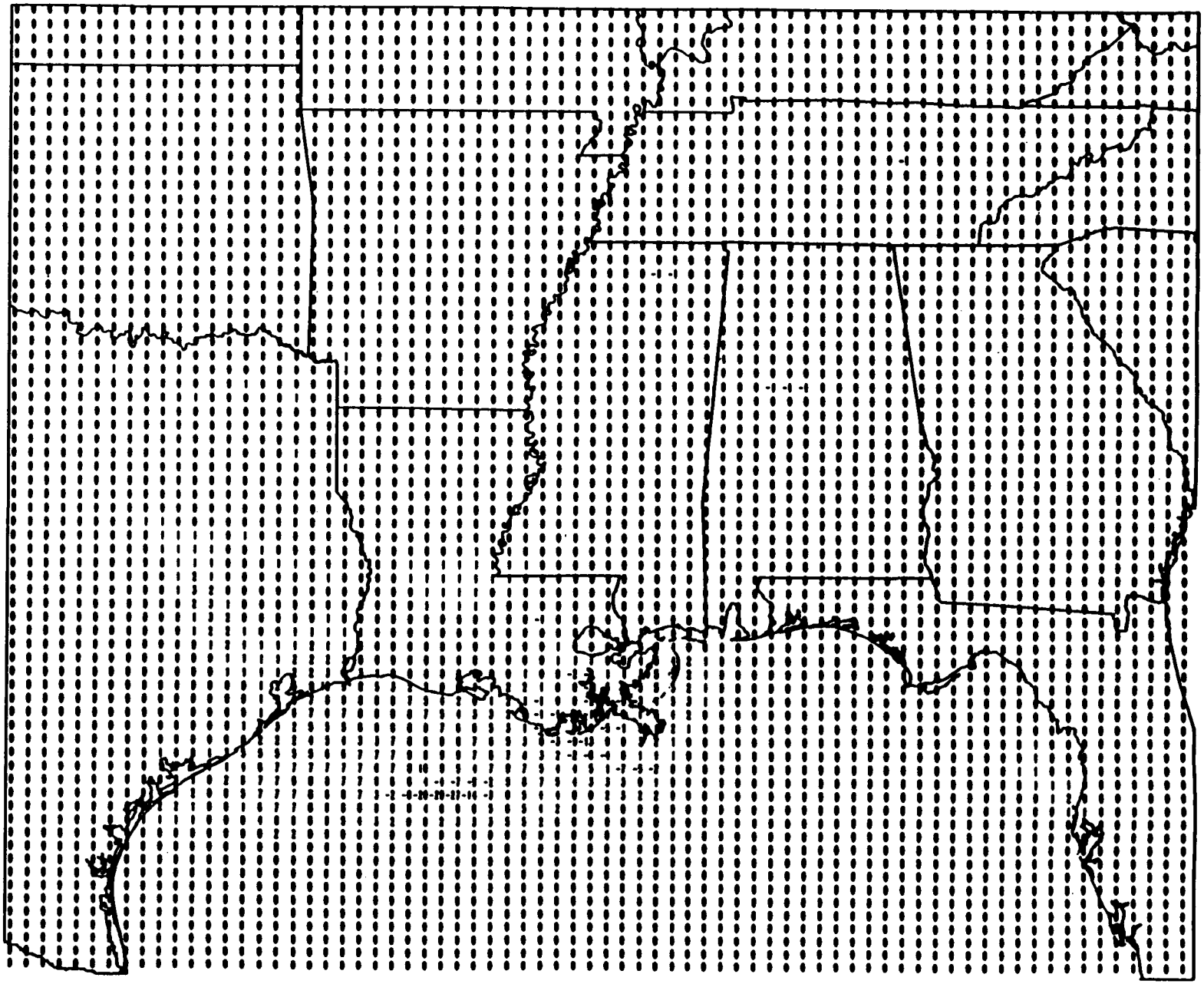

Difference: MMS Base With Double OCS - MMS Base
Daily Maximum Ozone, Layer 1 – AUGUST 4, 1988

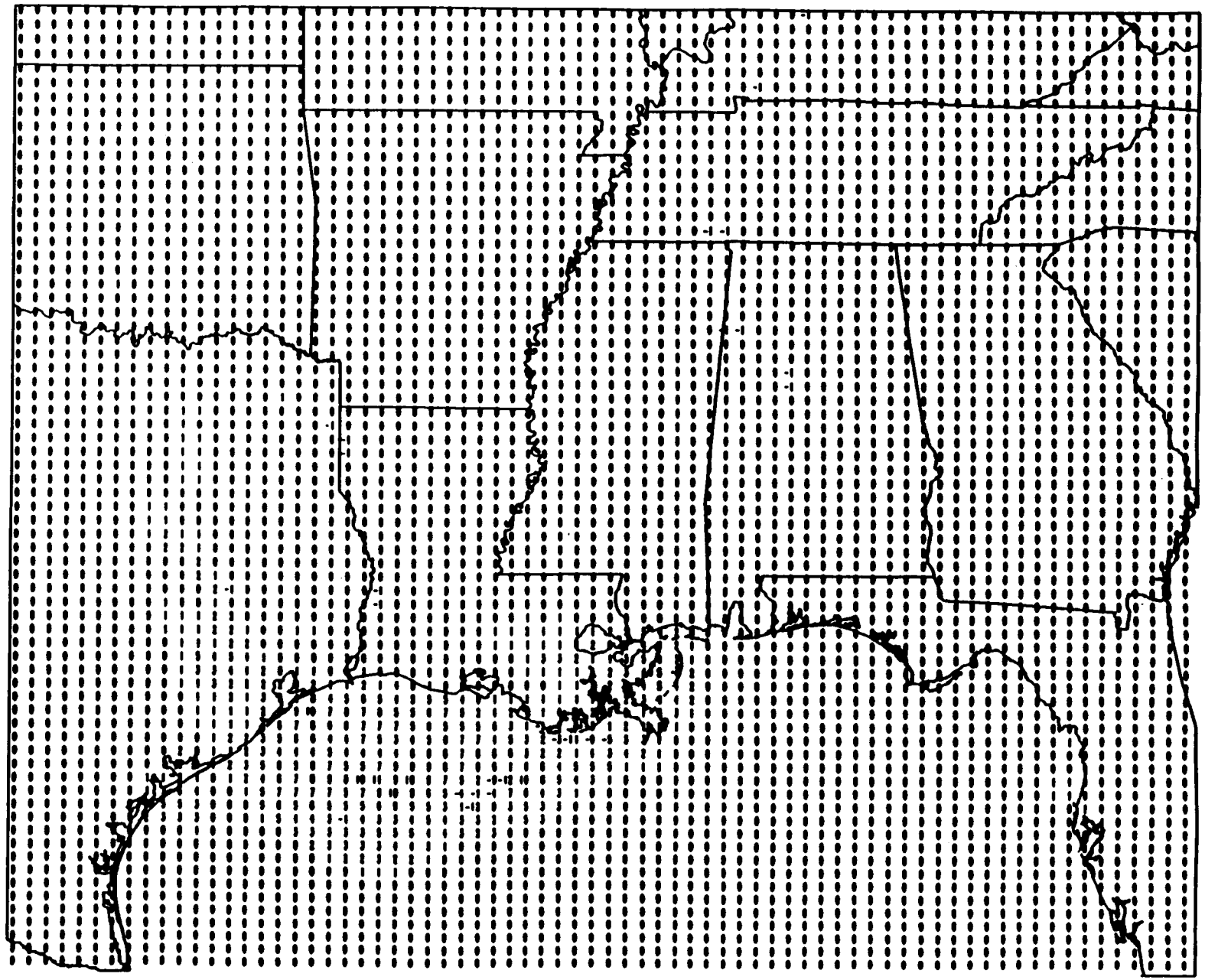

Difference: MMS Base With Double OCS - MMS Base
Daily Maximum Ozone, Layer 1 – AUGUST 5, 1988

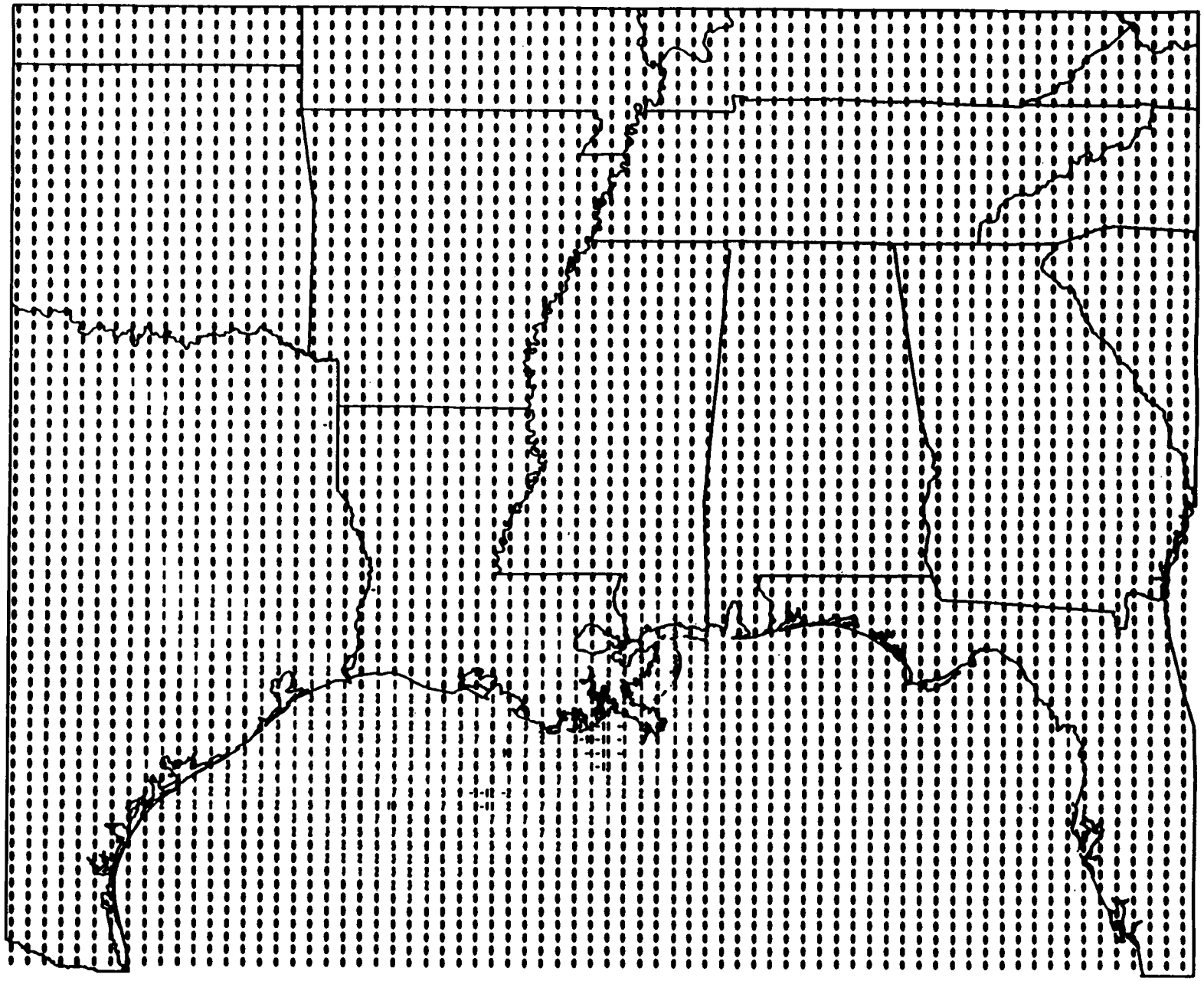

Difference: MMS Base With Double OCS - MMS Base
Daily Maximum Ozone, Layer 1 – AUGUST 6, 1988

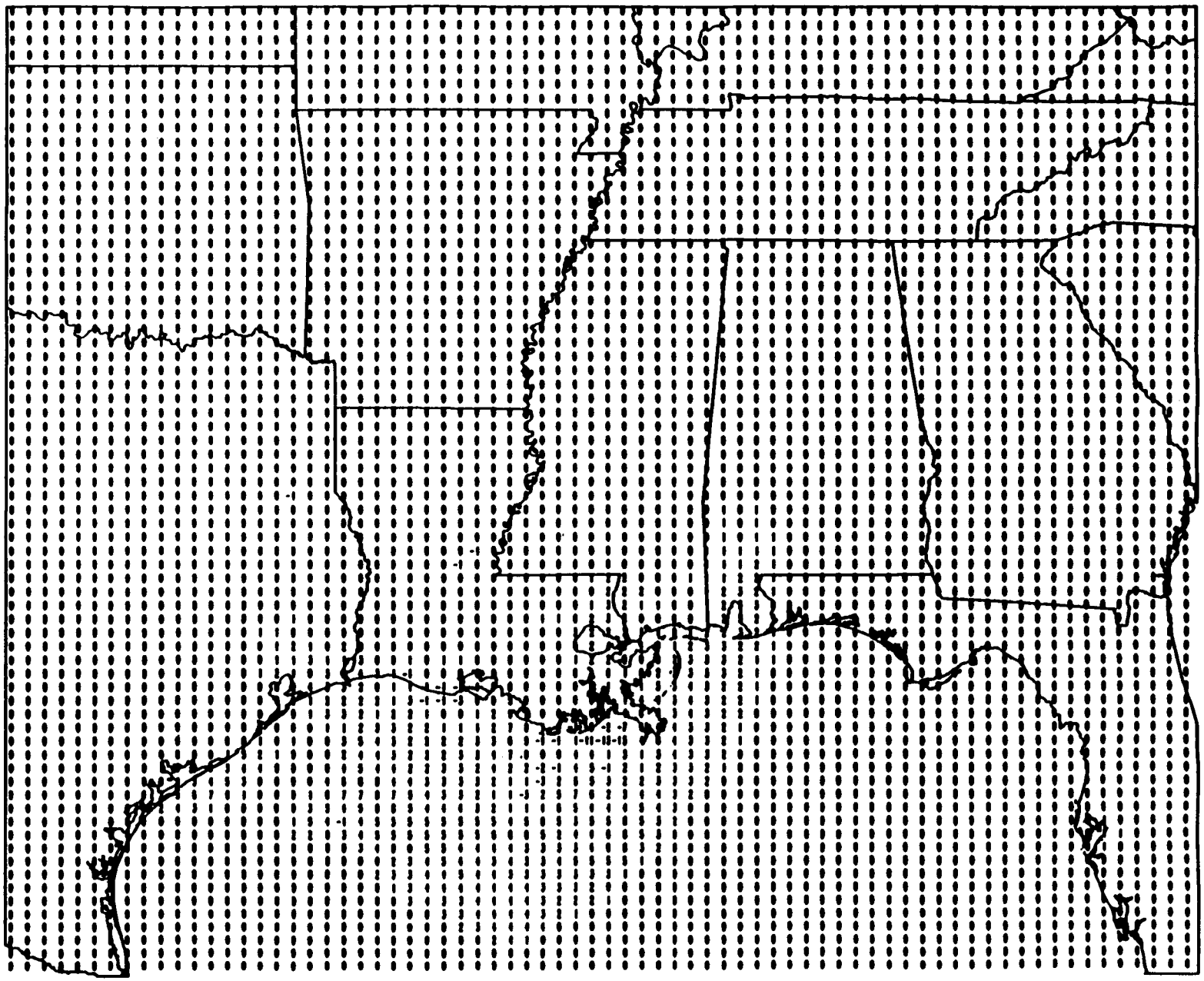

Episodic Ozone Concentration Difference
Between Without OCS Emissions and Base Case
For Episode #2, July 26, 1990 - July 31, 1990

Difference: MMS Base Without OCS - MMS Base
Episode Maximum Ozone, Layer 1 – July 26 – July 31, 1990

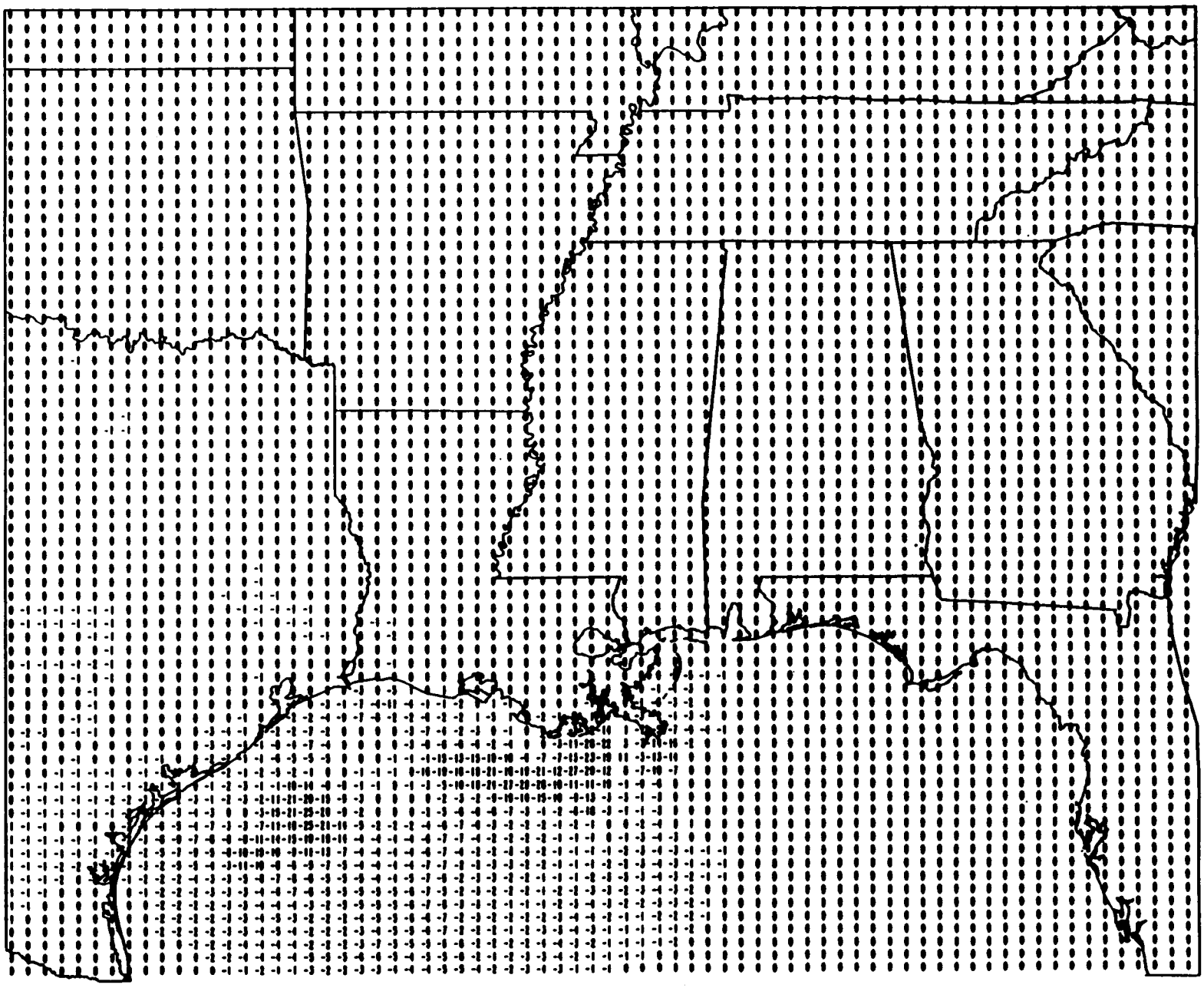

Daily Ozone Concentration Difference
Between Without OCS Emissions and Base Case
For Episode #2, July 26, 1990 - July 31, 1990

Difference: MMS Base Without OCS - MMS Base
Daily Maximum Ozone, Layer 1 – JULY 26, 1990

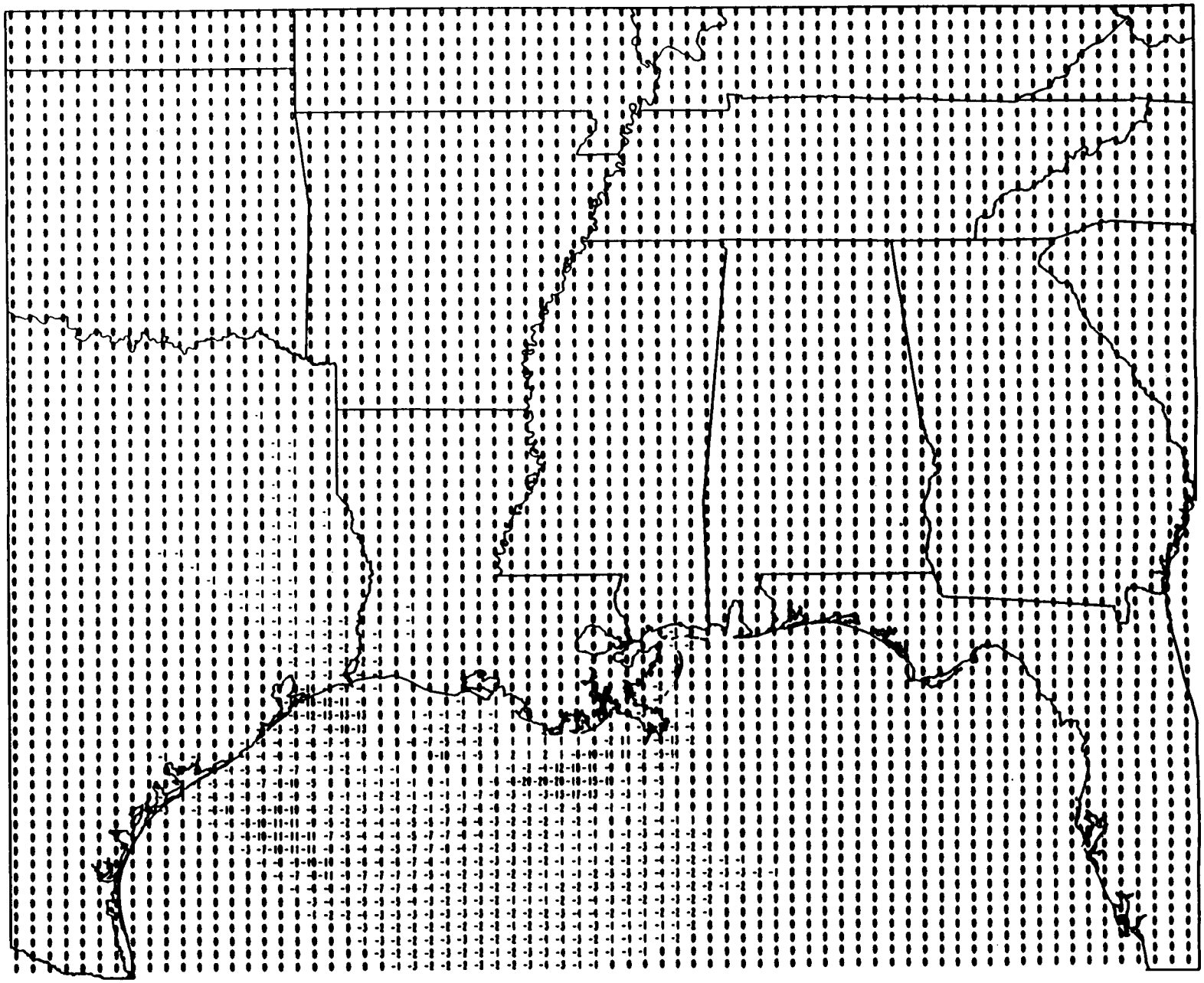

Difference: MMS Base Without OCS - MMS Base
Daily Maximum Ozone, Layer 1 – JULY 27, 1990

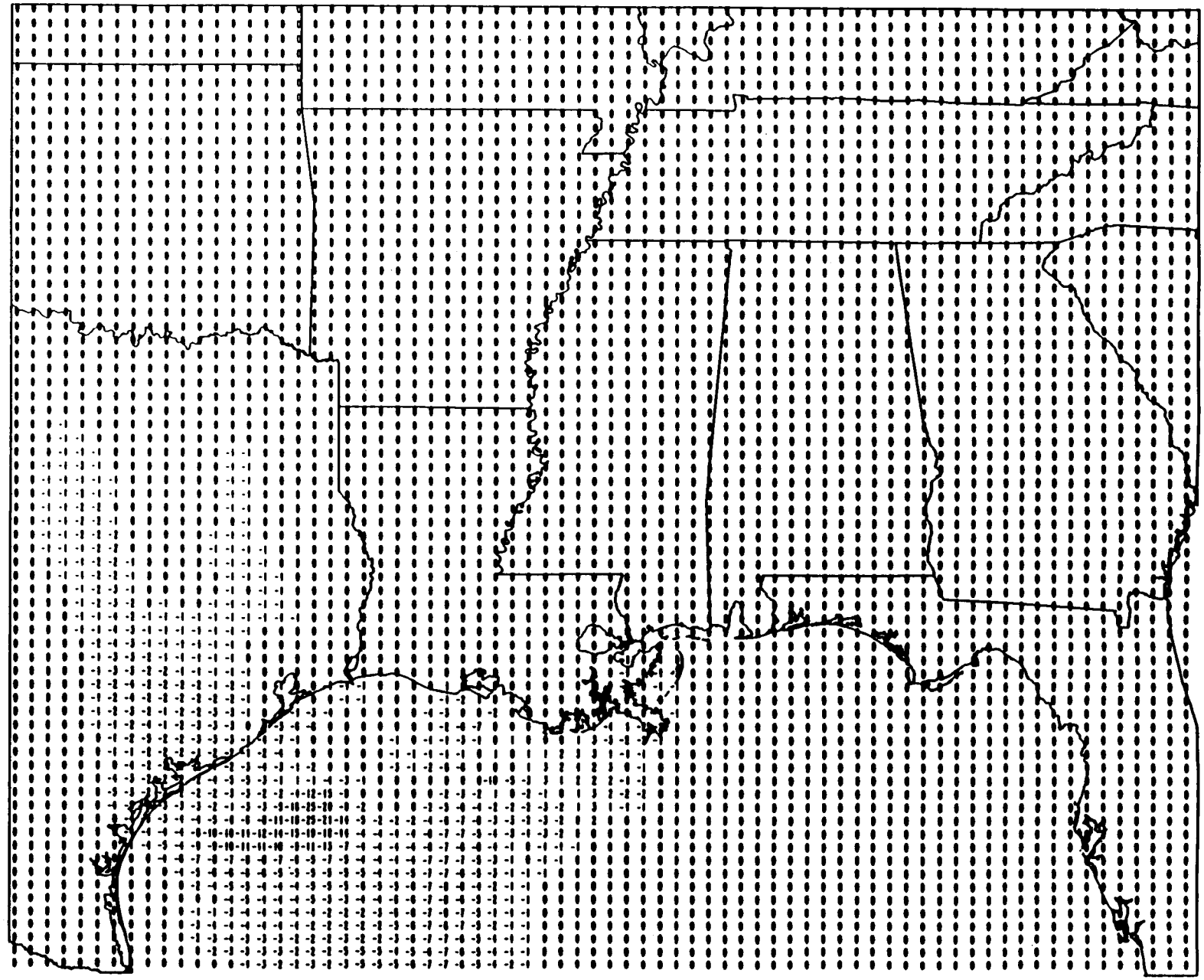

Difference: MMS Base Without OCS - MMS Base
Daily Maximum Ozone, Layer 1 – JULY 28, 1990

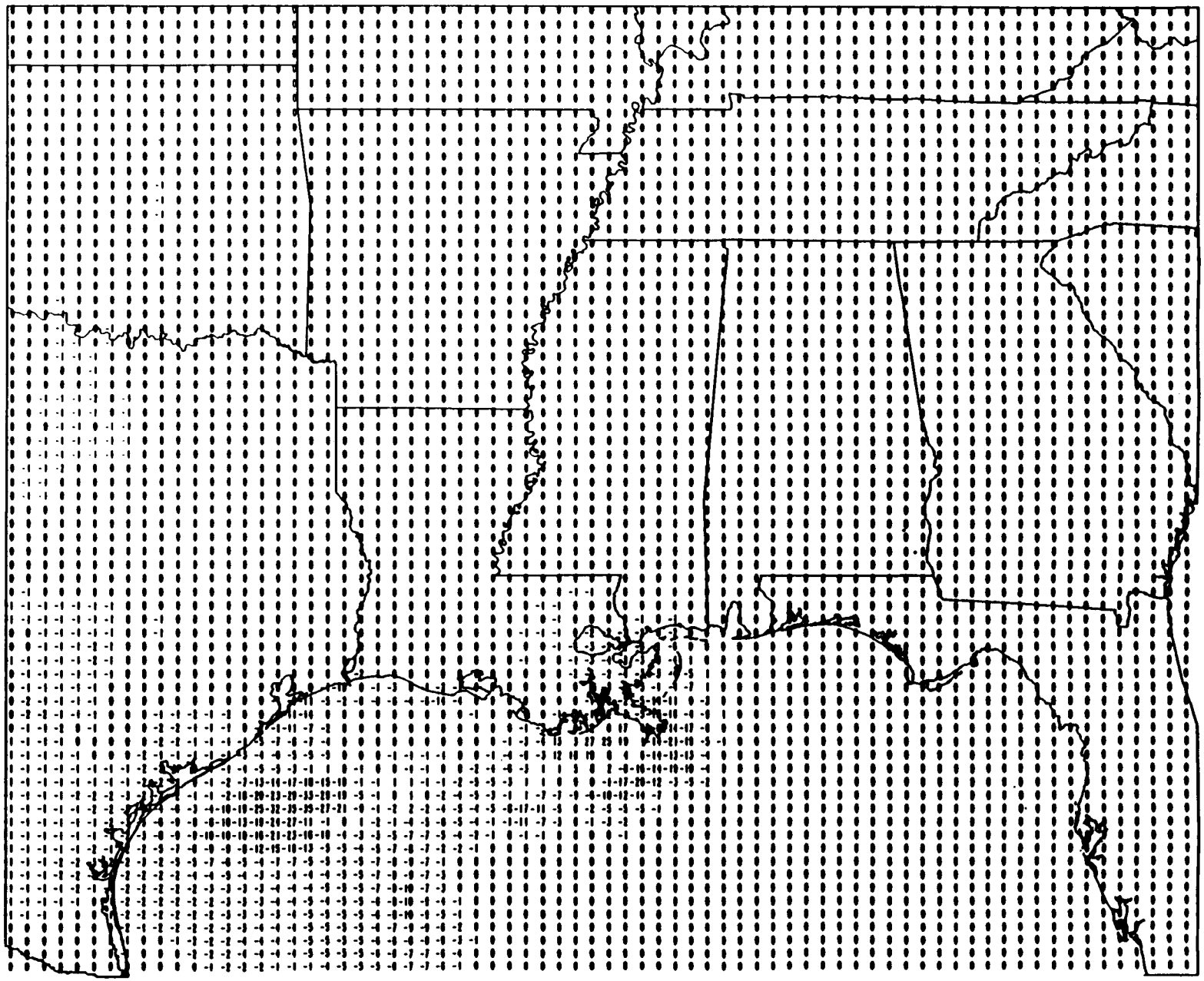

Difference: MMS Base Without OCS - MMS Base
Daily Maximum Ozone, Layer 1 – JULY 29, 1990

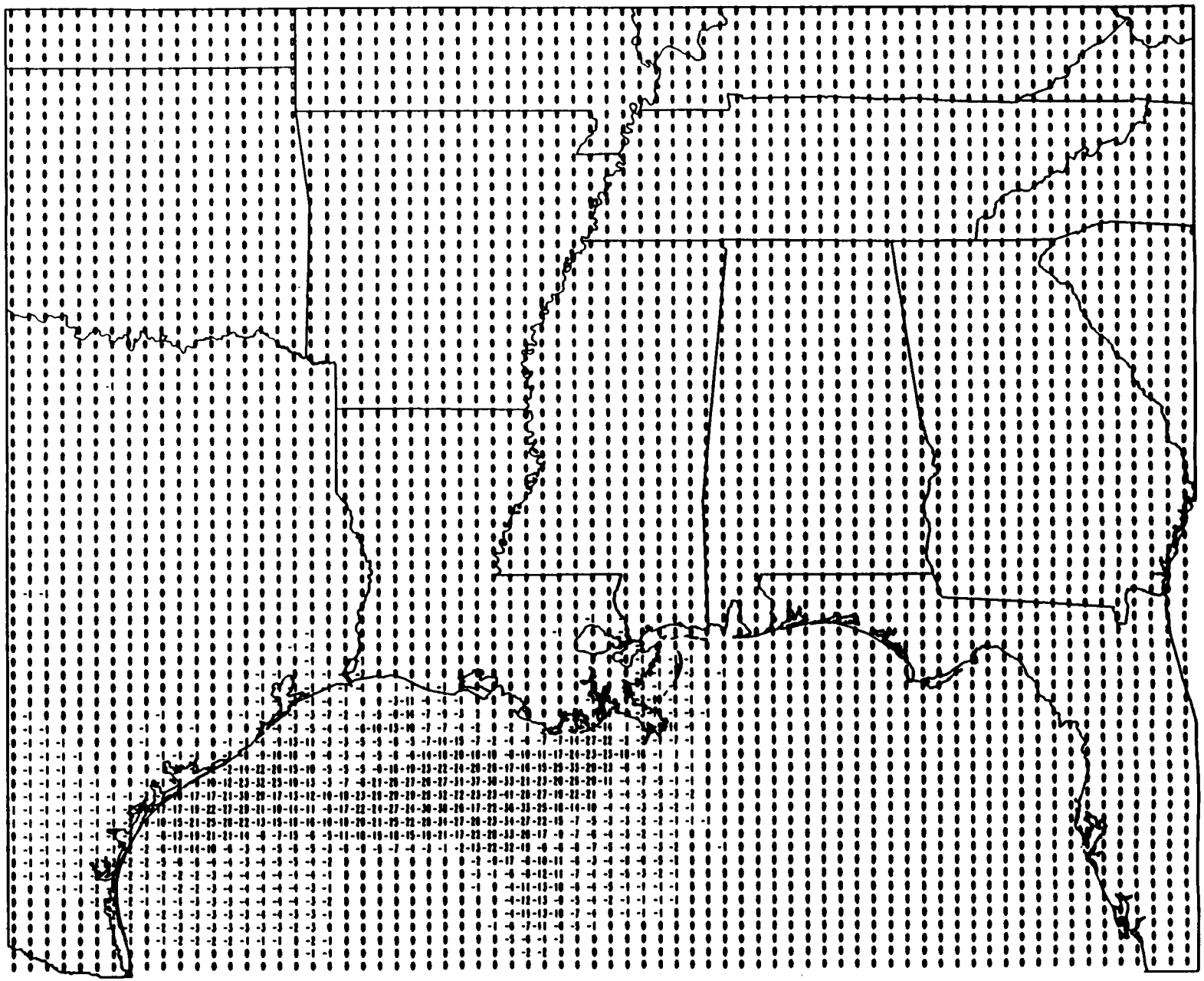

Difference: MMS Base Without OCS - MMS Base
Daily Maximum Ozone, Layer 1 – JULY 30, 1990

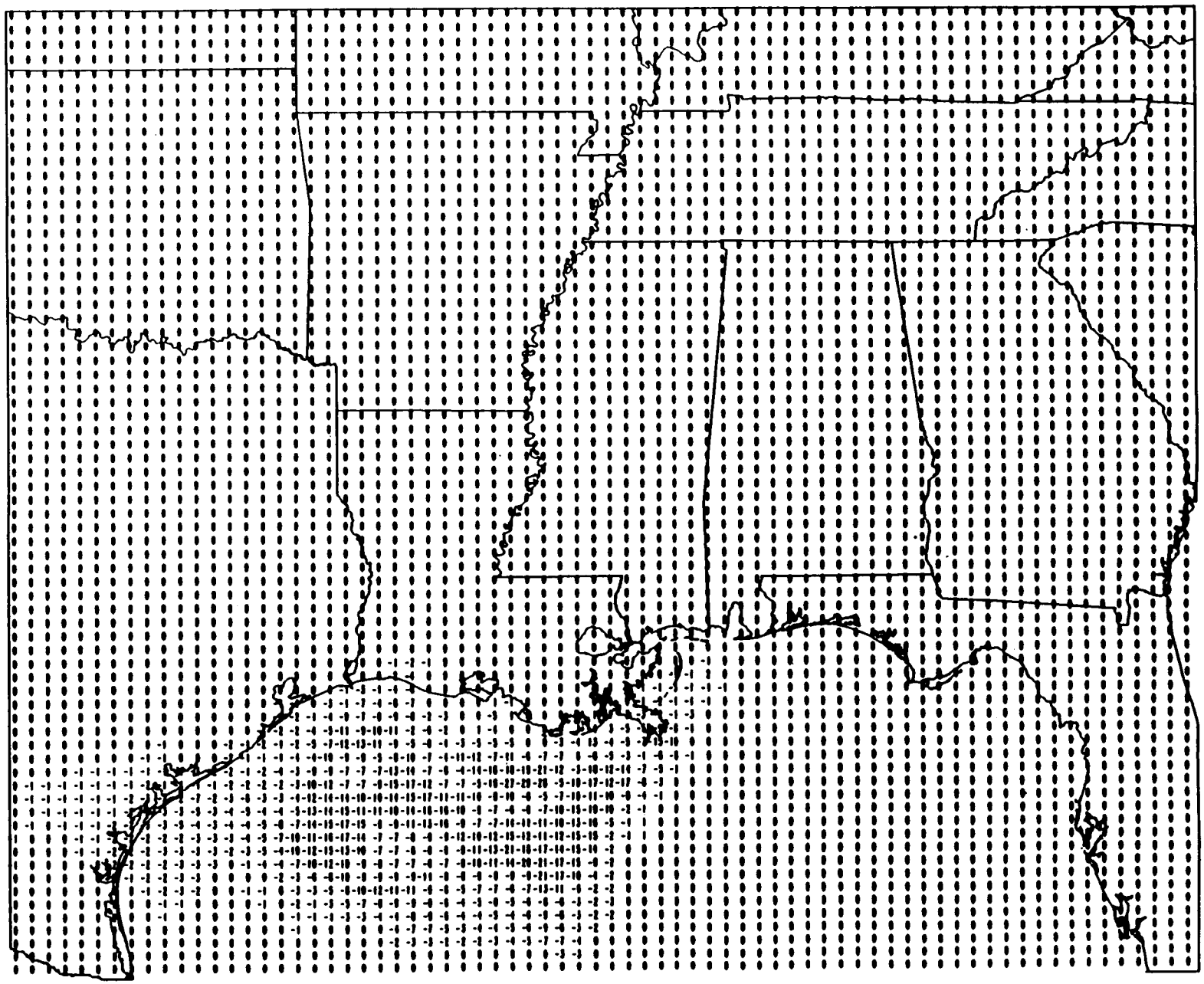

Difference: MMS Base Without OCS - MMS Base
Daily Maximum Ozone, Layer 1 – JULY 31, 1990

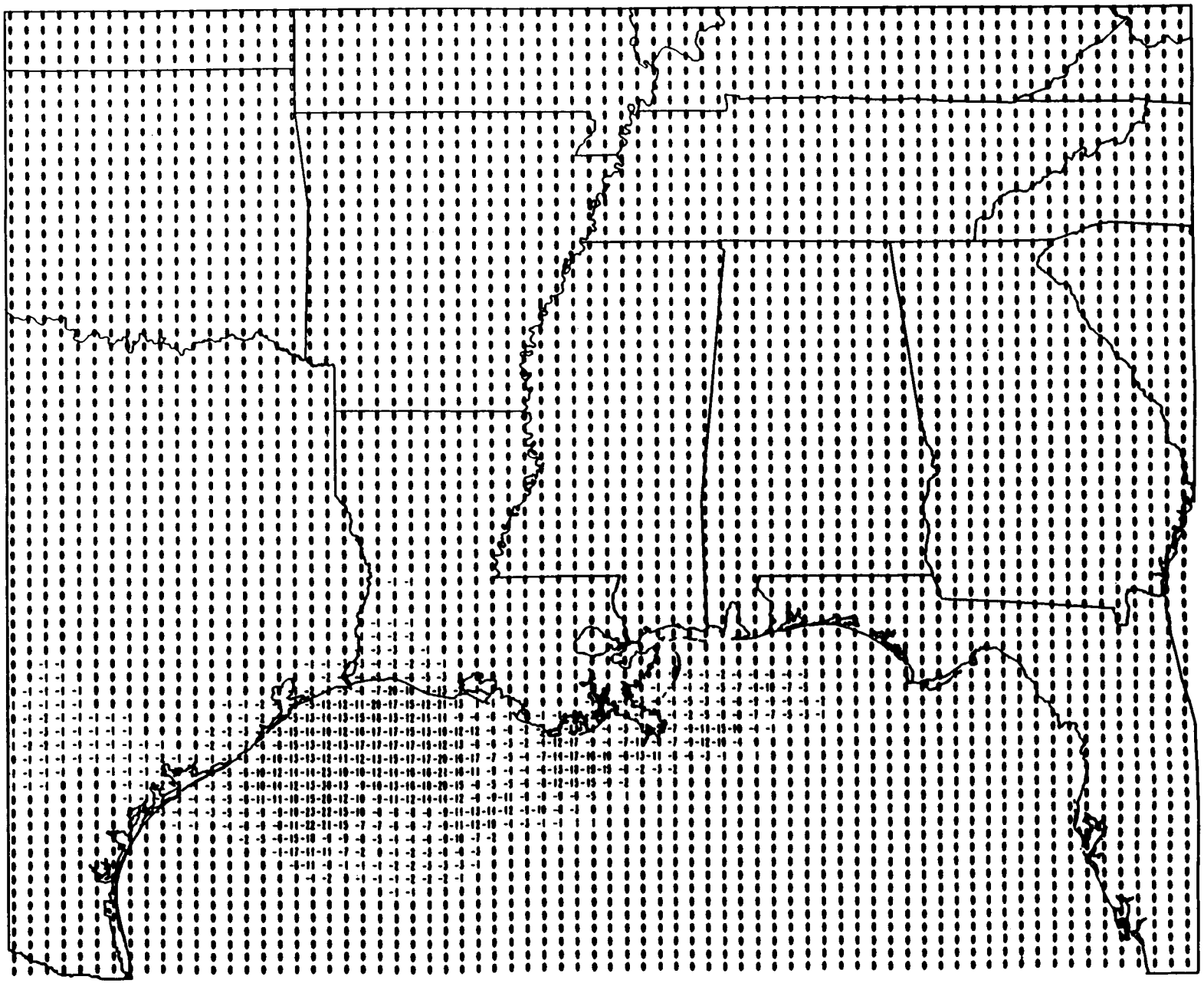

Episodic Ozone Concentration Difference
Between Double OCS Emissions and Base Case
For Episode #2, July 26, 1990 - July 31, 1990

Difference: MMS Base With Double OCS - MMS Base
Episode Maximum Ozone, Layer 1 – July 26 – July 31, 1990

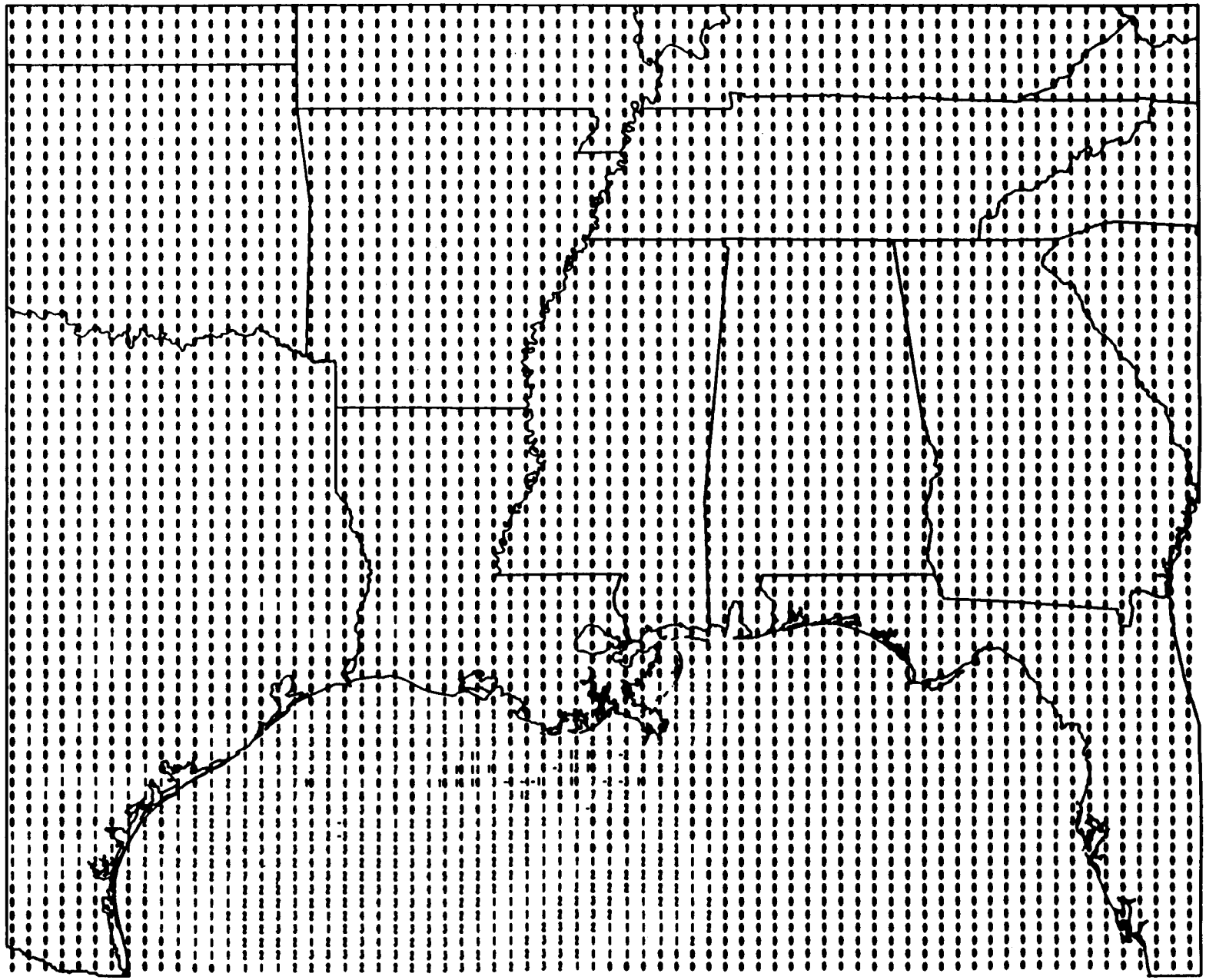

Daily Ozone Concentration Difference
Between Double OCS Emissions and Base Case
For Episode #2, July 26, 1990 - July 31, 1990

Difference: MMS Base With Double OCS - MMS Base
Daily Maximum Ozone, Layer 1 – JULY 26, 1990

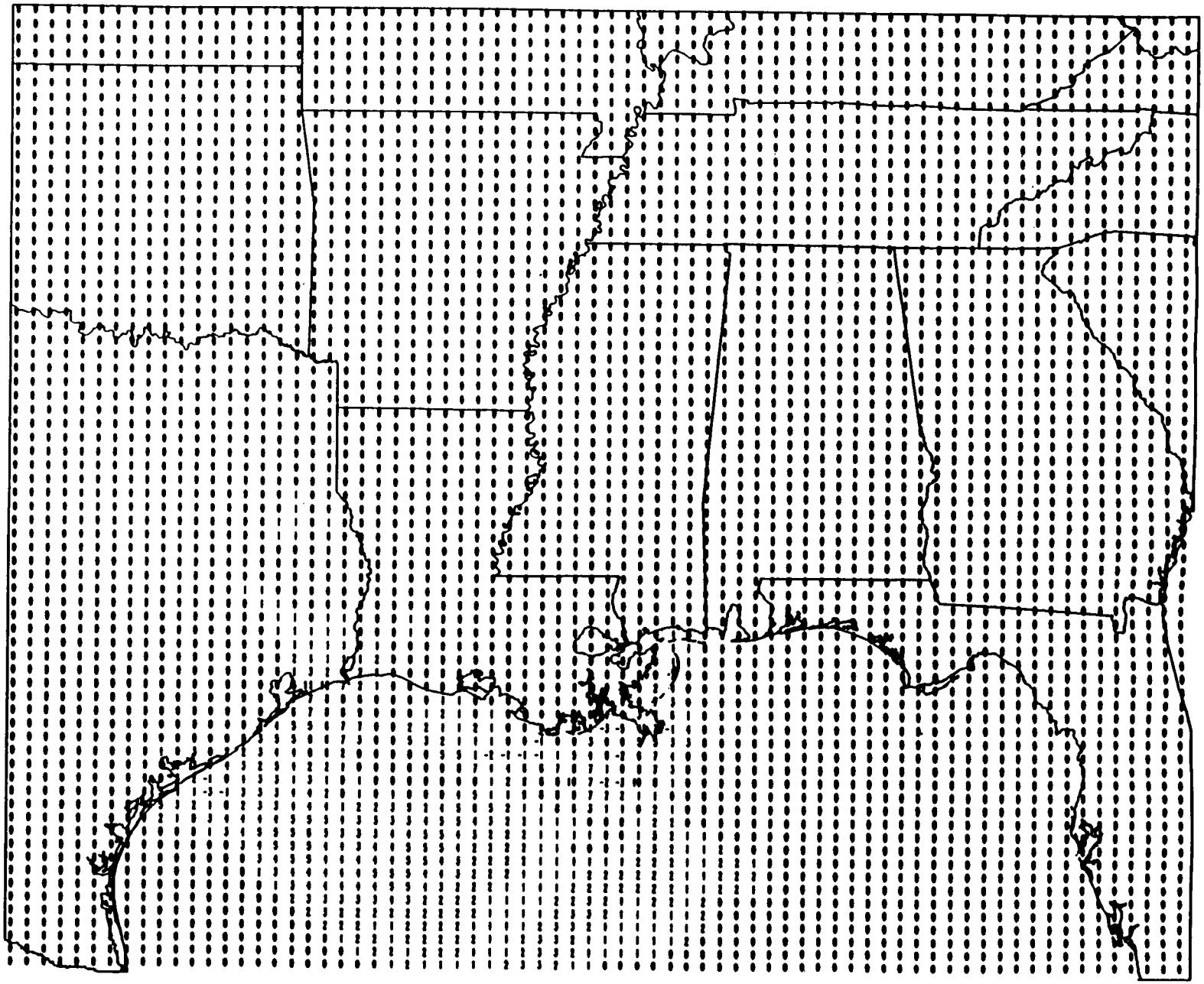

Difference: MMS Base With Double OCS - MMS Base
Daily Maximum Ozone, Layer 1 – JULY 27, 1990

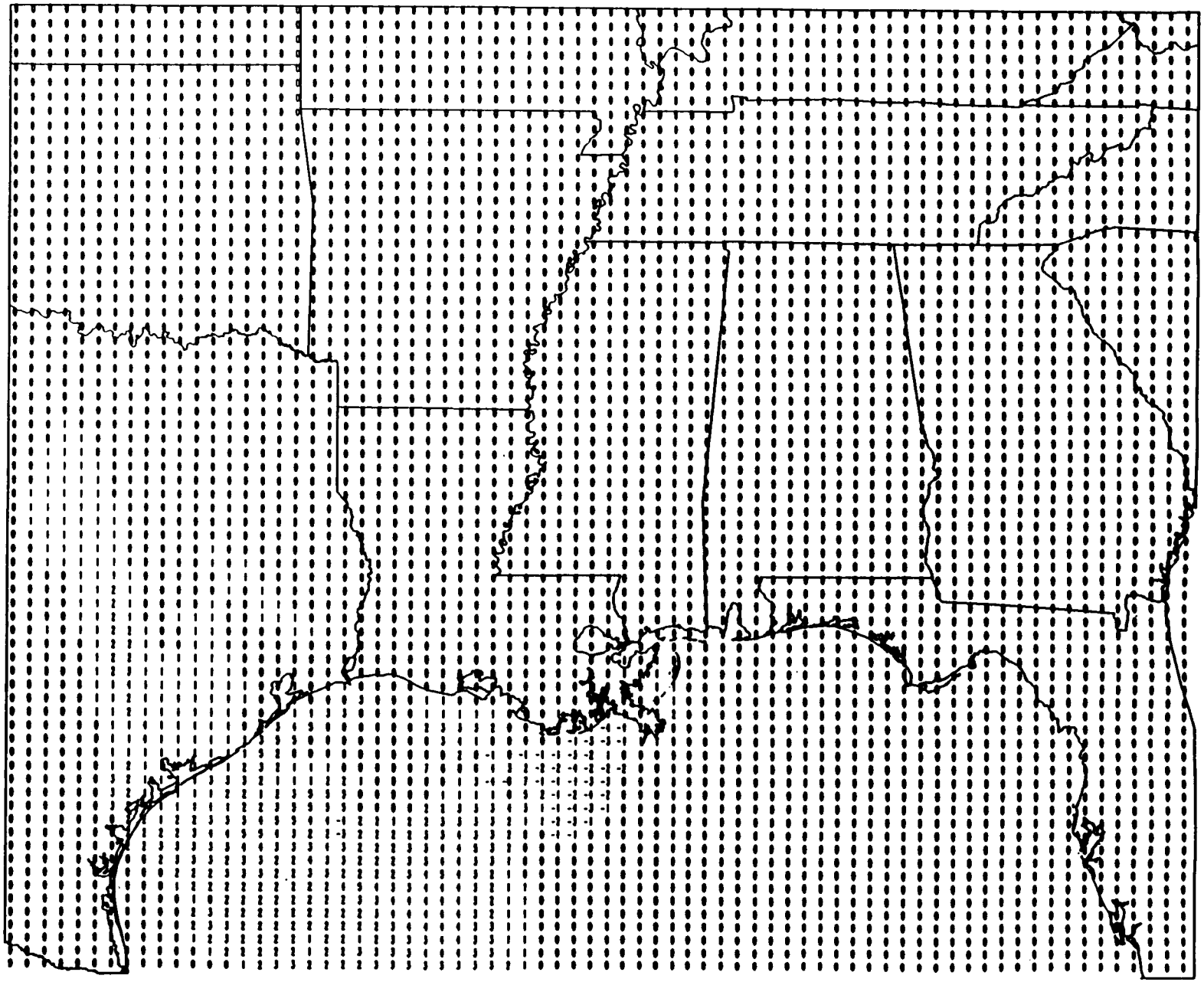

Difference: MMS Base With Double OCS - MMS Base
Daily Maximum Ozone, Layer 1 – JULY 28, 1990

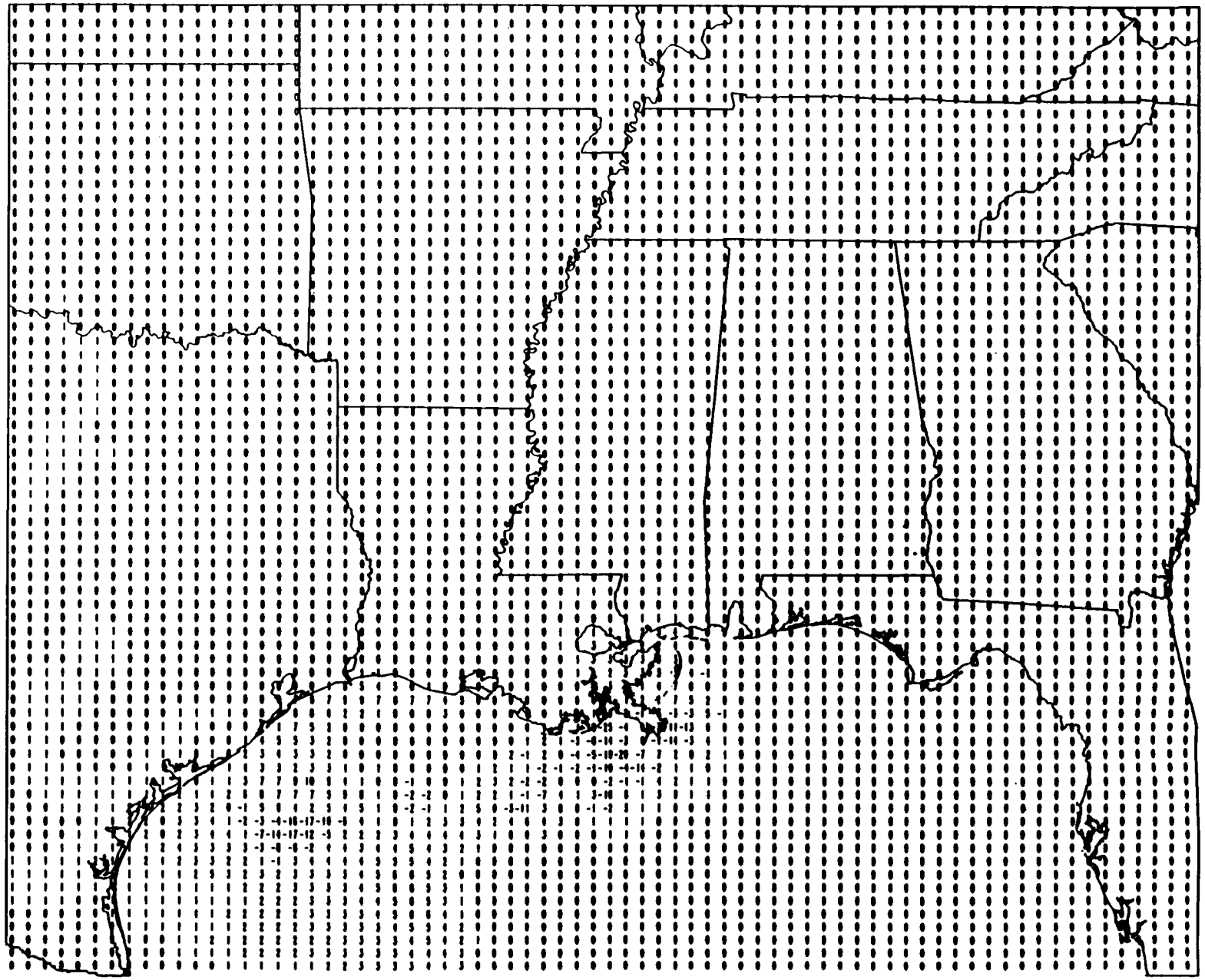

Difference: MMS Base With Double OCS - MMS Base
Daily Maximum Ozone, Layer 1 – JULY 29, 1990

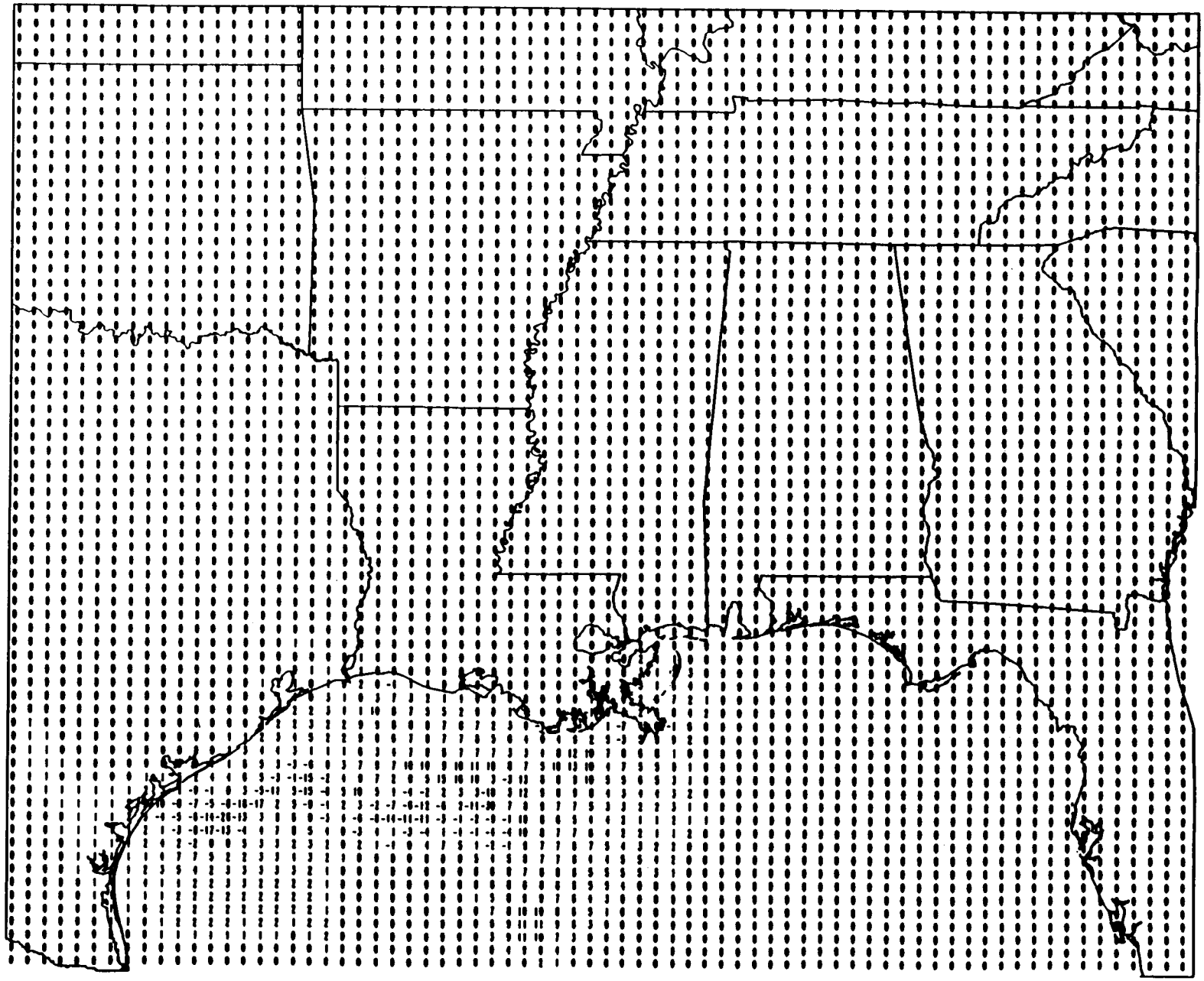

Difference: MMS Base With Double OCS - MMS Base
Daily Maximum Ozone, Layer 1 – JULY 30, 1990

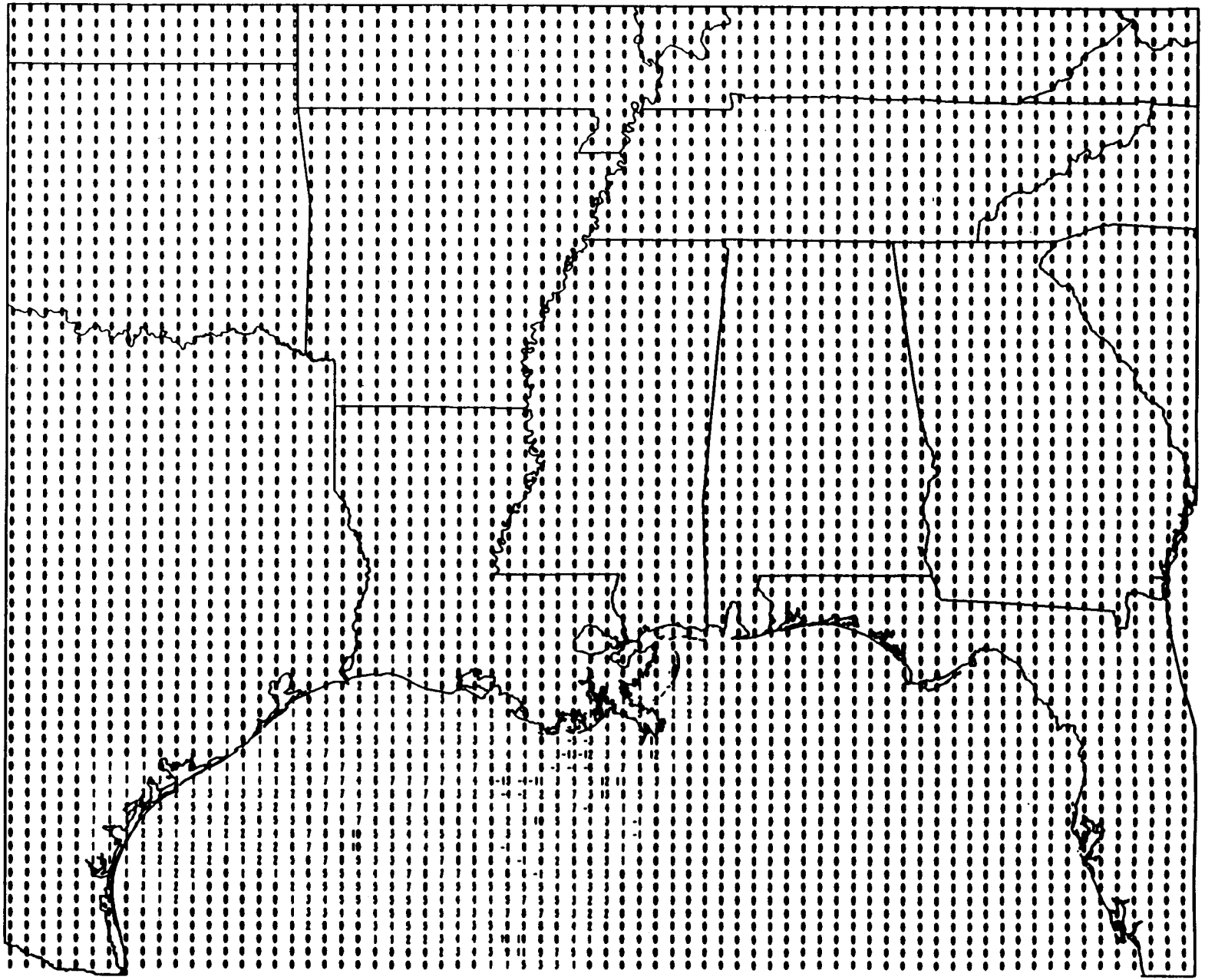

Difference: MMS Base With Double OCS - MMS Base
Daily Maximum Ozone, Layer 1 – JULY 31, 1990

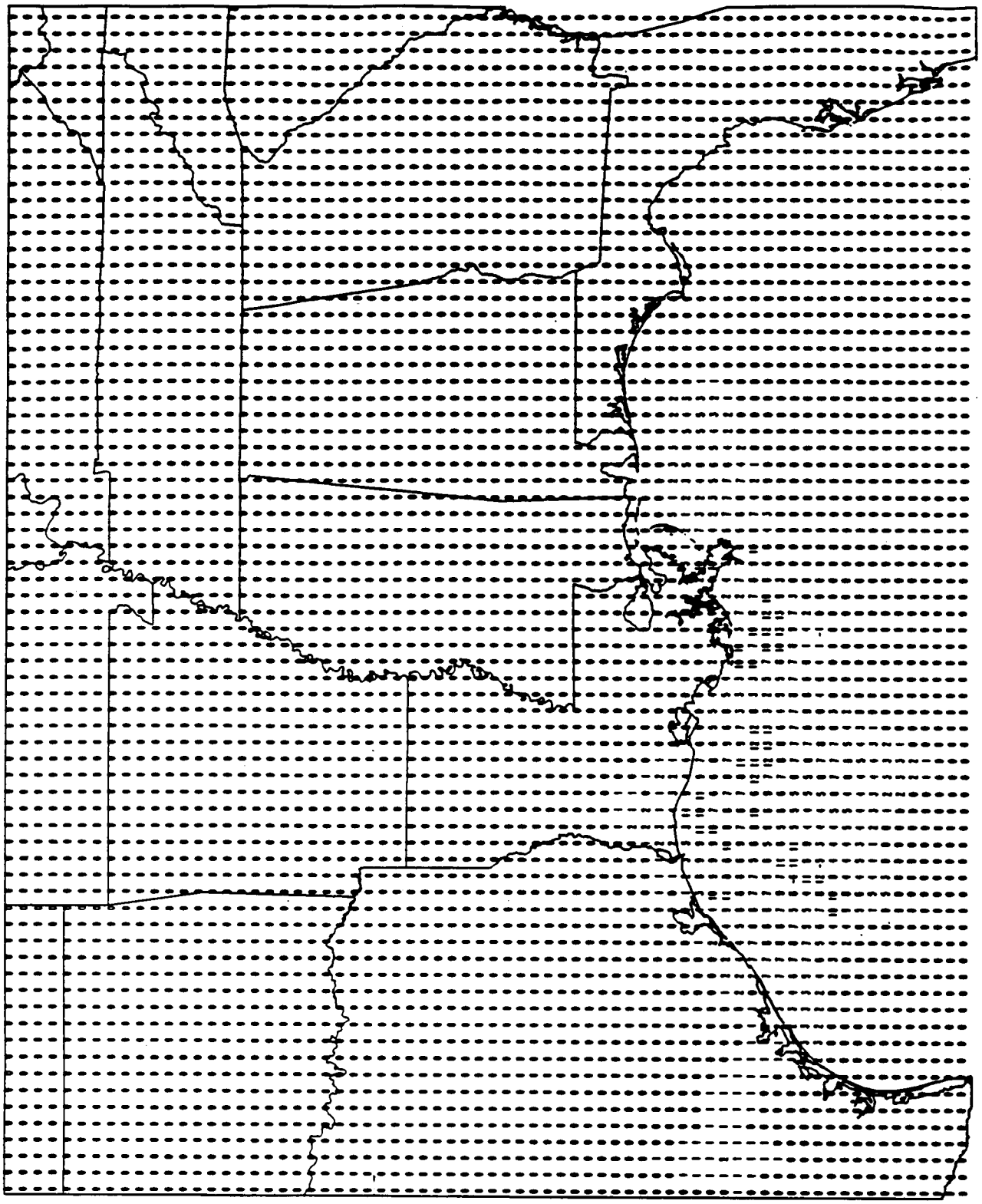

*U.S. G.P.O.:1993-301-078:80406

As the Nation's principal conservation agency, the Department of the Interior has responsibility for most of our nationally-owned public lands and natural resources. This includes fostering sound use of our land and water resources; protecting our fish, wildlife, and biological diversity; preserving the environmental and cultural values of our national parks and historical places; and providing for the enjoyment of life through outdoor recreation. The Department assesses our energy and mineral resources and works to ensure that their development is in the best interests of all our people by encouraging stewardship and citizen participation in their care. The Department also has a major responsibility for American Indian reservation communities and for people who live in island territories under U.S. administration.